April 2008
Research Report: UCPRC-RR-2008-07

Full-Depth Pavement Reclamation with Foamed Asphalt: Final Report

Authors:
D. Jones, P. Fu, J. Harvey, and F. Halles

Partnered Pavement Research Program (PPRC) Contract Strategic Plan Element 4:12:
Full-Depth Reclamation with Foamed Asphalt

PREPARED FOR:

California Department of Transportation
Division of Research and Innovation
Office of Roadway Research

PREPARED BY:

University of California
Pavement Research Center
UC Davis, UC Berkeley

DOCUMENT RETRIEVAL PAGE			Research Report: UCPRC-RR-2008-07
Title: Full-Depth Pavement Reclamation with Foamed Asphalt: Final Report			
Authors: D. Jones, P. Fu, J. Harvey, and F. Halles			
Prepared for: Caltrans	**FHWA No.:** CA101069C	**Work Submitted Date:** October 30, 2008	**Date**: April 2008
Strategic Plan Element No: 4.12	**Status:** Final		**Version No:** 03/31/10

Abstract:

A comprehensive study on full-depth reclamation (FDR) of pavements with foamed asphalt has been completed for the California Department of Transportation by the University of California Pavement Research Center. A literature review revealed that very little research had been carried out on the reclamation of thick asphalt pavements (multiple overlays over a relatively weak base or subgrade). A mechanistic sensitivity analysis was carried out to identify key variables in the design of recycled pavements consisting primarily of recycled asphalt pavement. The findings of this analysis and the literature review were used to formulate a work plan for laboratory and field studies to address issues specific to recycling these thick asphalt pavements.

A number of FDR projects were observed during the course of the study. Material was collected for a comprehensive laboratory investigation, which identified a number of key issues pertaining to mix design, including appropriate test methods for California, preparation of specimens (mixing moisture content and aggregate temperature), asphalt binder selection, target asphalt and active filler contents, aggregate gradations (fines content), specimen curing, and the interpretation of results. Visual assessments and Falling Weight Deflectometer testing were also carried out on selected projects at regular intervals. The study concluded that FDR with foamed asphalt combined with a cementitious filler is an appropriate pavement rehabilitation option for California. Projects should be carefully selected with special care given to roadside drainage. Appropriate mix and structural design procedures should be followed, and construction should be strictly controlled to ensure that optimal performance and life are obtained from the pavement. The following recommendations are made:

- FDR with foamed asphalt combined with a cementitious filler should be considered as a rehabilitation option on thick, cracked asphalt pavements on highways with an annual average daily traffic volume not exceeding 20,000 vehicles. The technology is particularly suited to pavements where multiple overlays have been placed over relatively weak supporting layers, and where cracks reflect through the overlay in a relatively short time. Higher traffic volumes can be considered provided that adequate strength and durability can be achieved with the in-place materials. Alternatively, the recycled layer can be used as a subbase under a new base layer.
- Project selection, mix design, and construction should be strictly controlled to ensure that optimal performance is obtained from the rehabilitated roadway.
- Full-depth reclamation with asphalt emulsions and partial-depth reclamation with asphalt emulsions and foamed asphalt should also be evaluated, and guidelines prepared for choosing the most appropriate technology for a given set of circumstances.

Keywords:

Full-depth recycling, Full-depth reclamation, Deep in situ recycling, Foamed asphalt, Foamed bitumen

Proposals for implementation:

Related documents:

Signatures:

D. Jones **1st Author**	J. Harvey **Technical Review**	D. Spinner **Editor**	J. Harvey **Principal Investigator**	T. J. Holland **Caltrans Contract Manager**

DISCLAIMER

The contents of this report reflect the views of the authors who are responsible for the facts and accuracy of the data presented herein. The contents do not necessarily reflect the official views or policies of the State of California or the Federal Highway Administration. This report does not constitute a standard, specification, or regulation.

PROJECT OBJECTIVES

The objective of this project was to develop guidelines for improved mix and structural design and construction for full-depth reclamation (FDR) of cracked asphalt concrete with foamed asphalt.

This objective will be met after completion of the following six tasks:

1. Perform literature survey, and technology and research scan.
2. Perform mechanistic sensitivity analysis.
3. Undertake assessment of Caltrans projects built to date based on available data.
4. Measure properties on Caltrans Full-Depth Pavement Reclamation with foamed asphalt projects to be built in the future.
5. Carry out laboratory testing to identify specimen preparation and test methods, and develop information for mix design, structural design, and construction guidelines.
6. Prepare interim guidelines for project selection, mix design, structural design, and construction.

This document covers Tasks 1 through 5.

ACKNOWLEDGMENTS

The University of California Pavement Research Center acknowledges the following individuals and organizations who shared experiences and/or provided assistance, information, documentation, or materials:

- The staff of the UCPRC laboratory who assisted with the preparation and testing of materials during the laboratory study
- Mr. Joseph Peterson and Ms. Julia Rockenstein, Caltrans
- Ms. Dawn Becky, Caltrans
- Staff from the Caltrans Colusa, Sierraville, and New Cuyama Maintenance Stations
- Prof. Kim Jenkins, University of Stellenbosch, South Africa
- Mr. Dave Collings, A.A. Loudon Consulting Engineers, South Africa
- Prof. Mofreh Saleh, University of Canterbury, New Zealand
- Mr. Hechter Theyse, Council for Scientific and Industrial Research, South Africa
- Mr. Panos Kokkas, Ms. Oleysa Tribukait and Ms. Darlene Comingor, County of Yolo, Department of Planning and Public Works
- Mr. John Rainey, Rainey Geotechnical
- The staff of Western Stabilization
- The staff of Durham Construction
- Shell, Paramount, and Valero refineries
- Graniterock Company and Granite Construction

EXECUTIVE SUMMARY

A comprehensive study on full-depth reclamation with foamed asphalt has been completed for the California Department of Transportation (Caltrans) by the University of California Pavement Research Center. The study, based on a series of work plans approved by Caltrans, included a literature review, a mechanistic sensitivity analysis of theoretical California pavement designs that incorporate foamed asphalt, bi-annual assessments of four full-depth reclamation with foamed asphalt projects, and a comprehensive, four-phase laboratory study. The project culminated in the preparation of interim guidelines for project selection, mix design, structural design, and construction (*Full-Depth Pavement Reclamation with Foamed Asphalt: Guidelines for Project Selection, Design and Construction*), which can be used in conjunction with the South African *Guidelines for the Design and Use of Foamed Bitumen Treated Materials* and the *Wirtgen Cold Recycling Manual.* The California guideline provides specific information for recycling thick asphalt pavements, and is based on the extensive laboratory testing program and the assessment of reclamation projects in the state.

A literature review of current practice revealed that, although considerable research has been carried out on the use of full-depth reclamation with foamed asphalt on pavements consisting of relatively thick granular layers and thin surface treatments, very little research had been carried out on full-depth reclamation of thick asphalt pavements with foamed asphalt (multiple overlays over a relatively weak base or subgrade). A mechanistic sensitivity analysis was therefore carried out to identify key variables in the design of recycled pavements consisting primarily of recycled thick asphalt pavement. The findings of the literature review and the sensitivity analysis were used to formulate a work plan for laboratory and field studies that would address the issues specific to recycling these thick asphalt pavements. A comprehensive write-up of the literature was not included in this report as similar reviews have been documented by other researchers.

A number of recently completed construction projects (03-COL-20, 05-SB,SLO-33, 07-Ven-33, 03-SIE-89) were visited, and construction on projects on state and county routes was observed. Large quantities of material for laboratory testing were collected from these projects. Visual assessments and Falling Weight Deflectometer (FWD) testing were carried out in the spring and fall each year during the course of the study. Key observations include:

- Some fatigue cracking was evident on sections of the 03-COL-20 (PM10.2/28.2, EA03-339004) project towards the end of the study, some eight years after construction. The project was considered a success by Caltrans, given that a design life equivalent to about five years of traffic was expected.

- On the 03-SIE-89 (PM20.0/29.6, EA03-0A7004) project, random areas of cracking (thermal and fatigue) were observed along the length of the road after about four years of trafficking. The cracks were sealed the following year. A microsurfacing was applied over the entire section as a pavement preservation intervention in 2008 (seven-years after construction).
- On the first Route-33 project constructed (05-SB,SLO-33-PM0.0/12.6, EA05-OA4004), severe distress in the form of alligator cracking and deformation was observed within 12 months after construction (2005) on a number of sections of the road. A forensic investigation attributed this distress to a combination of poor drainage (blocked culverts and filled-in side drains) and the incomplete drying of the recycled layer (studies have shown that foamed asphalt-treated layers only gain strength when the compaction moisture has dried back sufficiently). No active filler was used in this project, which may have also contributed to the poor initial strength. Areas of deformation continued to appear throughout the period of evaluation. FWD measurements indicated that these problems were all associated with weak subgrades and low base stiffness, and not with the surfacing.
- On the second Route 33 project (07-VEN-33-PM48.5/57.5, EA07-249304), constructed 12 months later in 2006, no distress was observed apart from some isolated cracking associated with slope instability. Construction was monitored and a number of concerns were noted with respect to the addition of water, quality control behind the recyclers, and the lack of attention given to drainage.
- FWD measurements on all of the sections indicated that the asphalt concrete layer stiffness was only influenced by temperature, with the values comparable between the different test subsections. Asphalt concrete stiffnesses on distressed and intact subsections on the same project were not significantly different. The moisture content in the pavement structure had a significant influence on the foamed asphalt layer stiffness, with differences as high as 40 percent between wet and dry seasons, which was of a higher relative magnitude than the seasonal variation of subgrade stiffness.
- The effects of temperature on foamed asphalt mix stiffness were quantified by field measurements. The average temperature sensitivity coefficient for the four sections on 03-COL-20 and 07-VEN-33 in Ventura County was 1.3 psi/°F (0.016 MPa/°C).

Heavy Vehicle Simulator (HVS) testing was carried out on one of the projects (Route 89); however, the test site was not representative of the mainline (or typical foamed asphalt pavements) and little useful information was gained. The HVS study is documented in a separate report.

A comprehensive laboratory investigation was carried out in four phases in conjunction with the field assessments. Although a comprehensive factorial design was prepared at the beginning of the study, it was clear that the number of tests required to complete the full factorial was impractical in terms of material

requirements and laboratory resources. A phased approach was therefore adopted, which entailed a series of small experiments based on a series of partial factorial experimental designs. By following this approach, researchers were able to gain an understanding of key issues influencing the performance of foamed asphalt mixes, and use the findings to adjust the testing program and relevant factorial elements to make the best use of resources. The testing was carried out on material sourced from two projects. This material consisted of predominantly recycled asphalt pavement (RAP) (± 90 percent) together with a small percentage (± 10 percent) of the natural aggregate from the underlying layer. The aggregates (RAP plus underlying layer) were of granitic origin and quartzitic origin for the two projects respectively, and although representative of a relatively large proportion of California, the results, specifically those pertaining to active and semi-active fillers, are not necessarily applicable for all materials found in the state. No recycling projects were undertaken on other representative aggregate types (e.g., basalt) during the UCPRC study and therefore tests with these materials could not be undertaken. The phases included:

- Phase 1 included specimen preparation procedures, test methods, and the development and assessment of analysis techniques. These formed the basis for testing in the later phases of the study. Foamability characteristics of a selection of California asphalts, and the temperature sensitivity of mixes were also assessed in this phase. A method to visually evaluate the fracture faces of tested specimens in a consistent way was developed in addition to these assessments.
- Phase 2 covered investigations into the effects of asphalt binder properties, recycled asphalt pavement (RAP) sources, RAP gradations, mixing moisture content, and mixing temperature on foamed asphalt mix properties. It also investigated different laboratory test methods for assessing the strength and stiffness characteristics of foamed asphalt mixes, and the development of an anisotropic model relating laboratory stiffness tests to field stress states. This work was performed on specimens without active or semi-active fillers so that the effects of the asphalt alone could be evaluated.
- Phase 3 extended the objectives of Phase 2 with more detailed investigations on variables related to RAP sources and asphalt binder characteristics.
- Phase 4 focused on the role and effects of active, semi-active, and inert fillers on foamed asphalt mix performance, as well as issues pertaining to curing.

The findings of the laboratory study identified a number of key issues that have been incorporated into the mix design guideline. These include appropriate test methods for California, preparation of specimens (mixing moisture content and aggregate temperature), asphalt binder selection, target asphalt and active filler contents, aggregate gradations (fines content), specimen curing, and the interpretation of results.

Based on field and laboratory results, a small analysis was carried out to determine appropriate gravel factors for foamed asphalt-treated materials. Assuming a mix design of 3.0 percent foamed asphalt and between 1.0 and 2.0 percent portland cement for the foamed asphalt base, as well as a period of curing, a Gravel Factor of 1.4 is recommended as an interim for designing foamed asphalt-treated pavements in California, until additional information from long-term field studies is obtained. This is based on a range of between 1.32 and 1.47 for wet and dry seasons, respectively.

The study concluded that full-depth reclamation with foamed asphalt combined with a cementitious filler is an appropriate pavement rehabilitation option for California. Projects should be carefully selected with special care being given to roadside drainage. Appropriate mix and structural design procedures should be followed, and construction should be strictly controlled to ensure that optimal performance and life is obtained from the pavement. Premature failures will in most instances be attributed to poor project selection (e.g., weak subgrades and/or poor drainage), or poor construction (e.g., poor asphalt dispersion, incorrect mixing moisture content, poor compaction, and poor surface finish).

The following recommendations are made:

- Full-depth reclamation with foamed asphalt combined with a cementitious filler should be considered as a rehabilitation option on thick, cracked asphalt pavements on highways with an annual average daily traffic volume not exceeding 20,000 vehicles per day, provided that an appropriate pavement design can be achieved. The technology is particularly suited to pavements where multiple overlays have been placed over a relatively weak base course layer, and where cracks reflect through the overlay in a relatively short time. Higher traffic volumes can be considered provided that adequate strength and durability can be achieved with the in-place materials. Alternatively, the recycled layer can be used as a subbase underneath a new base layer.
- Project selection, mix design, and construction should be strictly controlled to ensure that optimal performance is obtained from the rehabilitated roadway.
- Full-depth reclamation with asphalt emulsions and partial-depth reclamation with asphalt emulsions and foamed asphalt should also be evaluated, and guidelines prepared for choosing the most appropriate technology for a given set of circumstances.

TABLE OF CONTENTS

LIST OF TABLES

LIST OF FIGURES

ABBREVIATIONS USED IN THE TEXT

CAL/APT	Caltrans Accelerated Pavement Testing
Caltrans	California Department of Transportation
CSB	Cemented subbase
CT	Computed Tomography (X-ray)
CTB	Cement-treated base
DISR	Deep in-situ recycling
DGAC	Dense-graded asphalt concrete
DSLR	Digital single-lens reflex camera
DCP	Dynamic Cone Penetrometer
ESAL	Equivalent Standard Axle Load
EKF	Extended Kalman Filter method
FWD	Falling Weight Deflectometer
FOBack	Finite element Open source Backcalculation
FFAC	Fracture Face Asphalt Coverage
FFIA	Fracture Face Image Analysis
FFRC	Free-Free Resonant Column (resilient modulus or test)
FDR	Full-depth recycling/pavement reclamation
GE	Gravel Equivalent
HVS	Heavy Vehicle Simulator
HMA	Hot-mix asphalt
ITS	Indirect Tensile Strength
LEAP2	Layered Elastic Analysis Program
LVDT	Linear Variable Displacement Transducer
MMC	Mixing moisture content
MDD	Multi-depth Deflectometer
OGAC	Open-graded asphalt concrete
OMC	Optimum moisture content
PPRC SPE 4.12	Partnered Pavement Research Center Strategic Plan Element 4.12
PM	Post mile
PMS	Pavement Management System
PG	Performance Grade binder
RAC-G	Rubberized asphalt concrete, gap-graded
RAC O	Rubberized asphalt concrete, open-graded
RAP	Reclaimed asphalt pavement
RMS	Root Mean Square
TSR	Tensile Strength Retained
UCS	Unconfined or Uniaxial Compressive Strength test
UCPRC	University of California Pavement Research Center

CONVERSION FACTORS

SI* (MODERN METRIC) CONVERSION FACTORS				
Symbol	**Convert From**	**Convert To**	**Symbol**	**Conversion**
LENGTH				
mm	millimeters	inches	in	mm x 0.039
m	meters	feet	ft	m x 3.28
km	kilometers	mile	mile	km x 1.609
AREA				
mm^2	square millimeters	square inches	in^2	mm^2 x 0.0016
m^2	square meters	square feet	ft^2	m^2 x 10.764
VOLUME				
m^3	cubic meters	cubic feet	ft^3	m^3 x 35.314
MASS				
kg	kilograms	pounds	lb	kg x 2.202
TEMPERATURE (exact degrees)				
C	Celsius	Fahrenheit	F	°C x 1.8 + 32
FORCE and PRESSURE or STRESS				
N	newtons	poundforce	lbf	N x 0.225
kPa	kilopascals	poundforce/square inch	lbf/in^2	kPa x 0.145

*SI is the symbol for the International System of Units. Appropriate rounding should be made to comply with Section 4 of ASTM E380. (Revised March 2003)

1. INTRODUCTION

1.1 Background

Full-depth reclamation/recycling (FDR), or deep in-situ recycling (DISR), of damaged asphalt concrete pavement with foamed asphalt to provide a stabilized base for a new asphalt concrete wearing course is a pavement rehabilitation strategy of increasing interest worldwide. It offers a rapid rehabilitation process, with minimal disruption to traffic. Most importantly, it reuses aggregates in the pavement, thereby minimizing the environmental impacts associated with extraction and transport of new aggregates.

In March 2000 the technology was presented to California Department of Transportation (Caltrans) pavement engineers at the South African Pavement Technology Workshop, which was held at the University of California Pavement Research Center (UCPRC) facilities in Richmond (UC Berkeley), as part of the Caltrans Accelerated Pavement Testing (CAL/APT) contract. Caltrans built its first project with this technology soon after (a 10 mile [16 km] pilot study on Route 20 in Colusa County). Caltrans also approved a UCPRC study to investigate the use of the technology under California material, traffic, and environmental conditions.

Most Caltrans FDR projects are performed on pavements with thick, cracked asphalt concrete layers, which distinguishes California practice from that of other states and countries investigating and using this technology. Pavement technology in South Africa and Australia typically relies on good quality granular material or cement-treated base and subbase layers for the primary load-carrying capacity of the pavement, with the thin asphalt concrete (<2.0 in. [50 mm]) or aggregate surface treatment layers (chip seals) providing little or no structural integrity. Consequently, in those countries the recycled material consists mostly of recycled natural aggregate and cracked cement-stabilized layers, which is accordingly reflected in their research and experience. Practice in Europe has been intermediate between that of California and South Africa, with the recycled material generally consisting of a mix of asphalt bound and natural aggregate materials.

1.2 Project Objectives

The research presented in this report is part of Partnered Pavement Research Center Strategic Plan Element 4.12 (PPRC SPE 4.12), titled "Development of Mix and Structural Design and Construction Guidelines for Full-Depth Reclamation (FDR) of Cracked Asphalt Concrete as Stabilized or Unstabilized Bases" being undertaken for Caltrans by the UCPRC. The objective of the study is to adapt, modify, and

improve existing mix design, structural design, and construction guidelines for full-depth reclamation (FDR) of cracked asphalt concrete with foamed asphalt to suit California conditions.

1.3 Overall Project Organization

This UCPRC project is a comprehensive study, carried out in a series of phases, involving the following primary elements *(1)*:

- Phase 1
  - Literature review, and technology and research scan.
  - Mechanistic sensitivity analysis.
- Phase 2
  - Assessment of Caltrans projects built to date based on field monitoring and previously collected data.
  - Accelerated Pavement Testing (Heavy Vehicle Simulator [HVS]) experiment.
  - Assessment of planned Caltrans projects prior to construction.
- Phase 3
  - Laboratory testing to identify specimen preparation and test methods, and develop information for mix design, structural design, and construction guidelines.
- Phase 4
  - Project selection, mix design, structural design, and construction guidelines.

Deliverables

The reports prepared during this study document background studies, data from construction, HVS tests, laboratory tests, subsequent analyses, and recommendations. On completion of the study this suite of documents will include:

- One first-level report covering the HVS study on Route 89;
- One detailed research report (this document) detailing the various tasks completed in the study;
- One guideline documenting project selection, mix design, structural design, and construction procedures; and
- One four-page summary report and one longer, more detailed summary report capturing the entire study's conclusions.

A series of conference and journal papers documenting various components of the study have also been prepared.

1.4 Structure and Content of this Report

This report presents an overview of the work carried out to meet the objectives of the study, and is organized as follows:

- Chapter 2 provides a summary of the literature.
- Chapter 3 presents findings of the mechanistic sensitivity analysis, which provided direction for subsequent laboratory testing and structural design considerations.
- Chapter 4 summarizes the bi-annual visual and Falling Weight Deflectometer assessments on four FDR projects in California.
- Chapter 5 introduces the laboratory study.
- Chapter 6 covers the first phase of laboratory testing, which familiarized the research team with the equipment, procedures, and test methods, and provided a basic understanding of the attributes of typical California foamed asphalt mixes.
- Chapter 7 summarizes the second phase of laboratory testing, which included investigations into:
  - The effects of asphalt binder properties, recycled asphalt pavement (RAP) sources, RAP gradations, and mixing moisture content on foamed asphalt mix properties;
  - Assessment of different laboratory test methods for measuring the strength and stiffness characteristics of foamed asphalt mixes; and
  - Development of an anisotropic model relating laboratory stiffness tests to field stress states.
- Chapter 8 provides an overview of Phase 3 of the laboratory study, which extended the objectives of Phase 2 with more detailed investigations on variables related to RAP sources and asphalt binder characteristics.
- Chapter 9 details the final phase of laboratory testing, which focused on the role and effects of active fillers and curing procedures.
- Chapter 10 summarizes the derivation of a recommended Gravel Factor for foamed asphalt-treated layers.
- Chapter 11 summarizes key issues for consideration in the guideline documentation.
- Chapter 12 provides conclusions and recommendations.

1.5 Terminology

A variety of terms are used for describing the recycling of pavements, including but not limited to full-depth recycling or reclamation, partial-depth recycling or reclamation, deep in-situ recycling, cold in-place recycling (cold foam recycling/reclamation), and hot in-place recycling. In this document, the terms "full-depth reclamation," abbreviated as FDR, and "full-depth reclamation with foamed asphalt," abbreviated as FDR-foamed asphalt or FDR-FA are used throughout.

1.6 Measurement Units

Use of metric units was Caltrans practice when this project was begun, and during much of its execution. Metric units have always been used by the UCPRC in the design and layout of HVS test tracks, and for laboratory and field measurements and data storage. Caltrans has recently returned to the use of U.S. standard units. In this report, English metric and units (provided in parentheses after the English units) are provided in general discussion. In keeping with convention, only metric units are used in laboratory and field data analyses. A conversion table is provided on Page iv at the beginning of this report.

2. LITERATURE SURVEY

2.1 Introduction

Comprehensive literature surveys on full-depth pavement reclamation with foamed asphalt (FDR-foamed asphalt) have been undertaken by a number of practitioners *(2-5)*. Another similar general review was considered unnecessary. Instead, a review of new literature on key issues pertaining to the University of California Pavement Research Center (UCPRC) work plan was carried out, summarizing the basic conclusions of previous research and the conditions under which those conclusions were drawn. Gaps between current understanding and actual performance observation were identified, together with research needs for application of the technology under California conditions. Although foamed asphalt stabilization can be used in both in-place full-depth reclamation (FDR) and in plant mixes, only the former is considered in this study.

Soil stabilization with foamed asphalt (or bitumen as it is referred to in the literature elsewhere) is a relatively old technology, but has had limited application until recently due to patent restrictions and a lack of suitable application equipment. Recently, developments in full-depth reclamation equipment, more stringent environmental and traffic delay concerns, and expiration of the patent has led to increasing interest in the technology. Recent research and implementation was mostly undertaken in South Africa and Australia, but a number of states in the U.S. and some European and Asian counties are now also implementing the technology and reporting on research. The technology was presented to Caltrans pavement engineers by the UCPRC at a South African Pavement Technology Workshop in 2000. Since then, the technology has been investigated as a means to recycle cracked asphalt pavement into a stabilized base, thereby eliminating reflective cracking associated with overlay rehabilitation technologies, and reducing the quantities of aggregate and the length of construction periods associated with conventional reconstruction procedures. FDR-foamed asphalt generally also permits placement of the asphalt overlay after recycling faster than do current FDR technologies using cement and standard asphalt emulsions. Although extensive state-of-the-practice reviews have been carried out *(4,5)* and relatively comprehensive guidelines *(3,6)* are available, these are mostly applicable to reclamation of relatively thin asphalt surfacings over thicker granular or lightly cemented bases. Only limited published research is available on the use of the technology in recycling thick, cracked asphalt pavements.

2.2 Background

Asphalt or bitumen foaming is a process in which a small quantity of water is injected into hot asphalt, temporarily transforming it to foam. The viscosity of the asphalt is greatly reduced, facilitating easy mixing with aggregates or recycled asphalt pavement (RAP) at ambient temperature. The foaming process is accomplished in a specially designed expansion chamber after which it is injected from nozzles onto the loose aggregate. The bubbles break down after a period lasting between a few seconds up to 60 seconds (depending on the properties of the asphalt, and ambient and aggregate temperatures) after which the binder returns to its original state.

The technology was first developed at Iowa State University in 1956 by Professor Ladis Csanyi while researching the viscosity of asphalt binders and the effects of steam injection on this property. Mobil Oil Australia acquired the patent rights in 1968, and improved the process by using water at ambient temperature rather than steam, thus making this process more practical for field application.

Foamed asphalt stabilization differs from asphalt emulsion stabilization in a number of ways. Particle coating differs in that foamed asphalt tends to coat the smaller aggregate particles and fines (smaller than 0.08 in. [2.0 mm]) forming a mastic that adheres to larger particles, whereas asphalt emulsion tends to coat the larger particles, to which the uncoated fine particles adhere. The strength, stiffness, and water susceptibility of these two mixes are reportedly similar if the parent aggregates, asphalt content, and active filler content are all the same *(7)*. However, foamed asphalt has been favored in the past due to shorter curing times and resultant earlier opening to traffic linked to the lower water contents in foamed asphalt stabilization compared to those in emulsion treatments. Ramanujam and Jones *(8)* reported that foamed asphalt-treated sections performed better than emulsion-treated sections, which became slick and showed signs of permanent deformation after rain during construction and prior to sealing. Recent developments in emulsion technology have apparently addressed some of the past limitations, although limited published information is available.

Active (portland cement, lime) and/or inert (fly ash, mineral fines) fillers are usually added to foamed asphalt mixes to improve certain properties, including workability, stiffness, and strength, or to reduce moisture sensitivity. The behavior of the mix will depend on the application rate of the filler and the asphalt binder content (Figure 2.1), and appropriate choices need to be made depending on the desired result. In California, FDR will primarily be used to rehabilitate cracked pavements and to counter the effects of reflective cracking from lower layers (original asphalt concrete wearing course and overlays and/or cement treated bases). Different combinations of asphalt binder and filler will result in a base with properties similar to unbound granular materials (very low binder and filler contents), cemented materials

(low binder and high active filler content), or asphaltic materials (high binder and low active filler content).

2.2.1 Unbound Granular Materials

If the pavement is recycled and compacted without the addition of foamed asphalt or active filler, the new base will behave in a similar manner to one constructed with conventional granular materials. Although the binder in the original asphalt concrete may provide some cementation, the stabilizing effect will be limited because of extensive aging and inconsistent distribution through the new layer. A base constructed with this material is unlikely to crack, but thicker hot-mix asphalt (HMA) surfacings may be necessary to prevent permanent deformation and/or fatigue associated with lower strength and stiffness of the unbound materials. The savings on asphalt binder and cement costs are generally insignificant compared to the high cost of thicker HMA surfacings.

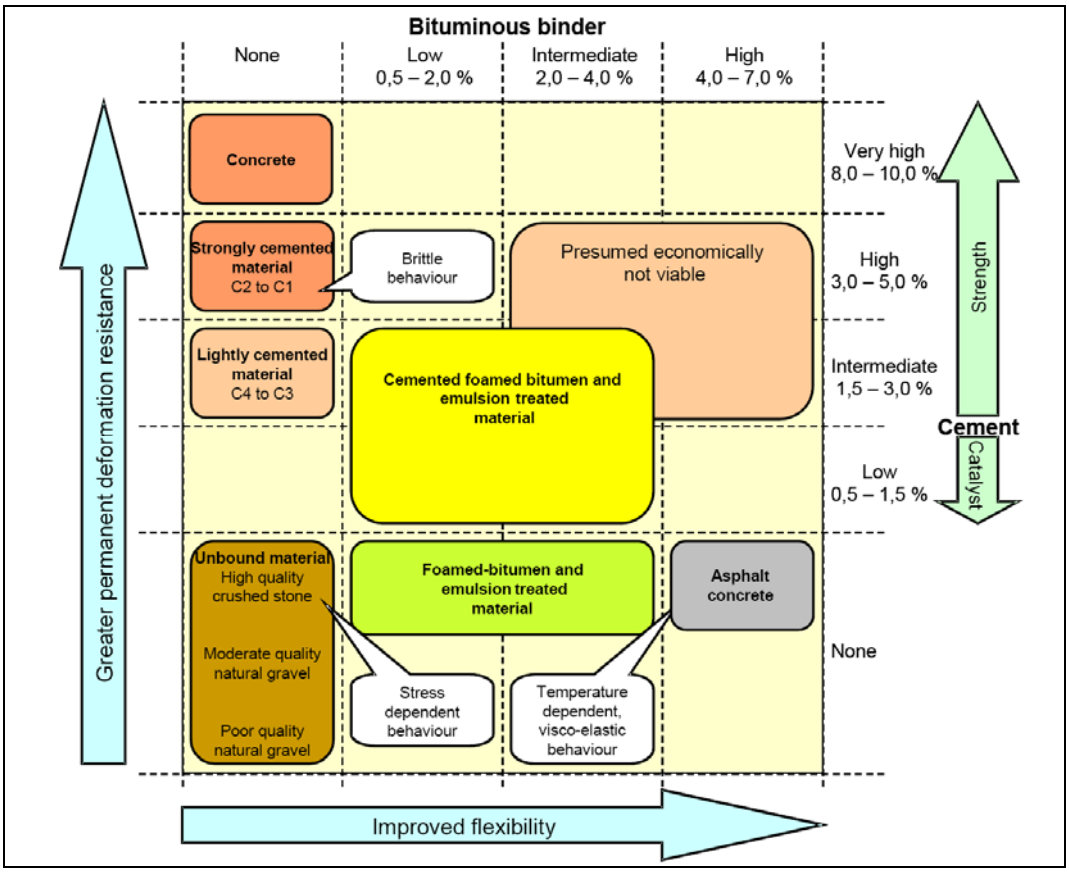

Figure 2.1: Matrix of the basic characteristics of road-building materials. ***(9)***

2.2.2 Cemented Materials

When higher percentages of cement (more than 2.0 percent) and moderate amounts of foamed asphalt (less than 2.0 percent) are mixed with the RAP, the properties of the treated material will be similar to

those of conventional cement-treated materials. Increasing cement contents correspond to decreasing stress dependency and moisture susceptibility. However, higher cement contents result in materials that typically have high stiffness (resilient modulus) and tensile strength, but are prone to shrinkage, which may induce cracking. Lower flexibility can also lead to early fatigue cracking. Although, these shrinkage and fatigue cracks are often discrete, with the cemented material between cracks retaining considerable stiffness and strength, they tend to eventually reflect through the HMA surfacing, which will require some form of overlay at a relatively early stage. Elimination of reflection cracking is one of the goals of FDR.

2.2.3 Asphaltic Materials

Higher asphalt contents (higher than 4.0 percent) with lower cement contents (less than 2.0 percent) result in materials with lower stress dependency, little or no shrinkage, and improved fatigue life. However, these materials are subject to permanent deformation and more rapid fatigue damage of the HMA surfacing resulting from the relatively high tensile strains associated with the low stiffness of the recycled base. They are also more sensitive to temperature change.

2.3 Foamed Asphalt Properties of Interest

The performance of a foamed asphalt base is dependent on a number of properties. These need to be understood in order to ensure that mix-designs are optimal and that construction procedures are adjusted appropriately. Issues and properties of interest in the UCPRC study include:

- Preparation of representative laboratory specimens (Sections 6.3, 8.3, and 9.11)
- Moisture sensitivity and testing under unsoaked and soaked conditions (Section 6.3)
- Foaming properties of the asphalt binder (Sections 6.4)
- Temperature sensitivity of foam asphalt-treated materials (Section 6.5)
- Influence of mixing moisture content on foam asphalt distribution (Section 7.5)
- Strength of foamed asphalt mixes (Section 7.3 and Chapters 8 and 9)
- Stiffness and fatigue properties of foamed asphalt mixes (Sections 7.4 and 9.7)
- Influence of fines content on mix performance (Sections 8.4 and 9.4)
- Influence of asphalt source on mix performance (Section 8.5)
- Influence of different active fillers on mix performance (Section 9.6)
- Cracking properties (Section 9.9)

2.4 Structural Design

The most complete structural design guides for pavement structures with foamed asphalt are published in the South African *Interim Technical Guideline: The Design and Use of Foamed Bitumen Treated*

Materials (3) and the *Wirtgen Cold Recycling Manual (6)*. Empirical design charts and mechanistic-empirical design guides and equations are provided in those documents. The design equations and charts in the South Africa guideline were developed based on mechanistic-empirical principles and calibrated with results from one South African HVS test *(10)* and later updated with results from a second HVS test on a different recycled roadway *(11)*. The design guides in the Wirtgen manual are based on a combination of South African HVS testing and laboratory and field performance, as well as international laboratory and field studies.

Limited unpublished research on determining Gravel Equivalent values for foamed asphalt-treated materials has been carried out by Caltrans.

2.4.1 South African Guidelines

The South African guideline offers two approaches to the structural design of pavements with foamed asphalt, namely a catalog (lower volume roads and lower reliability) and a mechanistic-empirical approach (higher volume roads and higher reliability).

In the mechanistic-empirical approach, the service life of the foamed asphalt-treated base is divided into two phases. In the first phase, termed the "effective fatigue phase," the stiffness of the treated base decreases under repetitive loading from a high initial value until a stiffness value similar to the parent aggregate is reached. The number of load repetitions required to reach this state is termed the "effective fatigue life." The stiffness reduction is attributed to the breaking down of the cohesive bonds. Thereafter, the stiffness remains relatively constant in a phase termed "equivalent granular state." In later research, these three terms were renamed to "constant stiffness state," "stiffness reduction phase," and "Phase-1 life" *(11)* in order to equate performance of foamed asphalt bases with that of cement-treated bases in line with terminology used in the South African mechanistic pavement design analysis method *(12)*. The Phase-1 life is believed to be related to the ratio of maximum principal strain to the strain-at-break of the treated material in a flexural beam strength test and can be expressed as follows (Equation 2.1):

$$N_{eff} = a\left(SR_{\varepsilon}\right)^{b} \tag{2.1}$$

where:
- N_{eff} = phase 1 fatigue life;
- SR = strain ratio, where $SR_{\varepsilon} = \varepsilon/\varepsilon_b$;
- ε = the maximum tensile strain at the bottom of the layer;
- ε_b = the strain-at-break from laboratory flexural beam tests;
- a, b = regression constants.

In the following "constant stiffness phase," the development of fatigue cracking in the HMA surfacing will be accelerated due to the reduced base stiffness. Confinement of the underlying layers will also be

reduced. The critical failure mode in this phase is permanent deformation (rutting), believed to be related to load repetition, relative density, stress ratio, and the ratio of cement and asphalt contents. Permanent deformation equations from the South African guidelines and later updates are shown in Equations 2.2 and 2.3:

$$N_{PD,FB} = \frac{1}{30} 10^{[C_1 + C_2 RD + C_3 PS - C_4 SR + C_5 (cem/bit)]} \quad (2.2)$$

where: $N_{PD,FB}$ = structural capacity (load repetitions);
RD = relative density;
PS = plastic strain (%);
SR = stress ratio;
cem/bit = ratio of cement and asphalt contents (%);
C_1- C_5 = regression constants.

$$\log N = c_1 + SR^3 (c_2 + c_3 CEM + c_4 BIN^2) + c_5 RD + c_6 SAT + c_7 PS + c_8 CEM \quad (2.3)$$

where: N = load repetitions;
CEM = cement content (%);
BIN = asphalt binder content (%);
SAT = saturation level (%);
C_1- C_8 = regression constants.

A major shortcoming of the South African guideline equations is the limited calibration with field performance *(10,13)*. The structures on which the models were calibrated represent only two structure types. In both calibration projects, recycled materials were aggregate and cement-treated aggregate respectively, with very little RAP from the thin surface treatments. After recycling, the roads were again surfaced with chip seals that did not contribute to the structural integrity of the roads. In California, the pavement structures typically selected for recycling with foamed asphalt will have multiple layers of asphalt materials (up to 8.0 in. [200 mm] and thicker) and will be surfaced after recycling with at least 2.0 in. (50 mm) of HMA. Therefore, in typical South African projects, shear failure at the top of the treated base will be a more critical failure mode than fatigue (tension) at the bottom of the layer, and hence the failure mechanisms assumed in the South African guidelines and the transfer functions based on them are probably not appropriate for California applications.

The mix designs of the treated materials in the two projects were also similar, with the first having 1.8 percent residual binder and 2.0 percent cement, and the second 2.3 percent residual binder and 1.0 percent cement. These materials would be classified as FB2 (UCS of 1,400 to 2,000 kPa and ITS of 100 to 300 kPa [UCS of 200 to 290 psi and ITS of 15 to 45 psi]) or FB3 (UCS of 700 to 1,400 kPa and ITS of 300 to 500 kPa [UCS of 100 to 200 psi and ITS of 44 to 73 psi]) in the South African guideline. The models were not calibrated against projects with stronger FB1 (UCS of 1,400 to 2,000 kPa and ITS of 300 to 500 kPa) materials.

An extensive study by Collings, et al. *(14)* on a nine-year-old road recycled with foamed asphalt indicated considerable inconsistency between actual performance and that predicted by the method in the guideline. No significant resilient modulus reduction was observed, and after nine years there was no substantial difference in the stiffness of two identical structures that had significantly different traffic and loading histories.

The South African structural design method for foamed asphalt-treated layers is currently being rewritten based on additional research carried out since the original guideline was prepared.

2.4.2 Wirtgen Manual

The Wirtgen manual provides three approaches for structural design, namely structural numbers, mechanistic-empirical, and stress ratio limits. Choice of method is linked to traffic and required reliability. The structural number approach is based on the *AASHTO Guide for the Design of Pavement Structures (15)*, while the mechanistic empirical approach is based on the South African guideline.

The stress ratio limit approach was developed by Jenkins *(4)* and is based on research performed at the Delft University of Technology. This research showed that when a granular material in a pavement structure is subjected to loading, the ratio of the maximum deviator stresses induced in the granular layer relative to the strength of that material (i.e., the stress ratio) will determine the rate of permanent deformation or rutting. Similar findings have been found in a number of other research projects around the world. Jenkins found that this deviator stress ratio should be limited to between 0.40 and 0.45 for foamed asphalt materials in order to ensure satisfactory material performance. The method is described in the Wirtgen manual *(6)*.

2.5 Life-Cycle Costs

The determination of accurate life-cycle costs and cost-benefits of recycling pavements with foamed asphalt as an alternative to more conventional techniques (overlay or reconstruction) is difficult given that there is very little documented long-term performance data for foamed asphalt treated roads available. Therefore, only scenarios based on estimated lives and failure modes can be used to obtain an indication of the potential benefits.

3. MECHANISTIC SENSITIVITY ANALYSIS

3.1 Introduction

The designs of full-depth foamed asphalt recycled pavements in California to date have been largely empirical and based on a visual survey of the road, coring, test pits, and laboratory testing focused on Indirect Tensile Strength (ITS) and R-value tests. The results have been used to determine the depth of recycling and to prepare a mix design. Mix designs have typically required between 2.0 percent and 3.0 percent foamed asphalt and between 1.0 percent and 1.5 percent portland cement or other active filler. Design lives have typically been calculated for five years due to a lack of reliable performance prediction models and limited practical experience. The first Caltrans full-depth reclamation with foamed asphalt (FDR-foamed asphalt) section on State Highway 20 in Colusa County built in 2000 exceeded this design life without the development of any significant distress, indicating that current performance expectations may be somewhat conservative. However, other projects with design lives of ten years in California and in other states have shown significant early distresses, indicating knowledge gaps in the key issues influencing performance. A mechanistic sensitivity analysis was therefore included in the work plan for the University of California Pavement Research Center (UCPRC) study *(1)* to identify key properties affecting the expected performance of materials recycled with foamed asphalt, the expected distress mechanisms (failure modes), as well as the likely reasons for the variability of observed performance over time.

3.2 Objectives

The objectives of this part of the UCPRC study included:

- Identification of the key properties affecting expected performance of materials recycled with foamed asphalt,
- Identification of the expected distress mechanisms of materials recycled with foamed asphalt, and
- Preliminary estimation of the acceptable ranges of the properties of FDR-foamed asphalt materials for a range of typical Caltrans rehabilitation pavement structures.

These objectives were met by undertaking a mechanistic sensitivity analysis on a factorial of typical Caltrans pavement structures. The analysis included materials in the three overlapping classes of FDR-foamed asphalt materials, namely granular, cemented, and asphaltic materials, and was expected to identify gaps in the existing knowledge with regard to properties and existing performance models. A range of properties for each type of material were considered in the analysis, simulating the effects of

different mix designs, and using properties and performance models for existing similar materials. The following variables were included in the factorial in addition to the FDR-foamed asphalt mix variables:

- Stiffness of underlying layers,
- Thickness of the FDR-foamed asphalt layer, and
- Thickness and stiffness of the asphalt concrete surface layers.

This sensitivity analysis was carried out prior to the laboratory and field tests discussed in the following chapters, during which the key material properties identified were measured. The models used in this analysis were proposed by various researchers in the literature, but only very limited validation studies had been reported. The limitations of this preliminary sensitivity analysis should therefore be considered when interpreting its results.

3.3 Background

3.3.1 Roles of Foamed Asphalt and Active Fillers in Mix Properties

The asphalt binder and active filler (e.g., cement) contents are the two main variables in a foamed asphalt mix design. Depending on the quantities added, mixes from the same parent material may behave as a granular material (low asphalt and cement contents), a cemented material (higher cement content), or an asphalt-bound material (higher foamed asphalt content). Mixes in each category have different properties, are suited to different existing pavement conditions, and will have different inputs in the structural design (see Section 2.2).

Test results from comprehensive laboratory studies in South Africa *(16,17)* clearly demonstrated the roles of foamed asphalt and cement in the mix properties. In flexural beam tests, both the stiffness and flexural strength (stress-at-break) increased significantly with increasing cement content, but the flexibility (strain-at-break) was reduced. Conversely, flexibility was significantly improved by increasing the asphalt content, but stiffness was reduced. Based on these findings, fatigue of the foamed asphalt layer was incorporated as the primary distress mechanism in the South African design method *(3)*. The transfer function in the design model uses tensile strain at the bottom of the FDR-foamed asphalt layer as the critical response, which implies a "fatigue type" distress, with fatigue life a function of the material properties (fatigue resistance or flexibility) and the structural response under traffic load. Increasing the cement content reduces the tensile strain in the foamed asphalt layer by increasing stiffness at the expense of flexibility, while an increase in the asphalt content improves flexibility but may also increase strain by reducing stiffness. A trade-off between asphalt and cement content is therefore required to optimize the design, which will depend on the project parameters (e.g., recycling depth, percentages asphalt concrete and granular base recycled, quality of the subgrade, and local environmental characteristics), and the project constraints (e.g., budget and pavement profile requirement).

3.3.2 Transfer Functions

Balancing the stiffness and flexibility of the foamed asphalt layer to achieve maximum service life within certain constraints was the main focus of this sensitivity analysis. Fatigue of the foamed asphalt layer was the critical distress mode considered because the tensile strains in the asphalt concrete overlay are typically relatively small before the foamed asphalt layer has lost most of its stiffness under traffic loading. Additionally, the rutting of the subgrade was also considered since another important role of the foamed asphalt layer is to provide protection to the underlying layers. Transfer functions for fatigue in the foamed asphalt layer and rutting in the subgrade were selected as described below.

Foamed Asphalt Fatigue

The transfer function to calculate the "effective fatigue life" or "Phase-1 life" *(11)* suggested in the South African guideline is:

$$N_f = 10^{(a-b[\varepsilon_t/\varepsilon_b])} \quad (3.1)$$

where: N_f = effective fatigue life of foamed asphalt layer
ε_t = the maximum tensile strain at the bottom of the layer
ε_b = the strain-at-break from laboratory flexural beam test
a,b = regression coefficients related to a reliability requirement (e.g., for a South African Category B road where 90% reliability is required, a = 6.499 and b = 0.708).

This transfer function was developed in South Africa based on limited laboratory and HVS testing. Another more widely-used transfer function for fatigue life of conventional hot-mix asphalt (HMA) is shown in Equation 3.2 *(18)*.

$$N_f = 18.4(C)\left(4.325\times10^{-3}\left[\varepsilon_t\right]^{-3.291}\left|E^*\right|^{-0.854}\right) \quad (3.2)$$

where: C = a function of air voids and asphalt volume in HMA
$|E^*|$ = asphalt mixture stiffness modulus, in psi or kPa/6.894

These two transfer functions use the same response variable (maximum tensile strain ε_t) but different material property variables (ε_b or $|E^*|$). However, if it is considered that increasing the stiffness $|E^*|$ by adjusting the cement or asphalt contents usually decreases the flexibility (strain-at-break ε_b), then the basic idea is similar. Equation 3.2 was therefore modified for use in the sensitivity analysis as follows (Equation 3.3):

$$N_f = \alpha_0\left(\varepsilon_t\right)^{\alpha_1} E_{FA}^{\alpha_2} \quad (3.3)$$

where: E_{FA} = the stiffness or Young's modulus of the foamed asphalt mix
$\alpha_0, \alpha_1, \alpha_2$ = regression coefficients as functions of material properties $\alpha_0>0$, $\alpha_1, \alpha_2<0$

Equation 3.3 was considered more appropriate for use in the sensitivity analysis because E_{FA} is also an input parameter in a mechanistic analysis, while strain-at-break (ε_b) is not.

Subgrade Rutting

Equation 3.4 *(18)* was adopted for subgrade rutting in the sensitivity analysis.

$$N_r = \left(\frac{0.0105}{\varepsilon_v} \right)^{1/0.223} \quad (3.4)$$

where: N_r = rutting life (in terms of load repetition) of the pavement structure assuming minimal rutting of the asphalt concrete layer

ε_v = maximum vertical strain at the top of the layer (compressive is positive).

3.4 Sensitivity Analysis

3.4.1 Input Variables

Five structure scenarios that could potentially be used in California were analyzed with the foamed asphalt layer stiffness and thickness as the sensitivity analysis input variables (Figure 3.1 and Table 3.1). The values for the existing underlying layers (subgrade) and the new asphalt concrete wearing course overlay were fixed for this analysis. Structures A through D were combinations of stiff or soft subgrade, with or without aggregate subbase. Structure E had a cement-treated subbase layer under the existing asphalt concrete layer (this is an unlikely pavement structure in California, but was included for comparison purposes). The load was a single wheel with 40 kN (9,000 lb) vertical load and 700 kPa (100 psi) tire contact pressure. For structure type E, the cement-treated base (CTB) layer in the original pavement became the cemented subbase (CSB) layer after recycling.

The sensitivity coefficients of the tensile strain in the foamed asphalt layer and subgrade rutting life to the two variables in the structural design (stiffness and thickness of the foamed asphalt layer) were obtained by mechanistic analysis and regression.

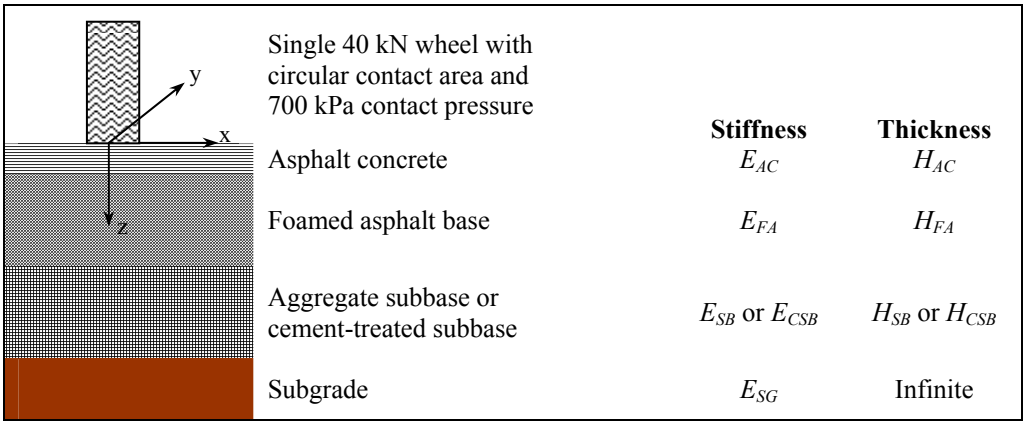

Figure 3.1: Assumed load and pavement structure.

Table 3.1: Mechanistic Analysis Parameters for Each Pavement Structure

Parameter	Structure				
	A	B	C	D	E
E_{AC} (MPa)	2,000	2,000	2,000	2,000	2,000
H_{AC} (mm)	50	50	50	50	50
E_{FA} (MPa)	Variable: 400 ~ 2,000				
H_{FA} (mm)	Variable: 150 ~ 300				
E_{SB} (MPa)	-	250 MPa	-	250 MPa	-
H_{SB} (mm)	-	250 mm	-	250 mm	-
E_{CSB} (MPa)	-	-	-	-	3,500 MPa
H_{CSB} (mm)	-	-	-	-	270 mm
E_{SG} (MPa)	100	100	60	60	100
Note: The Poisson's ratios for all the materials are assumed to be 0.35.					

3.4.2 Responses Under Loading

The strain responses under the assumed load were calculated using *LEAP2* (Layered Elastic Analysis Program *[19]*). Full bonding was assumed between all layers.

For Structures A through D, the horizontal strain at the bottom of the foamed asphalt layer immediately under the center of the load was the maximum first principal strain in this layer, which is consistent with the assumptions of Equation 3.2. Consequently this strain was used as ε_t in Equation 3.3.

For Structure E, the analysis was more complicated due to the presence of the stiffer cement-treated subbase layer under the foamed asphalt layer. Along the symmetry axis where x = 0 and y = 0, there is a local maximum value of the first principal strain at mid-depth of the foamed asphalt layer. The tensile strain at the bottom of the layer is relatively small since it is constrained by the cemented layer. The contours of the first principal strain within the asphalt concrete and foamed asphalt layers for a typical structure (with E_{FA} = 800 MPa (116 ksi) and H_{FA} = 200 mm [8 in.]) are shown in Figure 3.2, where this local maximum first principal strain is marked as $\varepsilon_{p,axis}$. This local maximum value was used as the critical tensile strain ε_t in Equation 3.3 for this scenario.

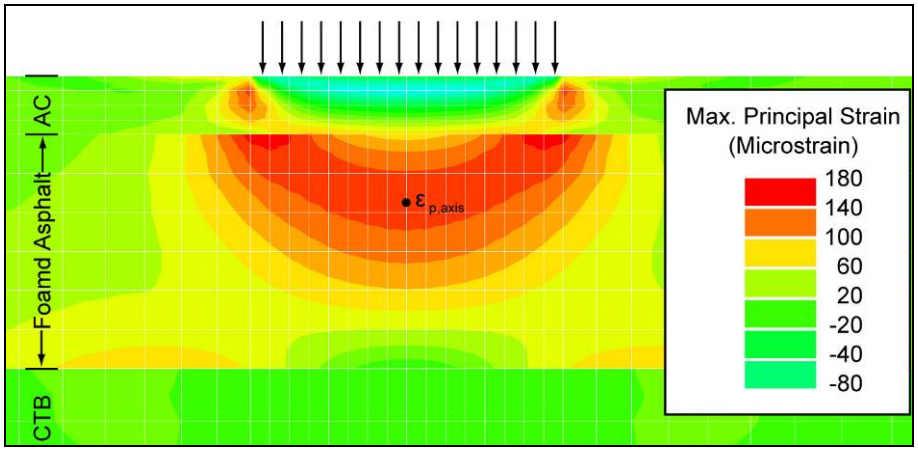

Figure 3.2: Contours of the first principal strain for a typical structure in Structure E.

3.4.3 Structural Response versus Layer Thickness and Stiffness

The effects of E_{FA} and H_{FA} on the output variables, tensile strain of the foamed asphalt layer, and the rutting life (calculated in equivalent standard axle loads [ESALs]) of the subgrade for Structure A are shown in Figure 3.3, which indicates that as stiffness and thickness of the foamed asphalt layer increase, the tensile strain in the foamed asphalt layer decreases and rutting life increases. The behavior of Structures A through D is similar in terms of the effects of E_{FA} and H_{FA} on the output variables.

3.4.4 Proposed Regression Model

Based on the above observations, the relation between the strain responses (or the life) and the foamed asphalt layer stiffness and thickness can be expressed by the following regression equation (Equation 3.5). The effects of E_{FA} and H_{FA} are different for Structure E, but the equation is still applicable.

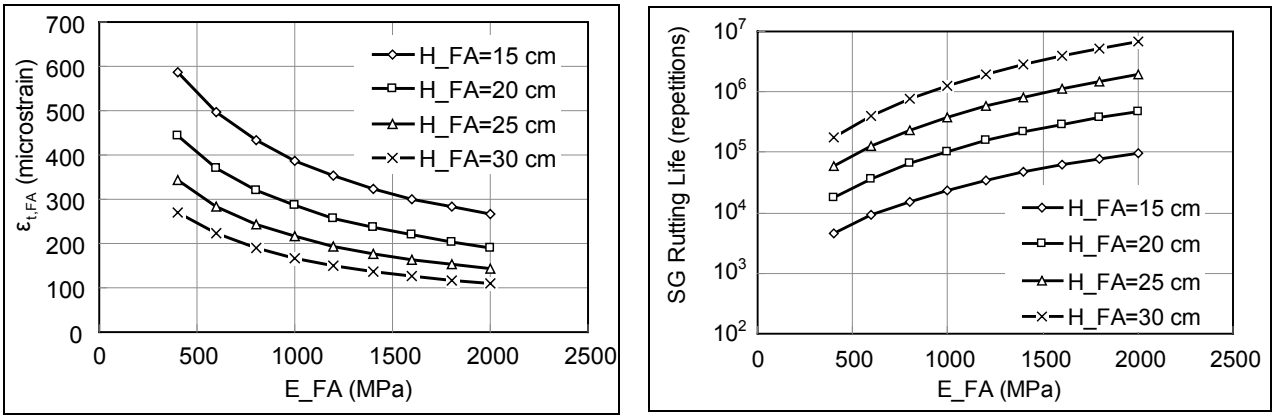

(a) Strain responses **(b) Subgrade rutting life**

Figure 3.3: Strain responses and subgrade rutting life of structures in Structure A.

$$\ln A(E_{FA}, H_{FA}) = \ln A_0 + \beta_1 \ln\left(\frac{H_{FA}}{H_{FA,0}}\right) + \beta_2 \ln\left(\frac{E_{FA}}{E_{FA,0}}\right) \quad (3.5)$$

where:
- $A(E_{FA}, H_{FA})$ = the response (the tensile strain at the bottom of the foamed asphalt or the rutting life of the structure)
- $E_{FA,0}$, $H_{FA,0}$ = the stiffness and the thickness of the foamed asphalt layer for a "standard" case (800 MPa and 20 mm in this study)
- A_0 = the tensile strain at the bottom of the foamed asphalt or rutting life for the "standard" case (i.e., $A_0 = A(E_{FA,0}, H_{FA,0})$
- β_1 β_2 = regression constants. These two constants can be regarded as "sensitivity coefficients." Each characterizes the sensitivity of the response to a variable. If H_{FA} is increased by 10%, the tensile strain will increase by $10\beta_1$%.

The sensitivity coefficients (β_1, β_2) of the tensile strain in the foamed asphalt layer and subgrade rutting life to the two structural design variables (stiffness and thickness of the foamed asphalt layer) were derived by mechanistic analysis and regression. The advantages of increasing the stiffness or flexibility for a given condition were determined by comparing the sensitivity coefficients and the constant in Equation 3.5.

The regression results for Equation 3.5 are shown in Table 3.2. The R^2 values for most cases are larger than 0.995 which indicates that Equation 3.5 is reasonable.

Table 3.2: Sensitivity Analysis Regression Results

Structure	$\varepsilon_{p.axis}$ or $\varepsilon_{t.FA}$ (microstrain)			$\varepsilon_{v,SG}$ (microstrain)			Rutting Life (Repetitions)		
	A_0	β_1	β_2	A_0	β_1	β_2	A_0	β_1	β_2
A	322	-1.22	-0.53	875	-1.29	-0.47	77,401	5.77	2.12
B	199	-1.12	-0.35	363	-0.94	-0.27	4,088,002	4.21	1.20
C	380	-1.26	-0.60	1,075	-1.33	-0.51	29,614	5.96	2.31
D	210	-1.10	-0.34	446	-0.96	-0.27	1,365,229	4.31	1.22
E	142	0.14	-1.11	141	-0.62	-0.20	253,235,912	2.80	0.91

The following observations were made from the regression results.

- For all cases, β_1 and β_2 for subgrade rutting life were always positive. Increasing the foamed asphalt stiffness or thickness always increased the rutting life due to the better protection provided to the subgrade. For the two scenarios without a subbase layer (Structures A and C), the rutting life for the standard case was relatively short. Doubling the foamed asphalt stiffness did not improve rutting life to an acceptable value and these results therefore indicate that the presence of a relatively stiff subbase is needed to protect the subgrade.
- The presence of a subbase layer under the foamed asphalt layer reduced the tensile strain in this layer by up to 40 percent for the standard cases (from 322 µstrain to 190 µstrain or from 380 µstrain to 210 µstrain). Conversely, the change of subgrade stiffness from 60 MPa to 100 MPa (8.7 to 14.5 ksi) with no subbase only reduced the tensile strain by 10 to 15 percent. This confirms the previous conclusion that a granular subbase layer under the foamed asphalt recycled layer is beneficial.
- For most scenarios β_1 was approximately three times larger than β_2. As an example, increasing the foamed asphalt thickness by 33 percent (from 6.0 in. to 8.0 in. [150 mm to 200 mm]) or doubling the foamed asphalt stiffness resulted in the same reduction of tensile strain in the foamed asphalt layer and increase in rutting life. An increase in the thickness of the foamed asphalt layer by 2.0 in. (50 mm) might be more appropriate in many instances, since increasing the stiffness would normally require an increase in the cement content. This decision would, however, depend on factors such as the comparative costs of increasing the recycled depth versus adding more cement, the consistency of recycling depth, and the potential for reduced fatigue resistance if the thicker foamed asphalt layer cannot be adequately compacted.
- For Structures A through D, the presence of an aggregate subbase reduced both β_1 and β_2, with much greater impact to β_2 compared to β_1. With a subbase present, increasing the foamed asphalt layer stiffness is much less effective than increasing the layer thickness.

- For Structure E, β_1 for $\varepsilon_{t,FA}$ was positive. This implies that increasing the thickness of the foamed asphalt layer will increase the tensile strain in this layer, which will decrease its fatigue life. The responses for the standard case and the two sensitivity coefficients are all much smaller than for the other four structures. The foamed asphalt layer in this structure prevents the propagation of reflection cracking from the cracked cement-treated subbase, and provides a uniform support to the asphalt concrete layer. Most of the structural capacity in the pavement is provided by the cemented subbase. Foamed asphalt bases with granular material properties (as opposed to asphaltic or cemented) would be sufficient for this structure.
- For Structure E, the calculated rutting life using Equation 3.4 was significantly higher than 50 million repetitions, which was beyond the range for which this equation was calibrated *(18)*. This implies that rutting in unbound layers is unlikely to occur in a structure with a thick cement-treated subbase (note that this structure was included for control purposes and is not typical in California).

Equation 3.3 can be rewritten to semiquantitatively consider the tradeoff between stiffness and flexibility on fatigue life of the foamed asphalt layer, as follows (Equation 3.6):

$$\ln N_f = \ln\alpha_0 + \ln\varepsilon_t + \alpha_2 \ln E_{FA} \tag{3.6}$$

If $A = \varepsilon_t$ and $A_0 = \varepsilon_{t,0}$, then substituting Equation 3.5 into Equation 3.6, results in (Equation 3.7):

$$\ln N_f = \ln\left(\alpha_0 \varepsilon_{t,0}^{\alpha_1} \left[\frac{H_{FA}}{H_{FA,0}} \right]^{\alpha_1\beta_1} E_{FA,0}^{-\alpha_1\beta_2} \right) + (\alpha_1\beta_2 + \alpha_2) \ln E_{FA} \tag{3.7}$$

where: $\alpha_1, \alpha_2, \beta_2 < 0$

The benefit in terms of increased fatigue life of the foamed asphalt layer by increasing its stiffness by adding more cement depends on the value of $(\alpha_1\beta_2 + \alpha_2)$. If the value is greater than zero, the treatment will be beneficial. It should be noted that the values of α_1 and α_2 may differ for different parent materials, different compaction levels, and even different cement contents.

3.4.5 Example

The following example uses test results from studies in South Africa *(16)*. These results are shown in Figure 3.4 which shows strain-at-break versus stiffness in flexural beam tests for the same parent material (ferricrete) with different cement and asphalt contents. Combining these data with Equation 3.3, which was developed in the same study, a new fatigue transfer function (Equation 3.8) can be derived in the same format as Equation 3.3.

$$N_f = 1.077 \times 10^{10} \left(\varepsilon_t\right)^{-1.23} E_{FA}^{-0.988} \quad (3.8)$$

where: ε_t = is the tensile strain in the foamed asphalt layer
E_{FA} = the stiffness of the foamed asphalt layer in MPa

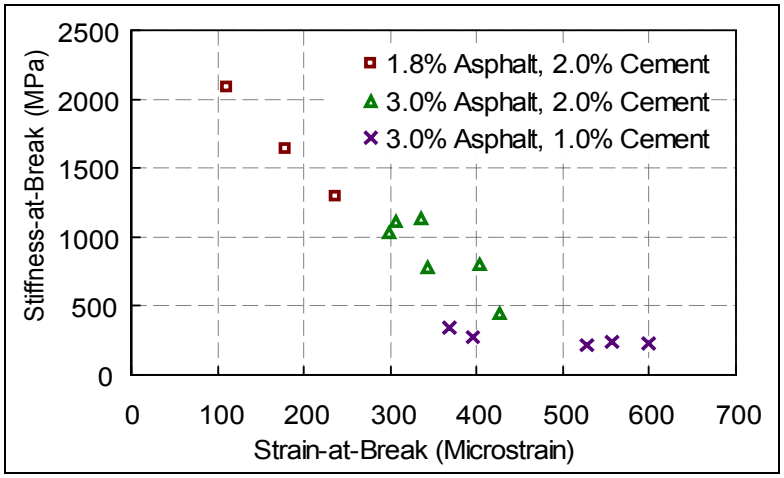

Figure 3.4: Typical relationship between strain-at-break and flexural stiffness.

When comparing Equation 3.8 with Equation 3.3, it can be seen that $\alpha_1 = -1.23$ and $\alpha_2 = -0.988$. For Structures A through D, $(\alpha_1\beta_2 + \alpha_2)$ was within the range of -0.57 to -0.25. Therefore flexibility of the foamed asphalt mix was more desirable than stiffness. Doubling the stiffness reduced the fatigue life by between 25 and 57 percent.

3.5 Summary of Observations

The findings indicated by the results of the sensitivity analysis can be summarized as follows:

- The presence of an aggregate or cement-treated subbase will have a significantly beneficial influence on the performance of an FDR-foamed asphalt-treated layer and asphalt concrete surfacing. Reduced life can be expected if the milling depth breaks through the existing aggregate or cement-treated base into the subgrade. Retaining a portion of the existing base layer should be considered when identifying candidate projects and preparing structural designs incorporating a foamed asphalt layer. On roads with thin existing aggregate base layers, consideration can be given to importing a layer of aggregate base material, spreading it on the surface to the desired thickness, and then incorporating it into the recycled layer in order to retain the existing base as a subbase in the new structure.
- Increasing the thickness of the recycled layer (i.e., increasing the recycling depth) will be beneficial, provided that adequate compaction can be achieved at the bottom of the layer.

- Foamed asphalt layer designs with lower binder and cement contents (i.e., similar behavior to granular materials) should only be considered for pavements with an underlying cement-treated subbase.
- Depending on certain structural and material characteristics, increasing foamed asphalt stiffness by adding cement can either reduce or increase the fatigue life of structures. A sensitivity analysis is necessary to determine whether flexibility or stiffness is more desirable for a specific structure.

4. ASSESSMENT OF PROJECTS BUILT TO DATE

4.1 Introduction

A number of full-depth reclamation (FDR)-foamed asphalt projects were carried out by Caltrans in various districts before and during the course of the University of California Pavement Research Center (UCPRC) study. Four of these projects were evaluated to gather information on project selection, construction, and long-term performance. A number of other projects undertaken by county and city authorities as well as projects in other countries were also assessed during the course of the UCPRC study. The following tasks were identified in the work plan for this work phase:

- Analyze the variability of measured as-built properties to determine ranges of values;
- Compare pavement performance for sections with different as-built properties within each project;
- Compare pavement performance between projects with different FDR-foamed asphalt mix designs, structural designs, traffic levels, and environmental conditions;
- Identify potential failure modes of FDR-foamed asphalt projects for environmental and traffic conditions in California;
- Relate field performance back to laboratory test results and performance predictions from mix and structural designs; and
- Determine whether FDR-foamed asphalt materials built to date have properties similar to those of cemented, asphalt-bound, or granular materials in terms of:
  - Sensitivity of stiffness to curing time, temperature, season, and load
  - Damage under traffic loading and environment
  - Permanent deformation

The work plan called for comprehensive visual assessments; Falling Weight Deflectometer (FWD), Dynamic Cone Penetrometer (DCP), and density measurements; and the periodic removal of cores for laboratory testing. Visual assessments and FWD measurements were undertaken biannually, however, the road closure programs did not allow for the other testing.

The four sections assessed were on Route 20, Route 33 (two projects), and Route 89. A Heavy Vehicle Simulator (HVS) experiment was also carried out on the Route 89 project.

4.1.1 Test Sections

Route 20, Colusa County (03-COL-20)

This 9.5 mile (15.3 km) project was the first FDR-foamed asphalt project undertaken by Caltrans and was constructed in 2001 between Postmile (PM) 10.2 and PM 19.7, prior to the start of the UCPRC study. The preconstruction assessment and construction activities were not observed. The project was first assessed in April 2006, and thereafter at approximately six-monthly intervals (spring and fall) up to the spring of 2008.

The project consisted of a two-lane highway partly traversing a mountainous cut-and-fill area (25 percent of the total length) and partly on a 0.5-to-1.3 ft (0.15-to-0.4 m) high embankment over flat Central Valley topography through agricultural lands. Subgrade soils in the valley portion of the road consist of silty/clay alluvial deposits. Prior to construction, the average two-way traffic was 6,200 vehicles per day, and the average annual equivalent standard axle load (ESAL) was 326,000 as estimated in 2000 *(20)*. Route-20 is one of the main routes connecting US-101 (and Route 1 on the coast) and Interstate 5 in the Central Valley.

The mix design proposed 2.5 percent AR-4000 asphalt binder (approximately equivalent to PG64-16) and 1.5 percent portland cement. The existing road had a long and complex maintenance history, and consequently the thickness of the asphalt concrete layer varied significantly along its length. The nominal foamed asphalt-treated base layer thickness was 9.0 in. (225 mm) and contained between 60 and 100 percent recycled asphalt pavement (RAP) and between zero and 40 percent of the original underlying granular base material. Indirect Tensile Strength (ITS) tests were carried out by Caltrans to determine the mix design. The average ITS values for the adopted mix design was 90 psi (612 kPa) for unsoaked (dry) specimens and 50 psi (347 kPa) for soaked specimens. After construction of the foamed asphalt-treated layer, the road was surfaced with 1.8 in. (45 mm) of dense-graded asphalt concrete (DGAC), and a 0.8 in. (20 mm) open-graded asphalt concrete (OGAC) friction course. The Caltrans Office of North Region Materials (Marysville, CA) compiled a report *(21)* entitled *Final Completion Report for Cold Foam in Place Reclamation Col-20 PM 10.2 – 28.2* in August 2006 that contains more detailed information about the project.

The average local annual precipitation for the city of Williams (on the eastern end of the section) is 16 in. (400 mm) (records from 1971–2000), 85 percent of which occurs between October and March.

Route 89, Sierra County (03-SIE-89)

This project covers a distance of 10 mile (16 km) between the intersection of Route 89 and Route 49, and the Sierra-Plumas County Line. The road is mostly in undulating/mountainous forest terrain. In 2002, the average two-way traffic was 1,550 vehicles per day, and the average annual equivalent standard axle load (ESAL) was 49,000 *(20)*. Traffic consists of a mix of heavy trucks (timber) and general traffic linking Interstate 80 with a number of small communities. Prior to reclamation, the road consisted of multiple layers of asphalt concrete on in situ weathered granite subgrade. The road had extensive thermal and fatigue cracking. The nominal existing asphalt concrete thickness for the FDR design was 6.0 in. (150 mm), although actual thickness varied as a result of repairs during the life of the road. ITS tests on foamed asphalt mixes were performed by Caltrans to determine the mix design. A foamed asphalt content of 2.5 percent of the dry aggregate mass and portland cement content of 1.0 percent was adopted as the mix design, which resulted in average unsoaked ITS values of 45 psi to 60 psi (300 kPa to 390 kPa), depending on the location of the test materials. Construction took place in the summer of 2002 with a nominal recycling depth of 8.0 in. (200 mm). The road was surfaced with 1.8 in. (45 mm) of dense-graded asphalt concrete.

The area through which the road traverses has warm, dry summers and cold winters, with temperatures below 32°F (0°C) common. Precipitation falls primarily in winter in the form of rain and snow. The average local annual precipitation for Sierraville, 5.0 mile (8.0 km) south of the section is 24 in. (620 mm) (records from 1948–2007), most of which falls between November and April. Annual average snowfall is 70 in. (1,775 mm), most of which falls between December and April.

Route 33, Santa Barbara/San Luis Obispo Counties (05-SB,SLO-33)

This 10.9 mile (17.5 km) Capital Maintenance Project is a two-lane highway between the junction of Route 33 and Route 166 and the Santa Barbara-Ventura County Line. Of the total length, 2.6 mile (4.2 km) is in San Luis Obispo County and the remainder in Santa Barbara County. The road traverses predominantly irrigated agricultural areas and overlies a fine silty subgrade material of sandstone origin. Prior to construction, the average two-way traffic was 1,000 vehicles per day, and the average annual equivalent standard axle load (ESAL) was 13,000 *(20)*. The traffic consists primarily of heavy trucks transporting local agriculture products and aggregates produced at two quarries. The road could potentially be used as an alternative route for Interstate 5 in the event of a prolonged closure. The road showed extensive, severe alligator and block cracking prior to rehabilitation. The nominal existing asphalt concrete thickness for the FDR design was 7.0 in. (175 mm). However, actual thickness varied between 4.3 in (110 mm) and 21 in (530 mm), attributed to repairs of subgrade-related failures over the life of the road. ITS tests on foamed asphalt mixes were performed by Caltrans to determine the mix design. A

foamed asphalt content of 3.0 percent of the dry aggregate mass with no active filler was adopted as the mix design, which resulted in average ITS values of 46 psi (314 kPa) for unsoaked (dry) specimens and 19 psi (131 kPa) for soaked specimens, considerably lower than those on other projects. Construction took place in the summer of 2005 with a nominal recycling depth of 9.0 in. (225 mm). The road was surfaced with 2.5 in. (60 mm) of RAC-G (gap-graded rubberized asphalt concrete) and 1.0 in.(25 mm) of RAC-O (open-graded rubberized asphalt concrete).

According to historical climate records of the nearest weather station (Cuyama), located at the northern end of the project, the average local annual precipitation is 6.0 in. (150 mm) (records between 1948 and 1973), 77 percent of which occurs between November and March.

Route 33, Ventura County (07-VEN-33)

This 9.0 mile (14.5 km) two-lane Capital Maintenance Project is located in the Cuyama Valley between PM 48.5 and PM 57.5, from Lockwood Valley Road to the Ventura-Santa Barbara County Line. The road traverses rolling terrain including cut-and-fill areas that are susceptible to landslides. The subgrade is primarily of weathered sandstone origin. The average two-way traffic in 2002 was 360 vehicles per day, and the average annual equivalent standard axle load (ESAL) was 7,000 *(20)*. This is considered a low traffic volume road but it could potentially be used as an alternative route for Interstate 5 in the event of a prolonged closure.

Prior to rehabilitation, the road showed extensive and severe alligator and block cracking (see Section 4.4.4). This road was rehabilitated in the summer of 2006. The mix design called for a recycling depth of 8.0 in.(200 mm) with the addition of 2.8 percent foamed asphalt and 2.0 percent cement kiln dust, covered by a 1.8 in. (45 mm) dense-graded asphalt concrete wearing course. The nominal existing asphalt concrete thickness for the FDR design was 6.0 in. (150 mm), however, actual thickness varied between 6.0 in. (150 mm) and 22 in. (550 mm), with variation attributed to repairs of subgrade-related failures over the life of the road.

According to historical climate records of the nearest weather station (the Ozena Valley Ranch), located at the southern end of the project, the average local annual precipitation is 8.8 in. (222 mm) (records between 1948 and 1964), 81 percent of which occurs between November and March.

4.2 Heavy Vehicle Simulator (HVS) Study on Route 89

The HVS testing carried out on a turnout adjacent to Route 89 at PM 27 (km 44) is discussed in a separate report *(22)*. A summary of the key findings is provided below.

The original workplan was based on HVS testing being carried out in the northbound lane, with traffic being diverted to the southbound lane and widened shoulder. Due to safety reasons, the HVS test section was moved to a turnout. Material was imported to provide the support layers for the test section, but differed from that of the main roadway. The base layer of the test section was constructed with excess reclaimed asphalt concrete treated with foamed asphalt and cement from the main roadway, and not as a full-depth recycled layer per se. This material had been stockpiled for about a week before construction of the HVS sections and was therefore not necessarily representative of typical FDR-foamed asphalt pavement. The recycled material had an R-value of 82. The test section base layer was primed with an SS-1 emulsion before being surfaced with 2.0 in. (50 mm) of asphalt concrete. Construction was not monitored by the UCPRC.

HVS trafficking on the sections commenced in August 2003 and was completed in May 2004. During this period a total of 1,863,595 load repetitions were applied across the four test sections. One test was carried out with controlled water flow across the surface. A temperature chamber was used to maintain the pavement temperature at 68°F ± 7°F (20°C ± 4°C) for two of the tests, and at 41°F ± 7°F (5°C ± 4°C) for one test. The last test (wet) was carried out at ambient temperatures. A dual tire (100 psi [690 kPa] pressure) and bidirectional loading with lateral wander was used in all tests.

Findings and observations based on the data collected during this HVS study include:

- Results from field surveys done prior to, during, and after HVS testing showed that the pavement structure of the HVS test sections was not representative of the mainline and foamed asphalt-treated, recycled pavement in general. The base layer thickness on the HVS test sections varied between 3.0 in. and 4 in. (75 mm and 100 mm), compared to the design thickness of 8.0 in. (200 mm). The base layer was supported by a weak clay-like layer and decomposed granite subgrade. A very weak support layer was identified in the vicinity of one of the sections and test-pit results show that the moisture content in the subgrade of this section exceeded 20 percent.
- The mode of distress of the HVS test sections differed between favorable conditions in summer and fall and unfavorable conditions in winter and spring. The mode of distress before the onset of winter consisted of gradual deformation of the pavement resulting in a terminal surface rut with limited fatigue cracking. After the winter, the mode changed to a more rapid rate of rutting and on the two sections tested during spring, shear failure of the base layer occurred in certain locations. These sections also showed extensive fatigue cracking, but this was probably caused by the weak soft base layer (low resilient modulus) with large plastic deformations generating high tensile strains in the asphalt concrete surfacing layer.

- The pavement structure of the HVS test sections showed sensitivity to high moisture contents in terms of elastic and plastic response. The resilient modulus of the base layer decreased during the winter and spring, and the rut rate increased. Although not to the same extent, a reduction in base layer resilient modulus on the mainline was also observed from FWD results. It is not clear whether the reduction in base layer resilient modulus was permanent. If it is, early fatigue of the asphalt surfacing layer is likely.
- The pavement bearing capacity only exceeded the design value under favorable conditions in the fall and early winter. However, the pavement structure of the HVS test sections was not representative of the mainline pavement structure and therefore not representative of the bearing capacity of foamed asphalt-treated, recycled pavements. The bearing capacity of the pavement is subject to seasonal effects and cannot be estimated from a single HVS test result.

Based on the above findings and the limitations associated with testing on an unrepresentative section, no recommendations as to the use of full-depth reclamation with foamed asphalt in rehabilitation strategies were made after completion of the experiment.

4.3 Bi-Annual Monitoring Study

A timeline of construction and performance assessments is provided in Figure 4.1. The bi-annual monitoring study included a visual assessment and FWD testing on the four selected FDR-foamed asphalt projects in California. The visual assessment included an evaluation of any distress apparent on the surface as well as any potential influencing factors, such as drainage condition and roadside activities. Any recent maintenance on the road was also assessed. FWD testing was undertaken with the UCPRC Heavy Weight Deflectometer, which is configured with a segmented 300-mm (12 in.) diameter load plate and eight deflection sensors (Table 4.1). At each drop point, three load levels were applied and each load level was applied once. Target loads for the pavement sections were 30 kN, 40 kN, and 50 kN (6,750, 9,000 and 11,250 lb).

Action	2001				2002				2005				2006				2007				2008	
	W	S_p	S_u	F	W	S_p	S_u	F	W	S_p	S_u	F	W	S_p	S_u	F	W	S_p	S_u	F	W	S_p
Route 20			C											A		A		A		A		A
Route 89							C							A		A		A		A		A
Route 33[1]											C			A		A		A		A		A
Route 33[2]														C		A		A		A		A

[1] San Luis Obispo and Santa Barbara Counties
[2] Ventura County

W = winter S_p = spring S_u = summer F = fall
C = Construction A = Assessment

Figure 4.1: Timeline of construction and assessments.

Table 4.1: UCPRC FWD Sensor Locations

Sensor Number	Distance from Center of Load Plate (mm [in.])	
1	0	(0)
2	210	(8.3)
3	315	(12.4)
4	475	(18.7)
5	630	(24.8)
6	925	(36.4)
7	1,535	(60.4)
8*	1,985	(78.2)
* The eighth sensor was not used in the analysis.		

4.4 Visual Assessments

4.4.1 Route 20 (03-COL-20)

The project was divided into three sections for the purpose of visual assessments. The first section covered half of the project from its start near Williams (PM 15.0 through PM 19.7) and was relatively straight and level. The second section, also straight and level, ran from approximately PM 12.0 to PM 15.0, while the third section covered the hilly terrain between PM 10.2 and PM 12.0. Drainage on the road was considered to be good.

Apart from longitudinal cracking (Figure 4.2) along the centerline and some mechanical damage, very little distress was observed on most of Section 1 during the course of the assessments. On the middle section, the same longitudinal crack along the centerline was observed. Isolated areas of fatigue cracking were noted in the inner wheelpath during the 2007 assessments (Figure 4.3). More areas of fatigue cracking, in both the inner and outer wheelpaths, were observed during the 2008 assessment (Figure 4.4). Some spalling of the cracks in the open-graded friction course was evident (Figure 4.5). There was no sign of pumping of fines through the cracks or of permanent deformation. The origin and cause of the cracking was not clear and no conclusions will be drawn until cores from the distressed areas can be studied. On the hill section, some longitudinal cracking in the asphalt was observed during the 2007 and 2008 assessments (Figure 4.6). These appeared to be top-down, construction, and slope/fill stability related cracks, not directly linked to the foamed asphalt base performance. Some spalling of the cracks was noted.

Figure 4.2: Centerline crack on 03-COL-20 (2006–2008).

Figure 4.3: Fatigue Cracking in inner wheelpath on 03-COL-20 (2007).

Figure 4.4: Fatigue cracking in outer wheelpath on 03-COL-20 (2008).

Figure 4.5: Spalled cracks through open-graded friction course on 03-COL-20 (2008).

Figure 4.6: Longitudinal cracks in hill section on 03-COL-20 (2007–2008).

4.4.2 Route 89 (03-SIE-89)

This section was first assessed in June 2006, about four years after construction. Random areas of cracking were observed along the length of the road as follows:

- Longitudinal/alligator cracking (Figure 4.7 and Figure 4.8) along the pavement edges, attributed to the lack of support on the sides of the road and possible weakening of the material caused by the ingress of water in the absence of sealed shoulders. This type of cracking covered between 10 and 20 percent of the project length.

- Thermal cracking (Figure 4.9) due to low temperatures in winter.
- Transverse fatigue cracking in a low-lying area, attributed to moist, weak subgrade materials (Figure 4.10).

Figure 4.7: Outer wheelpath cracking on 03-SIE-89.

Figure 4.8: Sealed outer wheelpath cracks on 03-SIE-89.

Figure 4.9: Thermal cracking on 03-SIE-89.

Figure 4.10: Sealed transverse cracks on 03-SIE-89.

Many of the cracks had been sealed prior to the spring 2007 assessment. No new cracks were observed, nor had distress deteriorated in the areas previously assessed. A pavement preservation surface treatment (microsurfacing) was applied to the road in the week prior to the final evaluation in June 2008 (Figure 4.11). It is not clear to what extent the road had deteriorated since the fall 2007 evaluation. However, judging by the thickness of the surfacing (0.4 in. [10 mm]), it is unlikely that any serious distress had occurred.

Figure 4.11: Pavement preservation treatment on 03-SIE-89.

4.4.3 Route 33 (05-SB,SLO-33)

Severe distress in the form of alligator cracking and deformation was observed at a number of locations along the road during the first assessment in April 2006 (Figure 4.12 through Figure 4.14). Most failures were in the northbound lane (upslope) on which most of the truck traffic was loaded. Fewer failures were noted on the southbound lane (downslope), where most of the truck traffic was unloaded. Clay particles that had pumped through the distresses were clearly visible in the failed areas. A follow-up assessment was carried out in July 2006. New areas of distress were noted (Figure 4.15) as were a number of digouts and patching with hot-mix asphalt that had been undertaken since the previous visit (Figure 4.16 and Figure 4.17). New distress was evident along the edges of these patches.

Figure 4.12: Early cracking with pumping on 05-SB,SLO-33 (April 2006).

Figure 4.13: Severe distress (1) on 05-SB,SLO-33 (April 2006).

Figure 4.14: Severe distress (2) on 05-SB,SLO-33 (April 2006).

Figure 4.15: Severe distress (3) on 05-SB,SLO-33 (July 2006).

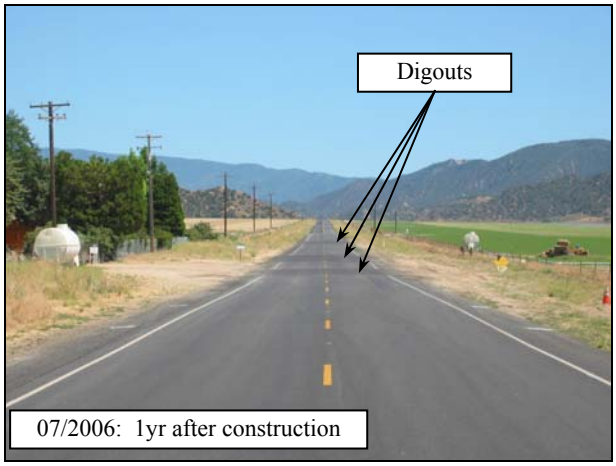

Figure 4.16: Digouts on 05-SB,SLO-33 (July 2006).

Figure 4.17: New distress next to digout on 05-SB,SLO-33 (July 2006).

The cause of distress was attributed in part to inadequate drainage associated with the filling in of side drains (Figure 4.18), blocked culverts (Figure 4.19), and regular irrigation in cultivated fields, orchards and vineyards along the road (Figure 4.20). Many of these fields had been ploughed perpendicular to the road with consequent channeling of water into the pavement structure (Figure 4.21).


Figure 4.18: Filled in side drains on 05-SB,SLO-33.

Figure 4.19: Blocked culvert on 05-SB,SLO-33.

Figure 4.20: Proximity of irrigated fields to damaged road on 05-SB,SLO-33.


Figure 4.21: Plough furrows perpendicular to road on 05-SB,SLO-33.

Some areas associated with poor construction quality control were also noted. These included poor construction joints leading to transverse cracks (Figure 4.22), scoring of the asphalt during paving or compaction (Figure 4.23), areas of very thin asphalt (Figure 4.24), and the compaction of trash into the hot asphalt (Figure 4.25).

Figure 4.22: Poor construction joint on 05-SB,SLO-33.

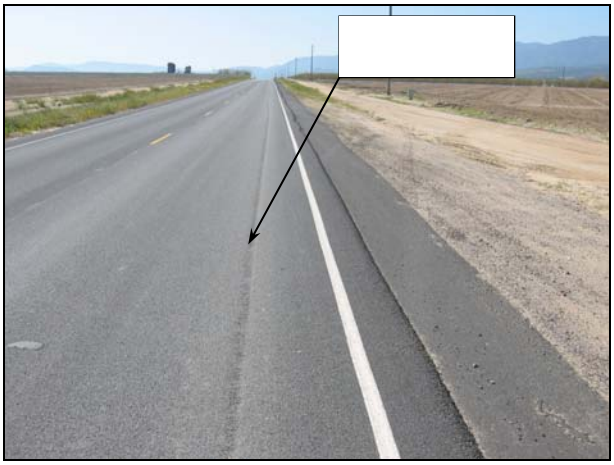

Figure 4.23: Construction defect on 05-SB,SLO-33.

Figure 4.24: Area of thin asphalt concrete on 05-SB,SLO-33.

Figure 4.25: Trash compacted into asphalt concrete on 05-SB,SLO-33.

New areas of distress, and distress in and around the previously patched areas were observed during subsequent assessments, particularly during the visits in spring 2007 and spring 2008 (Figure 4.26 and Figure 4.27). During later visits (in fall 2007 and spring 2008), distress was noted in areas where unsealed access roads appeared to channel water into the pavement structure (Figure 4.28).

Figure 4.26: New areas of distress on 05-SB,SLO-33 (May 2008).

Figure 4.27: New distress on previous digout on 05-SB,SLO-33 (May 2008).

Figure 4.28: Distress associated with access road drainage on 05-SB,SLO-33 (May 2008).

Forensic Investigation

A forensic investigation of the early distressed areas was carried out by Caltrans in July 2006 *(23)* and observed by the UCPRC. The investigation included a visual evaluation to identify areas of distress, selected coring and Dynamic Cone Penetrometer measurements, and the excavation of two test pits.

Observations in the test pits and of cores revealed a moist and apparently uncured foamed asphalt base, contaminated with plastic fines (Figure 4.29 through Figure 4.31). This condition was attributed to inadequate drainage on the road (as described above) and the associated high rainfall in the wet season following construction. The high moisture content prevented the drying out of the foamed asphalt treatment, which is critical for strength development (as discussed in Chapters 7 through 10). Clay pockets in the original underlying layers appeared to have been mixed into the foamed asphalt layer during the recycling process. This material would also have been influenced by the moisture, leading to shearing, loss of support, and subsequent pumping of the fines through the foamed asphalt layer (Figure 4.32 and Figure 4.33).

Figure 4.29: Test pit #1 on 05-SB,SLO-33.

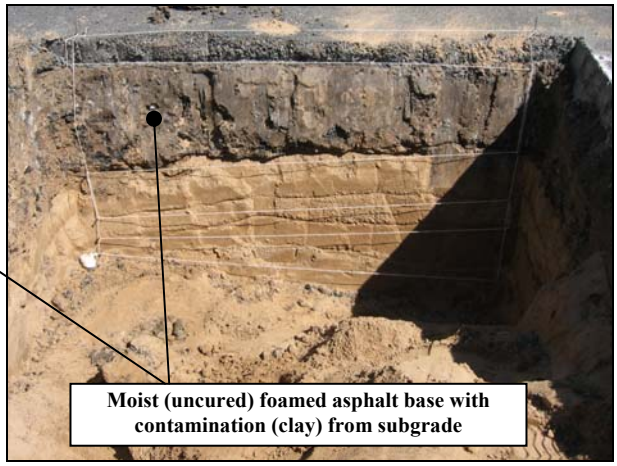

Figure 4.30: Test pit #2 on 05-SB,SLO-33.

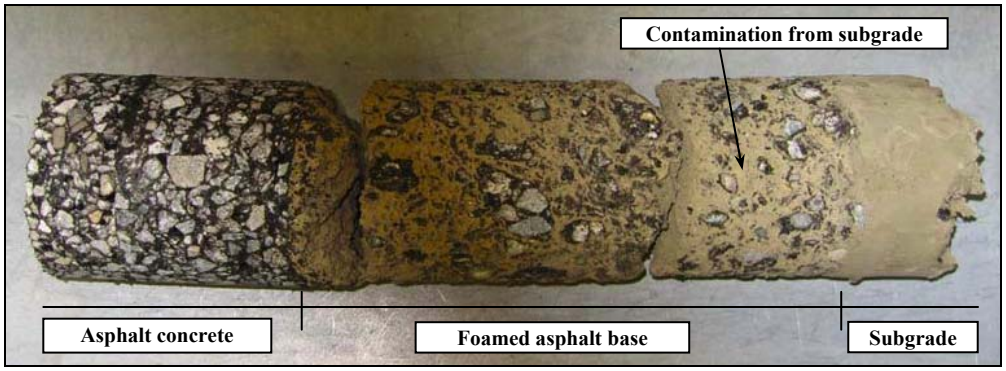

Figure 4.31: Core showing fines contamination. (1)
(Photo provided by J. Peterson, Caltrans)

Figure 4.32: Core showing fines contamination. (2)

Figure 4.33: Fines pumped through base and asphalt concrete.

4.4.4 Route 33 (07-VEN-33)

A visual evaluation and FWD measurements were carried out on the road prior to construction. The first two days of construction were observed and thereafter the project was assessed at the same time as the

Route 33 project in San Luis Obispo and Santa Barbara counties at approximately six-month intervals. A truckload of prepulverized material (no foamed asphalt) from the project was transported to the UCPRC for the laboratory investigation.

Preconstruction Assessment

The detailed preconstruction assessment (visual evaluation, test pits, coring, Dynamic Cone Penetrometer study, and mix design) on this project was undertaken by Caltrans in 2005, prior to the start of the UCPRC field study. However, a visual assessment and FWD measurements were carried out in early April 2006 to complement the Caltrans study and to familiarize UCPRC researchers with the project.

The UCPRC visual assessment revealed that the road was highly distressed over much of the 9-mile (14.5-km) section. Severe alligator cracking (Figure 4.34) was evident as well as some longitudinal and transverse cracking (Figure 4.35 and Figure 4.36), and some cracking associated with slope instability (Figure 4.37). Patching and areas of overlay were noted along some sections of the road (Figure 4.38 and Figure 4.39). One area that had been severely affected by a landslide was being reconstructed at the time of the investigation (Figure 4.40). Most drainage structures were blocked by soil and vegetation and some were damaged by erosion (Figure 4.41).

Figure 4.34: Preconstruction fatigue (alligator) cracking on 07-VEN-33.

Figure 4.35: Preconstruction transverse cracking on 07-VEN-33.

Figure 4.36: Preconstruction longitudinal cracking on 07-VEN-33.

Figure 4.37: Preconstruction cracking associated with slope instability on 07-VEN-33.

Figure 4.38: Preconstruction patching on 07-VEN-33.

Figure 4.39: Preconstruction maintenance overlay on 07-VEN-33.

Figure 4.40: Pre-construction landslide repair on 07-VEN-33.

Figure 4.41: Drainage structure on 07-VEN-33.

FWD measurements were carried out on selected subsections of the project. A full-length evaluation, although desirable, was not undertaken due to traffic closure limitations. The test sections are summarized in Table 4.2.

Table 4.2: Preconstruction FWD Test Sections on Route 33 (07-VEN-33)

Test Section	Start Point	End Point	Direction	Length (m)	Test Interval (m)
33Ven-A	PM 51.00,	PM 50.00	Southbound	1,600	16
33Ven-B	PM 48.50,	PM 50.00	Northbound	2,400	160
33Ven-C	PM 50.50,	PM 51.00	Northbound	1,600	16
33Ven-D	PM 54.00,	PM 54.90	Northbound	1,400	16

A simple calculation to determine a deflection modulus from the fifth sensor (~600 mm [23.6 in.]) on the FWD was used to approximate the subgrade modulus (see Section 4.7.2). The results of the study are plotted in Figure 4.42. The results indicate that most of the sections tested were considered to have adequate subgrade conditions. A deflection modulus of less than 45 MPa (6.5 ksi), shown on the plots, was considered as a warning that subgrade problems could occur. This interim threshold value was selected by comparing FWD results on good and distressed sections on the Route 33 FDR project in Santa Barbara/San Luis Obispo Counties, described above.

Based on the information provided by Caltrans and the limited evaluation by the UCPRC, the project was considered as an appropriate candidate for full-depth reclamation with foamed asphalt, although some concerns were noted with respect to variability in the thickness of the asphalt concrete and the condition of the drainage structures.

Construction Assessment

The first two days of construction were observed by the UCPRC. The pavement reclamation component was subcontracted by the prime contractor. The subcontractor employed a second contractor to allow for a tandem reclamation process, consisting of prepulverization followed by foamed asphalt injection. One lane was closed to traffic for construction. A pilot car directed traffic on the open lane. Two-way traffic was restored each evening. The following construction process was followed:

- The road was first prepulverized to a depth of between 4.0 in. and 11 in. (200 mm and 275 mm), depending on the thickness of the asphalt concrete (Figure 4.43).
- Cement kiln dust was then applied to the pulverized material at a rate of 2.0 percent by mass of aggregate (Figure 4.44), reportedly to increase the fines content and provide some early strength.

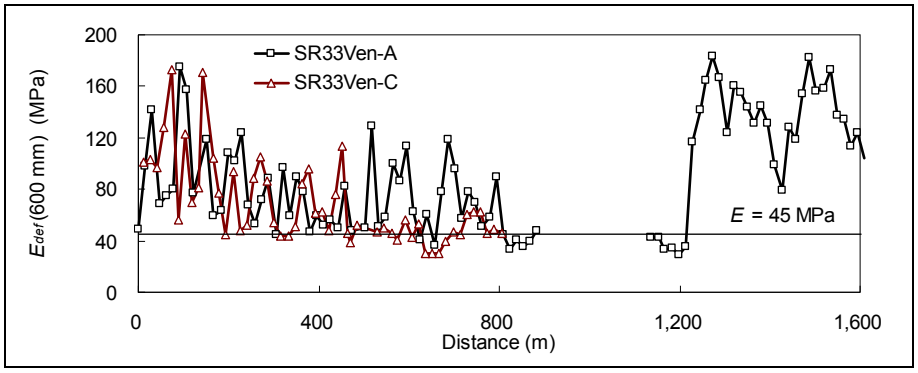

(a) Section 33Ven-A and 33Ven-C
(Distance 0 in 33Ven-C was at PM51.00, the end point of the test section to facilitate comparison)

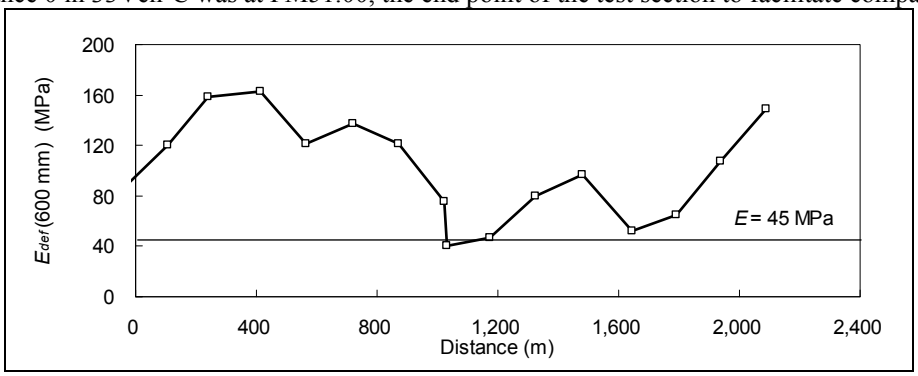

(b) Section 33Ven-B

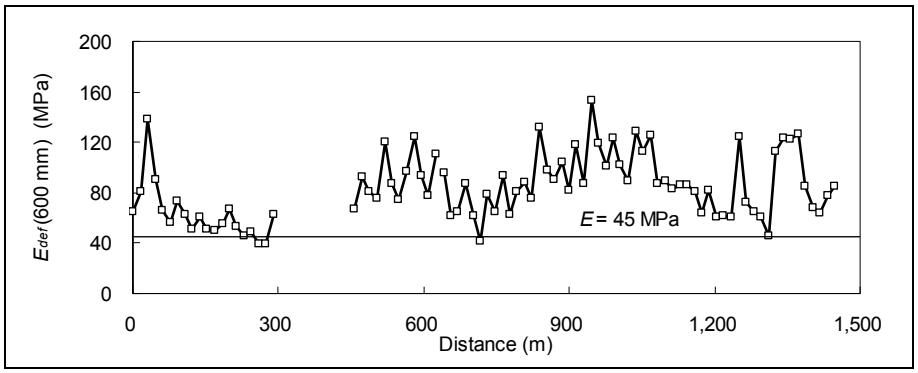

(c) Section 33Ven-D

Figure 4.42: Deflection modulus calculated from FWD testing on 07-VEN-33.

- The recycling machine and binder tanker followed, applying the foamed asphalt at a rate of between 3.0 and 3.5 percent depending on the fines content of the material (Figure 4.45 and Figure 4.46). A water tanker was not included as part of the recycling train; instead the compaction water was added at periodic intervals by a separate tanker. Checks on the mix were made by the crew at periodic intervals. Observations indicated that the second pass of the recycling machine tended to break down the material more than was considered desirable. Similar observations where made in the test pits on the SR33-San Luis Obispo Project, as well as observations on other FDR projects where the road was prepulverized before addition of the foamed asphalt. The exclusion of a water tanker from

the recycling train appeared to result in poor distribution of the compaction water through the recycled layer.

Figure 4.43: Prepulverization on on 07-VEN-33.

Figure 4.44: Cement kiln dust application on 07-VEN-33.

Figure 4.45: Foamed asphalt injection (Train 1) on 07-VEN-33.

Figure 4.46: Foamed asphalt injection (Train 2) on 07-VEN-33.

- A padfoot roller (11 ton) followed the recycling train for initial compaction (Figure 4.47). Water was added from a tanker at periodic intervals during the process (Figure 4.48). One padfoot roller served both recycling trains.
- Once initial compaction had been completed with the padfoot roller (no impressions left on the road surface), a grader was used to shape the road and a steel vibratory roller (11 ton) for additional compaction (Figure 4.49). Water was sprayed at periodic intervals.
- Final compaction was carried out with a pneumatic-tired roller (9 ton) after wetting of the surface (Figure 4.50).
- Random density measurements were taken with a nuclear gauge. Gravimetric moisture samples were not taken.

- The road was broomed and temporary markings painted onto the surface prior to opening to traffic (Figure 4.51 and Figure 4.52). A tightly knit surface was achieved over most of the surface (Figure 4.53), with isolated areas of aggregate segregation (Figure 4.54). One cracked area, attributed to incorrect compaction, was identified (Figure 4.55). This was reworked.

Figure 4.47: Initial compaction with padfoot roller on 07-VEN-33.

Figure 4.48: Water application behind recycling train on 07-VEN-33.

Figure 4.49: Shaping and compaction with steel wheel roller on 07-VEN-33.

Figure 4.50: Final compaction with rubber-tired roller on 07-VEN-33.

Figure 4.51: Brooming on 07-VEN-33.

Figure 4.52: Temporary striping application on 07-VEN-33.

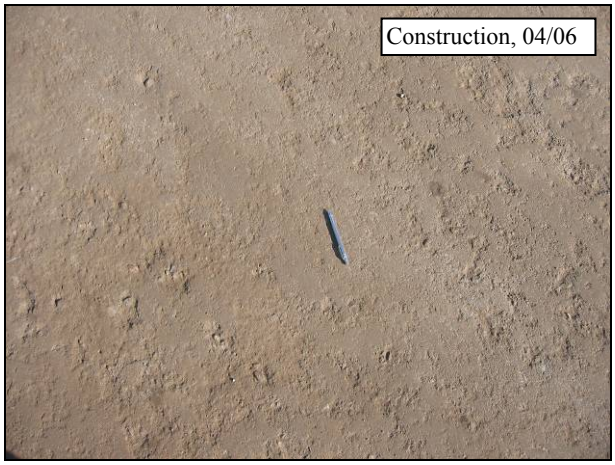

Figure 4.53: Surface ready for traffic on 07-VEN-33.

Figure 4.54: Area of segregated aggregate on 07-VEN-33.

Figure 4.55: Area demarcated for rework on 07-VEN-33.

Postconstruction Assessments

The road was monitored in June and November 2006, May and November 2007, and May 2008. The first assessment was carried out immediately after construction and no significant problems, apart from blocked drainage structures, were noted. The November 2006 assessment was carried out during light rainfall. The road appeared to be performing well, apart from isolated areas of longitudinal cracking (Figure 4.56 and Figure 4.57), transverse cracking along the edge of the road (Figure 4.58), some areas of shearing in the asphalt concrete (Figure 4.59), and some small areas of roughness (Figure 4.60). Cracking around the striping (Figure 4.61 and Figure 4.62) was observed along most of the road. Erosion from slopes was noted in cut areas (Figure 4.63). Most drainage structures remained blocked with vegetation, soil, and excess asphalt concrete from the paving process (Figure 4.64 and Figure 4.65).

Figure 4.56: Longitudinal crack on 07-VEN-33.

Figure 4.57: Longitudinal crack and loss of oversize stone on 07-VEN-33.

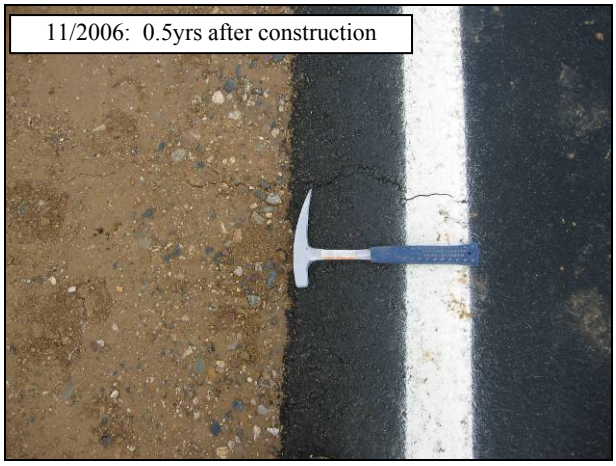

Figure 4.58: Transverse cracking on 07-VEN-33.

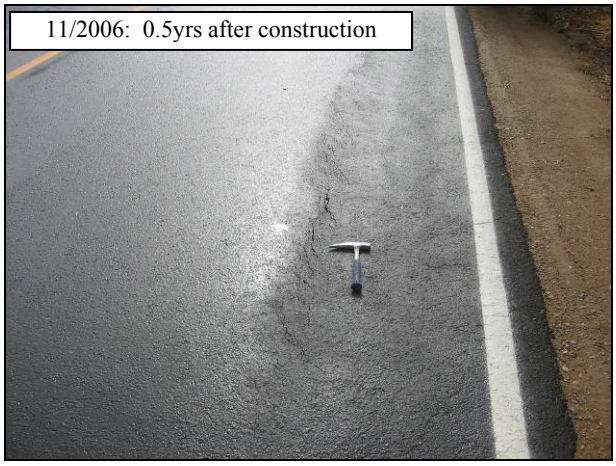

Figure 4.59: Shearing in the asphalt concrete on 07-VEN-33.

Figure 4.60: Roughness in asphalt concrete on 07-VEN-33.

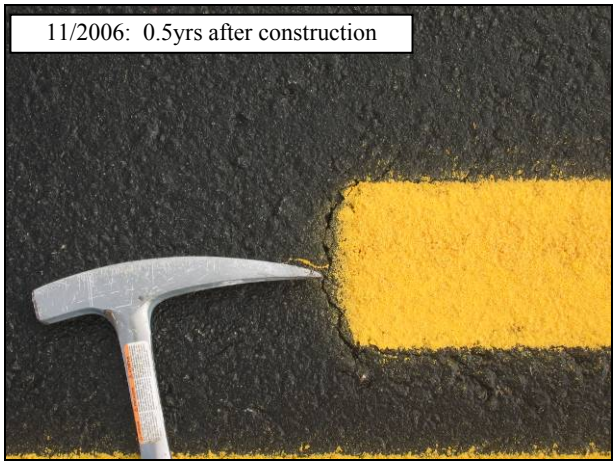

Figure 4.61: Cracking around centerline striping on 07-VEN-33.

Figure 4.62: Cracking around edge striping on 07-VEN-33.

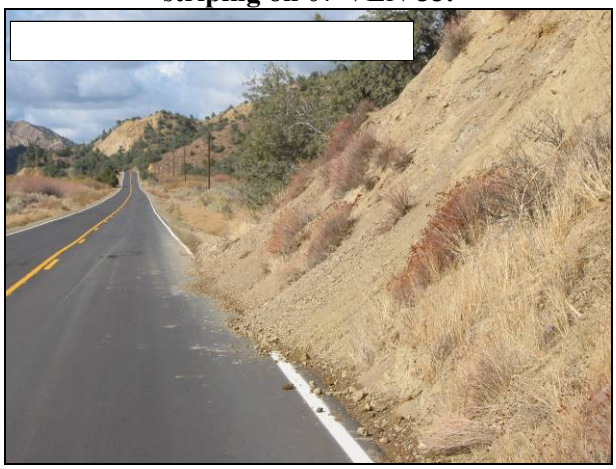

Figure 4.63: Debris from slope instability on 07-VEN-33.

Figure 4.64: Blocked drain. (1) on 07-VEN-33.

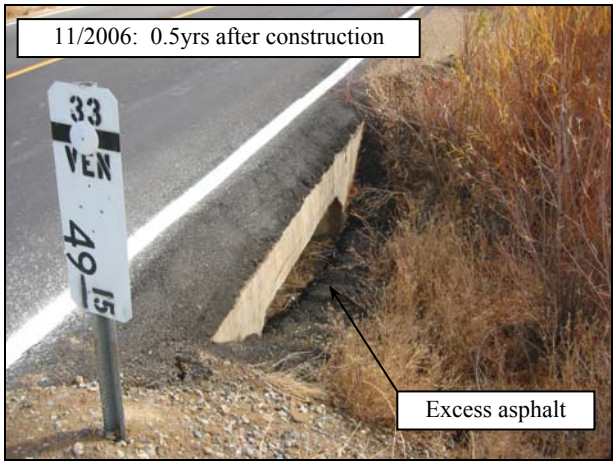

Figure 4.65: Blocked drain, including excess asphalt concrete from paving on 07-VEN-33. (2)

Subsequent assessments revealed no further significant distress apart from some additional longitudinal cracks (Figure 4.66 and Figure 4.67). A major landslide occurred in July 2006 (Figure 4.68), requiring reconstruction of a section of the road. The drains had not been cleared at the time of the final assessment in May 2008.

Figure 4.66: Longitudinal cracking on 07-VEN-33 (April 2007).

Figure 4.67: Longitudinal cracking on 07-VEN-33 (May 2008).

Figure 4.68: Damage associated with landslide (July 2006).

4.5 Other Projects

A number of other non-Caltrans projects were assessed during the course of the experiment. These included projects on county, city, and forest roads. They are not discussed in this document; however, key learning points are included in the recommendations and were used in the preparation of the guideline documentation.

4.6 Falling Weight Deflectometer Assessments

4.6.1 Test Strategy

The resilient modulus of foamed asphalt mixes is influenced by many environmental factors, including temperature and moisture content. These conditions cannot be controlled during field testing and thus the measured values only reflect the material properties for the conditions at the time of testing. The FWD test plans were designed to quantify and differentiate these effects where possible.

The climate patterns for the Route 20 and Route 33 projects are similar, with concentrated rainfall between November and March, and little or no precipitation in the dry season. In each year, tests on each project were performed once in spring (May or June), when moisture content in the foamed asphalt-treated base was relatively high, and once in the fall when the material was relatively dry.

Testing on Route 20 and Route 33 (07-VEN-33) evaluated resilient modulus behavior of the foamed asphalt-treated base materials. Two test subsections were selected for each project and each section was tested twice on each day to obtain modulus measurements in two different temperature ranges. This allowed normalization of the measured modulus to a standard reference temperature. The available traffic closure arrangements were different for these two projects. Route 20 has high traffic volumes; therefore traffic closures were on fixed segments while a rolling closure was used on Route 33-Ventura, which had lighter traffic volumes. Consequently, the FWD tests on Route 20 covered shorter segments with a shorter test interval compared to the longer test sections and intervals on Route 33-Ventura.

All FWD measurements were taken in the outer wheelpath.

4.6.2 Test Subsections

Route 20 (03-COL-20)

Two test sections (each 500 m [1,650 ft] long and denoted as 20-A and 20-B respectively) were selected on the road for FWD testing (Table 4.3), based on the availability of historical data from Caltrans. The test interval was 16 m (53 ft). Testing was carried out in the spring and fall of each year (before and after the dry season) in June and October 2006, and May and October 2007. Tests were carried out early in the morning and later in the afternoon to quantify the effects of temperature on resilient modulus. The location of the test points was precisely controlled (tolerance of ±0.5 m [1.6 ft]) to ensure that the load was applied at the same point each time.

Table 4.3: FWD Test Sections on Route 20

Test Section	Start Point	End Point	Lane	Length (m)	Test Interval (m)
20-A	PM 19.15	PM 18.85	Westbound	512	16
20-B	PM 15.75	PM 16.05	Eastbound	512	16
Note: The segment between 0 m and 112 m on Section 20-A had high variation and the data were discarded in the analysis.					

Route 33 (05-SB,SLO-33)

Ten test subsections, denoted as 33SS-A through 33SS-J, were selected for this project (Table 4.4). These covered approximately 40 percent of the total length of the project, allowing comparisons between areas with good and poor performance. The planned test interval was 40 m (130 ft), but 20 m (66 ft) and 80 m

(260 ft) intervals were also used depending on weather conditions and the available traffic closure windows. FWD tests were performed in June and November 2006, and in May and November 2007, with morning and afternoon measurements taken on selected sections to compare the effects of temperature.

Table 4.4: FWD Test Sections on Route 33 (05-SB,SLO-33)

Test Section	Start Point[1]	End Point	Lane	Length (m)	Test Interval (m)	Distress in May 2008
33SS-A	SL PM 2.5	SL PM 2.0	Southbound	880	40	N
33SS-B	SB PM 8.0	SB PM 7.5	Southbound	800	40	N
33SS-C	SB PM 5.0	SB PM 4.5	Southbound	800	40	N
33SS-D[2]	SB PM 0.0	SB PM 0.5	Northbound	800	40	N
33SS-E	SB PM 1.0	SB PM 1.5	Northbound	800	40	Y
33SS-F[3]	SB PM 1.5	SB PM 2.0	Northbound	800	40	N
33SS-G[4]	SB PM 2.0	SB PM 2.6	Northbound	1,040	40	Y
33SS-H	SB PM 6.0	SB PM 6.5	Northbound	800	40	Y
33SS-I	SL PM 1.0	SL PM 1.5	Northbound	800	40	N
33SS-J[5]	SL PM 2.0	SL PM 2.5	Northbound	880	40	Y

Notes:
[1] SB: Santa Barbara County; SL: San Luis Obispo County
[2] 200 m was tested on this segment in June 2006. Mean values were calculated from the 200-m section only.
[3] Section 33SS-F was not included in the first round of testing in June 2006.
[4] Test results for 400 to 800 m of Section 33SS-G were used to calculate mean values. Distresses appeared at approximately 800 m.
[5] Section 33SS-J was only tested in June 2006 and May 2007.

Several localized distresses, mainly alligator cracking associated with pavement deformation/rutting, were identified on Route 33 (05-SB,SLO-33) in the spring of 2006. These were repaired by Caltrans during the course of the study. Patched segments were excluded from the analysis because of the inconsistent pavement structure. The terms "distressed" and "intact" are used in this chapter to describe the general condition of these areas. Distressed implies that visible distress, typically fatigue cracking and deformation, was observed on the sections during the assessments, while intact areas did not exhibit any signs of serious distress during the final visual assessment in May 2008. Testing on the road compared the material properties of subsections showing distress with those of sections considered to be in good condition. Subsections with a total length of more than 8,000 m (0.5 miles) were tested on this project. Most subsections were tested only once per day, which rendered normalization of modulus against temperature difficult. Temperature was therefore treated as a random variable in the analysis.

Route 33 (07-VEN-33)

Two test subsections, denoted as 33Ven-A and 33Ven-B, were selected for this project (Table 4.5). Choice of subsection was limited by the alignment of the road and consequent safety concerns during closures. The planned test interval was 40 m (130 ft), but 20 m (66 ft) and 80 m (260 ft) intervals were also occasionally used depending on weather conditions and the available traffic closure windows. FWD tests

were performed in June and November 2006, and in May and November 2007. Where possible, two sets of measurements were taken on each day (early morning and later in the afternoon).

Table 4.5: Test Sections on Route 33 (07-VEN-33)

Test Section	Start Point	End Point	Lane	Length (m)	Test Interval (m)
33Ven-A	PM 51.00	PM 50.00	Southbound	1,600	40
33Ven-B	PM 48.50	PM 50.00	Northbound	2,400	40

Route 89 (03-SIE-89)

FWD testing was carried out on this project in a similar manner to the Route 20 and Route 33 evaluations. However, satisfactory backcalculation of the FWD deflections was not possible due to high spatial variation of subgrade properties along the length of the road, the limited thickness of the asphalt concrete (1.9 in. [47 mm]), and unreliable calculations of subsurface temperature attributed to most of the road being in shade from the forest during testing. No results from this project are presented in this report.

4.6.3 Backcalculation Methods

Backcalculation of the FWD data was performed using *FOBack* (Finite element Open source Backcalculation), developed at the UCPRC for research purposes. The deflection calculation engine in *FOBack* is based on the finite element method using an eight-node, isoparametric quadrilateral element for axisymmetric applications. Small element sizes (approximately 20 mm x 20 mm [0.8 in.]) were used in the finite element mesh in the area close to the load and the axis of symmetry. The element sizes were gradually increased in both the radial (horizontal) and vertical directions. The dimensions of the entire model were larger than 100 m x 100 m (330 ft) and therefore the boundary effect was considered negligible. A typical finite element model consisted of approximately 1,000 elements and 3,000 nodes. *LEAP2*, a Layered Elastic Analysis Program *(19)* was used to validate the calculation results of this finite element module and satisfactory agreement was achieved.

The error minimization or modulus optimization algorithm used in *FOBack* is the constrained Extended Kalman Filter (EKF) method, developed at the UCPRC *(24)*. An average Root Mean Square (RMS) error lower than 1.0 percent was achieved for all test sections reported, indicating satisfactory fitting to the measured deflections.

4.6.4 Subsurface Temperature Calculations

The subsurface pavement temperatures at the mid-depth of the asphalt concrete layer (combining HMA, OGFC, RHMA-G, and RHM-O where applicable) and at the mid-depth of the foamed asphalt-treated base layer were calculated in accordance with AASHTO T-317 (*Prediction of Asphalt-Bound Pavement Layer*

Temperatures). The equation used in this procedure calculates pavement temperature at any depth based on the average air temperature at the site on the day before testing, the pavement surface temperature measured with an infrared thermometer during testing, and the time when the test on this point was performed. This equation was originally developed and calibrated for hot-mix asphalt, and not for foamed asphalt mixes, but was considered the best available model in the absence of direct measurements of temperature in the foamed asphalt layer.

4.6.5 Local Precipitation in 2006 and 2007

The in-place moisture content of the foamed asphalt-treated materials in the FWD test sections was not measured directly during the study. The general moisture condition was inferred qualitatively and comparatively on the basis of the local rainfall history and the drainage condition of the pavement structures. The precipitation measured at Williams, close to the Route 20 section, and at three weather stations in a 34 mile to 56 mile (55 km to 90 km) radius of the Route 33 sections (no nearby records were available) during the two relevant years is summarized in Table 4.6 (July 1 to June 30 of the following year).

Table 4.6: Summary of Rainfall near Test Sections

Road	Station	Relative Location	07/01/2005–06/30/06		2006–2007 season	
			Precip. (mm)	% of Normal	Precip. (mm)	% of Normal
Route 20	Williams	20 km east	594	143	232	56
Route 33	Bakersfield	80 km northeast	174	105	78	47
	Santa Maria	90 km west	439	122	130	36
	Ojai	55 km south	652	117	174	31

Notes:
- Data were compiled according to the "Western U.S. Climate Historical Summaries" available at the Western Regional Climate Center *(www.wrcc.dri.edu).*
- The normal annual precipitation is the thirty year (1971 to 2000) mean value measured by the same weather station.
- The two projects on Route 33: SR33Ven and SR33SS are discussed together.
- The nearest weather station to Route 33 is the New Cuyama Fire Station, but the precipitation data for this period could not be obtained.

Total precipitation in the 2005/2006 rain season was slightly or moderately higher than normal at all four reference weather stations. In contrast, the 2006/2007 rain season had lower than average rainfall. It can be inferred that at the same test location, both the foamed asphalt layer and the subgrade would have been drier in the spring and fall of 2007 than in the corresponding seasons in 2006.

4.6.6 Resilient Modulus Characterization of Route 20 and Route 33 (Ventura)

Backcalculation Results

The backcalculated resilient moduli of the asphalt concrete layer (E_{AC}), the foamed asphalt layer (E_{FA}) and the subgrade (E_{SG}) for Subsection SR20-A as measured in 2006 are plotted in Figure 4.69 as an example.

Detailed results for all sections are provided in Appendix A. Results for the morning and afternoon tests respectively are plotted separately in Figure 4.69(c), while the subgrade modulus values plotted in Appendix A are the average of the morning and afternoon test results.

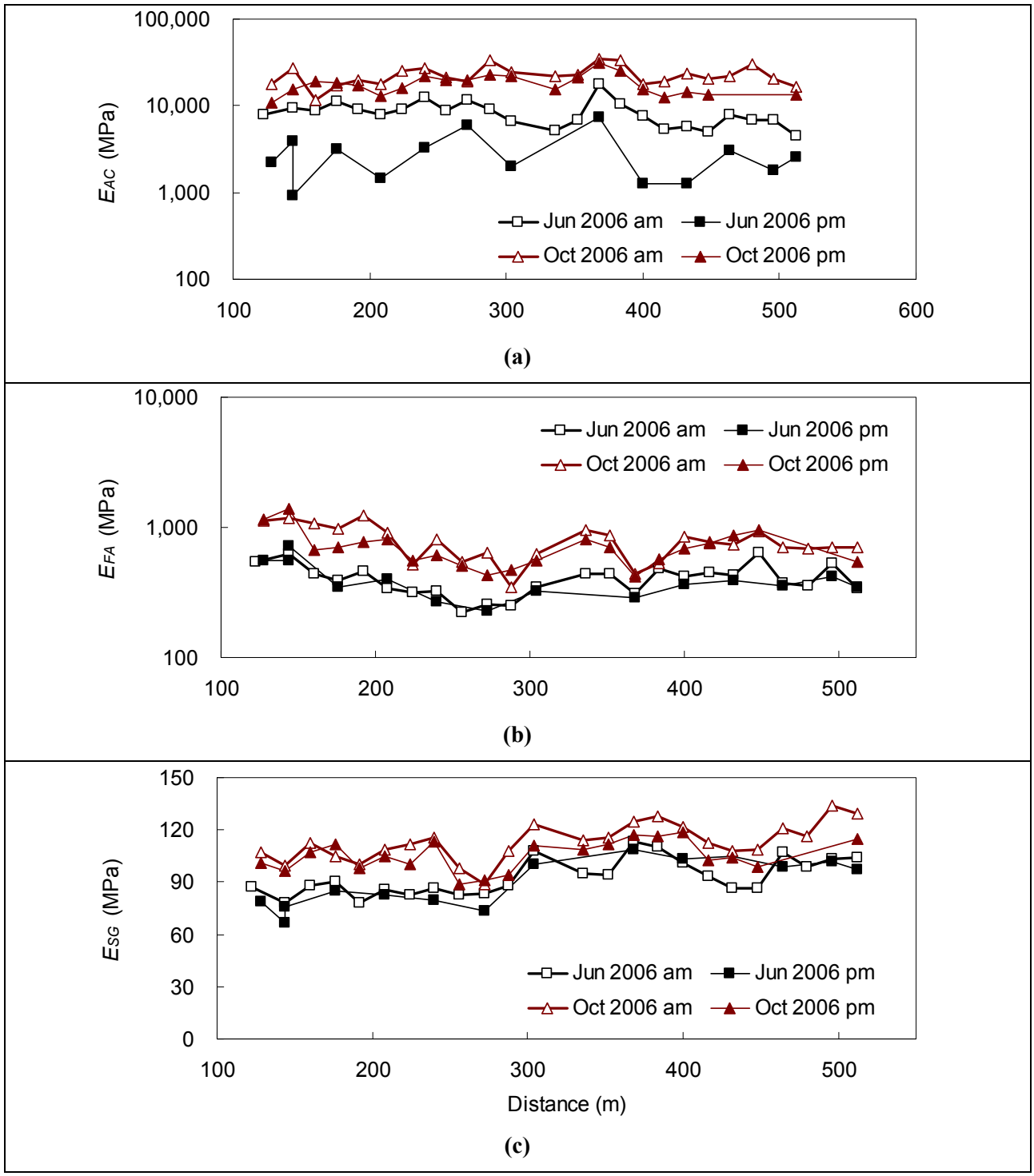

Figure 4.69: Backcalculated Resilient Modulus for Section SR20-A.
([a] Asphalt concrete layer; [b] foamed asphalt-treated layer; and [c] for the subgrade)
(Data for 0 to 112 m were discarded due to high variance.)

The results show that the moduli of the asphalt concrete were higher in October than June, indicating lower surface temperatures. The stiffness of the foamed asphalt layer was also higher in October than June, indicating cooler temperatures and less moisture. Daily temperature variation had consistent but minor effects on the subgrade modulus as discussed in Harvey et al. *(25)*. As the asphalt concrete temperature increased, the backcalculated subgrade stiffness generally dropped, possibly due to less confinement provided by the less-stiff foamed asphalt and asphalt concrete layers. The consistent trends of the backcalculated modulus of both the foamed asphalt material and the subgrade along the road for the four rounds of tests provided confidence in the backcalculation results.

Asphalt Concrete Modulus

It was assumed that the resilient moduli of the asphalt concrete layer and foamed asphalt-treated layers within each relatively uniform subsection follow log-normal distributions respectively, and that the resilient modulus of the subgrade follows a normal distribution. The mean values for each subsection are calculated accordingly.

The backcalculated resilient modulus (E_{AC}) values for the asphalt concrete layer (mean value of each section) for the two sections on Route 20 are plotted in Figure 4.70 against the average temperature (T_{AC}) at the mid-depth of this layer. The temperature sensitivity coefficient (defined in Section 6.5) of the asphalt concrete stiffness was determined as 2.5 psi/°F (0.031 MPa/°C) by simple linear regression. This implies that the stiffness of this asphalt concrete material doubles when the temperature decreases by 18°F (10°C).

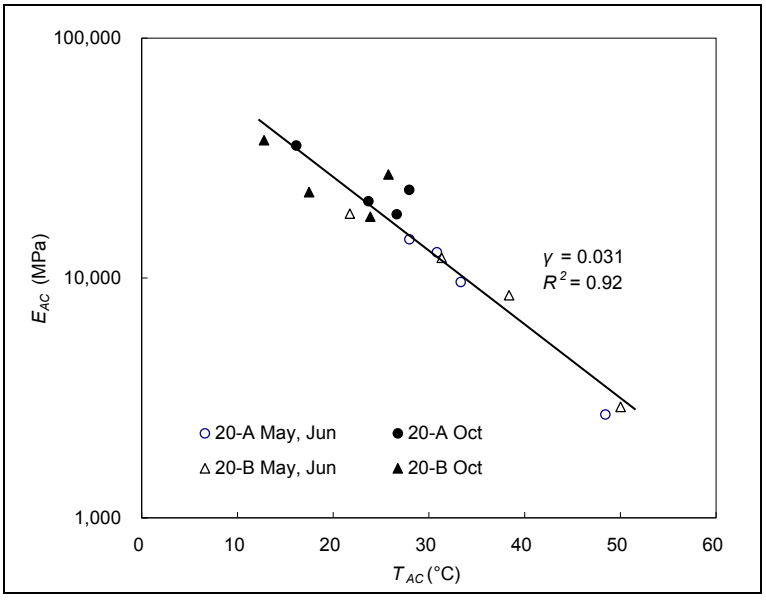

Figure 4.70: Temperature dependency of backcalculated AC modulus on Route 20.

All the data points align closely with the regression line indicating that the only major factor affecting the asphalt concrete resilient modulus was temperature. Traffic loading between May 2006 and November 2007 did not cause any perceivable damage to the asphalt concrete layer. The asphalt concrete resilient moduli measured in spring and in fall were not significantly different after being normalized to a reference temperature.

A similar analysis was attempted on the Route 33-Ventura sections, but the asphalt concrete stiffness tended to be overestimated because of the thin layer thickness (difficult in FWD backcalculation), and realistic plots (similar to Figure 4.70) for this road were not possible.

Normalizing Foamed Asphalt Stiffness against Temperature

Mean backcalculated foamed asphalt layer modulus (E_{FA}) values for each section on Route 20 and Route 33-Ventura were plotted on a log scale as shown in Figure 4.71.

The data points for the spring measurements formed a straight line, indicating that the resilient modulus of the foamed asphalt material in each test subsection was not significantly different between the two assessments in 2006 and 2007. One resilient modulus value at the reference temperature (68°F [20°C]) was therefore used to represent the stiffness of the foamed asphalt mix in each subsection during spring. Data points measured in the fall of each year did not form a single straight line, indicating that the resilient modulus of the foamed asphalt mixes was significantly higher in the fall of 2007 than in the fall of 2006. This was attributed to the lower rainfall during the 2006-2007 rain season (i.e., the materials in the fall of 2007 were significantly drier than in the fall of 2006). This stiffness change from 2006 to 2007 was not attributed to strength gain in the material (curing) given that the road was already five years old at the time of the evaluation, or to the action of traffic loading, as the E_{FA} values for 2007 would have been lower if they had been damaged by traffic.

It should be noted that the afternoon (higher temperature) test result of June 2006 for test Subsection 20-A appears to be off the regression line. This could be an outlier, or it may imply that there is an upper limit for temperature beyond which the relation shown in Equation 6.4 in Chapter 6 is not valid. This data point was not included in the temperature normalization. Due to traffic closure limitations, Subsection 33Ven-B was only tested once (one temperature) in the fall of 2006, therefore the same temperature sensitivity coefficient as determined for the fall 2007 test was used for temperature normalization of the 2006 data for this section.

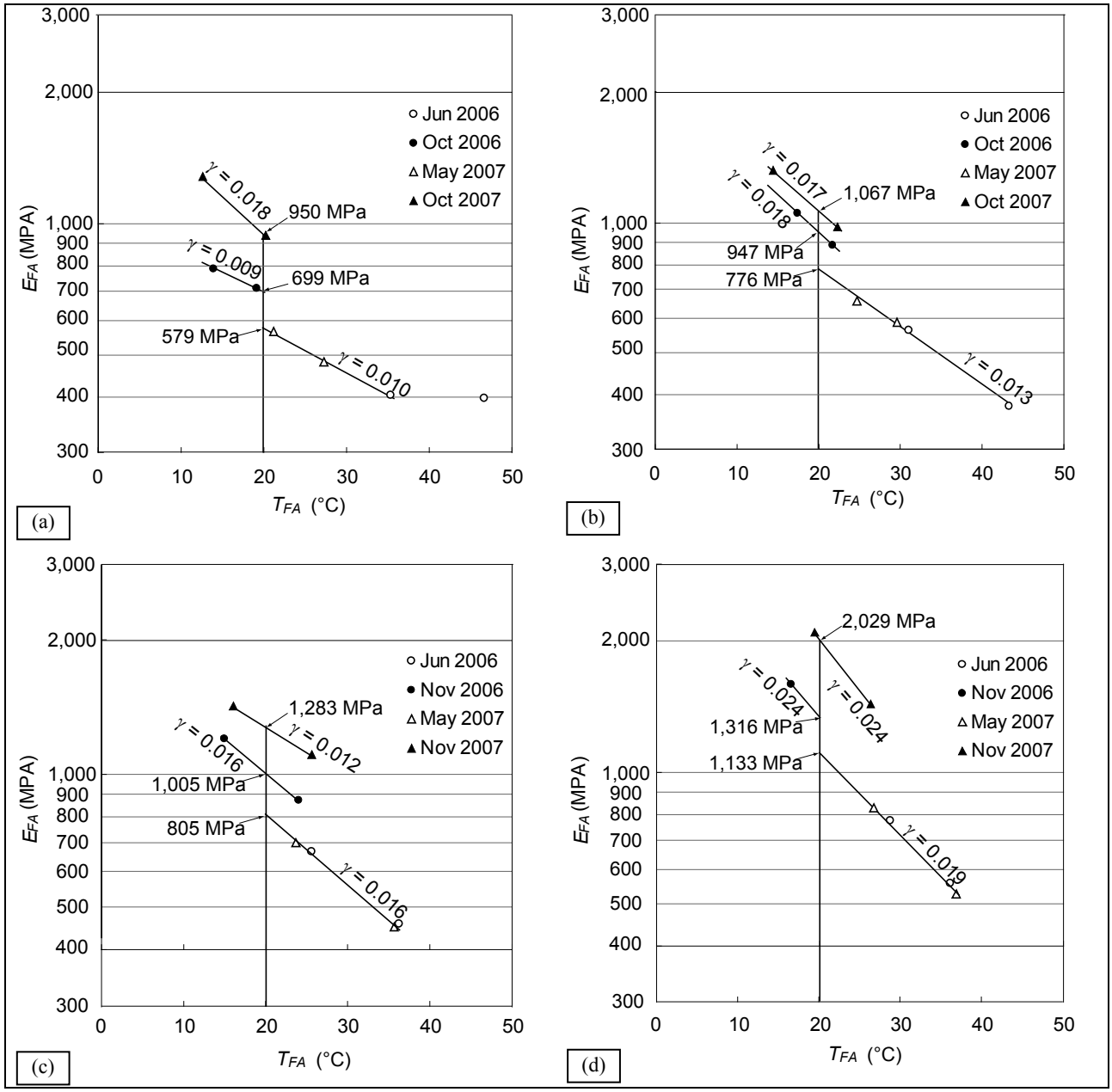

Figure 4.71: Mean FA Resilient Modulus values after temperature normalization.
([a] Section 20-A, [b] Section 20-B, [c] Section 33Ven-A, [d] Section 33Ven-B. E_{FA} is plotted on a log scale, but the axis is only partially shown for clarity. The temperature sensitivity of the resilient modulus γ is defined in Equation 6.4 in Section 6.5.)

Test Results

The mean stiffness values for the foamed asphalt layer and the subgrade of each section are summarized in Table 4.7.

The seasonal variation of the subgrade stiffness can be used to infer general moisture content change in the pavement structures, which is the primary factor affecting subgrade stiffness fluctuation. It is assumed

that for each section the moisture content changes in the foamed asphalt-treated base layer and in the subgrade are positively correlated.

Table 4.7: Test Results for Route 20 and Route 33 (Ventura)

06/2006	35.4	405	46.6	398	579	91
05/2007	21.2	567	27.3	482	579	99
10/2006	13.9	789	19.2	711	699	109
10/2007	12.6	1,285	20.3	939	950	111
06/2006	31.1	563	43.4	377	776	56
05/2007	24.6	659	29.6	588	776	62
10/2006	17.5	1,052	21.7	883	947	66
10/2007	14.5	1,317	22.3	978	1,067	74
06/2006	25.7	665	36.2	458	805	73
05/2007	23.7	698	35.6	451	805	98
10/2006	15.0	1,203	24.0	870	1,005	111
10/2007	16.0	1,428	25.5	1,104	1,283	160
	Section 33-Ventura-B					
06/2006	28.8	777	36.1	557	1,133	85
05/2007	26.7	829	36.8	527	1,133	99
10/2006	16.6	1,590	-	-	1,316	123
10/2007	19.4	2,099	26.3	1435	2,029	154

Subgrade stiffnesses measured in 2007 were significantly higher than the values measured in the corresponding seasons in 2006. This was consistently reflected in the calculated subgrade modulus indicating that the amount of local rainfall (snow is very rare at the project sites) in the previous rain season was the primary factor affecting moisture content in the pavement structures.

The drainage condition also affects the moisture condition of pavement materials. The two test sections on Route 20 were both situated on an embankment crossing irrigated agricultural fields. The two test sections on Route 33-Ventura were mostly surrounded by shrub grassland. Consequently, materials on Route 33-Ventura would be expected to be drier than the materials in Route 20, and their moisture content more sensitive to the amount of precipitation. The subgrade modulus (E_{SG}) values for Route 33-Ventura were between 16 and 34 percent higher in 2007 than in 2006, while the increase for Route 20 was only between 2.0 and 12 percent.

The effects of moisture on the foamed asphalt resilient moduli is conceptually illustrated in Figure 4.72, which includes the estimated relative moisture conditions of the field material as well as the moisture conditions used in the laboratory study (Chapters 7 through 9). The resilient modulus of the foamed asphalt is more sensitive to moisture change when the in-place moisture content is relatively low (i.e., late

summer and the fall). This explains why the foamed asphalt layer modulus (E_{FA}) values were similar for spring 2006 and spring 2007, but significantly different for fall 2006 and fall 2007. Simulating real field moisture conditions in a laboratory is difficult in that the distribution of the water at a micro scale has a greater effect on material behavior than the bulk moisture content of the material. The wetting and drying cycles that occur in the field are difficult to measure accurately and then duplicate in a laboratory. The relation shown in Figure 4.72, based on field measurements, confidently depicts the most fundamental effects of moisture on the resilient modulus of foamed asphalt mixes, despite its qualitative and conceptual nature.

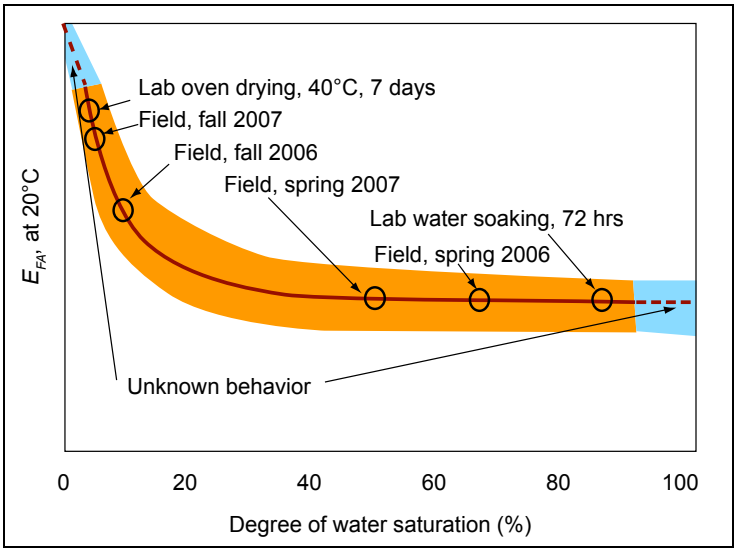

Figure 4.72: Conceptual illustration of moisture sensitivity of foamed asphalt modulus.

Normalized foamed asphalt layer modulus (E_{FA}) values of the four sections are summarized in Table 4.8. The percentage reduction of the foamed asphalt mix resilient modulus attributed to moisture conditioning in the field was calculated on the basis of comparing measured values in the spring (2006 and 2007) to the measured values in the fall of 2007 for the same section. When assessing the precipitation during the two rain seasons, stiffness measurements in the fall of 2007 were considered to be better reference values than those of the fall of 2006 for approximating the unsoaked condition tested in the laboratory. Based on these observations, stiffness reduction of the foamed asphalt materials under field moisture conditions in wet seasons could be as high as 30 to 45 percent compared to that in the dry seasons.

Table 4.8: Summary of Normalized Foamed Asphalt Layer Resilient Modulus

Test Section	E_{FA} (normalized to 20°C)			Stiffness Reduction due to Moisture Conditioning (%)
	Spring 2006/07	Fall 2006	Fall 2007	
20-A	579	699	950	39
20-B	776	947	1,067	27
33-Ven-A	805	1,005	1,283	37
33-Ven-B	1,133	1,316	2,029	44

These results are supported by laboratory testing discussed in Chapter 7 where the triaxial resilient modulus reduction of foamed asphalt mixes due to water soaking was between 5 and 30 percent (Section 7.4.5). An additional reduction of between 15 and 40 percent can be expected if the substantial reduction of stiffness in tensile stress states is taken into account (Section 7.7). These two mechanisms (compression/shearing by triaxial tests and tension by flexural beam tests) need to be combined to explain the stiffness reduction observed in the field, as the use of triaxial tests alone might suggest design values that are not sufficiently conservative.

4.6.7 Resilient Modulus Characterization of Route 33 (05-SB,SLO-33)

This part of the report compares the distressed and intact FWD subsections on Route 33 in Santa Barbara and San Luis Obispo counties.

Asphalt Concrete Stiffness

Figure 4.73 shows the backcalculated asphalt concrete layer stiffness (mean value of each section) against the calculated subsurface temperature at the mid-depth (1.8 in. [45 mm]) of the asphalt concrete layer. Data for the two test seasons (spring and fall), as well as for subsections in distressed and intact condition are plotted with different symbols. All data points form a straight line, which implies that the only factor affecting the backcalculated asphalt concrete stiffness was temperature. There was no significant difference in asphalt concrete properties between the intact and distressed subsections. The temperature sensitivity coefficient for this asphalt concrete was calculated as 0.027 using a simple linear regression, indicating that stiffness doubles if the temperature decreases by 20°F (11°C).

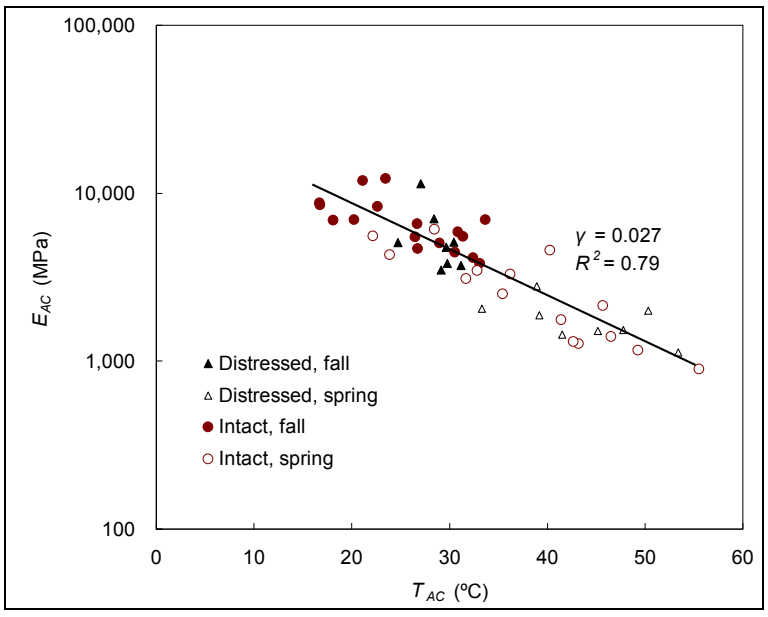

Figure 4.73: Temperature dependency of backcalculated AC modulus on SR33-SB/SLO.

Foamed Asphalt Layer and Subgrade Stiffnesses

The backcalculated foamed asphalt base layer and subgrade stiffnesses (mean values of each subsection) are summarized in Table 4.9. The calculated mid-depth temperatures (T_{FA}) in the foamed asphalt base layer are shown in the table, together with the visual condition as of May 2008. The mean values for certain subsections were calculated on a selected segment to minimize the influence of patched areas and segments showing high spatial variation.

Table 4.9: Test Results for Route 33 in Santa Barbara and San Luis Obispo Counties[1]

06/2006	30.8	437	47.3	285	62
05/2007	17.6	934	27.0	468	76
11/2006	20.4	536	35.0	403	68
11/2007	15.6	971	25.4	718	76
06/2006	32.6	322	–	–	63
05/2007	19.6	503	–	–	69
11/2006	21.3	344	35.2	262	64
11/2007	16.3	667	26.2	431	72
06/2006	34.8	692	–	–	62
05/2007	21.4	1173	–	–	82
11/2006	23.8	741	–	–	71
11/2007	18.0	1135	27.0	957	91
06/2006	38.0	143	44.8	112	67
05/2007	23.1	207	–	–	69
11/2006	25.6	152	–	–	70
11/2007	18.8	178	–	–	75
06/2006	39.3	56	–	–	42
05/2007	24.8	76	–	–	47
11/2006	26.6	63	–	–	49
11/2007	19.9	73	26.0	58	51
06/2006	–	-	–	–	–
05/2007	25.8	232	–	–	83
11/2006	27.8	181	–	–	85
11/2007	21.1	221	26.2	166	85
06/2006	41.1	114	–	–	52
05/2007	27.2	120	–	–	47
11/2006	30.4	90	–	–	49
11/2007	21.3	142	25.1	109	58
	Section 33-SB/SLO-H (0 m - 800 m, distressed)				
06/2006	39.7	111	–	–	46
05/2007	27.4	140	–	–	47
11/2006	31.0	118	–	–	48
11/2007	23.2	155	–	–	51

[1] There was insufficient data collected from this project to accurately determine a temperature normalized modulus (E_{FA}) for the foamed asphalt base.

Table 4.9: Test Results for Route 33 in Santa Barbara and San Luis Obispo Counties[1] *(cont.)*

06/2006	41.0	477	–	–	89
05/2007	27.4	726	–	–	101
11/2006	33.0	589	–	–	94
11/2007	24.4	755	–	–	101
	Section 33-SB/SLO-J (0 m - 600 m, distressed)				
06/2006	45.4	137	–	–	47
05/2007	–	–	–	–	–
11/2006	33.3	132	–	–	46
11/2007	–	–	–	–	–

[1] There was insufficient data collected from this project to accurately determine a temperature normalized modulus (E_{FA}) for the foamed asphalt base.

Box plots for subgrade modulus (E_{SG}) and foamed asphalt-treated base modulus (E_{FA}) as measured in November 2007 are shown in Figure 4.74 and Figure 4.75 respectively. These show all results (instead of just means of each subsection) and therefore a higher variation was expected. The results indicate that the subgrade and foamed asphalt layers in the distressed subsections were significantly weaker compared to the intact subsections. It is interesting to note that the modulus of the foamed asphalt layer in the distressed subsections had smaller variation than that in the intact sections. This is attributed to the foamed asphalt mixes in these subsections all having a modulus approaching the lower limit value for this type of material (i.e., similar to an equivalent untreated material).

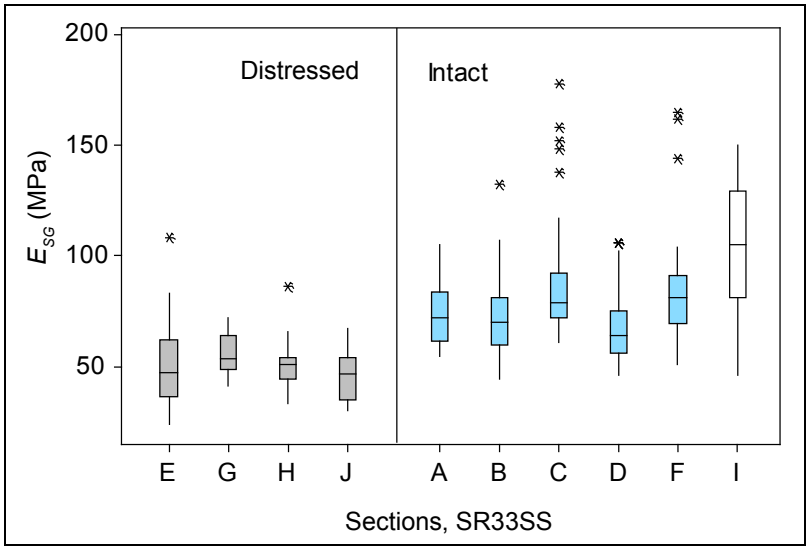

Figure 4.74: Subgrade modulus for all sections on Route 33 (SB,SLO) (11/2007).

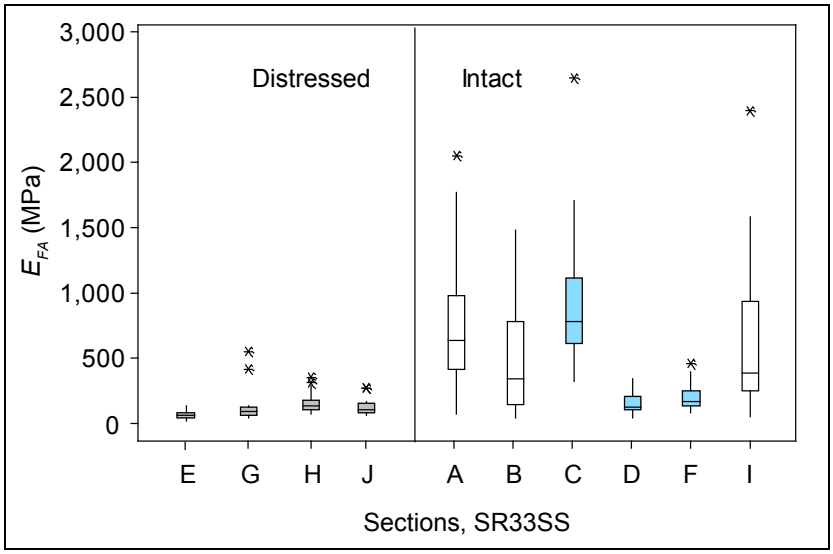

Figure 4.75: Foamed asphalt layer modulus for all sections on SR33-SB/SLO (11/2007).

Based on this data, Section 33SB/SLO-D and Section 33SB/SLO-F, which appeared intact during the May 2008 visual assessment, are likely to show evidence of distress before the remaining intact sections (it should be noted that distress was observed close to the start of Section 33SB/SLO-F). The foamed asphalt materials in these two subsections were only marginally stiffer than that of the distressed subsections, but the subgrade was moderately stiffer (or drier), which probably delayed the onset of distress. This confirms the importance of the support provided by the subgrade or subbase layers materials in obtaining greater stiffness in the foamed asphalt layer, as predicted in the sensitivity study in Chapter 3.

Figure 4.76 and Figure 4.77 show box plots for subgrade modulus (E_{SG}) and foamed asphalt-treated base modulus (E_{FA}) for the four evaluations times. Mean values for the distressed and intact sections are grouped together. There is a clear boundary for subgrade modulus (approximately 60 MPa [8.7 ksi]) differentiating the distressed and intact sections. A similar trend was observed for foamed asphalt-treated base stiffness with all distressed sections having a mean resilient modulus lower than 155 MPa (22.5 ksi), compared to the sections with no visible distress, which had much higher stiffnesses, depending on the temperature and moisture condition when tested. The foamed asphalt mix modulus measured each spring was lower than that measured each fall. This is attributed in part to the difference in moisture content and part to the difference in temperature. Insufficient data were collected to quantitatively differentiate these two effects in a similar manner to the other roads.

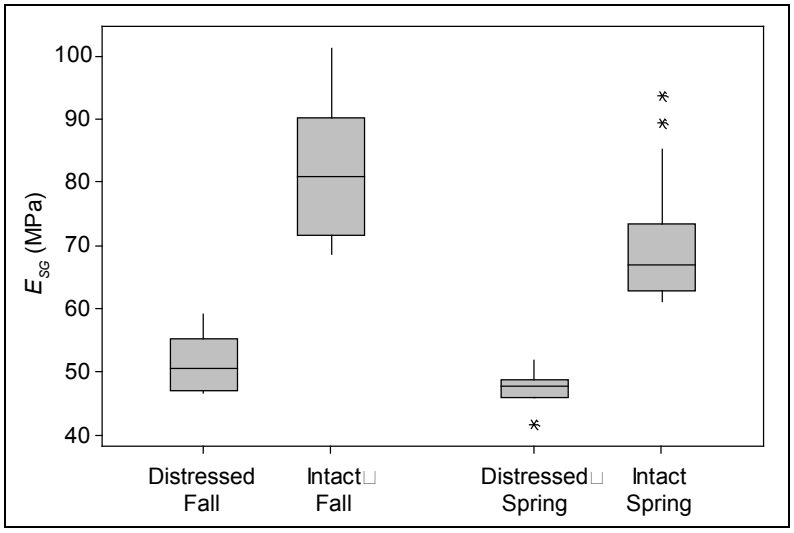

Figure 4.76: Subgrade modulus for all sections on SR33-SB/SLO.

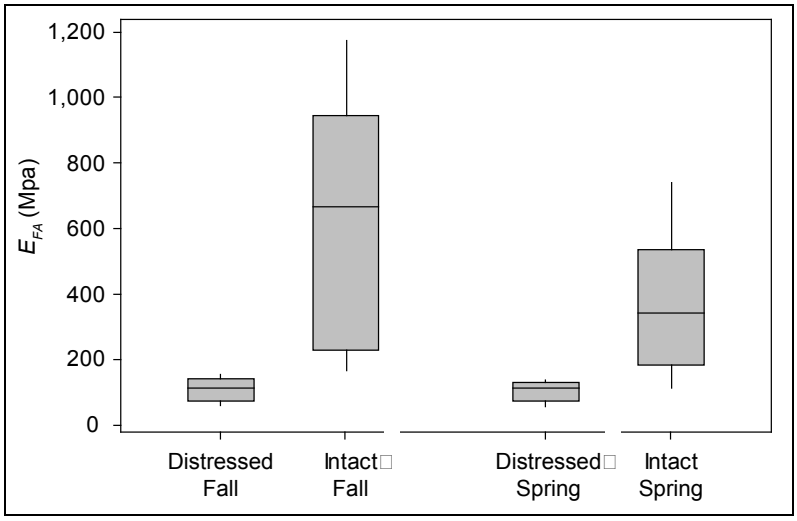

Figure 4.77: Foamed asphalt layer modulus for all sections on SR33-SB/SLO.

4.6.8 Summary

FWD testing and associated backcalculation of the data are useful for assessing the effects of temperature and moisture content on the properties of the different layers in a recycled pavement.

In this study, the asphalt concrete layer stiffness for the same project was only influenced by temperature, with the values comparable between the different test subsections. Asphalt concrete stiffnesses on distressed and intact subsections on the same project were not significantly different.

The moisture content in the pavement structure had a significant influence on the foamed asphalt layer stiffness. Moisture content varied with local precipitation and was also affected by drainage conditions.

The differences in stiffness measured in the wet and dry seasons respectively was as high as 40 percent, which is of a higher relative magnitude than the seasonal variation of subgrade stiffness.

The effects of temperature on foamed asphalt mix stiffness were quantified by field measurements. The average temperature sensitivity coefficient for the four sections on Route 20 and Route 33 in Ventura County was 1.3 psi/°F (0.016 MPa/°C), which is close to the value measured in the laboratory (Section 6.5.5).

The distressed sections on Route 33 in Santa Barbara and San Luis Obispo counties had significantly lower subgrade stiffnesses than the intact sections, which was attributed to poor drainage conditions. Based on the observations in two test pits, it was concluded that the foamed asphalt in these areas had not cured as of November 2007, more than two years after construction, because of excessive moisture in the layer. This is supported by extensive laboratory testing discussed in Chapters 7 through 10, which showed that strength development of foamed asphalt mixes without cement was entirely dependent on evaporation of the compaction moisture and excess in-place moisture.

4.7 Preconstruction Assessment with Falling Weight Deflectometer

4.7.1 Introduction

Prematurely failed areas in FDR-foamed asphalt projects are often associated with weak or soft subgrade materials and/or inadequate drainage, which lead to conditions of inadequate support for the upper pavement layers. The FWD has been successfully used in conjunction with visual assessments, cores, and DCP measurements to identify problem areas on candidate reclamation projects. A method for preconstruction FWD is discussed below.

4.7.2 Using Deflection Modulus to Approximate Subgrade Modulus

Preconstruction site evaluation often involves testing pavements with severe alligator cracking, which violates the continuity assumption for modulus backcalculation based on FWD data. A simple method is proposed for approximating the subgrade modulus from the deflection measured by one of the FWD sensors. The Boussinesq's equation for this calculation is shown below (Equation 4.1):

$$E_{def}(r) = \frac{(1-v^2)\times P}{\pi \times r \times d} \quad (4.1)$$

where: E_{def} = modulus;
P = the applied load;
v = Poisson's ratio, generally using 0.35;
r = the distance from the load center to the measured deflection;
d = measured deflection at r.

For a layered pavement structure the calculated deflection modulus is a function of the distance (r) at which the deflection is measured. For typical California FDR-foamed asphalt structures, it was found that $E_{def}(r)$ at r = 600 mm (24 in.), typically the distance of the fifth sensor on FWD equipment, is a reasonable indicator of subgrade modulus (i.e., E_{def}(600 mm) ≈ E_{SG}). Validation for this finding is provided through a comparison of pre- and postconstruction measurements on the Route 33 project in Ventura County.

4.7.3 Comparison of Pre- and Post-Construction FWD Measurements

Comparisons between preconstruction deflection modulus (E_{def}(600 mm)) and postconstruction backcalculated subgrade modulus (E_{SG}) are shown in Figure 4.78. Test results for the spring measurements in 2006 and 2007 are shown as they were less stiff than the corresponding fall measurements and therefore provide a more useful example. For both sections, E_{def}(600 mm) matched E_{SG}, reasonably well with a consistent trend. In 2007, the E_{SG} was slightly higher given that the subgrade material was probably drier due to the lower precipitation in the previous months.

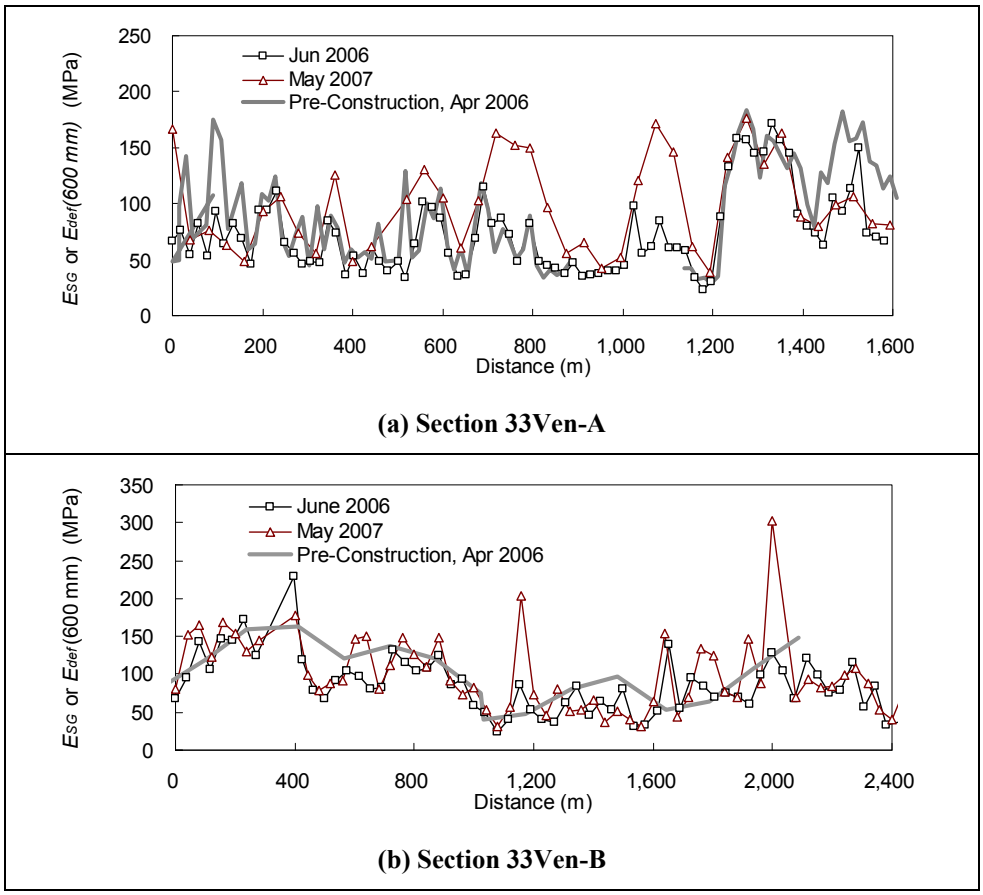

Figure 4.78: Comparison between pre- and postconstruction modulus determinations.

4.7.4 Interim Guidelines for Preconstruction FWD Testing

The following interim procedure is proposed for identifying weak subgrade areas with an FWD during the project design process. This procedure will be updated as more test data are collected.

- Testing should be carried out at the end of the rain season, when subgrade moisture is likely to be highest.
- The recommended test interval is 20 m (66 ft), which allows for a testing productivity of approximately one lane-km/hour (0.62 lane-miles/hour). A longer test interval can be adopted if there are constraints such as limited traffic closure schedules; however, this increases the potential for missing weaker sections.
- The lane with the worst existing condition should be tested unless each lane is designed separately, in which case both lanes should be tested.
- Testing should be carried out between the wheelpaths to minimize the effects of severe wheelpath cracking on the seating of the FWD load and sensors.
- The following criteria should be used in interpreting the deflection data from the 600 mm sensor (load normalized to 566 kPa [82 psi], or 40 kN [9,000 lb]):
  - If the calculated deflection modulus E_{def}(600 mm) is greater than 45 MPa (6.5 ksi) (equivalent to a 0.37 mm [15 mils] deflection measured by the 600 mm [24 in.] sensor), the subgrade should not require any specific improvement.
  - If the calculated deflection modulus E_{def}(600 mm) is between 45 MPa and 25 MPa (6.5 ksi and 2.6 ksi.) (equivalent to between 0.37 mm and 1.25 mm [14.6 and 49 mils] deflection measured by the 600 mm sensor, subgrade-related problems are likely and corrective action should be taken prior to reclamation of the pavement. This could include, but is not limited to, excavation and replacement of the weak material, reinforcement, raising the embankment, and/or provision of additional drainage. (For example, in Figure 4.78, the segment from 1,140 m to 1,220 m [3,740 to 4,000 ft] on Section 33Ven-A may require special treatment.)
  - If the calculated deflection modulus E_{def}(600 mm) is less than 25 MPa (equivalent to more than 1.25 mm (49 mils) deflection measured by the 600 mm sensor), a more detailed survey should be undertaken and appropriate actions or reconstruction options considered.

4.8 Assessment of Planned Projects

The UCPRC was only notified of one project prior to construction, namely the Route 33 rehabilitation in Ventura County. This project is discussed in Section 4.4.4.

4.9 Summary of Recommendations

Recommendations for project selection and construction are discussed in Chapter 11, based on observations on the four projects discussed in this chapter and on observations from other non-Caltrans projects. Key issues relating to observations in this chapter include:

- Project Selection and Design:
  - A comprehensive field evaluation should be carried out by the project designer, with the assistance from the District Materials Office, prior to deciding on whether FDR-foamed asphalt is an appropriate strategy for a particular project. This should include a visual assessment of the road, drainage structures, and adjacent land use practices (especially agriculture and associated irrigation), an FWD assessment, coring, DCP measurements, and material sampling.
  - Active fillers (cement or other appropriate filler) should be included in all mix designs to ensure adequate early strength development.
- Test Section Construction:
  - Test section construction should be closely monitored to ensure that performance data collected during monitoring can be appropriately analyzed and causes for poor performance correctly attributed. Test sections should be representative of the project being evaluated.
  - Construction quality appears to be a concern and quality control/quality assurance needs to be adequately addressed in the project specifications and strictly enforced. The costs of independent quality control are typically more than offset by longer pavement life.
- Postconstruction Performance:
  - The cause of early failures should be determined and appropriate corrective actions taken prior to undertaking expensive repairs (e.g., digouts) to ensure that the same failure does not re-occur. For example, the digouts on Route 33 should have been initiated after drainage problems had been identified and corrected. Many premature failures can be eliminated with proper field evaluation and design practice prior to construction.
- Pre-pulverization should only be considered on very thick pavements as two passes can break the material down to a finer than desirable grading.
- Mixing moisture should be carefully controlled. Water should be added during recycling from a tanker coupled to the recycler and not at a later time.
- A padfoot roller should be assigned to each recycling train and initial compaction should be completed prior to the application of additional water.
- Density and moisture content measurements should follow a strict pattern. Equipment should be appropriately calibrated for the specific mix and material. Cores should be taken periodically to validate the measurements.

5. LABORATORY STUDY: OVERVIEW

5.1 Introduction

Most large laboratory studies on foamed asphalt mixes have been carried out with primarily natural aggregates. As discussed in previous sections, most reclamation projects in California are on pavements consisting of multiple layers of asphalt concrete, with natural aggregates comprising between 10 and 25 percent of the mix. The University of California Pavement Research Center (UCPRC) study therefore concentrated on predominantly recycled asphalt pavement (RAP) materials. Key issues identified from the experiences of earlier studies by other practitioners formed the basis for the design of the testing program.

5.2 Laboratory Study Phases

The laboratory study was divided into four phases and each is discussed in a separate chapter. A comprehensive factorial design was prepared at the beginning of the study. However, it was clear that the number of tests required to complete the full factorial was impractical in terms of material requirements and laboratory resources. A phased approach was therefore adopted in the plan, which entailed a series of small experiments based on a series of partial factorial experimental designs. By following this approach, researchers were able to gain an understanding of key issues influencing the performance of foamed asphalt mixes, and use these to adjust the testing program and relevant factorial elements accordingly to make the best use of resources.

In the first phase (Chapter 6), specimen preparation procedures, test methods, and analysis techniques were assessed and developed. This formed the basis for testing in the later phases of the study. The foam and foamability characteristics of a selection of California asphalts, and the temperature sensitivity of mixes were also assessed in this phase. A method to visually evaluate the fracture faces of tested specimens in a consistent way was developed in addition to these assessments.

Phase 2 (Chapter 7) covered investigations into the effects of asphalt binder properties, RAP sources, RAP gradations, mixing moisture content, and mixing temperature on foamed asphalt mix properties. It also investigated different laboratory test methods for assessing the strength and stiffness characteristics of foamed asphalt mixes, and the development of an anisotropic model relating laboratory stiffness tests to field stress states. This work was performed on specimens without active or semi-active fillers so that the effects of the asphalt alone could be evaluated.

The third phase (Chapter 8) extended the objectives of Phase 2 with more detailed investigations on variables related to RAP sources and asphalt binder characteristics.

The final phase (Chapter 9) of laboratory testing focused on the role and effects of active, semi-active, and inert fillers on foamed asphalt mix performance, as well as issues pertaining to curing.

5.3 Materials

5.3.1 Aggregates

A large supply of representative material was critical for undertaking the laboratory study and three different reclamation projects were identified in California from which materials were collected. The first was on Route 33 in Ventura County (see Chapter 4). Material from this site was collected from a pre-pulverization run where no foamed asphalt was added. Aggregates in the RAP were of predominantly granitic origin, while those in the underlying layer were of quartzitic (alluvial) origin. The second project sample came from Route 88 in Amador County, where a section of road was pulverized as part of a realignment project. Aggregates in the RAP and underlying layer were of granitic origin. The material produced here was the same as that of a typical pre-pulverization run on a foamed asphalt reclamation project, and it was undertaken by the same contractor employed on the Route 33 project, using the same recycling equipment. Samples from the third project were from an access road in Sacramento. Aggregates in the RAP and underlying layer were of granitic origin, with similar characteristics to the Route 88 material. The pulverization depth on the sections where material was sampled was approximately 8.0 in. (200 mm), consisting of between 6.0 in. and 7.0 in. (150 mm and 175 mm) of cracked asphalt concrete and between 1.0 in. and 2.0 in. (25 mm and 50 mm) of aggregate base.

Material from the third project was not subjected to comprehensive testing due to the similarity in characteristics between it and the Route 88 material.

Although the Route 33 and Route 88 materials are representative of a relatively large proportion of California roads, aggregate chemistry of materials (e.g., basalt) occurring in other parts of the state could influence the behavior of foamed asphalt-treated materials, specifically with regard to active and semi-active fillers. However, during the period of the UCPRC study there were no reclamation projects performed on roads constructed of other commonly used materials in California. Since these materials could not be assessed, the results from Phase 4 of the laboratory study are not necessarily applicable to all reclamation projects in California. A range of active fillers should therefore be tested when developing mix designs until sufficient knowledge and experience on a spectrum of California materials has been accumulated.

Gradings and aggregate characteristics from the projects were compared with material sampled from other projects where different recycling machines (Wirtgen, Caterpillar, Terrex) were used. No significant differences were observed and comparative tests between materials recycled by different equipment were considered unnecessary.

Early familiarization tests, discussed in Section 6.3 were carried out on processed RAP sourced from an asphalt plant north of Sacramento, California.

Considerable time was devoted to understanding the effects of fine materials on performance. Gradings and specifically the fines content were adjusted in many of the experiments to assess these effects. In all instances, course aggregate fractions for these adjustments were obtained from Graniterock Company's A.R. Wilson Quarry near Aromas, California, and fines, in the form of bag-house dust, were obtained from Graniterock's asphalt plant at the same quarry.

5.3.2 Asphalt Binders

Asphalt binders were sourced from three different refineries in California. Details on the binders and the reasons for selecting a particular binder for specific tests are discussed in the relevant sections in the following chapters.

5.4 Test Methods

A number of different test methods were used in the study. These are discussed in the relevant sections under each phase in the following chapters.

6. LABORATORY STUDY: PHASE 1

6.1 Introduction

The first phase of the laboratory study was carried out to familiarize the research team with equipment, procedures, and test methods, and to obtain a basic understanding of the attributes of typical California foamed asphalt mixes before more detailed testing was carried out in the later phases. Tasks in this phase included:

- Assessment of specimen preparation procedures and test methods.
- Assessment of the foamability characteristics of California asphalts.
- Assessment of the temperature sensitivity of foamed asphalt mix stiffness.
- Development of techniques for analyzing fracture faces of tested Indirect Tensile Strength and Flexural Beam test specimens.

6.2 Experiment Design

A testing factorial was not prepared for the assessment of specimen preparation procedures and test methods or for the assessment of the temperature sensitivity of foamed asphalt mixes. Instead, an iterative testing program was followed, with the findings from earlier stages dictating procedures in subsequent stages until a sound understanding of the principles was obtained. In assessing the temperature sensitivity of mix stiffness, one material and one binder type were used to produce the three specimens. The only variable considered in this study was asphalt content (three values). The factorial followed in the study on foamability characteristics is discussed in Section 6.4.

All foamed asphalt was produced with a Wirtgen WLB-10 laboratory foaming unit. The aggregate was mixed in a custom-built pugmill, with the foam injected directly during mixing.

6.2.1 Materials

Aggregate

The Recycled Asphalt Pavement (RAP) material used in this phase was sourced from a Granite Construction hot-mix asphalt (HMA) plant in Sacramento, California. This RAP material was plant processed with a controlled gradation, and is used in some HMA products as a substitute for more expensive virgin aggregates. The gradation as supplied was somewhat fine (Figure 6.1, Gradation-1) and was modified with crushed aggregate (100 percent passing 19 mm [0.75 in.]) sourced from Graniterock's A.R. Wilson Quarry, to obtain a coarser gradation (Figure 6.1, Gradation-3). A finer gradation was also

produced by modifying Gradation-3 with additional fines (100 percent passing 0.075 mm [#200]), also obtained from the A.R. Wilson Quarry (Figure 6.1, Gradation-2). Gradations-1, -2 and -3 had 9.6 percent, 9.3 percent, and 5.3 percent passing the 0.075 mm (#200) sieve by mass respectively.

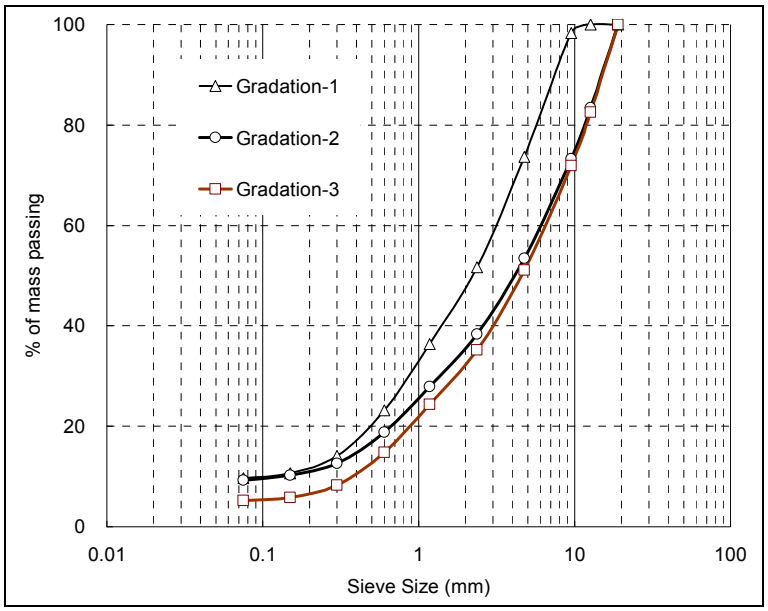

Figure 6.1: RAP gradation for Phase 1 laboratory study.

Asphalt Binder

One AR-4000 asphalt binder (approximately equivalent to PG64-16) was used for the assessment of specimen preparation procedures and test methods, and in the temperature sensitivity study. The binders used in the foamability study are discussed in Section 6.4.

6.3 Assessment of Specimen Preparation Procedures and Test Methods

This task was considered as exploratory and the procedures for specimen fabrication and testing were therefore developed incrementally, with changes and improvements based on the reasonableness and repeatability of the results. Procedures assessed in this task included:

- Comparison of strength tests,
- Specimen fabrication and testing procedures for triaxial resilient modulus tests and flexural beam tests,
- Testing under soaked and unsoaked conditions,
- Specimen curing,
- Differentiating the effects of foamed asphalt and active filler,
- Optimizing mixing temperatures,
- Specimen compaction methods

The findings from these assessments are summarized below, with the adopted procedures discussed in more detail in the relevant sections in Chapters 8 and 9. The preliminary findings from this task differed in some instances from original expectations based on the literature review. Where appropriate, adjustments were made to the work plan for later testing.

6.3.1 Comparison of Test Methods

Comparison of ITS and UCS Tests

The strength test methods in the original work plan included the Unconfined Compressive Strength (UCS) test, the monotonic flexural beam test, and the triaxial strength test. Initially, the Indirect Tensile Strength (ITS) test was not included based on concerns raised in the literature with regard to reliability, repeatability, and reproducibility of the test results, feedback from experienced researchers and engineers, and UCPRC experience with this test on hot-mix asphalt. It was further reported *(26)* that ITS and UCS were indicators of similar and highly correlated properties of foamed asphalt mixes. However, given that the ITS test is widely used and relatively simple and that equipment for carrying out the test is readily available in California, it was included in this task to reassess its potential use in foamed asphalt mix design.

The results indicated that satisfactory results can be obtained from the ITS test provided that specimen preparation is strictly controlled and that sufficient replicates are tested. Observations also showed that specimen preparation and testing for the ITS test using equipment available at the UCPRC was faster than that for the UCS test. Therefore a more in-depth comparison between a number of strength tests was planned for and carried out in Phase 2 to investigate whether the ITS test could be used as the primary strength test method for later phases.

6.3.2 Revised Triaxial and Flexural Beam Test Procedures

Based on a series of exploratory tests during this phase of the UCPRC study, triaxial resilient modulus and flexural beam test procedures followed at the UCPRC were adjusted to suit the properties of foamed asphalt-treated materials. Adjustments to the AASHTO T307 (*Standard Method of Test for Determining the Resilient Modulus of Soils and Aggregate Materials*) triaxial resilient modulus test protocol included:

- A new specimen compaction method to control density more precisely and to minimize aggregate particle segregation, and
- Methods of quantifying the effects of different loading rates.

The flexural beam test procedure followed was loosely based on AASHTO T97 (*Standard Method of Test for Flexural Strength of Concrete [Using Simple Beam with Third-Point Loading]*). Details on the procedure used are provided in Section 7.2.3. Adjustments to the original protocol included:

- The specimen height was changed to 80 mm (3.2 in.) instead of 150 mm (6 in.) to allow single lift compaction, and
- The loading was displacement rate-controlled rather than stress rate-controlled.

Details on testing with these methods are discussed in Chapter 7.

Fatigue Beam Tests

Fatigue tests were tentatively included in the original work plan to study fatigue properties of foamed asphalt mixes. Mixed success has been reported in the literature with regard to fatigue testing of foamed asphalt mixes, with some tests unsuccessful *(17)* and others providing useable results *(8,27)*. However, realistic results only appeared achievable at low testing temperatures (5°C [41°F]). This was taken into consideration when including fatigue testing in the work plan. A larger beam specimen (450 mm x 150 mm x 80 mm [18x6x3.2 in.]) was allowed for in the experimental design in an attempt to overcome some of the problems with early testing by other practitioners. However, preliminary testing revealed that this large specimen, prepared without cement, was very difficult to handle, especially when soaked. In some instances, specimens collapsed under their own weight and the control of stress and strain levels was difficult. The results obtained were inconsistent and consequently fatigue testing was excluded from the work plan.

6.3.3 Testing under Unsoaked and Soaked Conditions

During initial laboratory testing, it was observed that foamed asphalt mixes, when tested after soaking, showed very different behavior compared to mixes tested in the unsoaked (dry) state. Compacted RAP materials generally have a relatively high strength in the unsoaked state, even without any stabilization agent. The addition of foamed asphalt and/or active fillers has limited additional influence on this unsoaked strength, making observation of any stabilization effects difficult. However, when tested after soaking, the effects of the stabilization were clearly apparent when comparing treated and untreated specimens. Since many pavements in California that are potentially suitable for FDR with foamed asphalt are subject to moisture problems, either from high rainfall, irrigation, or poor drainage conditions, an understanding of performance under soaked conditions was considered important. Although some practitioners have focused their research on the results of unsoaked testing, the UCPRC research work plan *(1)* was modified to include both soaked and unsoaked testing in all experiments.

6.3.4 Curing

During early testing, the results confirmed that the strength development mechanism of foamed asphalt mixes during curing is closely related to the loss of moisture, especially for mixes that do not contain cementitious fillers. In this exploratory study, several specimens were sealed immediately after compaction to prevent moisture loss and then subjected to strength tests at periodic intervals. No significant strength development was observed during the six-month observation period. This was consistent with the finding of Bowering *(28)* that foamed asphalt specimens do not develop full strength until most of the mixing moisture has evaporated. This was also consistent with the field investigation on Route 33 that showed very low stiffness in subsections with continuously high water contents (see Section 4.6.7). Initial studies showed that the temperature at which the evaporation process occurred appeared to be of lesser importance, provided that an upper limit of 50°C (122°F) was not exceeded. Asphalt binders typically used in foam applications will start to flow at temperatures higher than this, thereby changing the attributes of the material.

Strictly simulating field curing processes is difficult given the widely varying conditions experienced in California. There is also very little published data on the monitoring of field curing mechanisms of foamed asphalt pavement layers, or linking field curing to laboratory curing. In the UCPRC study, attention was given to producing uniformly cured specimens for investigating the stabilization effects of foamed testing rather than specifically studying curing mechanisms under certain limited conditions. After a series of experiments, a standard curing procedure was adopted for all tests where foamed asphalt stabilizing mechanisms were being assessed without the addition of active filler (all Phase 2 tests). This entailed extruding the specimen from the mold immediately after compaction (no initial curing in the mold), then placing the specimen in a forced draft oven at 40°C (104°F) for 72 hours (3 days) or 168 hours (7 days), depending on the test objectives and specimen dimensions. Specimens were not sealed or covered in any way. This procedure was based on procedures discussed by Ruckel *(29)*, with some modification. In tests where active fillers were added, curing procedures were adjusted depending on the specifics of the test and are detailed in Chapter 9. Curing mechanisms are discussed in more detail in Section 9.11.

6.3.5 Differentiating the Effects of Foamed Asphalt and Active Filler

The results of early tests indicated that the addition of portland cement, even in very small quantities (between one and two percent), significantly altered the behavior of foamed asphalt mixes, with the effects of the cement appearing to mask any effects of the foamed asphalt. This supported the initial recommendations in the work plan, which proposed that the stabilization effects of the foamed asphalt and foamed asphalt with active filler be investigated separately.

6.3.6 Mixing Temperature

Observations during early testing in this phase indicated that foamed asphalt dispersion was significantly influenced by the temperature of the RAP material during foam injection and mixing, and that aggregate temperatures needed to be controlled during specimen preparation. A small experiment was carried out to determine a minimum temperature at which mixing could take place. This study showed that inferior asphalt dispersion was likely if the aggregate temperature prior to foamed asphalt injection was lower than 20°C (68°F). Dispersion deteriorated with decreasing temperature. Based on this limited study, the acceptable temperature range for specimen preparation was set at 25°C to 30°C (77°F to 86°F).

A more in-depth study into the effects of mixing temperature on asphalt dispersion and associated performance was added to the work plan and is discussed in Section 7.6.

6.3.7 Specimen Compaction Methods

The original work plan *(1)* included a comparison of different compaction methods, as it was assumed that multiple compaction methods could be applied for the same test method. For instance 100 mm (4 in.) briquette specimens for the ITS test could be compacted by either the Marshall method or the kneading compactor, and cylindrical triaxial specimens could be compacted by compactors with or without kneading actions. A small study was undertaken to compare the following different compaction methods:

- California Kneading Compactor
- Marshall
- Modified Proctor
- Vibrating Hammer

The results of this study indicated that for each test type, there was generally only one compaction method that was technically optimal or practically feasible for the intended study. For ITS specimens, kneading compaction was considerably slower than Marshall compaction (two specimens per hour compared to ten specimens per hour), and thus not suited to the productivity requirements of this study (40 to 60 specimens per day). For triaxial specimens, the vibratory action of a compaction head without kneading yielded substantial segregation of the material. Based on experiences in this preliminary testing, one compaction method was selected for each test type, with emphasis shifted to comparing different strength/stiffness test methods instead of different compaction methods. The adopted compaction methods for each test were:

- 100 mm (4 in.) ITS: Marshall
- 152 mm (6 in.) ITS: Modified Proctor
- UCS: Modified Proctor
- Triaxial: Modified Proctor
- Beam: Vibrating hammer with kneading action

6.3.8 Summary of Recommendations from Preliminary Testing

The following recommendations were made based on the findings of this task:

- The ITS is potentially appropriate for mix design testing and performance studies, provided that sufficient replicates are tested, and that tests are repeated if there are significant differences between the replicate specimens of the same mix design and specimen preparation run.
- Fatigue beam testing using current specimen preparation procedures is not appropriate for testing foamed asphalt mixes, unless mixes with relatively high active filler contents are being assessed.
- All testing should be carried out on soaked specimens to obtain a valid indication of likely in-service conditions and to best understand the behavior of the foamed asphalt. Results from testing unsoaked and soaked specimens can be compared to obtain an indication of the moisture sensitivity of the material.
- The aggregate temperature during foam injection and mixing should be in the range of 25°C to 30°C (77°F to 86°F). Poor dispersion will be obtained at lower temperatures.

6.4 Assessment of Foamability Characteristics

The objective of this part of the study was to characterize the properties of the foam (foamability characteristics) of a typical range of asphalts expected to be used in California FDR-foamed asphalt projects. Tasks included:

- Measuring and optimizing the foam characteristics of a selection of asphalt types available in California, and
- Identifying potential problems with current methods of quantifying foam characteristics.

Only the foamability characteristics of the binders were investigated in this phase of the laboratory study. The effects of these characteristics on mix properties were investigated in Phases 2 and 3 of the laboratory study.

6.4.1 Quantifying Foam Characteristics

The determination of the foam characteristics of an asphalt binder entails measurements of the foam produced from that asphalt using specific equipment under specific conditions. The "foamability" or "foam potential" of a specific asphalt binder is a property that indicates the potential or capability of this asphalt to produce good quality foam. Asphalt with good foamability can produce foam with inferior foam characteristics if the test conditions are not optimized.

Many variables, both internal and external, are known to affect the foam characteristics of an asphalt binder. Comprehensive reviews of the literature on this topic were prepared by Jenkins *(4)* and Saleh and

Herrington *(5)* and are not repeated in this report. Saleh and Herrington's review showed that there was general consensus on the influence of different crude oil sources and the refining techniques used to produce the asphalts, but conflicting views on the effects of other factors, such as penetration grade and viscosity.

Foam characteristics are typically quantified in terms of the expansion ratio (ER) and the half-life ($\tau_{1/2}$). These are defined as follows *(3,6)*:

- The expansion ratio is a measure of the viscosity of the foam and will determine how well the binder will disperse in the mix. It is calculated as the ratio of the maximum volume of foam relative to the original volume of asphalt.
- The half-life is a measure of the stability of the foam and provides an indication of the rate of collapse of the foam during mixing. It is calculated as the time taken in seconds for the foam to collapse to half of its maximum volume.

Foam with a higher expansion ratio would be expected to have a larger surface area per unit mass and lower viscosity due to a thinner asphalt film. Consequently it is easier for this type of foam to coat more and finer aggregates. The half-life quantifies the stability of the foam. More stable foam has more effective time to interact with the aggregate, resulting in better coating of the particles. The two properties can be combined to determine a "foam index" *(3,4)*, which is based on the following assumptions:

- The decay of asphalt foam can be modeled with the equation for isotope decay.
- The lower limit of expansion ratio for workable (low viscosity) foam is four.
- The workability of foam can be characterized with the area between the expansion ratio decay curve and the line of ER=4 in the ER-time space.

The procedure for determining the foam index is discussed elsewhere in the literature and is not repeated in this report *(3,6)*.

For any given asphalt type, two controllable external factors, namely the asphalt temperature and the foamant water-to-asphalt ratio, affect the foam characteristics. The foamant water-to-asphalt ratio is defined as the ratio, by mass, of the quantity of the foamant water injected into the foaming chamber to the quantity of asphalt binder to be foamed. The foamant water creates the foam when it is injected into the hot asphalt. In the literature *(3,6)*, it is generally accepted that:

- For a given foamant water-to-asphalt ratio, increasing the asphalt temperature results in higher expansion ratios and longer half-life, and

- For a given asphalt temperature, increasing the foamant water-to-asphalt ratio, results in higher expansion ratios, but shorter half-life.

The procedure for assessing foam characteristics measures the properties of the foam when it is in an empty container.. However, foam characteristics are influenced by many variables in a mix, including, aggregate temperature, fines content, aggregate moisture content, presence of active filler, etc., and hence different asphalt binders with the same measured foam characteristics could behave differently when they contact the aggregate particles.

Saleh *(30)* proposed the use of the Brookfield rotational viscometer to directly measure the rotational viscosity of the foam over a time window of three to four minutes. This approach was proposed as an improvement over the more empirical procedure described above, but for practical reasons it has rarely been followed by other researchers.

6.4.2 Experiment Factorial

The experiment factorial for this part of the UCPRC study is summarized in Table 6.1.

Table 6.1: Experimental Design for Foamability Characteristics

Asphalt Source	3[1]	A, B, C[1]
Asphalt Performance Grade	4[2]	64-10, 64-16, 64-22, 70-10[2]
Asphalt Temperature (°C)	3[3]	150, 165, 175
Water/Asphalt Ratio (%)	5	1, 2, 3, 4, 5
Replicates	1	
Total Number of Foamability Tests	180	

[1] Original work plan considered two sources (Valley and Coastal).
[2] Original work plan considered two PG grades (64-10 and 64-16).
Refinery A: PG64-16, PG64-10 and PG70-10; Refinery B: PG64-22; and Refinery C: PG64-16.
[3] Original work plan considered five temperatures (140, 150, 160, 170, 180).

This design differs slightly from the proposal in the work plan *(1)*, which was changed to consider a broader spectrum of asphalt sources and performance grades, but fewer binder temperatures. The original experimental design considered testing asphalt binders from the primary California coastal and valley sources. Discussions with the representatives from various refineries revealed that the source of the crude oil is not a stable indicator of asphalt properties, as the oil is obtained from multiple sources (including imports), with source selection and blending dependent on availability, price, and performance grade (PG) requirements. In terms of the performance grade, binder produced from certain crude sources may not meet the required grade and hence blends of different crudes may be used. For example, one of the binders used in the UCPRC study was a mix of crude oils sourced from the San Joaquin Valley (approximately

90 percent) and from Ecuador (approximately 10 percent). Consequently the experimental design was altered to consider asphalt refinery brands as a differentiation of the oil source. Performance grade certification tests were performed by the suppliers (results are provided in Appendix B). Asphalt binders were sourced from three refineries in northern California, which are referred to anonymously as Refinery or Asphalt -A, -B and -C.

6.4.3 Test Procedure: General

The test procedure for determining foamability characteristics of the different binders was carried out according to the recommendations in the Wirtgen WLB10 operation manual *(31)*.

6.4.4 Test Procedure: Foaming Temperature Considerations

During the course of experimentation with the Wirtgen WLB10 Laboratory Foaming apparatus, certain anomalies were noted with the binder temperature settings. The equipment's heating element is located at the bottom of the binder tank (kettle) on the apparatus and this, together with the highly viscous properties of the binder, results in variation in temperature with depth in the tank. Temperature differences up to 5°C (9°F) were measured with a calibrated thermocouple at different positions in the tank. The apparatus thermometer probe is highly damped, and hence the value shown is more a "moving average" of the asphalt binder temperature over a certain period of time (as long as several minutes), rather than a real-time indicator.

After completion of a series of equipment checks in March 2007, it was noted that the tank thermometer recorded a lower temperature than that recorded with a calibrated digital thermocouple. The thermometer was replaced by the local Wirtgen agent in July 2007. Correlations between the values measured by the original thermometer, the new thermometer, and the digital thermocouple were obtained for the purpose of temperature correction (Figure 6.2). The study had continued in the period between identification of the thermometer problem and replacement of the part and temperature values were corrected using these correlations. All temperatures reported below are equivalent to the new thermometer measurements. Given that the original thermometer underestimated the temperature values, only those foamability measurements determined at the higher temperature ranges in the tests before July 2007 were considered in the analysis.

Experimentation also revealed that precise control of the temperature was not possible due to limitations of the equipment. Fewer temperatures were therefore considered in the experimental design and some variation in temperatures between tests was accepted.

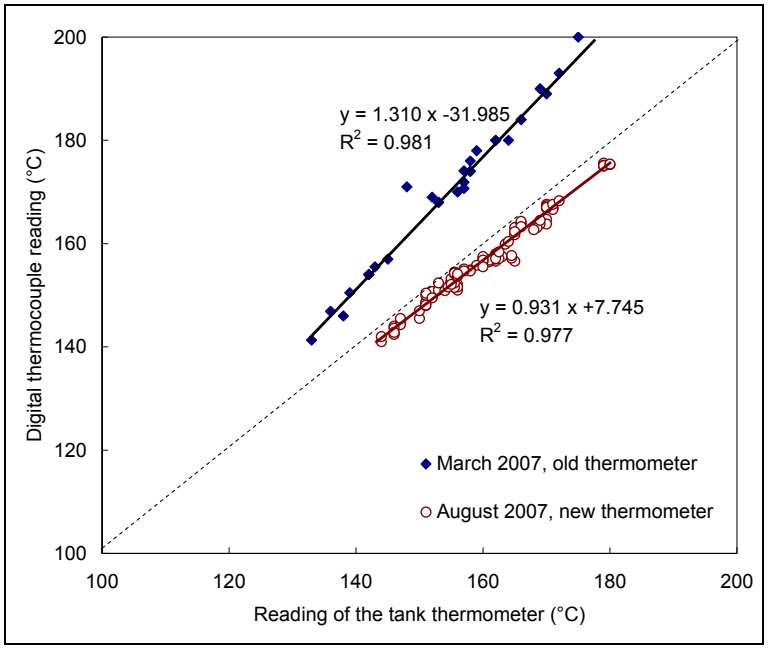

Figure 6.2: Correlation between WLB10 thermometers.

6.4.5 Test Procedure: Definition of the Half-Life

Two definitions for foam half-life have been reported in the literature:

- Jenkins *(4)* defines the half-life as "time measured in seconds for foamed bitumen to subside from the maximum volume to half of the maximum volume."
- The Wirtgen WLB10 operation manual *(31)* defines half-life as the time in seconds that the foam takes to dissipate to half of its maximum volume from the time the foam nozzle shuts off.

The definition in the South Africa guidelines *(3)* is vague but appears to follow Jenkins' definition. In practice, Jenkins' definition is considered somewhat subjective because the time point at which the foam reaches its maximum volume is difficult to identify. This is supported by Figure 6.3, which shows the decay curves of two hypothetical asphalt foams (Foam-A and Foam-B). According to Jenkins' definition, their half-lives are measured as *A1* and *B1* respectively; while the Wirtgen definition would be measured as *A2* and *B2*. The difference between the measurements by these two definitions is the time between the foam nozzle shutting off (at 0 seconds) and the foam reaching its peak volume. Depending on the binder, this can take a few seconds (e.g., Foam-B in Figure 6.3). The foam is stable and workable during this period and should therefore be included in the half-life, which is essentially a measure of foam stability.

In Figure 6.3, *A1* is similar to *B1*, but *B2* is considerably longer than *A2*. This would suggest that Foam-B is more stable than Foam-A and therefore *A2* and *B2* are considered to be more rational measurements.

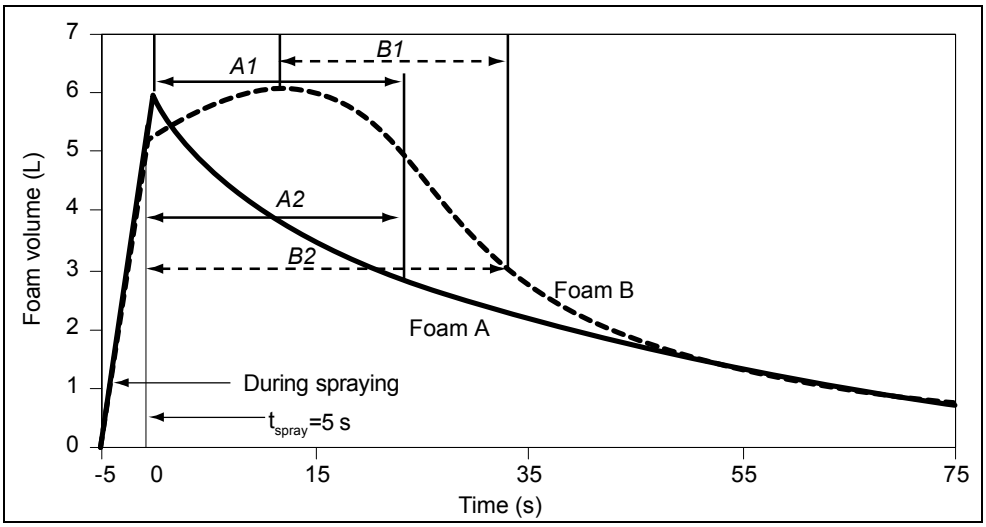

Figure 6.3: Two definitions of half-life of asphalt foam.

The Wirtgen prescribed procedure was thus considered more appropriate for the UCPRC study and was therefore adopted for the remainder of the study.

6.4.6 Test Results

The foam characteristics of each asphalt binder are shown in Table 6.2. Results are an average of multiple (two to four) measurements. It should be noted that the Refinery-A PG70-10 binder was only tested for foamability, and was not used in Phases 2 and 3 of the laboratory study. Two samples of Refinery-A PG64-16, obtained on different dates, were also tested.

Earlier research in the literature reported that "bitumens with lower viscosities foamed more readily and had higher foam ratios and half-lives than bitumens with higher viscosities, but the use of high viscosity bitumens resulted in superior aggregate coating" *(32)*. This behavior was not observed in the UCPRC study. The Refinery-A PG64-10 and PG70-10 produced foam similar to that of the Refinery-A PG64-16, although the viscosities were apparently higher. In the second phase of the UCPRC study, discussed in Chapter 7, it was found that binders with higher viscosity produced good quality foam, but that the strength of the mixes was lower due to insufficient coating of the aggregate particles, with the latter finding matching the literature.

Table 6.2: Foam Characteristics of Different Asphalt Binders

A PG64-16 (Sample 1 01/10/07)	150	168	–	14	21	23	23	–	–
	160	182	–	14	–	–	–	–	–
	165	189	–	–	24	25	23	–	–
	180	211	–	–	18	20	24	–	–
	150	168	–	18	11	17	16	–	–
	160	182	–	14	–	–	–	–	–
	165	189	–	–	6	8	12	–	–
	180	211	–	–	6	4	6	–	–
A PG64-16 (Sample 2 08/06/07)									
	150	–	–	17	21	19	–	–	–
	155	–	–	17	20	24	24	–	–
	160	–	–	17	22	24	19	–	–
	170	–	–	13	21	23	24	–	–
	180	–	–	13	17	–	–	–	–
	150	–	–	33	32	30	–	–	–
	155	–	–	27	26	23	22	–	–
	160	–	–	21	25	23	23	–	–
	170	–	–	29	14	13	16	–	–
	180	–	–	23	17	–	–	–	–
A PG64-10 (Sample 1 02/09/07)									
	150	168	8	16	19	21	19	–	–
	160	182	–	13	24	25	26	–	–
	165	187	–	–	–	–	–	23	–
	175	204	–	–	19	20	–	–	–
	150	168	50	17	19	23	34	–	–
	160	182	–	12	9	14	13	–	–
	165	189	–	–	–	–	–	17	–
	175	204	–	–	14	8	–	–	–
A PG70-10 (Sample 1 02/09/07)									
	150	168	7	14	19	20	22	18	15
	160	182	–	13	18	23	22	21	–
	175	204	–	10	18	20	24	22	–
	150	168	50	29	21	24	26	37	42
	160	182	–	19	14	16	20	23	–
	175	204	–	12	9	11	10	11	–
B PG64-16 (Sample 1 02/09/07)									
	150	–	–	6	6	6	6	–	–
	160	–	–	6	6	6	6	–	–
	175	–	–	6	6	6	6	–	–
			Half-Life (seconds)						
	150	–	–	NM[1]	NM	NM	NM	–	–
	160	–	–	NM	NM	NM	NM	–	–
	175	–	–	NM	NM	NM	NM	–	–

[1] NM - not measured. The expansion ratio was too low to allow accurate measurement of half-life.

Table 6.2: Foam Characteristics of Different Asphalt Binders *(cont.)*

C PG64-22 (Sample 1 08/08/07)	145	–	–	11	11	11	9	–	–
	155	–	–	12	13	18	–	–	–
	165	–	–	13	14	18	13	–	–
			Half-Life (seconds)						
	145	–	–	22	26	28	30	–	–
	155	–	–	15	14	10	–	–	–
	165	–	–	9	13	10	14	–	–

[1] NM - not measured. The expansion ratio was too low to allow accurate measurement of half-life.

The applicability of the foaming index described in the South African guideline *(3)* was also assessed for California binders. The theoretical base of this index is that an isotope decay type equation is applicable to the decay of asphalt foam. Decay curves were not measured quantitatively in the UCPRC study, but qualitative observations indicated that these curves are not applicable for the binders tested (Figure 6.4). Consequently, the use of the South African Foam Index as the objective function to optimize foaming parameters is not justified for California binders.

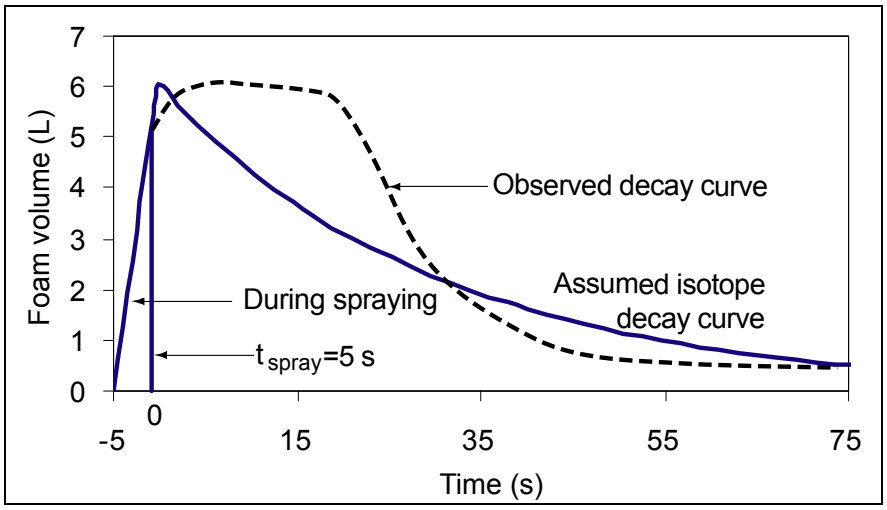

Figure 6.4: Theoretical and observed foam decay curve.
(Modified after Jenkins et al. *[33]*)

It is generally accepted that the foam characteristics of available binders should be checked in the project level design. The results from the UCPRC study (Section 8.5) confirmed the minimum requirements for the expansion ratio and half-life of 10 times and 12 seconds respectively, recommended by Muthen *(2)* in the South African study. It should be noted that the definitions of half-life in the UCPRC and South African studies differ, as discussed above, and therefore the UCPRC recommendation is a slight relaxation of the South African guideline.

The monitoring of full-depth reclamation projects in California and elsewhere has indicated that the temperature of the asphalt binder used in the foaming process cannot be precisely controlled. Ambient and aggregate temperatures will also vary during the course of each day of recycling. Consequently, rather than defining one "optimum" combination of foaming parameters (binder temperature and foamant water-to-asphalt ratio), an acceptance range of these two parameters, specifically the temperature should be determined in the mix design stage to serve as a guideline for construction. Within this range, the expansion ratio and the half-life should at least meet the minimum requirements discussed above. This implies that asphalt binders having higher foamability are less susceptible to the influence of field foaming conditions. The midpoint of this range can be determined by calculating a simple foam index. An index of the product of the expansion ratio and the half-life can be used as a guide, which is simpler than the foam index proposed in the literature *(3,4)*. In the mix design stage, the foamability check should at least cover a temperature range of 150°C to 180°C (302°F to 356°F) with intervals of 10°C (18°F), and a foaming water ratio range of 1.0 to 5.0 percent.

6.4.7 Summary of Recommendations for Foamability Characteristics

The following recommendations regarding foamability characteristics are made:

- Given that prediction of foamability characteristics for a specific performance grade or even refinery is considered impossible, these should always be checked whenever a new batch of asphalt binder is produced on any particular project.
- Sufficient material should be retained from the original mix design to check changes associated with the actual binder used in the project if the foamability characteristics of the binder change significantly.
- Foamability should be checked at regular intervals during each day of foaming (e.g., after each tanker change).
- The minimum requirements for the expansion ratio and half-life are 10 times and 12 seconds, respectively.
- An acceptance range of the binder temperature and the foamant water-to-asphalt ratio should be determined in the mix design stage to serve as a guideline for construction, instead of defining one "optimum" combination of foaming parameters.
- In the mix design stage, the foamability check should at least cover a temperature range of 150°C to 180°C (302°F to 356°F) with intervals of 10°C (18°F), and a foamant water-to-asphalt ratio range of 1.0 to 5.0 percent.

6.5 Assessment of Temperature Sensitivity of Foamed Asphalt Mix Stiffness

6.5.1 Introduction

Many of the properties of foamed asphalt mixes are temperature dependent because of the presence of the asphalt binder. California has a number of climate regions *(34)* and most FDR-foamed asphalt project locations have wide seasonal and daily temperature variation, both at the surface and in the pavement layers *(35)*. Knowledge of the temperature sensitivity of foamed asphalt mix properties is therefore important for interpreting field stiffness (e.g., FWD) data (i.e., normalizing the moduli to a reference temperature), and for analyzing performance in project level mix and structural designs, in which stiffness (i.e., Young's modulus) values at different temperatures are primary input parameters. However, only limited studies on the topic have been reported and a small-scale study was therefore carried out at the UCPRC to provide a reference for later field testing analyses, and for analyzing results from laboratory tests, most of which were carried out at 20°C (68°F).

Due to the exploratory and preparatory nature of this study, only a limited number of specimens were tested. The main objective was to investigate the potential interaction between the temperature dependency and stress dependency of foamed asphalt mix stiffness, and to propose a simple temperature sensitivity coefficient to be used in FWD data analyses, as summarized in Chapter 4. The test results served as reference values to check the validity or reasonableness of field measurements, rather than being directly used in a pavement design. All tests were performed on unsoaked specimens, prepared from a single RAP source with one binder type. No investigation on the temperature dependency of soaked specimen stiffness was carried out in this phase of the study.

6.5.2 Background

The temperature sensitivities of hot-mix asphalt (HMA) and foamed asphalt mix stiffnesses are generally similar in that they are dependent on the asphalt rheology. However their microstructures and the roles of the asphalt binder are different *(4)*. The stiffness of foamed asphalt mixes is fairly sensitive to the stress state of the specimen, especially the bulk stress, which is typical of weakly bound granular materials. Consequently, the effects of stress and the potential interaction between temperature and stress must also be considered when the effects of temperature on foamed asphalt mix stiffness are investigated.

Nataatmadja *(36)* reported that the stiffness of foamed asphalt mixes with asphalt contents of between 1.5 and 4.2 percent of the dry aggregate mass was reduced by between 30 and 44 percent when the temperature increased from 10°C to 40°C (50°F to 104°F). Saleh *(30)* investigated the temperature sensitivity of the resilient modulus of foamed asphalt mixes and the effects of asphalt binder temperature susceptibility and curing conditions. However both studies used the repetitive ITS test to measure the

resilient modulus, which yields a stress state different from the field stress state in a real pavement. In the UCPRC study, cyclic triaxial tests under different combinations of confining and deviator stresses were used to investigate the effects of stress states and temperature, as well as their potential interactions.

6.5.3 Materials and Test Methods

The material classified as "Gradation-2" described in Section 6.2 was used in this task. No active filler was added to ensure that a good understanding of the role of the foamed asphalt was obtained. One AR-4000 (approximately equivalent to PG64-16) binder was used throughout the experiment. The binder was heated to 150°C (302°F) and 2.0 percent foaming water was added. The expansion ratio of the foam was 12 and the half-life was 10 seconds. The aggregate temperature during mixing was not strictly controlled, potentially resulting in some variation in asphalt dispersion. Three triaxial specimens (nominal diameter of 152 mm [6 in.] and nominal height of 305 mm [12 in.]) were compacted following AASHTO T307-99 and cured in a forced draft oven at 50°C (122°F) for one week. Since no active filler was used, curing essentially involved drying (and redistribution of the moisture). Specimen details are listed in Table 6.3.

Table 6.3: Temperature Sensitivity Test Specimen Detail

Specimen	Bulk Specific Gravity	Nominal Foamed Asphalt Content (% dry aggregate mass)
A-15	2.256	1.5
B-30	2.157	3.0
C-45	2.061	4.5

The resilient modulus (M_r) test procedure followed the AASHTO T307-99 protocol, but with adjustments to the load sequence (Figure 6.5). Five confining stress levels (20, 35, 70, 105, and 140 kPa [3, 5, 10, 15, and 20 psi]) and three deviator stress levels for each confining stress were used. The deviator stress levels were relatively low and no significant structural damage was observed during testing. No temperature control chamber was available at the UCPRC when this study was undertaken and therefore the temperature of the specimen decreased gradually during testing. Surface temperature and the temperature at the specimen center were measured and the average value was used as the equivalent temperature of the specimen.

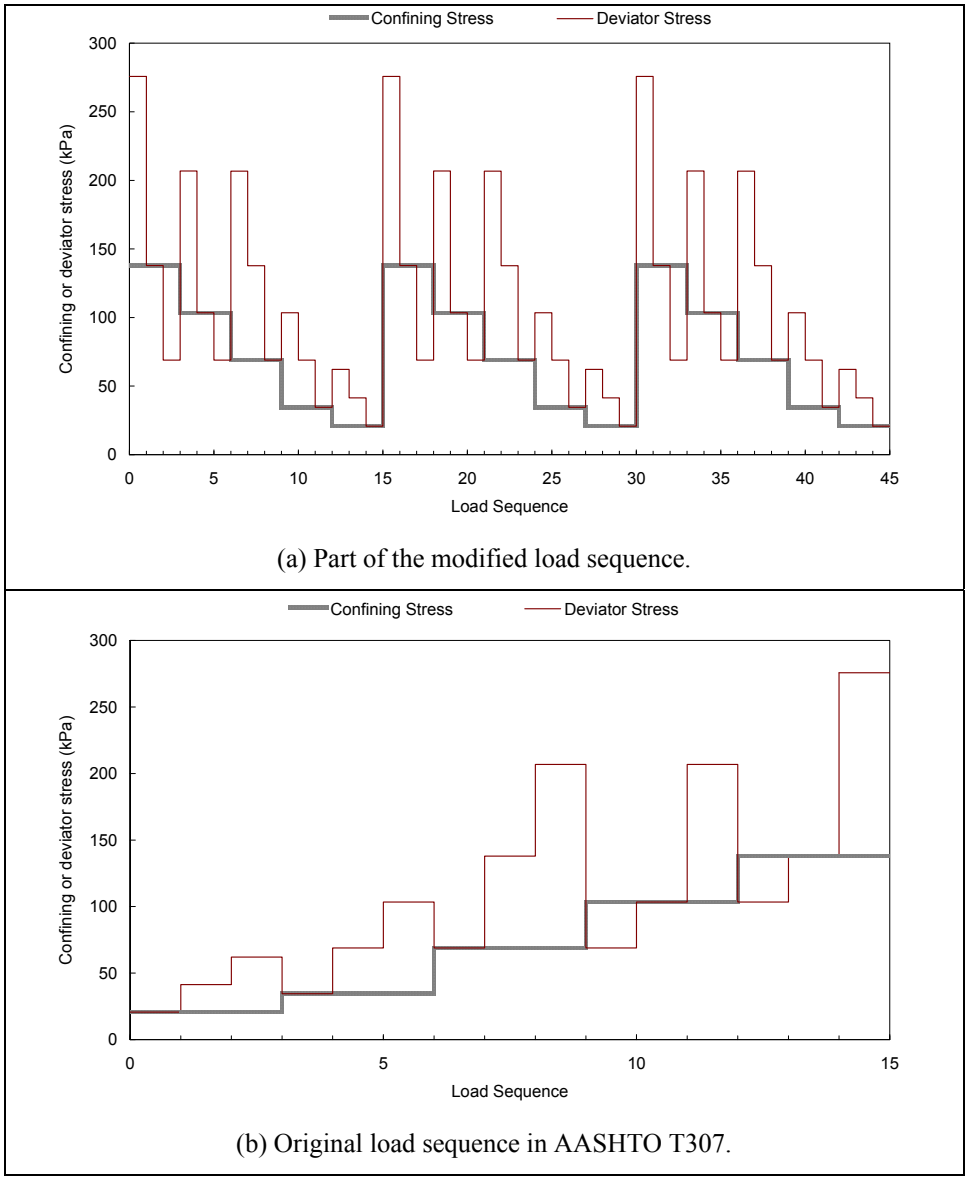

Figure 6.5: Load sequence of triaxial resilient modulus test.
(Combinations of confining stress and deviator stress)

6.5.4 Effects of Confining Stress, Deviator Stress, and Temperature

A number of observations were made with regard to the effects of confining stress, deviator stress, temperature, and their interactions on the measured resilient modulus of the foamed asphalt specimens. Since the three specimens had various foamed asphalt contents and density, the significance of each effect varies, as discussed below.

Effects of Bulk Stress

The resilient moduli measured at various temperatures and stress states for Specimen B-30 are plotted in Figure 6.6 with respect to the bulk stress $\theta = 3\sigma_0+\sigma_d$, where σ_0 is the confining stress and σ_d is the deviator

stress. Corresponding equivalent specimen temperatures are labeled for selected data points. The results indicate that as the bulk stress increased, the resilient modulus also increased. Lower stiffnesses were associated with higher temperatures. The relatively large variance of stiffness at each bulk stress level was attributed to the variation of temperature and deviator stress, which both affect stiffness, as well as to random errors inherent during testing and measuring. The significant stress dependency of the resilient modulus implies that the foamed asphalt mixes as tested can be classed as weakly bound granular materials.

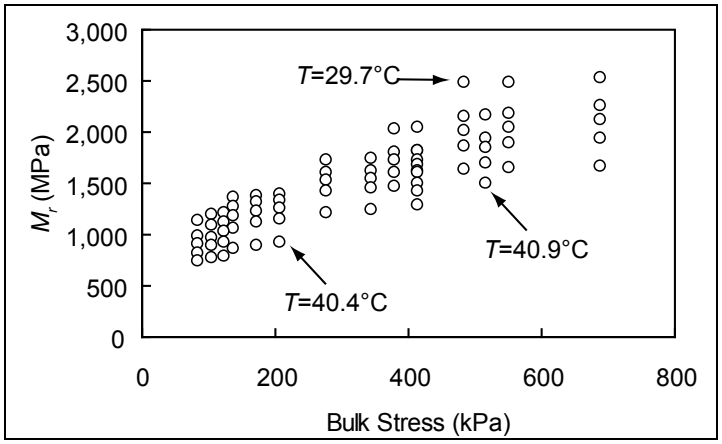

Figure 6.6: Dependency of resilient modulus on bulk stress.
(Specimen B-30; Equivalent specimen temperatures are shown for selected data points.)

Effect of Temperature

Figure 6.7 summarizes the relation between equivalent specimen temperature and resilient modulus for different bulk stresses on Specimen B-30 (the M_r axis is in log scale). Test results for one deviator stress ($\sigma_d = 2\sigma_0$) for each confining stress level are plotted as an example. The plot shows that resilient modulus-temperature curves for different confining stresses are generally parallel, which suggests that the effects of temperature and bulk stress are largely independent.

Deviator Stress and Its Interaction with Temperature

The deviator stress has two opposite effects on the triaxial stress state *(37)*. Increasing the deviator stress increases the bulk stress, which tends to increase the stiffness. However, it also increases the octahedral shear stress, which tends to reduce the stiffness. Figure 6.8 summarizes the overall effects of deviator stress at various temperatures for Specimen A-15 (σ_0 = 140 kPa and σ_0 = 70 kPa [10 and 20 psi]). As the temperature increases the materials tend to show more "stress-softening" behavior (i.e., the effect of deviator stress depends on temperature).

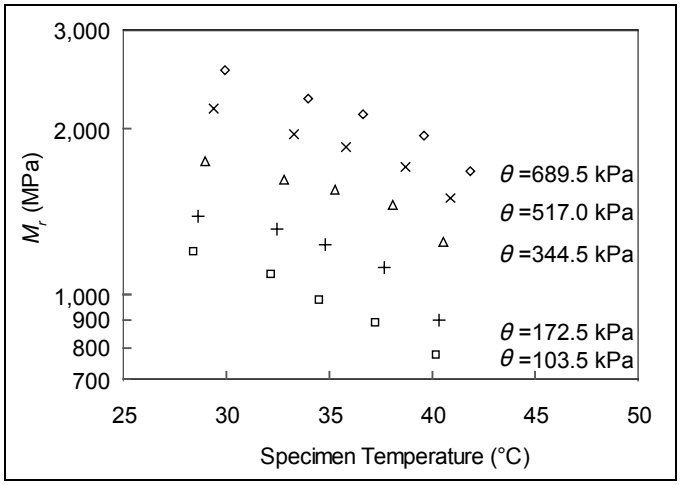

Figure 6.7: Effect of specimen temperature on resilient modulus.
(Specimen B-30; θ = bulk stress = sum of three principal stresses)

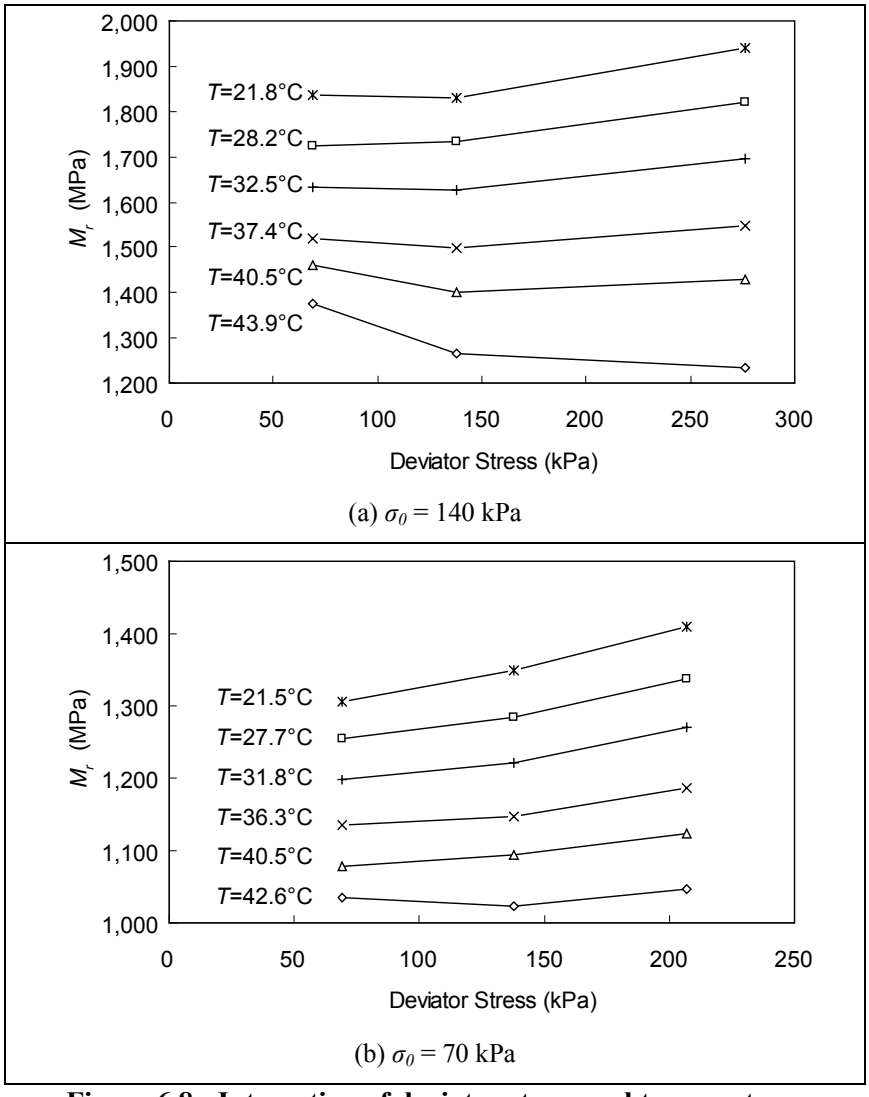

Figure 6.8: Interaction of deviator stress and temperature.
(Specimen A-15)

6.5.5 Model Development

Resilient Modulus Model Fitting

The resilient modulus of foamed asphalt is dependent on its stress state at a given temperature. This stress dependency is common for granular materials and Equation 6.1 is a general model proposed by Uzan *(37)*.

$$M_r = k_1 p_a \left(\frac{\theta}{p_a}\right)^{k_2} \left(\frac{\tau_{oct}}{p_a}\right)^{k_3} \quad (6.1)$$

where p_a = atmospheric pressure used to nondimensionalize stresses
σ_0 = confining stress
σ_d = deviator stress
θ = $3\sigma_0+\sigma_d$ = bulk stress
τ_{oct} = octahedral shear stress, and in the triaxial stress state $\tau_{oct} = \sqrt{2}\sigma_d/3$;
k_1, k_2, and k_3 are material related constants.

This model is modified as Equation 6.2 to take the effects of temperature into account.

$$M_r(T,\theta,\tau_{oct}) = M_{r0}(T)\left(\frac{\theta}{\theta_0}\right)^{k_4(T)} \left(\frac{\tau_{oct}}{\theta_{oct0}}\right)^{k_5(T)} \quad (6.2)$$

where $M_r(T,\theta,\tau_{oct})$ = resilient modulus of foamed asphalt at temperature T and stress state (θ,τ_{oct})
$M_{r0}(T)$ = resilient modulus at temperature T for a reference stress state (θ_0,τ_{oct0})
θ_0,τ_{oct0} = bulk stress and octahedral shear stress, respectively, for a reference stress state where σ_0 = 105 kPa and $\sigma_d = 2\sigma_0$
$k_4(T)$, $k_5(T)$ are material and temperature dependent constants.

The constants in this model are temperature dependent and therefore model fitting should ideally be based on resilient moduli measured at a constant temperature, which was not possible in this study (the triaxial equipment was not in a temperature chamber). As an alternative, model fitting was done for sequential subsets of fifteen combinations of confining pressure and deviator stress, which have the full combination of stress states tested, but with relatively small temperature variation. Model-fitting results are shown in Table 6.4 for the three specimens. The average temperature and the standard deviation of the temperature in each group are also shown. It should be noted that the $M_{r0}(T)$ values listed in the table are the model-fitting results and not the measured resilient modulus at corresponding temperature and stress state.

The following observations were made based on the model-fitting results:

- The R^2 values were all greater than 0.96, indicating that the proposed model captured the effects of the temperature and stress state reasonably well. The R^2 values at higher temperatures were generally larger.
- The resilient modulus for the reference stress state $M_{r0}(T)$ increases significantly with decreasing temperature.

- The indicator of the sensitivity of the resilient modulus to bulk stress, $k_4(T)$, showed a generally random fluctuation with changing temperature. This is consistent with the observation that little or no interaction is observed between the effects of temperature and bulk stress.
- The indicator of the softening effect associated with the octahedral shear stress, $K_5(T)$, showed a generally decreasing trend in absolute value as the temperature decreased. This is consistent with the observation that the stress-softening effect is more significant at higher temperatures. Weaker bonding between aggregates for softer asphalt binders is implied.

Table 6.4: Model Fitting Results for Specimens A-15, B-30, and C-45

Load Sequence	Temperature		$M_{r0}(T)$ (MPa)	$k_4(T)$	$k_5(T)$	R^2
	Average (°C)	Std. Deviation (°C)				
Specimen A-15 (1.5% Foamed Asphalt)						
1~15	42.7	0.74	1,156	0.466	-0.169	0.992
16~30	39.4	0.77	1,279	0.458	-0.139	0.992
31~45	36.4	0.69	1,337	0.457	-0.129	0.989
46~60	33.9	0.58	1,407	0.460	-0.126	0.986
61~75	31.9	0.46	1,452	0.467	-0.118	0.985
76~90	30.2	0.39	1,480	0.471	-0.128	0.982
91~105	28.9	0.33	1,514	0.480	-0.129	0.982
106~120	27.8	0.29	1,532	0.476	-0.125	0.982
121~135	22.0	0.18	1,604	0.467	-0.118	0.978
136~150	21.6	0.18	1,631	0.482	-0.115	0.982
Specimen B-30 (3.0% Foamed Asphalt)						
1~15	40.7	0.52	1,469	0.568	-0.147	0.994
16~30	38.2	0.75	1,718	0.513	-0.100	0.997
31~45	35.3	0.73	1,855	0.501	-0.100	0.994
46~60	32.9	0.61	1,951	0.483	-0.102	0.988
61~75	29.0	0.50	2,136	0.538	-0.147	0.982
Specimen C-45 (4.5% Foamed Asphalt)						
1~15	38.7	0.58	1,373	0.422	-0.134	0.991
16~30	36.3	0.77	1,520	0.419	-0.111	0.978
31~45	33.8	0.65	1,613	0.433	-0.107	0.973
46~60	31.7	0.54	1,688	0.443	-0.103	0.972
61~75	29.6	0.46	1,798	0.466	-0.108	0.973
76~90	28.3	0.33	1,848	0.473	-0.116	0.968
91~105	27.2	0.27	1,898	0.486	-0.120	0.963
106~120	26.2	0.23	1,937	0.495	-0.119	0.964

Temperature Sensitivity Coefficient

A temperature sensitive coefficient (γ) of resilient modulus (or stiffness) is proposed as shown in Equation 6.3 where T_0 is a reference temperature. This coefficient has to be a function of the stress state (θ, τ_{oct}) to take the interaction between the stress state and material temperature into account. According to the observations and analysis made previously, the absolute value of $k_4(T)$ is always more than four times greater than the absolute value of $k_5(T)$ and hence the effects of octahedral shear stress or deviator stress on resilient modulus are relatively insignificant. Consequently the interaction between the effects of temperature and stress state is also of lesser importance. If the interaction between the stress state and

temperature is ignored, Equation 6.3 can be simplified to Equation 6.4 without losing any significant explanatory power.

$$\gamma(\theta,\tau_{oct})=\frac{\log_{10}M_r(T,\theta,\tau_{oct})-\log_{10}M_r(T_0,\theta,\tau_{oct})}{T_0-T} \quad (6.3)$$

$$\gamma=\frac{\log_{10}M_{r0}(T)-\log_{10}M_{r0}(T_0)}{T_0-T} \quad (6.4)$$

The value of γ can be obtained by plotting M_{r0} versus temperature on a semi-logarithmic scale and measuring the slope, using data such as that found in Table 6.4. Each decrease in temperature by $0.301/\gamma$°C doubles the resilient modulus. The results for the three specimens are plotted in Figure 6.9. The temperature sensitivity coefficients are 0.0065, 0.0131, and 0.0115, for Specimens A-15, B-30, and C-45 respectively. This shows that increasing the foamed asphalt content in the range of 1.5 to 3.0 percent resulted in an increase in the temperature sensitivity of the stiffness. The test data showed that there was a minor decrease in temperature sensitivity when the asphalt content was increased above 3.0 percent, which was counterintuitive. It should be noted that only one sample was tested for each foamed asphalt content, and that other uncontrolled variables such as mixing temperature could have had a significant effect on asphalt distribution. In this preliminary qualitative study, the exact values of this coefficient were considered of less importance than the general observations.

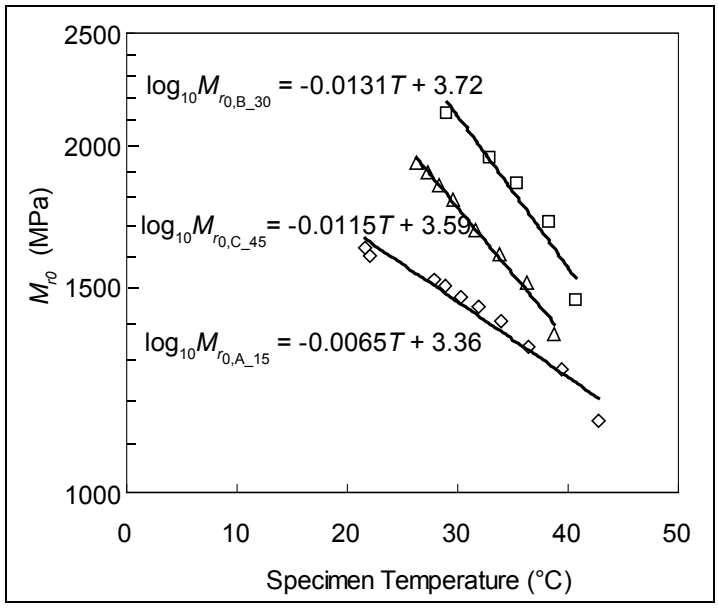

Figure 6.9: Relation between resilient modulus and temperature.

A simplified model combining Equations 6.2 and 6.4 to estimate the resilient modulus of a foamed asphalt mix for any combination of temperature and triaxial stress state is presented as Equation 6.5.

$$M_r(T,\theta,\tau_{oct}) = 10^{\alpha(T_0-T)} M_{r0}(T_0) \left(\frac{\theta}{\theta_0}\right)^{k_4} \left(\frac{\tau_{oct}}{\tau_{oct0}}\right)^{k_5} \quad (6.5)$$

This equation uses the same notation as Equations 6.2 and 6.4, except that $\bar{k}_4$ and $\bar{k}_5$ are the average values of $k_4(T)$ and $k_5(T)$ over various temperatures (i.e., the mean values of the corresponding columns in Table 6.4). Based on the regression results in Table 6.4 and Figure 6.9, the parameters for Specimen B-30 are:

$T_0 = 25°C$, $\gamma = 0.0131$, $M_{r0}(T_0) = 10^{3.72\text{-}0.0131T0}$, $\bar{k}_4 = 0.512$, and $\bar{k}_5 = -0.119$.

The calculated resilient modulus values of Specimen B-30 at various temperatures and stress states using Equation 6.5 are plotted in Figure 6.10 against the measured values from triaxial testing. A fairly good correspondence was achieved, implying that this model captures the effects of both the stress state and temperature on the resilient response of foamed asphalt-treated materials reasonably well.

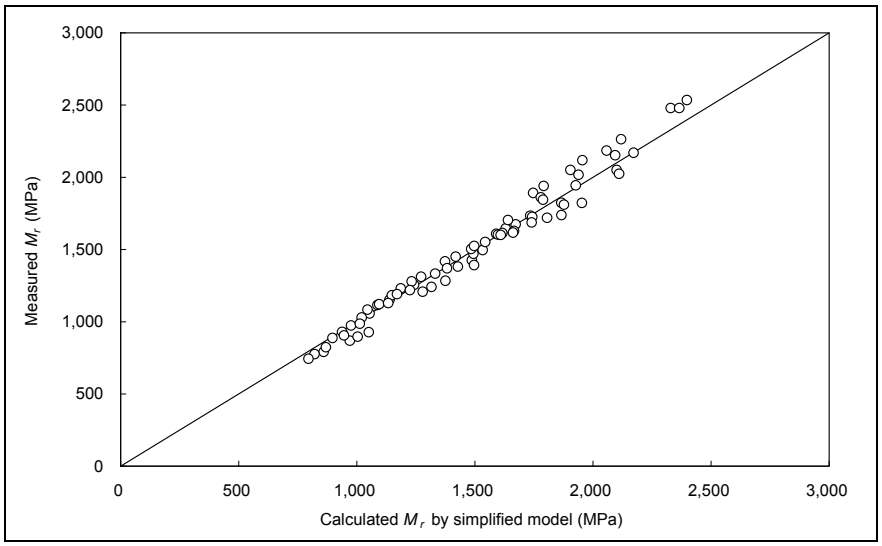

Figure 6.10: Comparison of measured and predicted resilient modulus.

6.5.6 Summary

The testing of three triaxial specimens with foamed asphalt contents between 1.5 and 4.5 percent and no active filler revealed that the hardening effect of the bulk stress dominates the effects of the deviator stress (or octahedral shear stress), and is largely independent of temperature. However, an interaction between the deviator stress and temperature was observed at higher temperatures, where the material tended to show more "stress-softening" behavior. Fitting the test data to a simple model quantitatively supported these observations. By ignoring the interactive effects of the stress state and temperature, a temperature sensitivity coefficient can be defined to characterize the temperature susceptibility of foamed asphalt mix

stiffness. This coefficient was later used in analyzing FWD test results from a number of roads recycled with foamed asphalt (discussed in Chapter 4). A simplified model with four material-related parameters was developed to predict the resilient modulus of foamed asphalt mixes at any triaxial stress state and temperature. The model was used to better understand the stabilization mechanisms of foamed asphalt without the influence of active fillers.

6.6 Fracture Face Image Analysis

The conventional research methodologies documented in the UCPRC work plan *(1)* are typically used to understand material behavior by studying the relationships between various design variables and laboratory-tested or field-measured properties. In some instances, the microscopic mechanics controlling the material behavior can be inferred indirectly, but more often only empirical relations between the variables and the properties are established and the microscopic mechanics are hypothesized. When knowledge of the microstructure is absent, extrapolating these empirical relations to a wider range of materials and construction practices than those included in the experimental work factorial can result in significant differences between measured and predicted properties. This part of the study, although not included in the work plan, was undertaken to develop a simple procedure for assessing microstructures of foam asphalt-treated mixes, specifically on the fracture faces of split ITS test specimens. The procedure was termed "fracture face image analysis" (FFIA) and essentially entails the quantification of the distribution of the asphalt mastic phase visible on fracture faces of laboratory-tested foamed asphalt specimens and then mapping this two-dimensional (2-D) distribution to the three-dimensional (3-D) asphalt mastic distribution features. This 3-D asphalt mastic distribution is considered an important microscopic structural characteristic of foamed asphalt mixes.

6.6.1 Fundamentals of Fracture Face Image Analysis

Microstructure Characteristics of Foamed Asphalt Mixes

The microscopic structure characteristics of foamed asphalt mixes and the processes that form this structure need to be considered before a method to quantify these features can be developed.

In the foaming process, hot asphalt cement (140°C to 180°C [285°F to 355°F]), water at ambient temperature, and compressed air are mixed in a specially designed chamber to form asphalt foam (or asphalt bubbles). During mixing, the foam is injected onto the agitated moist aggregate and as the bubbles burst they disperse the asphalt into the aggregate as variously sized, isolated droplets *(4)*, which coat and then bond the fine aggregate particles (mineral filler) together to form an asphalt mastic phase. The asphalt bubbles are not particularly stable when they contact the cooler aggregate, thus the foaming process usually lasts only a few seconds before the bubbles burst and cool down, increasing the viscosity of the

asphalt and reducing the workability of the mix. Consequently only a fraction of the mineral filler is coated with asphalt to form the asphalt mastic phase, leaving a considerable proportion of the fines as an uncoated mineral filler phase. This procedure is affected by many factors including the characteristics of the asphalt foam, the gradation of the aggregate, the mixing technique adopted, the moisture content and temperature of the aggregate, etc *(4)*.

After compaction and curing, a structure conceptually illustrated in Figure 6.11 is formed. This is theorized to have partially coated large aggregates that are "spot welded" with a fines mortar *(4)*, which is a mix of asphalt mastic (mixture of mineral filler and asphalt cement) and the sand fraction that is partially coated. In the UCPRC study, coated sand was considered to be part of the asphalt mastic phase and uncoated sand was considered to be mineral filler. In such a structure, three major phases can be identified:

- Large aggregate particles that form the aggregate skeleton;
- The asphalt mastic phase, which exists in the form of asphalt droplets bonding the aggregate skeleton together; and
- The mineral filler phase filling the voids in the skeleton.

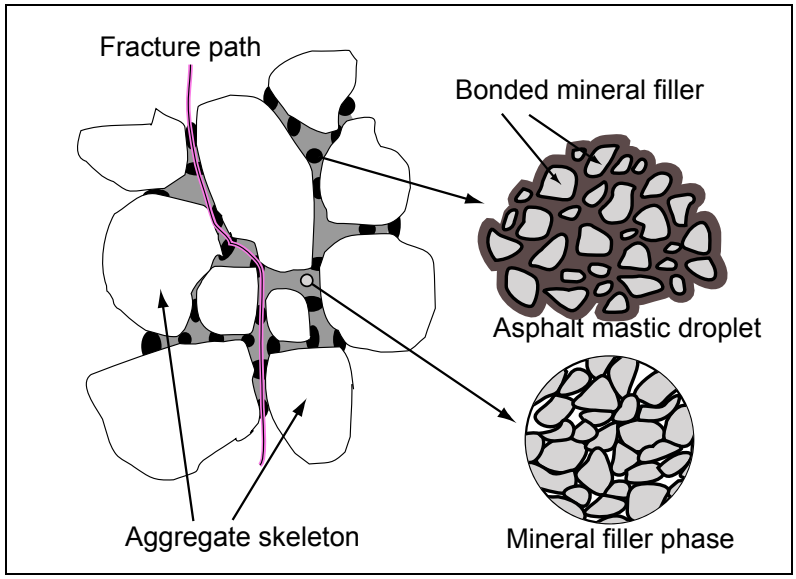

Figure 6.11: Microstructure of foamed asphalt mixes.

Air voids are considered as inclusions in the mastic and mineral filler phases and not as a separate phase. For the purposes of this study, the distribution of the air voids was considered as being of secondary importance compared to the distribution of the asphalt mastic and mineral filler phases.

Image Analysis of Hot-Mix Asphalt (HMA)

Various image analysis techniques have been developed in the literature to study the internal structural characteristics of conventional HMA or its constituents. They can be divided into three categories:

- Two-dimensional image analysis *(38-40);*
- Direct assessment of the three-dimensional structure using X-Ray Computed Tomography (CT) techniques to understand how the internal structure influences the material behavior *(41,42);* and
- Morphological characterization of coarse aggregate particles used in HMA *(43)*.

The applicability of these techniques is based on the internal microscopic structure features of HMA, which is different from that of foamed asphalt mixes. They can thus not be applied directly to foamed asphalt mixes for the following reasons:

- In good quality HMA, almost all the aggregate particles are coated by hot asphalt cement during the mixing process. HMA therefore should not have an uncoated mineral filler phase. Instead, the space between the skeleton formed by large aggregates is filled by the asphalt mastic phase and air voids.
- CT scanning relies on composition and density to differentiate materials. The constituents of foamed asphalt mixes are more complex and include materials of unknown origin and characteristics, which are mixed during the recycling process. The existence of the old oxidized asphalt concrete in foamed asphalt mixes also complicates the characterization of the asphalt mastic phase.
- Foamed asphalt mixes are somewhat brittle, and hence obtaining the flat and smooth cross section specimens required for these image analysis processes is difficult.

6.6.2 Analysis of Foamed Asphalt Mixes

Literature Review

Empirical criteria for assessing foamed asphalt materials were proposed by Ruckel et al. *(29)* to visually check the quality of asphalt dispersion in loose mixes. Jenkins *(4)* performed a statistical analysis on the size distribution of asphalt droplets in foamed asphalt-treated loose mixes to demonstrate how foamability of asphalt affects its dispersion. These qualitative visual inspections and semiquantitative analyses are similar to the first image analysis approach for HMA and granular base materials discussed in the previous section. Literature searches for quantitatively assessing the internal structure characteristics of foamed asphalt-treated material did not yield any applicable information.

Principles of Fracture Face Image Analysis (FFIA)

The basic principle of FFIA entails the quantification of the visible asphalt mastic distribution (two-dimensional [2-D]) on fracture faces of laboratory-tested specimens, and then using the results to imply

certain features of this distribution (three-dimensional [3-D]) in foamed asphalt mixes. In order to establish the 2-D/3-D mapping rules, the influence of the 3-D asphalt mastic distribution on the 2-D distribution on a fracture face first needs to be qualitatively analyzed.

Tensile-type laboratory tests, such as the monotonic flexural beam test or the indirect tensile strength (ITS) test, involve a process of crack initiation followed by crack propagation. When a crack propagates through a foamed asphalt mix, it either breaks the mineral filler phase, the asphalt mastic phase, or the interfaces between the asphalt mastic and the aggregates. Since the asphalt mastic phase and the mineral filler phase have distinct colors in most recycled materials, the quantity and distribution of asphalt spots seen on the fracture faces can be an indicator of the asphalt mastic distribution on the fracture face. Figure 6.12(a) shows a tested ITS specimen with a fracture breaking the specimen; Figure 6.12(b) shows the appearance of the two fracture faces, and Figure 6.12(c) shows the visible asphalt mastic spots on one of the faces identified using digital image processing techniques.

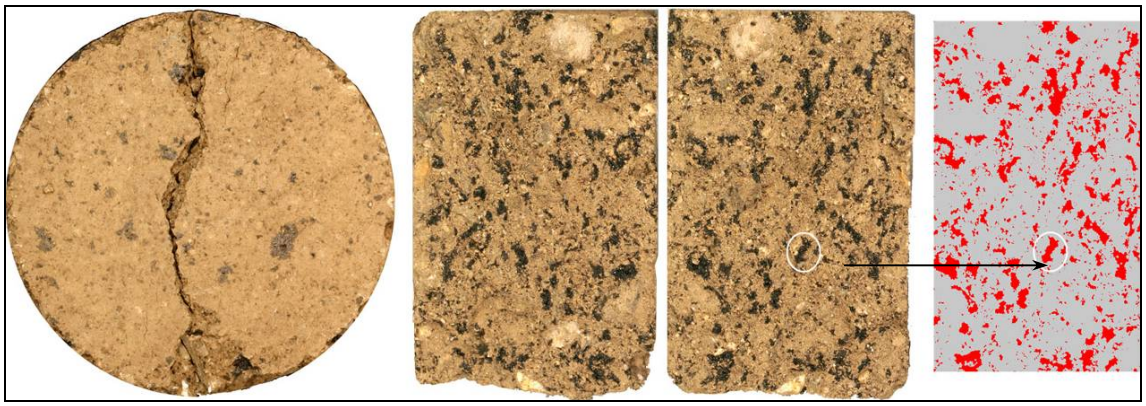

(a) (b) (c)

Figure 6.12: Tested ITS specimen and resulting fracture faces.

The fracture face asphalt coverage (FFAC) is defined as the ratio of the area of the mastic phase visible on a fracture face to the total area of the fracture face and is considered to be the simplest quantitative characterization of foamed asphalt fracture faces. In a digital image analysis, FFAC can be easily calculated by dividing the number of pixels representing the mastic phase, which is significantly darker, by the total number of pixels of the entire fracture face on a digital image. Care must be taken when assessing materials containing dark-colored minerals such as biotite, garnets, and tourmalines.

The two most fundamental volumetric characteristics of the asphalt mastic phase in a foamed asphalt mix are:

- Its total volume relative to the volume of the mineral filler phase, and
- The size distribution of the asphalt mastic droplets.

If the pattern in which the asphalt mastic and mineral fillers fill the voids in the aggregate skeleton is random and the mix is homogenous and isotropic in a global sense, the following simple mapping rules apply:

- If the size distribution of the asphalt mastic droplets is the same, then as the volumetric ratio of the asphalt mastic phase to the mineral filler phase increases, a higher ratio of the fracture face area will be covered by asphalt mastic.
- Given the same volumetric ratio of the asphalt mastic phase to the mineral filler phase, if the asphalt mastic exists in the form of a large number of small droplets (instead of a small number of large droplets) more uniformly distributed small asphalt mastic spots will be visible on the fracture faces as opposed to large concentrated asphalt spots.
- Given the same volumetric ratio of the asphalt mastic phase to the mineral filler phase, the mix where asphalt mastic exists in the form of a large number of small droplets (instead of a small number of large droplets) should also yield fracture faces with higher FFAC values.

The third mapping rule is not as intuitive or as apparent as the first two rules, and thus requires further clarification. A qualitative analysis of two idealized cases in Figure 6.13 illustrates these effects. Mix-A as shown in Figure 6.13(a) represents a structure with good asphalt dispersion featuring a large number of small asphalt droplets "gluing" the aggregate skeleton together. Mix-B, shown in Figure 6.13(b) represents a structure with inferior asphalt dispersion, with a few large asphalt droplets. The volumes of the asphalt mastic and mineral filler phases in the two mixes are the same, and the aggregate skeletons are similar. Assuming that the tensile strength of the mineral filler phase is weaker than that of the mastic phase (which is not always true as will be discussed later), when a crack propagates (from bottom to top) in Mix-A as a result of the action of external forces, it can propagate along either Path A1 or Path A2 since the lengths of the two paths and the numbers of asphalt bonds to break are similar. However, in Mix-B, the crack is more likely to propagate along Path B2, where it encounters fewer asphalt droplets. The fracture faces of Mix-A will show more black spots (broken mastic phase) in terms of both the number and the total area than those of Mix-B. At the same time, the tensile strength of Mix-A should be higher than that of Mix-B.

Given the aforementioned three rules, FFAC can be used as a quantitative indicator of the quality of foamed asphalt distribution for a given recycled material. Good quality foam distribution tends to bond more of the mineral filler to form the mastic phase. Consequently the volumetric ratio between the mastic phase and the mineral filler phase is higher. Foamed asphalt mixes with good foam distribution also tend to have a large number of small asphalt mastic droplets. For a given RAP and foamed asphalt content, mixes with higher FFAC values are thus preferable.

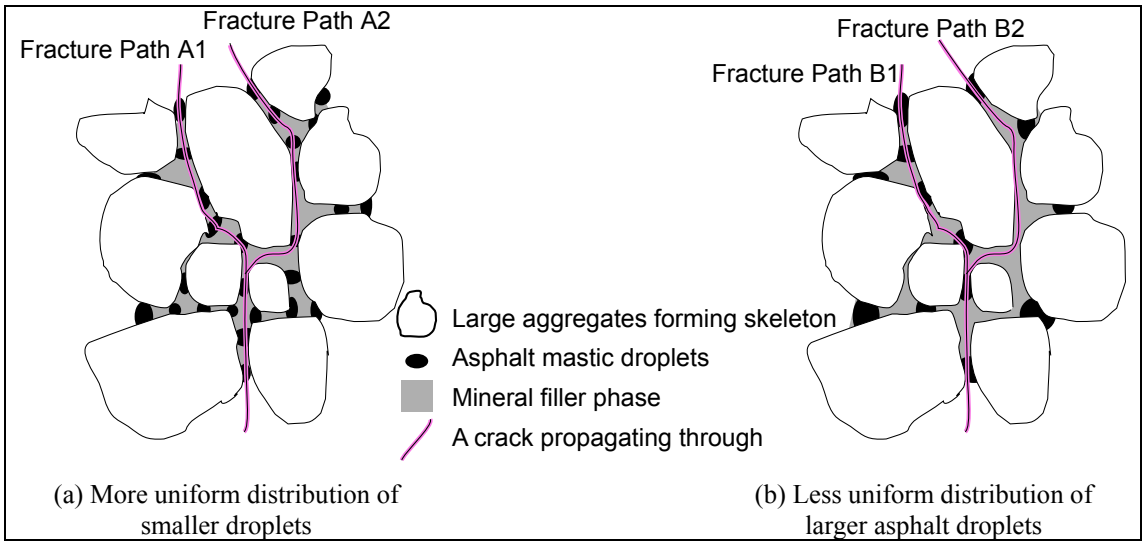

Figure 6.13: Effect of asphalt droplet size distribution on FFAC values.

Apart from the asphalt mastic phase distribution, the strength ratio between the asphalt mastic phase and the mineral filler phase also affects the FFAC values. For a given asphalt mastic dispersion pattern in a foamed asphalt mix, appearances of fracture faces are determined by the path through which the crack propagates. The strength of the mineral filler phase is sensitive to moisture conditioning, while the strength of the asphalt mastic phase is dependent on temperature and the loading rate, but less sensitive to moisture conditioning. Under certain circumstances, for example when testing at very high loading rates or when the mineral filler phase is substantially strengthened with portland cement (i.e., the mineral filler phase is stronger than the asphalt mastic phase), the crack in Figure 6.13(b) is more likely to propagate along Path B1 instead of Path B2. The fracture faces of Path B1 might have even higher FFAC values than those of Paths A1 or A2. This situation was considered to be undesirable in the UCPRC study because FFAC is expected to be a quantitative indicator of foamed asphalt distribution in the mix, with higher values representing better and more uniform dispersion. Preferred test conditions and limitations for FFAC are discussed in the following section.

The compaction methods used to fabricate specimens and the test methods (or the test boundary conditions) both have significant effects on FFAC values. Although the distribution of the asphalt mastic phase (i.e., asphalt droplets) in the loose mix is determined at the mixing stage, the specimen fabrication and compaction method employed will affect how the asphalt mastic phase is distributed in a specimen. The test method (or the test boundary condition) causing the fracture faces also affects the pattern of crack propagation through the specimens, thus affecting the FFAC. These concerns are addressed in the following sections of this report.

6.6.3 Preferred Test Conditions for FFAC

As shown in the above qualitative analyses, FFAC is primarily an indicator of the dispersion of the asphalt mastic phase in the foamed asphalt mix. It is also affected by other controllable factors, namely the relative strengths of different phases in the mix, the specimen fabrication and conditioning methods, and the test boundary conditions. FFAC should therefore only be used to assess specimens that were fabricated using the same method and were tested with the same test configuration (e.g., testing temperature and loading rate). It is suited for comparisons of asphalt mastic distributions as a function of other mix parameters such as asphalt type, asphalt content, mixing temperature, mixing moisture content, etc. on foamed asphalt mixes made from recycled aggregates with the same or similar gradations. FFAC analysis should not be used in the following instances:

- Direct comparisons of mixes with significantly different RAP gradations. It can be used for comparing small incremental changes in fines content.
- Direct comparisons of mixes containing different parent aggregates. Different aggregate color and mineralogy could influence the appearance of the material.
- Assessing unsoaked specimens and/or comparing unsoaked and soaked specimens. When considering moisture conditioning, the FFAC of soaked specimens is a more justifiable indicator than that for unsoaked specimens because the tensile strength of the mineral filler phase in unsoaked specimens can be close to or even greater than that of the asphalt mastic phase, in which case specimens with poorer asphalt distribution might show higher FFAC values.
- Assessing specimens containing active fillers and/or comparing specimens containing active fillers with those containing no active fillers. Portland cement and other active fillers can increase the strength of the mineral filler phase significantly and therefore fracture behavior will be different compared to that of specimens with no active filler.
- Comparing specimens that were not fabricated in the same way, e.g., using different compaction methods, specimen sizes, etc.

6.6.4 Image Processing Procedure

The procedure and equipment used to quantify FFAC on fracture faces are simple. The process is as follows:

1) Acquire images of laboratory strength test specimen fracture faces using a digital camera. ITS and flexural beam tests both yield relatively flat fracture faces that are ideal for image acquisition and analysis.
2) Normalize the brightness of the image.
3) Identify those pixels representing the asphalt mastic on the fracture face.
4) Identify and eliminate glare.

5) Count the pixels representing the asphalt mastic on the fracture face.
6) Calculate the FFAC value.

Digital image analysis software (Foamed Asphalt Fracture Face Image Analysis [FAFFIA]) was developed at the UCPRC to perform these operations.

Image Acquisition

In the UCPRC study, a digital single-lens reflex (DSLR) camera with a standard 50 mm focal length auto focus lens was used to acquire images of fracture faces. The image resolution was approximately 8 to 10 pixels/mm on the fracture surfaces. Although color images were acquired, only the red channel was used in this study because the mineral filler phase is brown and the contrast between the filler and the asphalt is most distinct in the red channel.

Lighting

The lighting configuration is critical. Light from multiple sources (between four and eight) placed at different angles must be cast onto the fracture faces to eliminate shadows on the uneven surface. These shadows influence the differentiation between the asphalt mastic and the mineral filler.

Threshold Brightness Selection

The choice of an appropriate threshold brightness value is also important. Once selected, pixels darker than the threshold value will be identified as asphalt mastic, while brighter pixels will be identified as the mineral filler phase. The boundary between the two phases is rarely distinct and the value is generally determined by a trial and error procedure until satisfactory differentiation between the two phases is achieved. Some subjectivity is inevitable but it is minimized through use of a photographic gray card, which is placed next to the specimen and included in the image to serve as a reference for normalizing the exposure. Since the colors of the asphalt mastic phase and the mineral filler phase are highly dependent on the parent materials, no universal threshold value is applicable for all mixes. Consistency in exposure normalization and threshold determination is important when comparing a number of specimens.

Glare Elimination

Glare on the asphalt mastic phase, caused by specular reflection of light from the asphalt binder, requires special treatment. The glare brightness is normally much higher than the threshold brightness and can therefore hide asphalt mastic areas. An iterative moving-average type algorithm is employed to eliminate this problem. In this process, the pixels surrounding each pixel that is brighter than the threshold brightness value are checked. The radius of this area is determined according to the resolution of the

image and the typical size of glare spots. In the UCPRC study, the glare area check radius was set at three pixels (equivalent to 0.3 mm to 0.5 mm). If more than 65 percent of the pixels in this check area are identified as mastic, the pixel is counted as asphalt mastic. Each iteration performs this check on every pixel and after several iterations most of the glare areas are satisfactorily eliminated (Figure 6.14).

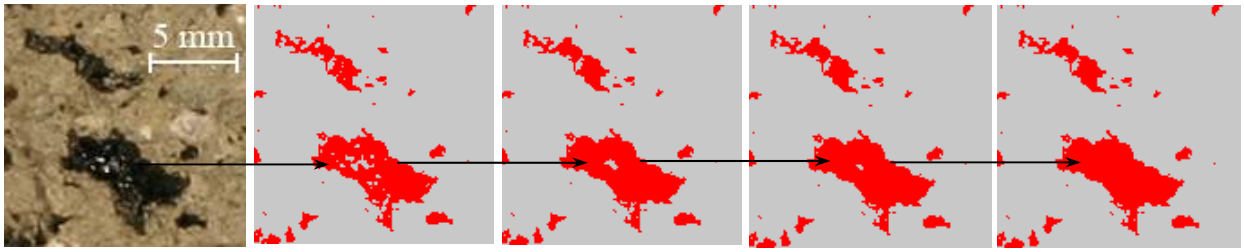

(a) Original image **(b) Processed image** **(c) Iteration 1** **(d) Iteration 2** **(e) Iteration 3**

Figure 6.14: Glare elimination on fracture face images.

6.6.5 Laboratory Applications of Fracture Face Image Analysis

FFAC is a useful quantitative indicator of asphalt dispersion in mixes with the same parent aggregates (without portland cement) and tested with the same test method after soaking. High values of FFAC generally indicate good asphalt dispersion. Fracture face image analysis was used extensively in the UCPRC study in analyzing and understanding the behavior of specimens treated only with foamed asphalt (i.e., no active fillers) in later phases of the laboratory study, before proceeding with investigations into the role of active fillers.

Although the procedure described is more suited to research, practitioners can use a simplified process of visually comparing the facture faces of tested ITS specimens to interpret asphalt mastic distribution features and to diagnose potential mix problems. The limitations discussed in Section 6.6.3 should be considered during any FFAC analysis. Table 6.5 can be used together with Figure 6.15 as an interim guideline for this diagnosis. The fracture faces shown in the figure are approximately 80 percent (80 mm x 50 mm [3.2 x 2 in.]) of the areas of the original fracture faces of the ITS specimens. Once these features and mix design problems are understood, mix design testing can proceed to assessing mix performance with active fillers.

Table 6.5: Interim Diagnosis Chart for Foamed Asphalt Mix Characteristics

Mix Characteristics	Test Results and Fracture Face Features	Example
• Ideal mix with good workability and moisture resistance	• High soaked ITS • Large number of uniformly distributed small asphalt spots • Medium to high FFAC	Figure 6.15(a)
• Low mixing temperature • High mixing moisture content	• Low and variable soaked ITS • Low and variable FFAC values • Large and concentrated asphalt spots	Figure 6.15(b)
• High mineral filler (fines) content • Low asphalt content	• Low soaked ITS • Low FFAC values • A few small asphalt spots	Figure 6.15(c)
• Low mineral filler (fines) content • Loose sandy mixes	• Moderate to low soaked ITS • High FFAC values • Many uniformly distributed moderate size asphalt spots	Figure 6.15(d)

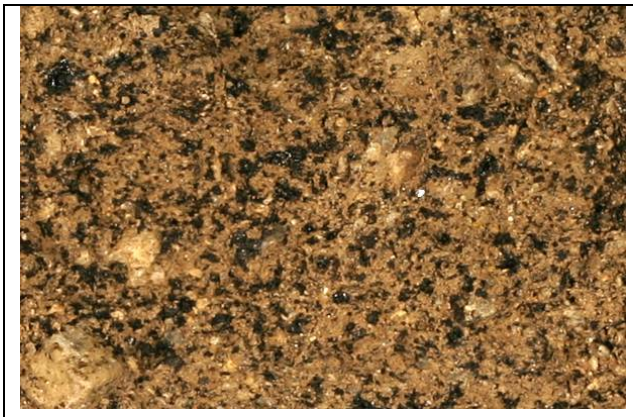

(a) Satisfactory mix

(b) Problematic mix: high mixing water content

(c) Problematic mix: high mineral filler content

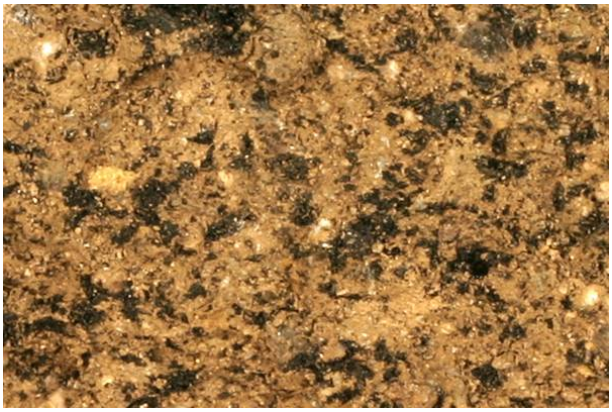

(d) Problematic mix: low mineral filler content

Figure 6.15: Typical fracture faces showing different symptoms.

6.6.6 Summary of Recommendations for Fracture Face Analysis

The following recommendations regarding the use of fracture face analysis are made:

- Analysis of the fracture faces of ITS specimens after testing can provide valuable insights into mix characteristics, simply by visual assessment. These visual procedures should be used by practitioners as a check during mix designs, while quantitative comparisons using digital image processing techniques are more suited to research analyses.
- Fracture face analysis is suitable for comparing asphalt mastic distributions as a function of other mix parameters, such as asphalt type, asphalt content, mixing temperature, mixing moisture content, etc., for foamed asphalt mixes made from recycled aggregates with the same or similar gradations.
- Fracture face is **not** suited to comparisons of mixes with different parent aggregates, significantly different gradations, fracture faces of specimens prepared with different fabrication procedures or tested with using different test procedures, or when portland cement or other active fillers have been included in the mix. Care should also be taken in interpreting the results if dark-colored minerals are present in the aggregates.

7. LABORATORY STUDY: PHASE 2

7.1 Introduction

The second phase of the laboratory study addressed additional issues identified in the work plan. These tasks included:

- An investigation into the effects of asphalt binder properties, RAP sources, and RAP gradations on foamed asphalt mix properties measured by different laboratory test methods. A limited experimental design was followed in order to obtain a better understanding of these effects using multiple test methods, with a more detailed study planned for Phase 3 that would assess more levels of each variable using a single test method.
- Comparison of different laboratory test methods for assessing the strength characteristics of foamed asphalt mixes.
- Comparison of different laboratory test methods for assessing the stiffness (or resilient modulus) characteristics of foamed asphalt mixes.
- A study into the effects of mixing moisture content on foamed asphalt mix properties.
- A study into the effects of mixing temperature on foamed asphalt mix properties.
- The development of an anisotropic model relating laboratory stiffness tests to field stress states.

This comprehensive laboratory study lasted 30 months, during which more than eight tons of RAP materials were processed and approximately 3,000 specimens fabricated. Consistency of the material supply was critical to the success of this study.

7.2 Experiment Design

7.2.1 Test Matrix

The general factorial design for this phase of the study is summarized in Table 7.1. This matrix was modified where necessary to suit the requirements of each task, with revised matrices provided in the relevant sections.

7.2.2 Materials

Aggregate

RAP materials collected from the Route 33 (Ventura County) and Route 88 (Amador County) projects were used in this phase. Three gradations (denoted as Gradations A, B, and C) were constituted from each source by sieving the RAP into four fractions with three sieve sizes (19 mm, 9.5 mm, and 4.75 mm

[3/4 in., 3/8 in., and #4]) and recombining them as shown in Figure 7.1. Plant pulverized RAP (sourced from Granite Construction), virgin aggregate, and baghouse dust (both sourced from Graniterock Company), were added to adjust the gradations where necessary. Materials retained on the 19 mm (3/4 in.) sieve were discarded. The preparation of these gradations ensured that consistent materials were used throughout the study.

Table 7.1: Factorial Design for Phase 2 Laboratory Study

Variable	No. of Factor Levels	Values
RAP Source	2	- Route 33 (Ventura County) - Route 88 (Amador County)
Aggregate gradation (See Figure 7.1)	3	- Original gradation as pulverized in the field - Coarse gradation (6.5% passing 0.075 mm by mass)[1] - Fine gradation with 20% passing 0.075 mm by mass
Binder source and type	2	- Refinery A PG64-16, optimized foaming characteristics - Refinery A PG64-10, optimized foaming characteristics
Test methods and associated specimen fabrication methods	6	- ITS (100 mm), Marshall compaction - ITS (152 mm), Modified Proctor compaction[2] - Flexural beam, vibratory hammer compaction - Triaxial Resilient Modulus, adjusted Modified Proctor compaction - UCS, adjusted Modified AASHTO compaction - Free-free resonant column (FFRC) resilient modulus tests on beam and triaxial specimens
Density for 100-mm ITS specimens	3	- 35 blows on each face - 50 blows on each face - 75 blows on each face

Replicates	2	- Two replicate batches for each mix.
		- For each batch of mix:
		  - 9 x 100 mm ITS specimens (3 compaction, 3 replicates)
		  - 2 x 152 mm ITS specimens
		  - 2 x beam specimens
		  - 1 x triaxial specimen

Water conditioning method	2	- 72 hours soaking (referred to as "soaked") - No conditioning (referred to as "unsoaked")
Fixed values		
Asphalt content (%)[3]	1	- 3
Active filler content (%)	1	- No active filler added
Curing method	1	- 40°C oven curing, unsealed, for 7 days
Testing temperature	1	- 20°C
Control	1	- One batch for each mix[4] - 9 x 100 mm ITS specimens (3 compaction, 3 replicates) - 1 x 152 mm ITS specimen - 1 x triaxial specimen

[1] 0.075 mm sieve equivalent to #200 sieve
[2] The 152 mm ITS tests were carried out on "soaked" specimens only.
[3] Asphalt contents are percent by mass of dry aggregate.
[4] Beam specimens were not prepared for the control mix as the untreated beams were too weak to be handled.

The assessment of the effects of gradation on the performance of foamed asphalt mixes, as defined in the work plan, was as follows:

- The SR33-A and SR88-A materials represented the average gradations as pulverized on each road, containing 8 and 10 percent fines passing the 0.075 mm (#200) sieve by mass, respectively.
- The SR33-B and SR88-B materials represented coarser gradations with 6.5 percent fines passing the 0.075 mm (#200) sieve.
- The SR33-C and SR88-C materials were produced by adding baghouse dust to SR33-B and SR88-B to produce materials with 20 percent passing the 0.075 mm (#200) sieve, thereby allowing assessment of the effects of higher fines contents on performance.

Basic properties of the materials are summarized in Table 7.2.

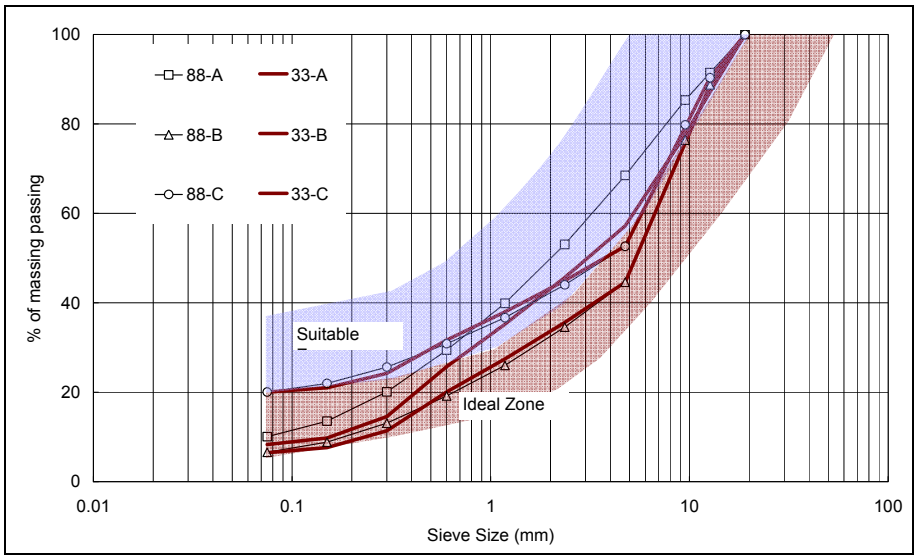

Figure 7.1: Phase 2 RAP gradation.
(Curves for 33-B and 88-B, and 33-C and 88-C overlap. "Ideal" and "suitable" zones follow South African guidelines [*3*])

Table 7.2: Basic Properties of the RAP Materials Used in Phase 2

Parameter	Material					
	33-A	33-B	33-C	88-A	88-B	88-C
Mineralogy of aggregates in the RAP	Granitic			Granitic		
Mineralogy of granular base included in RAP	Predominantly quartzitic gravel of alluvial origin (sourced from a river bed)			Sandy gravel of granitic origin		
Mineralogy of supplementary fines	Granite (crushed)					
Plasticity Index	NP[1]	NP	NP	NP	NP	NP
Optimum moisture content[2] (%) (Modified Proctor)	5.4	5.0	5.5	7.0	6.7	6.0
Max. Dry Density[2] (kg/m^3)	2,170	2,190	2,170	2,080	2,110	2,140
pH (AASHTO T289)	8.2	NM[3]	NM	6.7	NM	NM

[1] NP, nonplastic.
[2] Determined with Modified Proctor method (AASHTO T180)
[3] NM, not measured.

Detailed quantitative morphological analyses were not carried out on the RAP materials collected. A visual inspection showed that the aggregate angularities of the RAP from Route 33 and Route 88 were similar as illustrated in Figure 7.2. However, more aggregate particles from Route 33 were coated with an oxidized asphalt binder film compared to those from Route 88. Coated aggregate particles had a rougher surface texture than those of the uncoated particles (Figure 7.3).

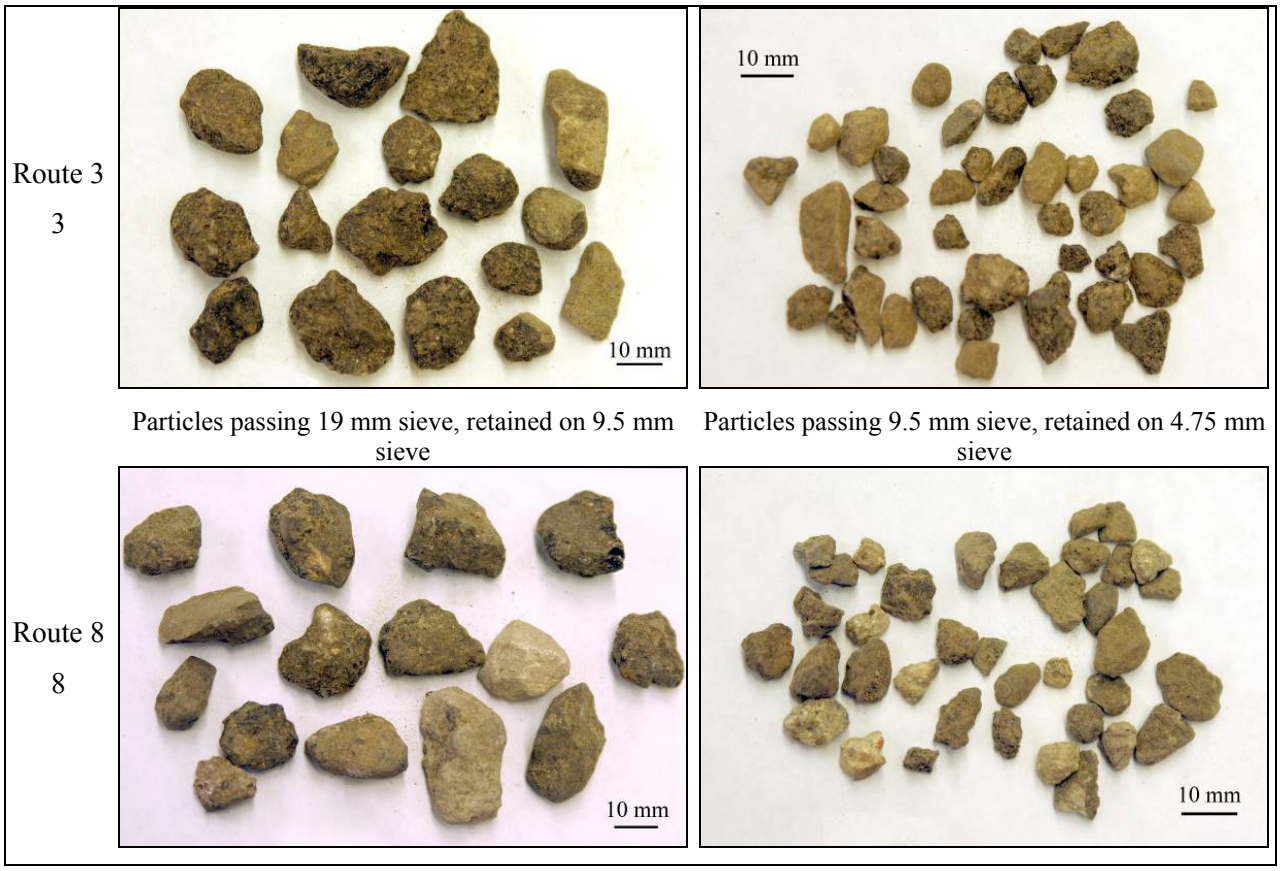

Figure 7.2: Visual properties of aggregates from Route 33 and Route 88.

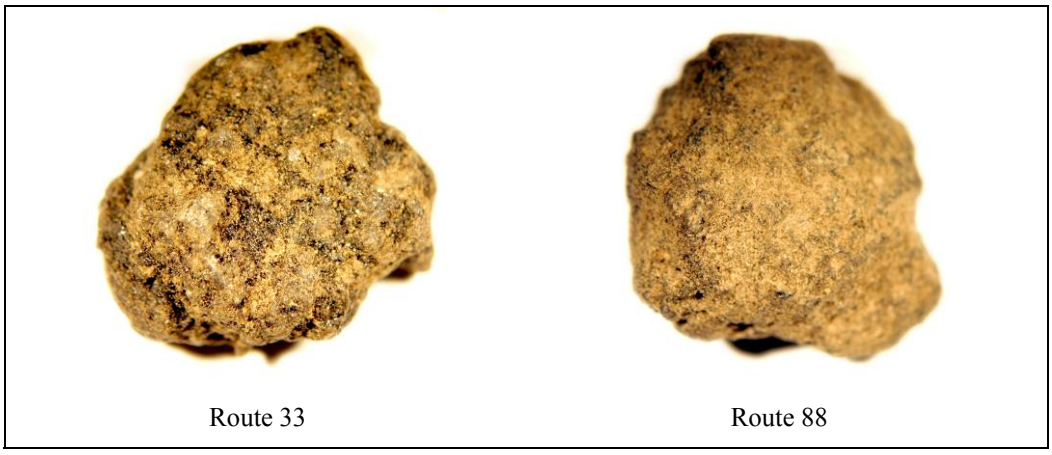

Figure 7.3: Surface texture of typical RAP particles.
(The diameter of both particles is approximately 5 mm.)

Asphalt Binder

Two grades of asphalt binder (PG64-16 and PG64-10) were used in this phase of testing. Both were sourced from Refinery A, and were reportedly produced from a blend of crude oils from the San Joaquin Valley (90 percent) and from Ecuador (10 percent). All foaming was carried out at 165°C (330°F) with 4 percent foaming water by mass of asphalt added. The average measured foam characteristics throughout this phase of laboratory testing are summarized in Table 7.3.

Table 7.3: Average Foam Characteristics for Phase 2 Testing

Binder	Expansion Ratio	Half-Life (seconds)
PG64-16	23	19.5
PG64-10	22	22.0

7.2.3 Specimen Fabrication and Test Procedures

Aggregate Mixing

Foamed asphalt was added to the aggregate following the standard procedures adopted in Phase 1. Precise temperature control of the loose mix was impractical, but the aggregate temperature was controlled between 25°C and 30°C (77°F to 86°F). The foamed asphalt content was fixed at three percent by mass of aggregate. For each mix type, one batch of loose mix (65 kg [143 lb] total) was prepared to fabricate the different types of specimens for laboratory testing detailed in the factorial design (Table 7.1 and Table 7.4). No active fillers were added in this phase.

Table 7.4: Specimen Preparation for Each Batch of Mix

Specimen Type	No. of Specimens	Compaction	Remarks
ITS (100 mm)	9	Marshall	- 3 compaction levels and 3 replicates per compaction level - 2 specimens for soaked testing and 1 for unsoaked testing per compaction level
ITS (152 mm)	1	Modified Proctor	- For soaked testing only
Flexural beam	2	Vibratory hammer	- 1 replicate for soaked testing and 1 for unsoaked testing
Triaxial	1	Adjusted Modified Proctor	- Each specimen subjected to resilient modulus testing in unsoaked condition, and then in soaked condition
UCS	1	Adjusted Modified Proctor	- For soaked testing only - Utilize the same specimens as the triaxial resilient modulus test
FFRC	2+1	Adjusted Modified Proctor	- Utilize the same specimens as the triaxial test (1 replicate) and the flexural beam test (2 replicates) - Unsoaked testing only
ITS: Indirect Tensile Strength UCS: Unconfined Compressive Strength FFRC: Free-free Resonant Column]			

Indirect Tensile Strength Test (100 mm)

Specimens with a nominal diameter of 100 mm (4 in.) and a nominal height of 63.5 mm (2.5 in.) were compacted following the Marshall compaction method *(44)*. Three compaction effort levels (35, 50, and 75 blows per face) were used and three replicate specimens were fabricated for each compaction effort. Two of the three replicate specimens at each compaction were tested after water conditioning, while the third specimen was tested dry. The same procedure was followed for the control specimens (no foamed asphalt).

The test setup prescribed in AASHTO T322 (*Standard Method of Test for Determining the Creep Compliance and Strength of Hot Mix Asphalt (HMA) Using the Indirect Tensile Test Device*) was followed as a slower loading rate (displacement controlled at a rate of 12.5 mm [0.5 in.] per minute of movement of the testing head) was desired. In later phases, the loading rate was changed to 50 mm (2 in.) per minute, which complied with AASHTO T283 [*Resistance of Compacted Bituminous Mixture to Moisture Induced Damage*]. ITS test results from Phase 2 were therefore not compared directly with results from the later phases. However, an approximate correlation between ITS values tested at the two loading rates was developed in Phase 3 and is discussed in Chapter 9.

Indirect Tensile Strength Test (152 mm)

Specimens with a nominal diameter of 152 mm (6 in.) and a nominal height of 116 mm (4.6 in.) were compacted following the Modified Proctor method (AASHTO T180 protocol), although the moisture content was not varied. One specimen was prepared from each batch of mix. The Modified Proctor (or modified AASHTO) density of the specimen at the compaction moisture content was calculated and used as the reference density for triaxial and beam specimen preparation. The treated specimen was cured and then moisture conditioned. In the control test (no foamed asphalt), specimens were tested in both unsoaked and soaked conditions.

The 152 mm ITS test was displacement controlled in a similar manner to the 100 mm ITS test. The strain rate was the same.

Triaxial Resilient Modulus Test

Cylindrical specimens with a nominal diameter of 152 mm (6 in.) and a height of 305 mm (12 in.) were prepared for Triaxial Resilient Modulus tests. Compaction procedures prescribed in AASHTO T180 and AASHTO T307 (vibratory impact hammer without kneading action) were both assessed. A modified version of AASHTO T180 was ultimately selected in which specimens were compacted in 12 lifts of 25 mm (1 in.) thick layers, with the mass of the mix of each layer calculated based on the 100 percent

modified AASHTO density obtained from the 152 mm ITS specimens. The method adopted provided specimens with less segregation, better bonding between lifts, and more precise density control.

The test procedure was modified from the AASHTO T307 test protocol. Resilient moduli at various confining stress levels, deviator stress levels, and loading rates were tested. The confining stress and deviator stress levels adopted were the same as those of AASHTO T307. For each combination of confining stress and deviator stress, haversine load pulses at four different loading rates were applied as follows:

- 0.05 second pulse width with 0.45 second relaxation,
- 0.1 second pulse width with 0.4 second relaxation,
- 0.2 second pulse width with 0.8 second relaxation, and
- 0.4 second pulse width with 0.6 second relaxation.

Since the Triaxial Resilient Modulus test was essentially nondestructive, each specimen was first tested for resilient modulus after dry curing, and then retested for resilient modulus after soaking.

Unconfined Compressive Strength Test

The Unconfined (or Uniaxial) Compressive Strength (UCS) test was performed on the same cylindrical specimens as the Triaxial Resilient Modulus test, which was assumed to be essentially nondestructive. On completion of the soaked resilient modulus test, the UCS test was carried out with displacement-controlled loading at a rate of 15 mm/min (0.6 in.).

Flexural Beam Test

A new monotonic flexural beam test procedure was developed for the UCPRC study. The nominal dimensions of the beam specimens were 560 mm x 152 mm x 80 mm (22 in. x6 in.x3.2 in.) (Figure 7.4). The quantity of moist material required to fabricate one beam was calculated based on the 100 percent modified AASHTO density determined during the 152 mm ITS test specimen preparation. The material was then compacted in a steel mold to the target volume by alternately applying two steel compaction heads (one flat and one curved, both with dimensions of 150 mm x 150 mm [6 in.]). The compaction heads were driven by a Hilti® TE 76P Combihammer with vibration force. Specimens were tested as extruded from the mold, with no cutting to final dimensions. Two beams were prepared from each batch, one for unsoaked testing and one for testing after soaking.

The flexural beam test configuration was similar to that of AASHTO T97, but the beam thickness was 80 mm (3.2 in.) instead of 150 mm (6 in.), and loading was displacement rate-controlled rather than stress

rate-controlled. The span length was 450 mm (18 in.) and loads were applied monotonically at the two third-points with a constant displacement rate of 25 mm/min. Two metal plates were glued at the midspan of the beam, with a linear variable displacement transducer (LVDT) attached to each metal plate to measure the deflection during testing (Figure 7.4).

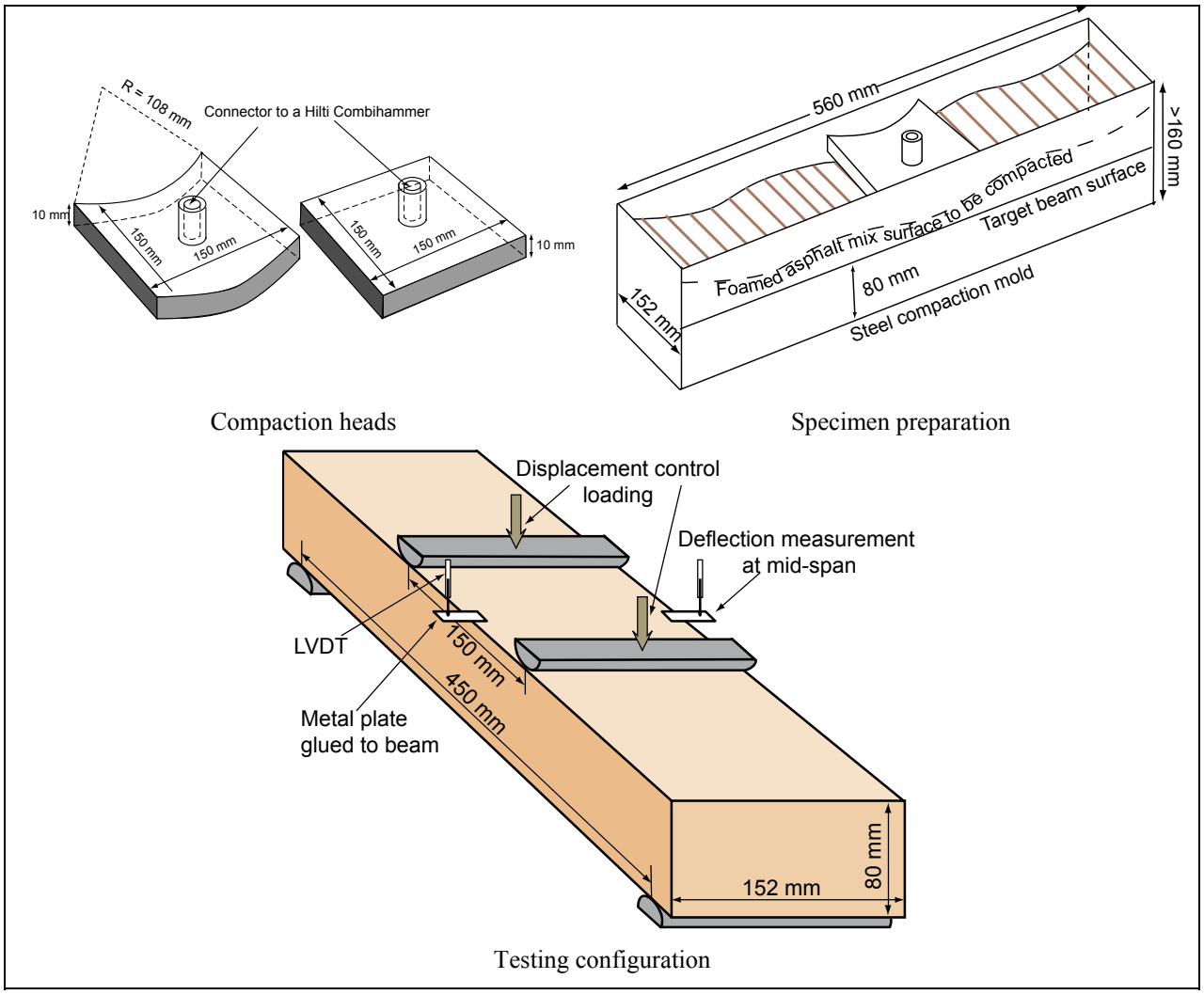

Figure 7.4: Flexural beam test preparation and configuration.

Free-Free Resonant Column Test

The Free-Free Resonant Column (FFRC) test was carried out on triaxial and beam specimens prior to destructive testing. The test setup was similar to that reported by Nazarian *(45)*, and Hilbrich and Scullion *(46)*. This test normally utilizes cylindrical specimens with a length-to-diameter ratio of 2 to 1 (similar to the triaxial test specimens), but beam specimens (ratio of 4.5 to 1) were also tested to obtain a larger data set. Since this test is nondestructive, all cylindrical and beam specimens were subjected to this test before the triaxial and flexural beam tests. The specimens were only tested in an unsoaked condition, as it was not possible to mount the accelerometer on soaked specimens.

Mixing Moisture Content

A target mixing moisture content of one percent lower than the optimum moisture content determined with the modified Proctor method (T180) was initially used for all tests. This moisture content was based on the findings of the literature review and experience of the UCPRC research team. A small study was also conducted as part of this phase to quantify the effects of different mixing moisture contents on foamed asphalt mixes (Section 7.5).

Curing and Water Conditioning

In this phase, all compacted specimens were cured, unsealed, in a forced draft oven at 40°C (105°F) for seven days. Specimens subjected to water conditioning were soaked in a water bath at 20°C (68°F) for 72 hours with water levels maintained at 100 mm (4 in.) above the top surface of the specimen. The prolonged drying and soaking durations were designed to represent critical field conditions, and to reduce the effects of different specimen sizes.

7.3 Assessment of Strength

The comparison of different laboratory test methods for assessing the strength characteristics of foamed asphalt mixes consisted of the following investigations:

- Effects of unsoaked versus soaked testing;
- Effects of compaction effort levels on density, and effects of density on strength;
- Effects of different binder grades; and
- Effects of different test methods.

7.3.1 Effects of Unsoaked versus Soaked Testing

Knowledge of the effect of soaking on foamed asphalt material behavior is important for understanding the behavior of treated materials in in-service pavements during fluctuating moisture conditions. The asphalt mastic phase of a foamed asphalt mix only partially coats aggregates, unlike HMA materials, where the aggregates are generally completely coated. In foamed asphalt mixes, the voids ratio and permeability are also substantially higher, and thus the mix properties are more sensitive to moisture conditioning. In California, the foamed asphalt-treated base layer is usually built on a thin granular subbase layer or directly on the subgrade and is therefore susceptible to seasonal moisture fluctuations. In farming areas, the situation is often aggravated by irrigation and land preparation practices that impact road drainage. This phenomenon was clearly observed in the seasonal field performance and stiffness monitoring program discussed in Chapter 4, as well as on other projects that were observed during the course of the UCPRC study. An example of FWD measurements on a section of road where side drains were used for transferring irrigation water compared to an adjacent section where this did not occur is

shown in Figure 7.5. The plot clearly shows the different response. Inadequate drainage was also identified as a primary cause of localized premature failure on the FDR-foamed asphalt project on Route 33 discussed in Chapter 4. These observations prompted a more in-depth comparison of unsoaked and soaked laboratory strength test results.

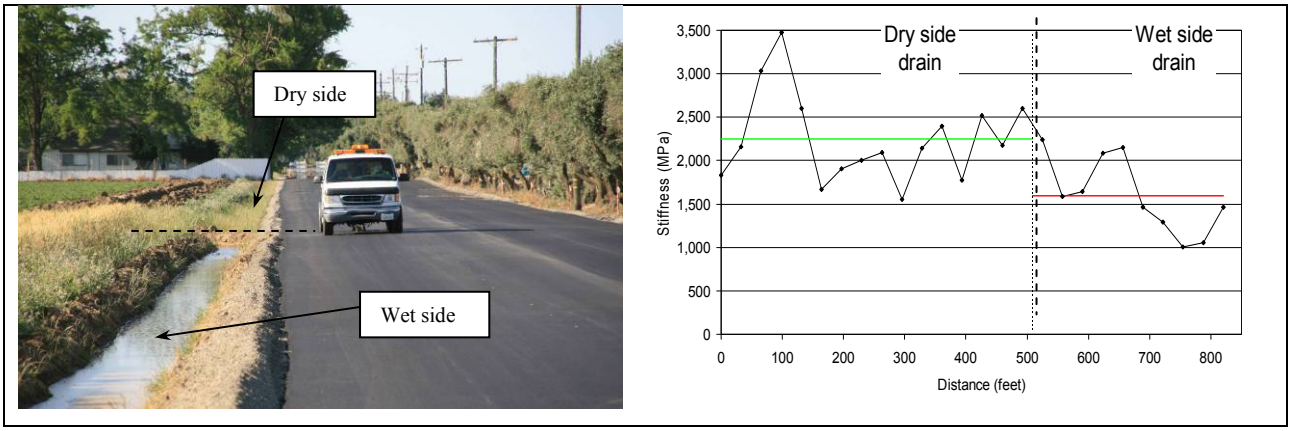

Figure 7.5: Effect of side drain water on foam asphalt base stiffness.
(FWD measurements taken 150 m [500 ft.] either side of boundary between wet and dry side drains)

Most laboratory test studies reported in the literature were based on strength testing, primarily using the Indirect Tensile Strength (ITS) test, under both unsoaked and soaked conditions. However, two different approaches have been employed for interpreting unsoaked and soaked test results:

- In the mix design and structural design procedures presented in the South African guidelines *(3)* and the *Wirtgen Cold Recycling Manual (6)*, unsoaked strengths (both the ITS and UCS) are recommended as the primary properties to be maximized, and minimum requirements for their moisture susceptibility are prescribed. The minimum required Tensile Strength Retained (TSR, in percentage) value, which is the ratio of unsoaked and soaked strengths, varies between 50 percent and 75 percent depending on local climate.
- Muthen *(2)* proposed that foamed asphalt specimens be tested at the most severe possible working environment (i.e., under soaked conditions). Romanoschi et al. *(47)*, Marquis et al. *(48)* and Kim and Lee *(49)* followed Muthen's philosophy to optimize mix design variables solely according to soaked strength values.

The different mechanisms that influence strength in a foamed asphalt-treated material need to be considered when studying the implications of unsoaked versus soaked laboratory testing. Cured, untreated RAP specimens (the control used in the UCPRC study) normally have measurable tensile strength, which can be generally attributed to three mechanisms:

- Weak chemical bonding. The aggregates and fines in the HMA and granular base materials in the original pavement being recycled may contain carbonates, oxides, silicates, organic matter, and other reactive components, which could precipitate at interparticle contacts and act as cementing agents *(50)*.
- Suction from the residual water. Specimens that have been subjected to oven curing at 40°C to 50°C (104°F to 122°F) still retain residual moisture after removal from the oven. According to Jenkins *(33)*, the moisture content of these specimens is generally between zero and 1.5 percent, but it is always lower than 4.0 percent. According to Lu et al.'s *(51)* calculation for an idealized spherical particle model, the tensile strength contributed by capillary suction in silts is typically several tens of kPa. Osmotic suction, which also contributes to the total suction, is often of the same magnitude as capillary suction.
- Adhesion of the old oxidized asphalt binder. Although the residual binder in RAP has been partially oxidized, it can still develop cohesion during compaction, with the level dependent on the extent of oxidization and the temperature at which the material is compacted. Compared to the other two mechanisms discussed above, it is considered to be of lesser importance.

These mechanisms are also applicable to foamed asphalt-treated materials. In addition to these, the foamed asphalt mastic bonds aggregate particles together providing additional tensile strength. During the UCPRC study, observations of the fractures induced by ITS and flexural beam testing revealed that the fracture seldom initiated and propagated through aggregate particles, except for some cases where the particles were cracked during compaction. In the following discussion, the three mechanisms listed above are assumed to all contribute to the tensile strength of the mineral filler phase.

If foamed asphalt specimens are tested for tensile strength in the unsoaked state, three of the mechanisms discussed above (weak chemical bonding, suction, and foamed asphalt bonding) will all contribute to the measured strength. However, when foamed asphalt specimens are soaked in water, most of the voids become saturated, and the weak chemical bonds between aggregates and the bonds created by suction are significantly weakened. The bonds formed by foamed asphalt are also negatively affected by soaking, but to a lesser extent. Therefore, under soaked conditions and in the absence of active fillers, the tensile strength of foamed asphalt mixes is primarily provided by the foamed asphalt, the bonding effects of which are readily measurable.

Table 7.5 and Figure 7.6 provide a summary of the results of strength testing using three different test methods (100 mm ITS, 152 mm ITS, and flexural beam), two different moisture conditions (unsoaked and soaked), two RAP sources (Route 33 and Route 88), and three gradations (in place [A], fine [B], and

course [C]). The results from the untreated controls are also included. The values shown for the treated specimens are an average of the two binder types (PG64-16 and PG64-10 both at asphalt content of 3.0 percent) and an average of the replicate specimens tested.

Table 7.5: Summary of Flexural and Tensile Strength Test Results

RAP Source	Tensile or Flexural Strength (kPa)								
	Unsoaked				Soaked				
	Control		3% Foam Asphalt		Control		3% Foam Asphalt		
	ITS 100 mm[1]	ITS 152 mm	ITS 100 mm[1]	Beam	ITS 100 mm[1]	ITS 152 mm	ITS 100 mm[1]	ITS 152 mm	Beam
33-A	725	632	979	1,550	74	113	170	142	265
33-B	756	613	857	1,261	76	92	209	122	213
33-C	287	246	616	1,036	10	28	95	104	87
88-A	318	300	505	800	66	60	187	222	205
88-B	172	244	555	856	46	34	236	148	204
88-C	64	198	486	711	0	20	128	125	72

[1] Only average of results for compaction with 75 blows shown.

The results indicate that the unsoaked control mixes of the SR33-A and SR33-B materials had much higher tensile strengths than the other control mix types. Although no X-Ray diffraction analyses were carried out, the higher strengths were attributed to a weak chemical reaction between the fines, given that the addition of 15 percent baghouse dust on the SR33-C mix (which diluted the existing fines) resulted in significantly lower strengths. The added mineral baghouse dust thus appeared to dominate the unsoaked strength of the SR33-C material. The weak cementation and suction were mostly eliminated after the specimens were subjected to water conditioning, with the SR33-A and SR33-B control mixes losing 80 to 90 percent of their unsoaked strength.

The foamed asphalt-treated mixes showed similar trends. Although the ITS and flexural beam strength values increased with the addition of the foamed asphalt, the unsoaked strengths still appeared to be dominated by the properties of the RAP. The unsoaked ITS values of the treated SR33-A and SR33-B materials were between 44 and 120 percent higher than those of the other four RAP materials. In contrast, the soaked tensile strengths of the SR33-A and SR33-B materials were similar or less (depending on the test method) than those of other RAP materials. This indicates that the properties (chemical bonding and suction) dominating the unsoaked strengths are not significant when the materials are soaked prior to testing. Consequently the stabilizing effects of foamed asphalt can be observed more clearly in the soaked condition, which is desirable for mix design purposes.

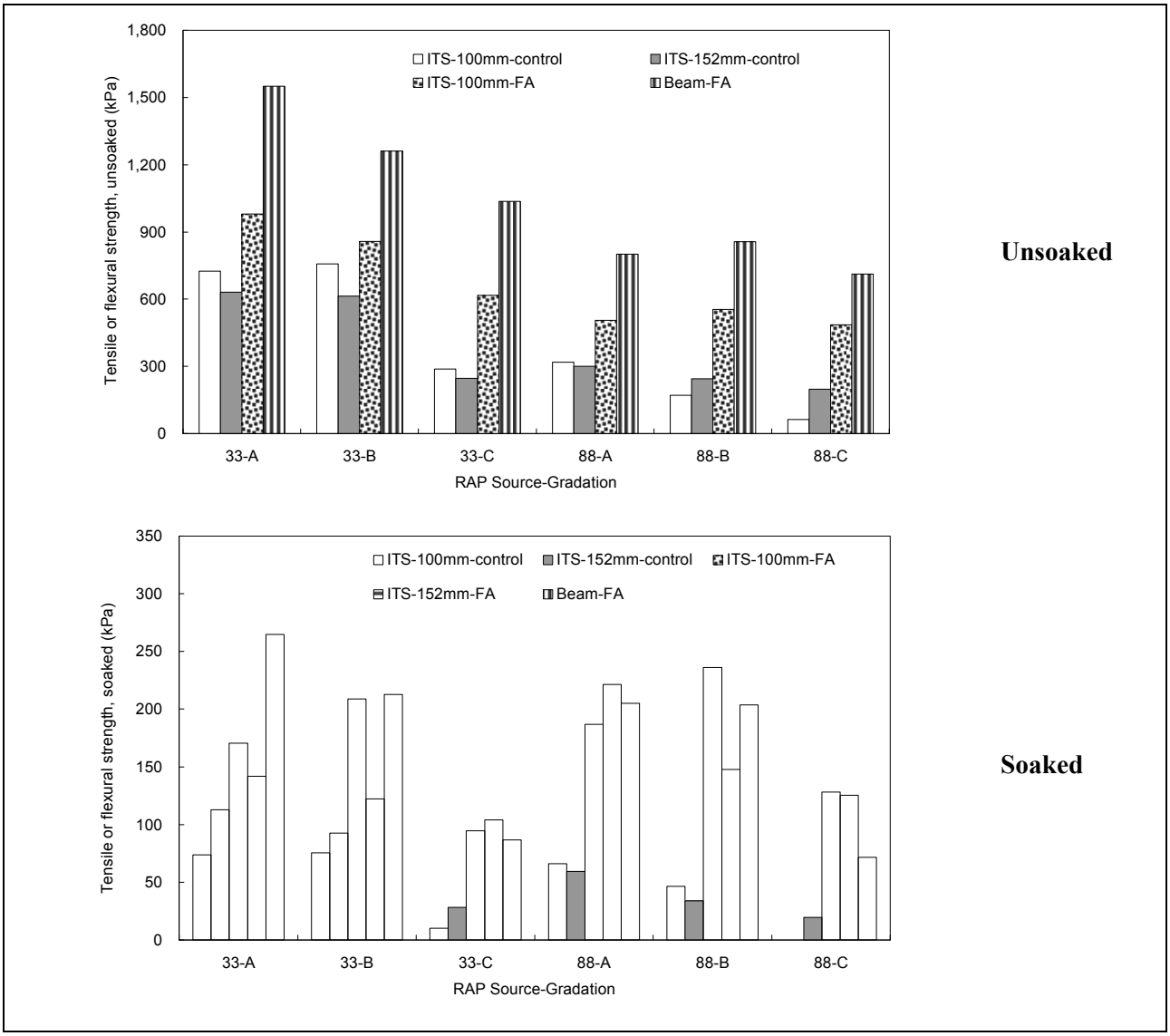

Figure 7.6: Comparison of unsoaked and soaked strength test results.
(FA = foamed asphalt-treated specimens)

7.3.2 Effects of Compaction Effort and Density

Three levels of compaction effort (35, 50, and 75 blows per face, or high, medium, and low) were used to compact the 100 mm-ITS specimens. The bulk specific gravity and soaked ITS test results are summarized in Table 7.6. Due to the large number of specimens to measure and the limited available resources, the well-established procedures for measuring bulk specific gravity of hot-mix asphalt were not followed. Instead, the diameter and height of each ITS specimen were measured, from which the bulk volume was calculated. Since the surfaces of specimens after curing were not perfectly smooth, a high variance was observed. However, the overall comparison of bulk specific gravities between different compaction effort levels should be valid, given that a standard procedure was consistently followed. Results shown in Table 7.6 are averages of the values for two binder grades, replicate batches of mixes,

and replicate specimens for each batch. Data shown in Figure 7.7 and Figure 7.8 are for individual batches of mixes.

Table 7.6: Effects of Compaction Effort on Density and Strength

RAP Source	75 Blows/Face		50 Blows/Face		35 Blows/Face	
	BSG	ITS	BSG	ITS	BSG	ITS
33-A	2.12	170	2.07	131	2.03	89
33-B	2.11	209	2.06	131	1.98	92
33-C	2.15	95	2.14	89	2.10	75
88-A	2.06	187	1.99	143	1.95	103
88-B	2.11	236	2.09	176	2.03	121
88-C	2.11	128	2.07	110	2.02	81
BSG: Bulk Specific Gravity						

On average, the resulting bulk densities of the specimens compacted with the medium compaction effort were two percent lower than the bulk densities of the specimens compacted with the higher effort (Figure 7.7), and soaked ITS values were 26 percent lower (Figure 7.8). Similarly, the density and strength reduction for the specimens compacted with the low compaction effort were 4 percent and 48 percent lower than those of the medium compaction effort, respectively. Figure 7.9 shows the effects of compaction effort on soaked strengths for each RAP and binder type The foamed asphalt mixes with coarse gradations were more sensitive to compaction effort (or density) than those with finer gradations.

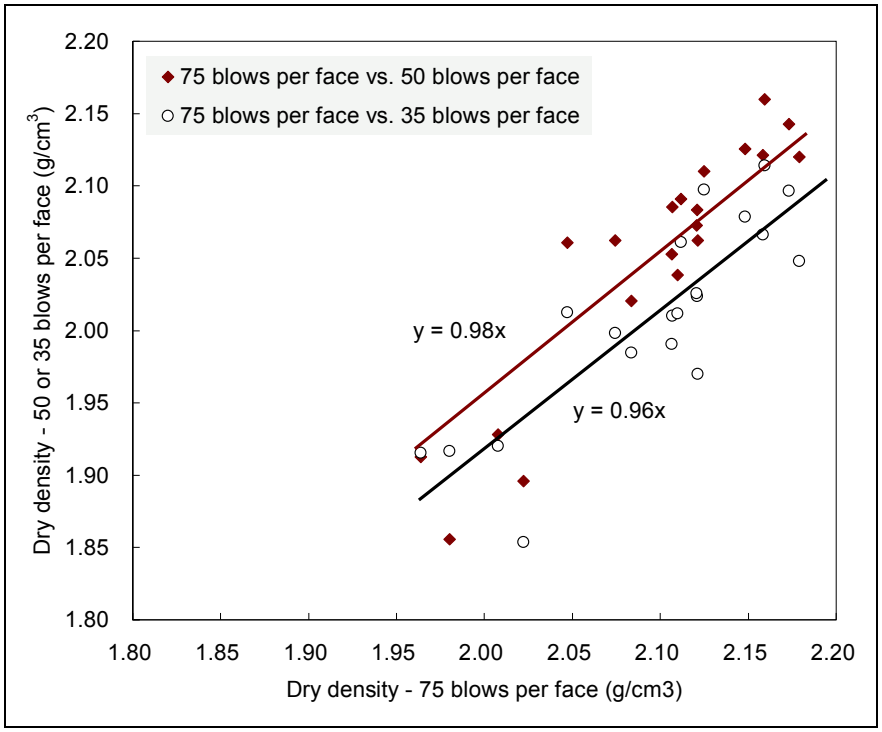

Figure 7.7: Effect of compaction effort on unsoaked density.

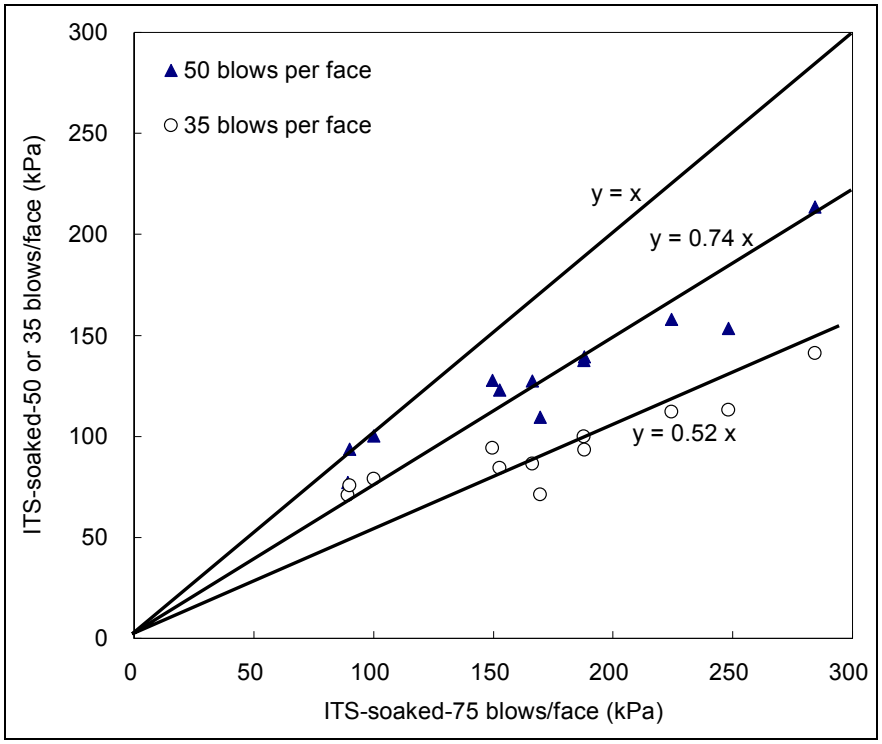

Figure 7.8: Effect of compaction effort on soaked ITS strength.

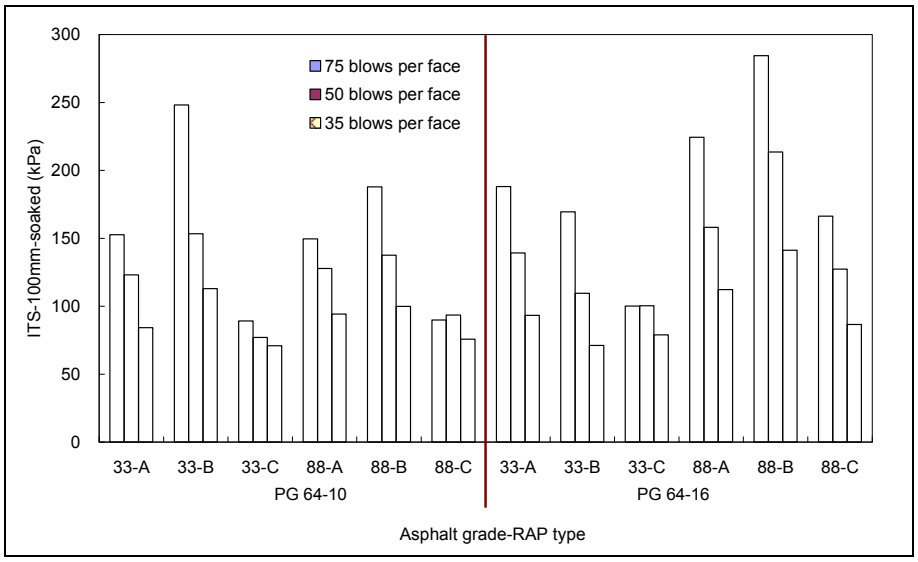

Figure 7.9: Effect of binder grade and compaction effort on soaked ITS strength.

7.3.3 Effects of Binder Grade

The effects of binder grade on the soaked strength of ITS (100 mm and 152 mm) and flexural beam specimens are summarized in Table 7.7 and Figure 7.10. The mixes treated with the softer (less viscous) PG64-16 asphalt generally had higher tensile strengths and better asphalt distribution represented by higher fracture face asphalt coverage (FFAC) values than the PG64-10 binder (see Section 6.6), with some exceptions.

Table 7.7: Effects of Asphalt Grade on Flexural or Tensile Strength

33-A	153	10	188	16
33-B	248	23	170	19
33-C	89	3	100	5
88-A	150	4	224	7
88-B	188	8	284	16
88-C	90	3	166	6
33-A	160	14	124	16
33-B	123	22	122	29
33-C	71	4	138	11
88-A	183	7	261	16
88-B	118	13	177	17
88-C	117	6	134	10
	Beam Flexural Strength, Soaked			
33-A	247	14	282	13
33-B	259	20	167	20
33-C	104	2	69	7
88-A	171	7	239	10
88-B	204	16	204	24
88-C	60	3	83	8

Two characteristics of an asphalt binder primarily determine the capacity of foamed asphalt to improve the tensile strength of granular materials:

- The level of dispersion of the asphalt through the mix, and
- The strength of bonding provided by the dispersed asphalt.

The grade of asphalt influences these characteristics in opposing ways:

- Results indicate that the softer asphalt (PG64-16) had better dispersion. Although the two grades used in this study have similar foaming characteristics in terms of the expansion ratio and half-life (Table 6.2), image analyses clearly show that the softer grade had significantly better dispersion. The softer asphalt had lower viscosity than the harder asphalt at the same temperature and same expansion ratio. When the asphalt bubbles collapsed, the softer asphalt film adhered to more of the finer aggregate particles.
- It can generally be assumed that the bonding provided by the harder asphalt should have higher strengths at the same temperature and loading rate, given the temperature sensitivity of the asphalt. Although this was observed, the test data clearly show that better dispersion, as determined using FFAC, had a larger influence on strength (Figure 7.10).

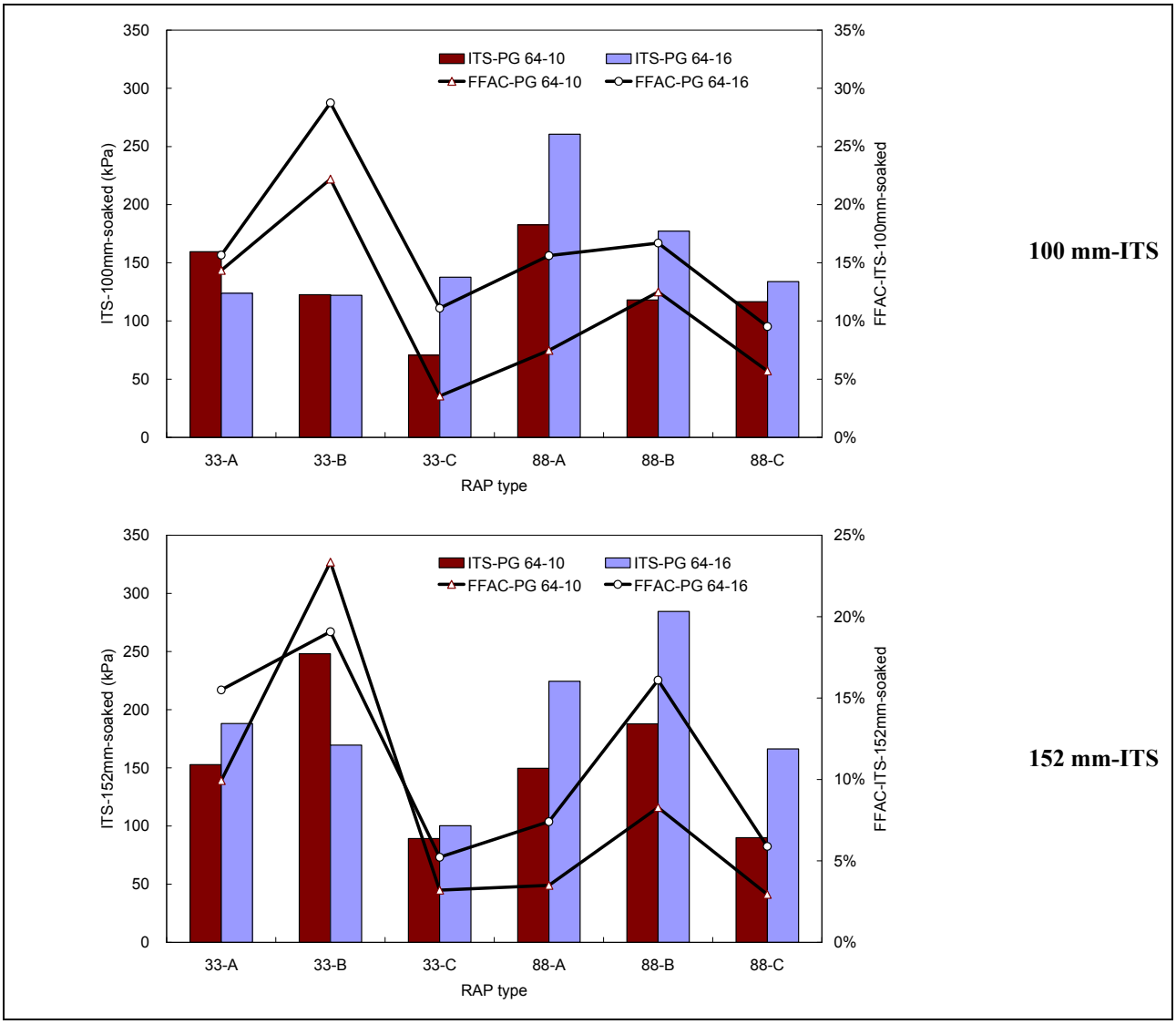

Figure 7.10: Effect of binder grade on strength.

7.3.4 Comparison of Different Test Methods

The ITS-100mm, ITS-152mm, UCS, and flexural beam tests all provided acceptable indications of the tensile strength of foamed asphalt-treated materials. A good correlation was obtained between the ITS-152mm test results and the UCS test results, supporting findings in the literature *(26)* (Figure 7.11).

All the tests assessed in the UCPRC study appeared to measure the same properties of the foamed asphalt mixes. This conclusion is based on analysis of the test results which revealed that:

- The measured tensile strength ranges determined with different methods on soaked specimens were similar, as shown in Table 7.5 and Figure 7.6.
- Performance in terms of asphalt grade, RAP source, and RAP gradation showed similar rankings. Softer asphalt grades showed higher strengths for all tests and mixes, with SR33-C and SR88-C materials showing significantly lower strengths than materials with other gradations. The

differences between the other four RAP types were within the range of measurement "noise." (Results from the Phase 3 study [Chapter 8] revealed that foamed asphalt mixes made with the SR33-A, SR33-B, SR88-A, and SR88-B RAP materials types had similar strength values.)

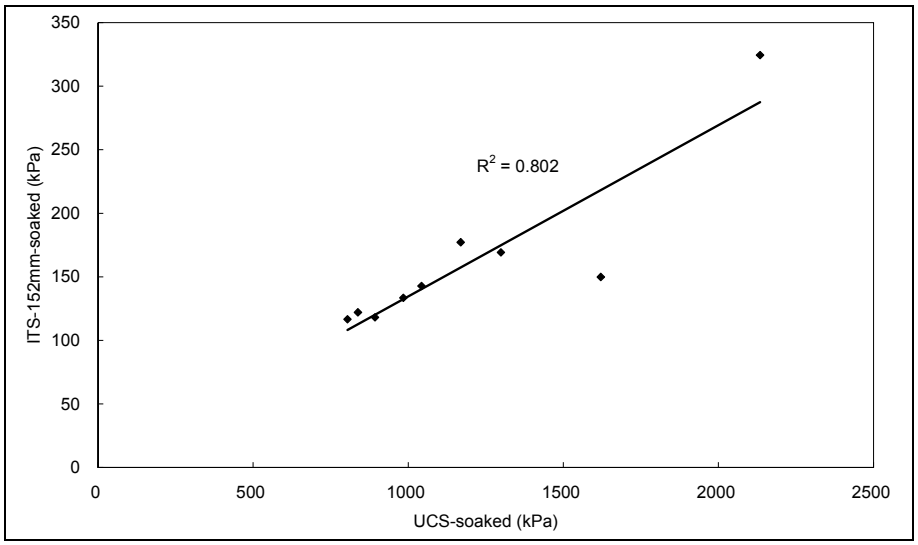

Figure 7.11: Comparison of ITS-152 mm and UCS test results

The ITS-100 mm test was found to be the easiest and most economical (in terms of time and material) to perform compared to the other tests, which showed no significant superiority in terms of results. It was therefore decided that the ITS test using 100-mm diameter specimens would be used as the primary test method for all subsequent material (tensile) strength testing in the UCPRC study. Adopting the ITS test allowed for more replicates to be tested and more levels of variables to be included in each experiment factorial than if the UCS test had been adopted. (The original work plan called for 492 strength tests. However, by adopting the ITS test, more than 2,500 strength tests were eventually carried out during the laboratory study, which provided considerably more insight into the performance of foamed asphalt-treated materials than the original plan would have provided.)

7.3.5 Summary of Recommendations for Strength Testing

The following recommendations regarding strength testing are made:

- All laboratory strength testing should be carried out in the soaked condition. Compared to unsoaked tests, strength tested after soaking better characterizes the stabilizing effects of foamed asphalt. Soaked conditions also better represent critical field conditions.
- The use of softer asphalt binder grades is encouraged, as these have better dispersion than harder binders for the same or similar foaming characteristics.
- The highest possible density should be strived for during construction, as higher strengths are obtained with increasing density.

- The ITS test (100 mm diameter, Marshall compaction) can be used for laboratory characterization of foamed asphalt mixes, provided that sufficient replicates are tested. It is considered a simple, economical, and reliable test method, capable of characterizing the stabilizing effects of foamed asphalt.

7.4 Assessment of Stiffness

7.4.1 Introduction

The resilient modulus of foamed asphalt-treated material characterizes its resistance to resilient deformation under applied loads. It is defined as the ratio of the amplitude of the applied stress to the amplitude of the resultant recoverable strain. Although the definition points to measuring "recoverable" deformation under cyclic loading, the initial elastic modulus measured in monotonically loaded tests is also often taken as the resilient modulus. In a typical full-depth recycled pavement structure, the resilient modulus of the foamed asphalt layer has a significant influence on the bending deformation and fatigue life of the asphalt concrete surfacing, as well as the distribution of the traffic load to reduce stresses in the underlying layers. The resilient modulus in a treated layer will change with changing moisture condition.

Although considerable research has been published on resilient modulus testing of foamed asphalt in the laboratory, no published research on testing resilient modulus using triaxial or flexural beam tests in the soaked condition could be located. This type of testing was considered fundamental for understanding the behavior of foamed asphalt mixes in California and was therefore included in the UCPRC study. The primary tasks included:

- An investigation of the effects of foamed asphalt treatment on stiffness behavior compared to untreated controls;
- Comparison of different laboratory test methods, and
- Prediction of field performance by combining stiffness values measured under different laboratory stress states (Section 7.7).

7.4.2 Background

As discussed elsewhere in this document, foamed asphalt mixes have characteristics different from those of hot-mix asphalt (HMA) and granular base materials. The fine aggregate particles in foamed asphalt mixes are only partially coated with asphalt binder during foaming to form an asphalt mastic phase, and a considerable proportion of the voids in the aggregate skeleton are filled with fine mineral particles (or mineral fillers) with no asphalt coating. Portland cement is frequently added to foamed asphalt mixes, but at relatively low contents (1.0 to 2.0 percent by mass of the dry aggregate) compared to foamed asphalt contents (2.0 to 3.5 percent by mass of aggregate). The foamed asphalt mix can thus be regarded as a

weak asphalt-bound material. It is well known that the strength, resilient modulus, and permanent deformation resistance of foamed asphalt mixes are dependent on the stress state *(52-54)*, which is typical of unbound or weakly bound granular materials. However, foamed asphalt mixes can withstand some tensile or bending deformation, and even show some fatigue resistance, which is typical of bound materials. This has been demonstrated by ITS tests *(36)*, monotonic flexural beam tests *(16,17)*, and cyclic flexural beam tests *(8,27)*.

Laboratory resilient modulus test methods and procedures used for assessing foamed asphalt mixes were all originally developed for granular, stabilized, or asphalt concrete materials. For instance, the Indirect Tensile Resilient Modulus Test (AASHTO TP31 [withdrawn in 2001], ASTM D4123 [withdrawn in 2003], and LTPP P07) and the cyclic flexural beam test for dynamic modulus and fatigue (AASHTO T321) were both originally developed for HMA materials, while the triaxial resilient modulus test (AASHTO T307) is a conventional test method for unbound granular materials. The cyclic flexural beam and triaxial resilient modulus tests were specifically designed to measure resilient modulus, whereas tests such as the triaxial permanent deformation and cyclic flexural fatigue beam tests were developed for other purposes, but provide data that can be used to calculate a resilient modulus.

Although these tests all quantify the stiffness of materials, the boundary conditions applied and the resultant stress states are significantly different. The flexural beam test to some degree simulates the stress state of the asphalt concrete layer under a wheel load, with tensile stress at the bottom and compressive stress at the top of the beam specimen, but no horizontal confinement stresses due to the absence of the lateral confinement that the materials would experience in the field. In contrast, the triaxial resilient modulus test applies various combinations of compressive confining and deviator stresses, but no tensile stress can be induced within the specimen in typical test setups. The stress state within a specimen subjected to the Indirect Tensile Resilient Modulus test is more complicated. According to elastic theories for a homogenous continuum, horizontal tensile strain and stress are induced within the cylindrical specimen subjected to narrow vertical strip loads. However, the applicability of such theories to foamed asphalt mixes, which present characteristics more typical of granular materials, is questionable.

The stress state in a foamed asphalt base layer subjected to traffic loading cannot be represented by any one of these laboratory tests alone. The stress state at certain locations is similar to that of a triaxial test, while at other locations (e.g., bottom of the foamed asphalt layer) tensile strain is induced, which is similar to the stress state at the bottom of a flexural beam specimen. Therefore, laboratory test results from any one test should be interpreted with caution when used for designing pavements and should not be assumed to be fully representative of the properties in the pavement structure.

The Indirect Tensile Resilient Modulus test is the most widely reported test method in the literature for assessing the resilient modulus of foamed asphalt mixes *(36,55,56)*, mainly because of the ready availability of the equipment. However, unrealistically high resilient modulus values (higher than 5,000 MPa [725 ksi]) were reported in most instances. Researchers who used the Triaxial Resilient Modulus Test *(7,53,58)*, the Triaxial Permanent Deformation Test *(16,17,58)*, the Monotonic Flexural Beam Test *(16,17)*, the Cyclic Flexural Beam Fatigue Test *(8,27)*, and the temperature-frequency sweep with Cyclic Flexural Beam Test *(27)* generally reported values within a range of between 500 MPa and 3,000 MPa (72.5 ksi and 435 ksi), which are consistent with backcalculation results from Falling Weight Deflectometer (FWD) and Multi-Depth Deflectometer (MDD) measurements on in-service pavements *(8,11,59)*. This discrepancy between results determined using the Indirect Tensile Resilient Modulus Test and other test methods is evident in studies where multiple test methods were carried out for the same materials *(8)*.

Given these discrepancies, the Indirect Tensile Resilient Modulus test is not considered appropriate for the mix and structural designs of foam asphalt projects. Instead, resilient moduli determined with triaxial or beam type tests appear to be more credible indicators and their test conditions are more relevant to field stress states. Two potential reasons are suggested below, but further investigation of the theories and models capable of capturing the semigranular nature of foamed asphalt mixes, such as discrete element methods *(60)* is needed to better understand the indirect tensile test.

- The calculation of stress in indirect tensile tests relies on more assumptions of continuum mechanics than does the calculation of stress in the triaxial or beam tests. In indirect tensile tests, loads are applied vertically through two narrow loading strips, and the horizontal tensile stresses are calculated using continuum mechanics principles, which have questionable applicability to foamed asphalt mixes. In triaxial tests, confining and deviator stresses are applied uniformly and the calculation of the resultant stresses generally only relies on the assumption that the internal stress should balance the applied external load. Internal stress conditions in bending beam specimens are similar in that the normal stress has to balance the applied bending moment on any transverse cross section. The Poisson's ratio is also used in calculating stress in the indirect tensile test while no assumed material-specific constant is involved in the stress calculation for the triaxial and beam tests.
- In indirect tensile tests, the width of the loading strips (13 mm [0.5 in.]) and the distance between the two gauges measuring deformation (25 mm [1 in.]) is smaller than or close to the dimension of the largest aggregate particles in the specimen. The specimen sizes for triaxial tests and flexural beam tests are much larger and stress distribution is more uniform, and thus less influenced by the mix particle size specified for the test.

The effect of water conditioning on foamed asphalt mix behavior is an important issue in foamed asphalt mix- and structural design. Compared to HMA materials, the voids ratio and permeability of foamed asphalt mixes are much higher, which renders the material properties highly sensitive to moisture conditioning. Limited resilient modulus measurements of soaked foamed asphalt mixes have been reported by Australian researchers *(8,36)*, but all research was based on the Indirect Tensile Resilient Modulus test. No published research on soaked foamed asphalt resilient modulus testing with triaxial or beam tests was found in the literature.

The resilient modulus of foamed asphalt mixes typically shows a temperature and loading rate dependency due to the presence of asphalt (both newly introduced foamed asphalt and partially oxidized asphalt from the original asphalt concrete surfacing layers). The temperature dependency of foamed asphalt mix resilient modulus and its interaction with stress dependency under triaxial test boundary conditions is discussed in Section 6.5. Temperature sensitivity coefficients (a dimensionless parameter defined in Section 6.5) from 0.0065 to 0.013 were measured. It was concluded that the effects of temperature and loading rate were of a less complicated and more predictable nature compared to the effects of water conditioning and stress state.

Frequency sweeps from cyclic flexural beam tests was reported by Twagira *et al. (27)*. The materials tested contained between 2.4 and 3.6 percent foamed asphalt and between zero and 1.0 percent portland cement, and results indicated that a 10-fold increase in loading frequency generally increased the measured resilient modulus by approximately 25 percent.

7.4.3 Revised Experiment Factorial for Stiffness Assessment

The Phase 2 factorial design presented in Table 7.1 was altered for this part of the study with changes to the original variables as shown in Table 7.8.

7.4.4 Free-Free Resonant Column Test (FFRC)

The FFRC test was performed on all flexural beam and triaxial specimens. Test results are summarized in Table 7.9 (unsoaked flexural strength of the beam specimens are also shown as a reference) and Figure 7.12 through Figure 7.14. It should be noted that the values shown in the table are averages of replicate batches and replicate specimens, whereas values shown in the figures are values for individual specimens or batches when applicable.

Table 7.8: Revised Factorial Design for Stiffness Assessment

Variable	No. of Values	Values
Test methods and associated specimen fabrication methods	3	- Flexural beam, vibratory hammer compaction - Triaxial Resilient Modulus, adjusted Modified Proctor compaction - Free-free resonant beam resilient modulus tests on beam and triaxial specimens
Replicates	2/1	- 2 x beam specimens - 1 x triaxial specimen
Fixed Values		
Control	1	- Untreated controls included in each test

Table 7.9: Free-Free Resonant Column Unsoaked Stiffness Test Results

RAP Source	Asphalt	M_r-FFRC-Beam (MPa)	M_r-FFRC-Triaxial (MPa)	Beam Flexural Strength (kPa)
33-A	PG64-10	10,192	-	1,523
33-A	PG64-16	11,526	8,429	1,569
33-B	PG64-10	10,952	9,818	1,361
33-B	PG64-16	10,183	8,603	1,153
33-C	PG64-10	8,493	7,415	1,015
33-C	PG64-16	8,085	7,238	1,052
88-A	PG64-10	6,212	5,905	888
88-A	PG64-16	5,273	-	707
88-B	PG64-10	6,739	6,009	830
88-B	PG64-16	6,925	6,152	877
88-C	PG64-10	5,852	6,643	738
88-C	PG64-16	5,651	5,912	681

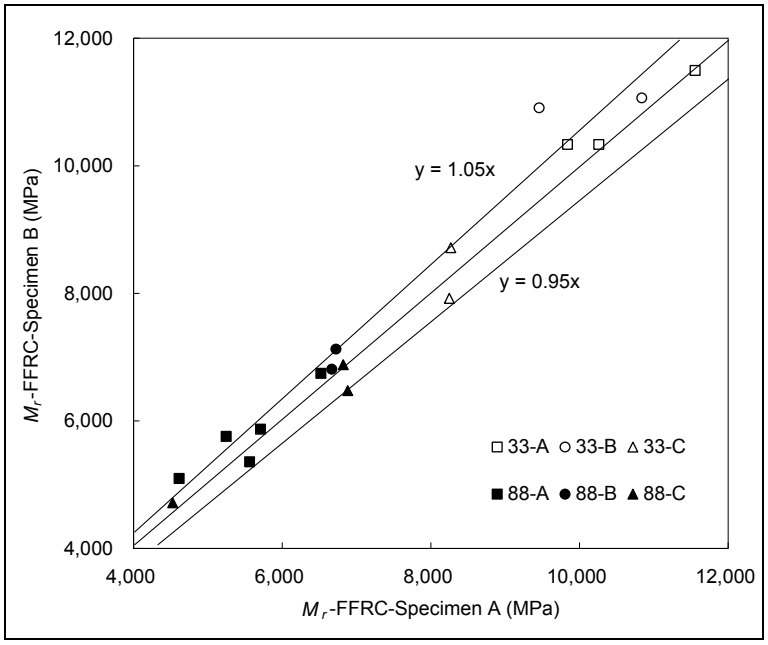

Figure 7.12: Repeatability of FFRC tests.

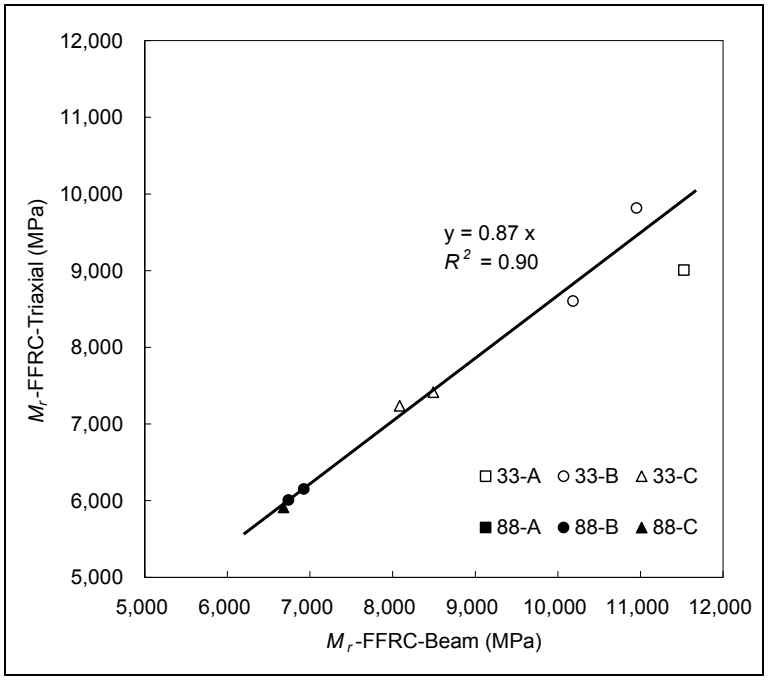

Figure 7.13: Correlation of beam and triaxial specimen FFRC resilient modulus values.

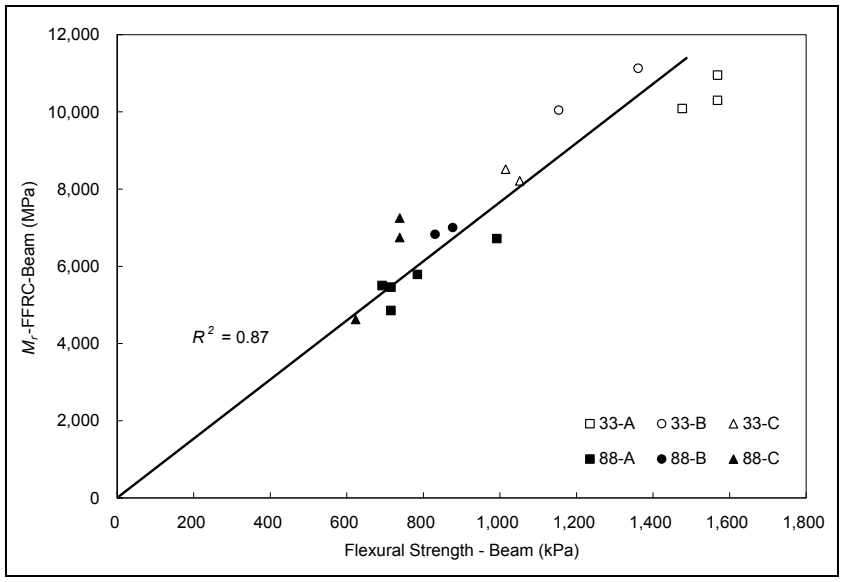

Figure 7.14: Correlation between FFRC resilient modulus and modulus of rupture.
(Tests carried out on the same beam)

Observations from the test results include:

- The repeatability of this test was considered acceptable. Figure 7.12 shows a comparison of the results for two replicate beams made from the same batch of mix. The relative difference was generally within 5 percent.
- There was a high correlation (Pearson correlation coefficient of 0.97) between the FFRC resilient modulus values for beam specimens and those for triaxial specimens made from the same batch of

mix (Figure 7.13). The FFRC resilient modulus values for triaxial specimens were consistently lower (by 13 percent on average) than the FFRC resilient modulus values for beam specimens. This is attributed in part to the aggregate particle orientation induced by compaction. During FFRC tests, the wave propagation direction in a triaxial specimen is the same as the direction of the compaction action, whereas in a beam specimen the FFRC test wave propagation is perpendicular to the direction of the compaction action.

- FFRC tests appeared to overestimate the resilient modulus of foamed asphalt mixes. The resilient modulus values determined from triaxial and flexural beam tests on the same mixes were generally lower than 2,000 MPa (290 ksi), while typical values of 4,000 MPa to 12,000 MPa (580 ksi to 1,740 ksi) were recorded during the FFRC tests. Given that the resilient modulus of foamed asphalt mixes is stress and loading rate dependent, the stress induced in FFRC tests is of very small amplitude and high frequency and thus has minimal relevance to the stress state induced by traffic loading on pavement structures. Higher frequencies and smaller strain amplitudes result in higher stiffness for asphalt bound materials.
- The FFRC modulus values for unsoaked specimens appeared to be very dependent on RAP source and gradation. The specimens prepared from SR33-A and SR33-B materials had significantly higher FFRC modulus than the other RAP sources and gradation. The same trend was observed in ITS test results (Table 7.5), and from the correlation between FFRC resilient modulus and modulus of rupture (stress-at-break) results of monotonic flexural beam tests (Figure 7.14). This was attributed to a combination of the mechanical properties and weak natural chemical bonding in the fines matrix of the Route 33 materials. These exhibited brittle, but stiff, properties especially at low stress levels, in the unsoaked state, but did not influence performance of the material in the soaked state. Dilution of the material with additional mineral fines (15 percent baghouse dust) reduced the effect of this bonding. (No X-ray diffraction tests were carried out on any of the materials, and results of pH tests indicated slight alkalinity on the Route 33 material [pH of 8.2 using AASHTO T289] and slight acidity [pH of 6.7] on the material sampled from Route 88, which did not show the same indications of chemical bonding. These pH values are typical of the natural materials and are not indicative of earlier modification with lime or cement).

In summary, the FFRC testing was found to be relatively simple and inexpensive to carry out with high repeatability, but given that the testing stress state is very different from the working stress state of foamed asphalt mixes in pavement structures, the results are considered to be of questionable value for pavement design.

7.4.5 Triaxial Resilient Modulus Test

All triaxial specimens were subjected to resilient modulus tests under unsoaked and then soaked conditions. Combinations of various load pulse durations, confining stresses, and deviator stresses were applied to each test. Equation 7.1, modified from Uzan's *(37)* general model by the addition of consideration of loading pulse durations, was used to fit the triaxial resilient modulus test data. An average R^2 value of 0.983 was achieved.

$$M_r = k_1 p_a \left(\frac{T}{0.1\text{sec}}\right)^{k_T} \left(\frac{\theta}{p_a}\right)^{k_2} \left(\frac{\tau_{oct}}{p_a}\right)^{k_3} \quad (7.1)$$

where p_a = atmospheric pressure used to nondimensionalize stresses
T = duration of the haversine load pulses
σ_0 = confining stress
σ_d = deviator stress
θ = $3\sigma_0+\sigma_d$ = bulk stress
τ_{oct} = octahedral shear stress, and in the triaxial stress state $\tau_{oct}=\sqrt{2}\sigma_d/3$
k_T, k_1, k_2, and k_3 are material-related constants.

Model fitting results are presented in Table 7.10. In triaxial test stress states, the resilient modulus of foamed asphalt mix is primarily a function of the confining stress (σ_0), the deviator stress (σ_d), and the loading rate (characterized by the haversine load pulse duration T), i.e., $M_r = M_r$ (σ_0, σ_d, T). Based on the fitting results, resilient modulus values at two reference stress states, $M_{r1} = M_r$(20 kPa, 62 kPa, 0.1 second) and $M_{r2} = M_r$(140 kPa, 105 kPa, 0.1 second) were calculated as shown in Table 7.10. The resilient modulus at low confining pressure and relatively high deviator stress levels is represented by M_{r1}, while M_{r2} represents the resilient modulus at high confining stress and relatively low deviator stress levels. Both stress states were used in the testing sequence of AASHTO T307, but the values shown were calculated on the basis of model fitting results.

Table 7.10: Triaxial Resilient Modulus Test Results

RAP Source	Unsoaked						Soaked						
	k_1	k_T	k_2	k_3	M_{r1} (MPa)	M_{r2} (MPa)	K_1	k_T	k_2	k_3	M_{r1} (MPa)	M_{r2} (MPa)	RMR[1] (%)
Foamed Asphalt-Treated Specimens													
33-A	10,433	-0.06	0.19	-0.03	1,131	1,467	7,406	-0.09	0.17	-0.06	833	1,026	72
33-B	9,794	-0.04	0.16	-0.01	1,038	1,298	8,153	-0.11	0.15	-0.06	916	1,106	87
33-C	9,450	-0.04	0.15	-0.03	1,015	1,235	5,469	-0.09	0.27	-0.10	664	920	70
88-A	8,467	-0.04	0.18	-0.05	941	1,188	7,864	-0.09	0.21	-0.05	881	1,163	96
88-B	8,560	-0.05	0.19	-0.03	938	1,205	6,672	-0.09	0.22	-0.06	763	1,006	82
88-C	7,528	-0.03	0.19	-0.05	842	1,078	4,600	-0.08	0.31	-0.10	564	837	72
Untreated Control Specimens													
33-A	10,901	-0.03	0.16	-0.05	1,211	1,484	8,004	-0.06	0.24	-0.05	908	1,239	79
33-B	9,240	-0.04	0.24	-0.04	1,031	1,420	6,953	-0.07	0.25	-0.10	833	1,131	80
33-C	6,469	-0.01	0.29	-0.19	880	1,199	NR[2]	NR	NR	NR	NR	NR	NR
88-A	8,369	-0.04	0.25	-0.07	967	1,332	3,693	-0.05	0.40	-0.16	495	807	56
88-B	9,278	-0.03	0.26	-0.10	1,116	1,548	3,553	-0.06	0.45	-0.17	487	845	49
88-C	8,447	-0.03	0.23	-0.08	983	1,322	NR	NR	NR	NR	NR	NR	NR

[1] RMR: Resilient Modulus Retained. In this case $RMR = \frac{1}{2}\left(\frac{Mr_{1-soaked}}{Mr_{1-dry}} + \frac{Mr_{2-soaked}}{Mr_{2-dry}}\right)$

[2] No result — specimens disintegrated during water conditioning.

A comparison of untreated control and foamed asphalt-treated test results in both soaked and unsoaked states resulted in the following observations:

- Soaked control mixes of SR33-A and SR33-B materials had significantly higher resilient moduli than specimens made with SR88-A and SR88-B materials. These results differed from other test results for the same materials discussed elsewhere in this report (e.g., ITS results), which indicated that the SR33-A and SR33-B and SR88-A and SR88-B materials had similar performance. The difference is attributed to the courser surface texture of the Route 33 aggregate (Figure 7.3), which may have influenced aggregate repositioning/reorientation under loading.
- Unsoaked foamed asphalt-treated materials had similar resilient modulus values to the control specimens in the unsoaked state, except for the treated SR33-C materials, which had a slightly higher resilient modulus (approximately 10 percent) than the same untreated specimens at both stress levels.
- Soaked foam asphalt-treated SR88-A and SR88-B materials had significantly higher resilient moduli compared to the untreated materials, especially at low confining stress levels. Untreated SR33-C and SR88-C materials did not withstand soaking and collapsed before testing, whereas the treated specimens of the same materials withstood soaking and retained an acceptable stiffness.
- The differences in soaked resilient moduli between SR33-A and SR33-B, and SR88-A and SR88-B materials were less significant for the foamed asphalt-treated mixes than for the untreated control mixes. In the control mixes, the characteristics of the aggregate (e.g., surface texture) probably dominated the resilient modulus behavior, while the presence of asphalt binder in the treated mixes dominated behavior.

The effects of the dispersed asphalt on the foamed asphalt mix resilient modulus behavior were also observed by tracking the change of material constants (k_T, k_1, k_2, and k_3) in Equation 7.1 with the difference in asphalt dispersion. Figure 7.15 shows the correlations between the Fracture Face Asphalt Coverage (FFAC) values of soaked 152 mm ITS specimens prepared from the same batch of material, and the four material constants in Equation 7.1 for soaked triaxial specimens. Data points with FFAC = 0 correspond to the values for the soaked untreated control materials. The untreated SR33-C and SR88-C material specimens collapsed during soaking and results are therefore not shown.

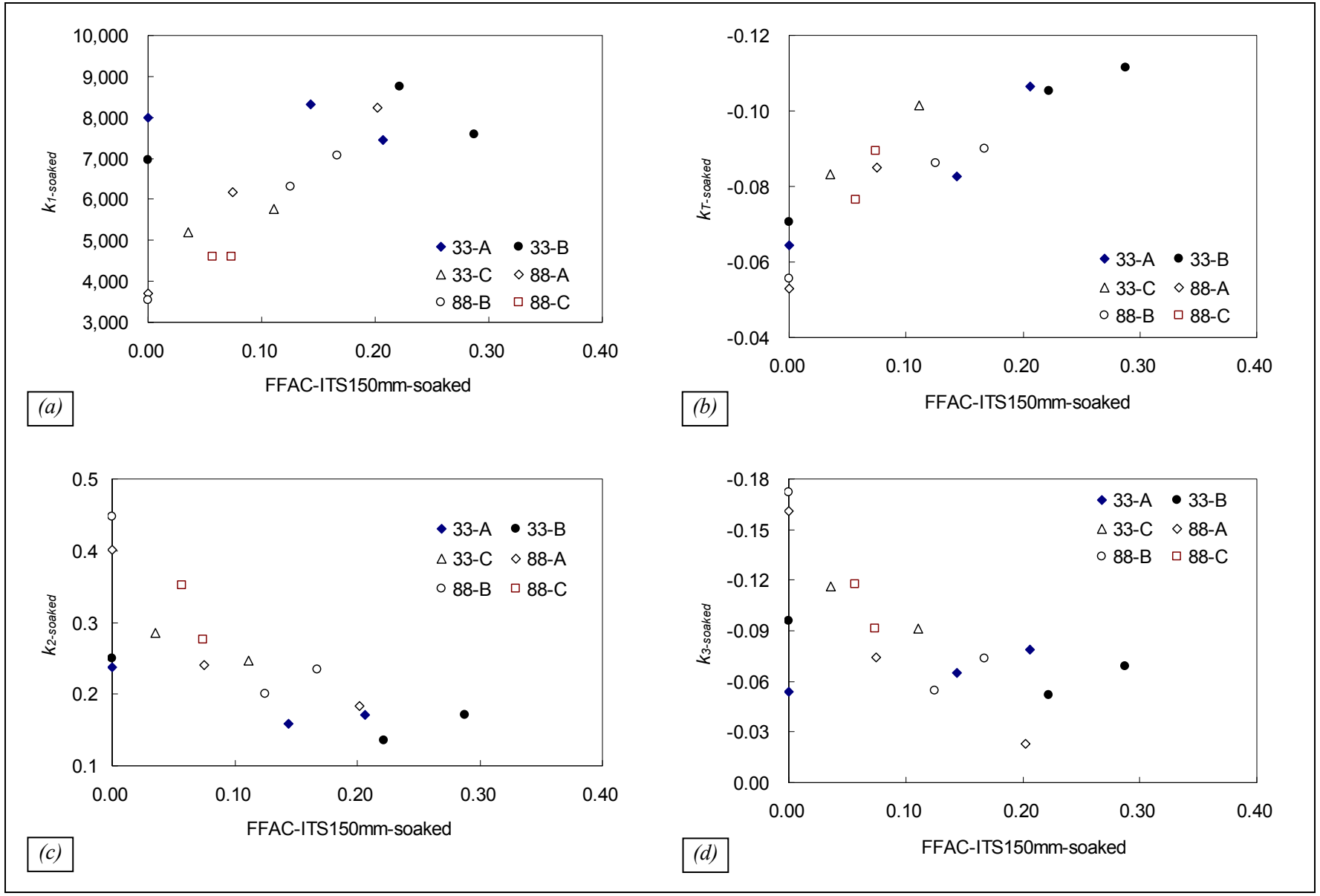

Figure 7.15: Correlation between FFAC and material constants for soaked resilient modulus
(a) FFAC vs. $k_{1\text{-soaked}}$ (b) FFAC vs. $k_{T\text{-soaked}}$ (c) FFAC vs. $k_{2\text{-soaked}}$ (d) FFAC vs. $k_{3\text{-soaked}}$

- The constants k_T, k_2 and k_3 represent the sensitivity of the foamed asphalt mix resilient modulus to loading rates (or load pulse durations), bulk stresses, and deviator stresses, respectively. The constant k_1 is a scalar term and if all the other parameters are the same, increasing k_1 values, results in increasing resilient modulus values at low confining stress levels. As the FFAC value increased (i.e., better asphalt dispersion in the mix), the resilient modulus at low confining stress levels also increased (Figure 7.15-a). The resilient modulus was more sensitive to loading rates (Figure 7.15-b), but less sensitive to bulk stress values (Figure 7.15-c) and deviator stress values (Figure 7.15-d). These effects were more significant for the SR88-A, SR88-B, SR88-C, and SR33-C materials compared to the SR33-A and SR33-B materials.

In summary, triaxial resilient modulus test results showed that foamed asphalt treatment did not always increase the absolute values of resilient modulus, under either unsoaked or soaked conditions. The foamed asphalt transformed the material behavior from that of typical unbound granular materials to that of partial asphalt-bound materials, with the resilient modulus more loading rate dependent but less stress dependent. The significance of this transforming effect also appeared to be influenced by certain characteristics of the RAP material. For example, RAP materials with coarser surface texture appeared to be less affected by foamed asphalt stabilization in triaxial stress states, during which aggregate particle interlocking and frictional sliding play significant roles in addition to the cohesion provided by the foamed asphalt.

7.4.6 Flexural Beam Test

The monotonic flexural beam test results for both unsoaked and soaked specimens are shown in Table 7.11. The parameter E^{bend} is the equivalent tangential Young's modulus for bending determined from the stress-strain curves. Strain-at-break (ε_b) was the calculated tensile strain at the bottom of the beam at the midspan, computed from the measured beam deflection when the deflection-load curve reached its peak. All calculations were based on Euler-Bernoulli beam theories. Values listed in Table 7.11 are the averages of pooled values for mixes treated with the PG64-16 and PG64-10 binders and for replicate specimens. Many of the metal deflection measurement plates detached after soaking and thus only a limited number of successful tests were completed for certain material gradations. Test results should therefore be interpreted with care since the variance could be large.

Table 7.11: Monotonic Flexural Beam Test Results

Sample	Unsoaked			Soaked			$\frac{E^{bend}_{soaked}}{E^{bend}_{dry}}$ (%)	$\frac{E^{bend}_{soaked}}{M_{r1-soaked}}$ (%)
	N^1	E^{bend}_{dry} (MPa)	ε_b	N^1	E^{bend}_{soaked} (MPa)	ε_b		
33-A	3	1,689	2,632	1	117	4,230	7	14
33-B	2	1,381	2,632	1	249	2,444	18	27
33-C	2	1,673	2,444	1	70	3,760	4	11
88-A	5	855	2,181	5	98	4,230	11	11
88-B	2	1,073	2,820	2	82	4,512	8	11
88-C	3	873	2,444	2	50	4,606	6	9

[1] *N:* number of specimens that were tested with successful deflection measurement.

The following observations were made:

- In the unsoaked state, beams made with materials sourced from Route 33 had higher bending stiffness than those made with materials sourced from Route 88. The difference in strain-at-break for the two materials sources was small. Interestingly, the amplitude of the equivalent Young's modulus for bending (E^{bend}) for unsoaked specimens were similar to that of the triaxial resilient modulus as shown in Table 7.5.
- When the beams were soaked, they lost between 82 and 94 percent of their stiffness, while the strain-at-break values had a moderate increase. Triaxial specimens lost an average of 21 percent of their stiffness when soaked. This was attributed to the different stress states associated with the two tests. Foamed asphalt materials with no active filler (e.g., portland cement) resist applied loading primarily by three mechanisms, namely interlocking and frictional sliding of the aggregate particles, bonding of the foamed asphalt, and bonding in the mineral filler phase (i.e., weak cementation and suction of residual water). These three mechanisms are insensitive to water conditioning, moderately sensitive to water conditioning, and notably sensitive to water conditioning, respectively. The first mechanism resists compression and shearing forces under confinement in triaxial stress states, and therefore has a dominant role in the behavior of soaked triaxial specimens when the other two mechanisms are impaired. Consequently water conditioning has a relatively limited effect on the triaxial resilient modulus. The third mechanism, which was relatively strong but brittle, contributed most of the deformation resistance in the unsoaked beam specimens. When beams are soaked, the first and third mechanisms contribute little in the unconfined state, and the foamed asphalt dominates in resisting tensile deformation, and hence the overall stiffness of beam specimens is highly sensitive to moisture damage. Since the asphalt bonding is more ductile than the bonding in the mineral filler phase, the strain-at-break increased moderately for soaked beams.

7.4.7 Summary

The following summary points were noted on conclusion of this task:

- The resilient modulus of foamed asphalt mixes is highly dependent on the stress state, but the available laboratory test methods cannot fully simulate the complexity of field stress states.
- The Free-Free Resonant Column test and indirect tensile resilient modulus test both yield stress states that are very different compared to those in a pavement. They appear to significantly overestimate the resilient modulus values of foamed asphalt mixes, and thus present problems for their use in pavement design.
- In triaxial resilient modulus tests, foamed asphalt transforms the material behavior from that of typical unbound granular materials to that of asphalt-bound materials. Limited increases in the resilient modulus values, attributed to the foamed asphalt treatment, were observed. The magnitude of increase also appeared to be dependent on certain characteristics of the granular materials being treated.
- The range of values of tangential Young's modulus for bending in flexural beam tests was similar to the resilient modulus determined from triaxial resilient modulus tests in the unsoaked state. However, the modulus reduction due to water conditioning for beam tests was between 85 and 95 percent, while that of triaxial tests was between 5 and 30 percent.
- The triaxial resilient modulus and flexural beam tests each partially represent the stress state in a foamed asphalt-treated base layer under traffic loading. Results of these two test types therefore need to be combined to better understand foamed asphalt mix behavior, as is discussed in Section 7.7.

7.5 Assessment of Mixing Moisture Content

7.5.1 Introduction

An assessment of the mixing moisture content of foamed asphalt mixes was included to investigate the effects of this variable on various mix properties, using a combination of laboratory testing and fracture face analysis. The *mixing moisture content* (MMC) is defined as the moisture content of the agitated granular material when foamed asphalt is injected. It should not be confused with the *optimum moisture content* (OMC), which is the moisture content at which maximum dry density is achieved during compaction. During field construction, the mixing moisture content in the recycling machine's mixing chamber is adjusted by the operator depending on the in-place moisture content of the material being recycled. In the laboratory, the mixing moisture content is adjusted in a similar manner by adding water to the pugmill while the material is being agitated, but before the foamed asphalt is injected.

A comprehensive review of the literature on the effects of the mixing moisture content was prepared by Saleh and Herrington *(5)* and is not repeated in this report. In summary, the moisture content in loose foamed asphalt mixes (precompaction) was found to influence asphalt dispersion, which in turn influences

the properties of the final product (postcompaction), including density, strength, and stiffness. The effects of mixing moisture content on density are well understood and laboratory testing and observations during field construction have shown that at relatively high surface temperatures (i.e., 40°C [104°F] and typical of California Central Valley summer construction conditions), the foamed asphalt complements the water in acting as a compaction aid. Based on these observations, the literature generally suggests compacting at a moisture content equivalent to between 70 and 85 percent of optimum (as determined with the modified AASHTO method [AASHTO T180]) to ensure that optimal compaction is achieved.

The effects of mixing moisture content on foamed asphalt dispersion are not as clearly understood and rigorous proof has not been reported in the literature due to the absence of an appropriate measure of quantifying asphalt dispersion or distribution in a mix. Fracture face image analysis was considered appropriate for assessing this effect.

7.5.2 Revised Experiment Factorial

The Phase 2 factorial design presented in Table 7.1 was altered for this part of the study as shown in Table 7.12. Only two RAP materials (SR33-A and SR88-C) and one asphalt type were used. A range of mixing moisture contents was added to the factorial as the main investigation variable. In all instances, the moisture content was adjusted after the injection of the foam and initial mixing to ensure that all specimens were compacted at the same moisture content. The actual measured mixing and compaction moisture contents are listed in Table 7.13.

Table 7.12: Revised Factorial Design for Mixing Moisture Content Study

Variable	No of values	Values
Rap source/gradation	2	- SR33-A - SR88-C
Target mixing moisture content	5/4	- SR33-A: 3%, 4%, 5%, and 6% - SR88-C: 3%, 4%, 5%, 6%, and 7%
Test methods and associated specimen fabrication methods	6	- ITS (100 mm), Marshall compaction, 75 blows/face - Triaxial resilient modulus, adjusted Modified Proctor compaction - UCS, adjusted Modified Proctor compaction
Replicates	2/1	- 4 x 100 mm ITS specimens (2 unsoaked, 2 soaked) - 1 x triaxial/UCS specimen (soaked)
Fixed Values		
Asphalt source and type	1	- Refinery A PG64-16
Target compaction moisture content	1	- SR33-A: 5% (unless mixing moisture content was higher) - SR88-C: 6% (unless mixing moisture content was higher)
Control	-	- Untreated controls were not relevant to this study

Table 7.13: Mixing and Compaction Moisture Contents

RAP Source	Mix	Target Mixing Moisture (%)	Measured Mixing Moisture (%)	Compaction Moisture (%)	OMC of Untreated RAP (%)
SR33-A	A	3.0	2.5	4.9	5.5
	B	4.0	3.7	5.1	
	C	5.0	4.8	4.8	
	D	6.0	6.0	6.0	
SR88-C	A	3.0	2.6	5.9	5.9
	B	4.0	4.0	6.5	
	C	5.0	4.6	6.0	
	D	6.0	6.3	6.3	
	E	7.0	7.1	7.1	

7.5.3 Visual Analysis of Loose Mix

Samples of loose mix collected prior to the injection of foam were observed through a low-powered microscope. Selected images of samples of the SR88-C mixes at various mixing moisture contents with various representative moisture contents are shown in Figure 7.16. The microstructures formed by the moist soil particles and their evolution with increasing moisture content are shown. No asphalt was added to these mixes.

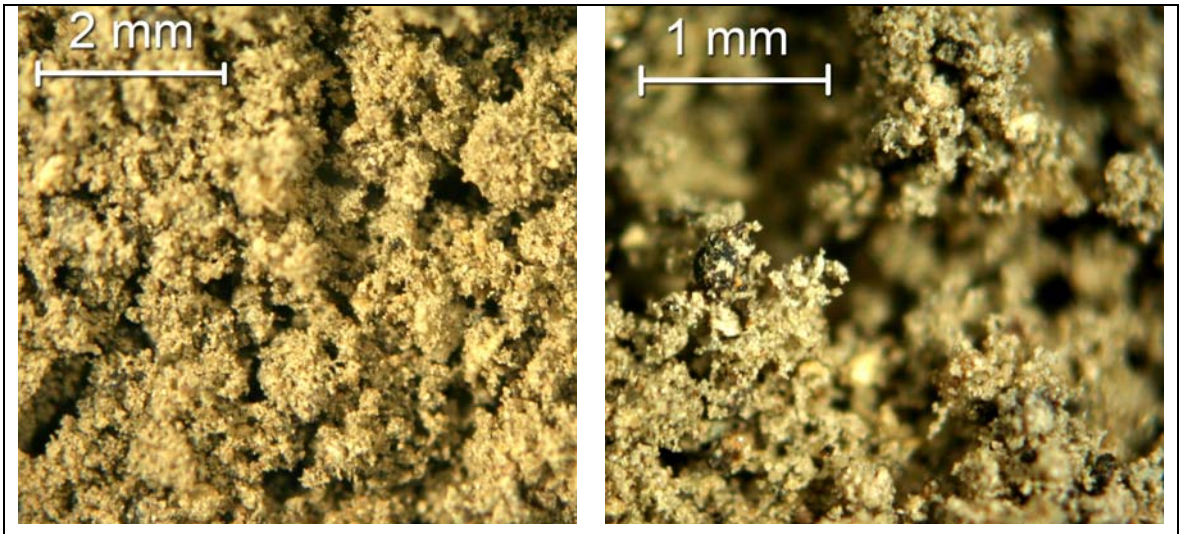

(a) Moisture Content = 2.5%

Figure 7.16: Microscope images of various mixing moisture contents.
(Uncompacted, no foamed asphalt added)

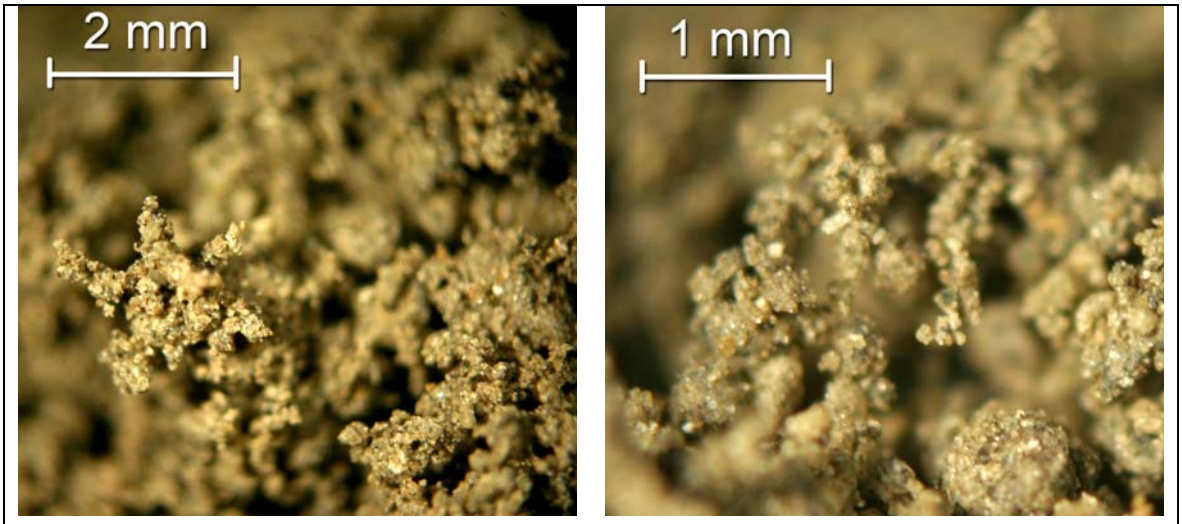

(b) Moisture content = 4.9%

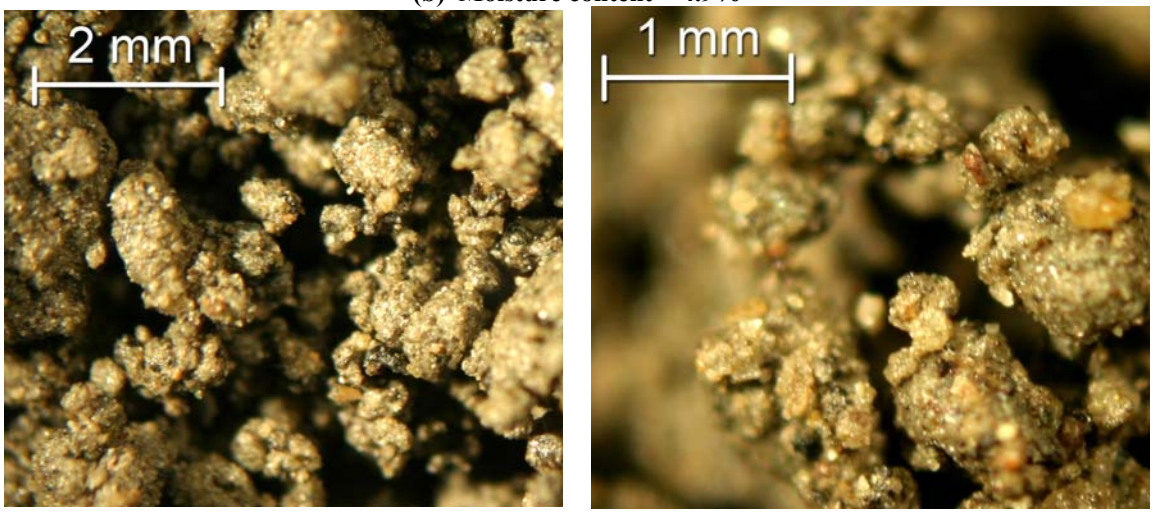

(c) Moisture content = 6.4%

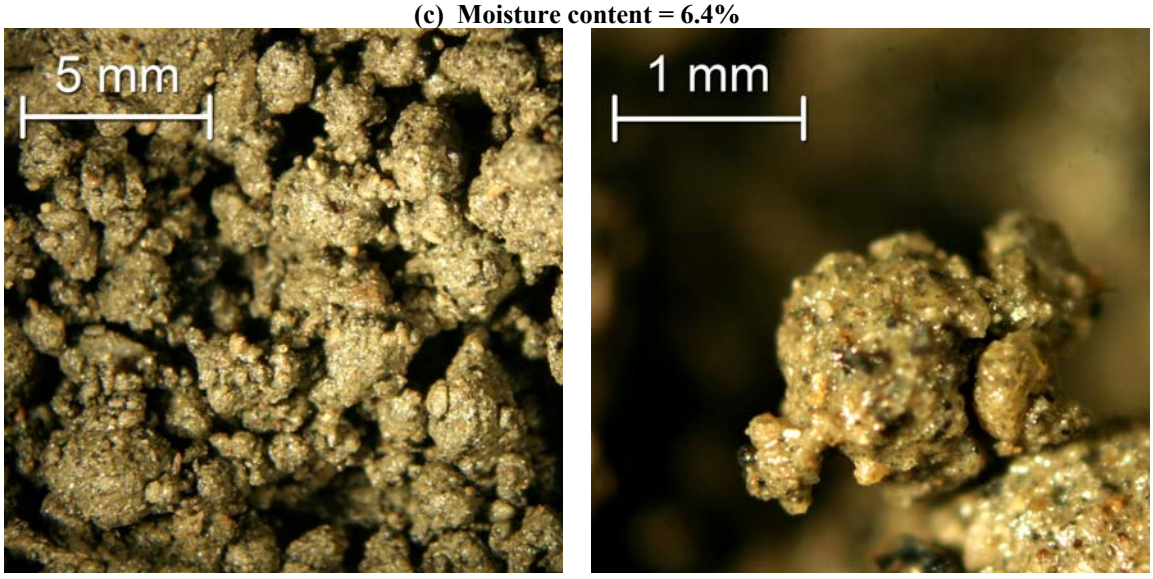

(d) Moisture content = 7.3%

Figure 7.16: Microscope images of various mixing moisture contents *(cont.)*
(Uncompacted, no foamed asphalt added)

In a moist, loose aggregate particle assembly, water bridges bond the particles primarily through capillary suction (Figure 7.17), with the suction forces providing tensile strength to the bond.

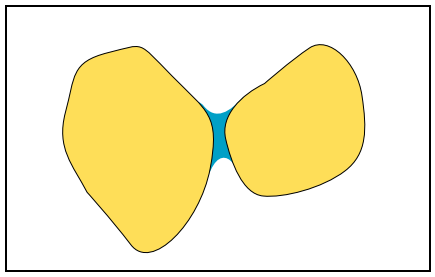

Figure 7.17: Soil particles connected by a water bridge.

As the mixing moisture content is increased from zero percent, the agglomeration state of the aggregate particles evolves through a series of states:

- State-A: No water exists in the loose mix and the aggregate particles are not attached to each other in any way.
- State-B: When the mixing moisture content is low, a few small aggregate particles are bonded together by water bridges to form a number of small clusters with each cluster containing a few fine particles (Figure 7.16a).
- State-C: As the mixing moisture content increases, a higher proportion of the aggregate particles (all sizes) are bonded together and various spatial structures are formed (Figure 7.16b and Figure 7.18).

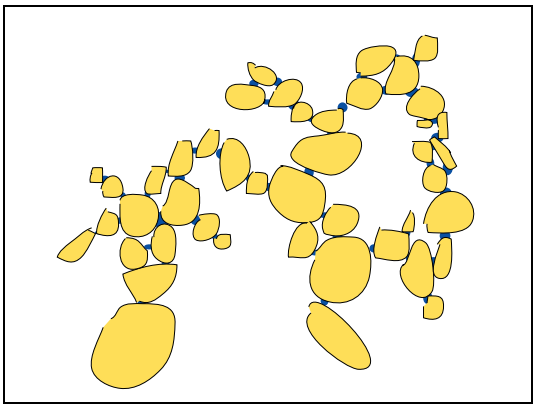

Figure 7.18: Fine particle spatial structure at low mixing moisture content (State-C).

- State-D: When the mixing moisture content is close to or higher than the optimum compaction moisture content, relatively large agglomerations are formed, in which fine particles form a paste that coats bigger aggregate particles (Figure 7.16c and d, and Figure 7.19).

There are no clear boundaries between these states. Based on the microscope assessment of the SR88-C materials, it is proposed that mixes in State-B would have a mixing moisture content lower than 2 percent; mixes in State-C would have mixing moisture contents in the vicinity of 5 percent, while mixes in State-D would have mixing moisture contents around 6.5 percent and higher.

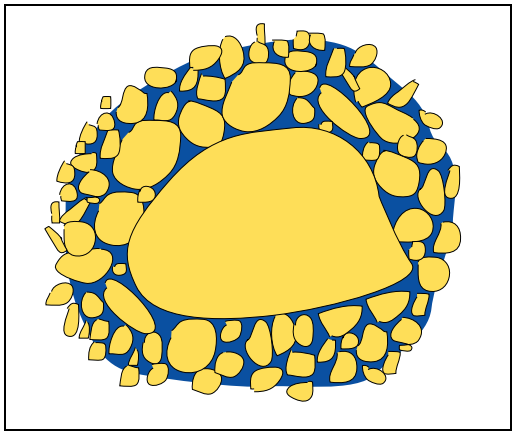

Figure 7.19: Particle agglomeration when mixing moisture content is high (State-D).

Visual assessments of the ITS specimen fracture faces, supported by the FFAC analysis, indicate that poor dispersion of foamed asphalt is likely if the mixing moisture content is in State-D, because the exposed surface area of the aggregate particles is small and the asphalt will have a concentrated distribution with a relatively high film thickness. Mixes in State-B typically have good asphalt distribution, but in practice the mixes might be too dry to achieve adequate compaction.

Mixes in State-C appear to have a good balance between mix workability (or compactability) and asphalt distribution. Insufficient data was collected during the UCPRC study to determine clear upper and lower limits for the compaction moisture content for this state, but 75 to 90 percent of the optimum compaction moisture content appears to be an appropriate starting point. These limits should be established during the mix design process. Although control of the mixing moisture content is generally applicable to all gradations of material, mixes with coarser gradations appear to be less sensitive to mixing moisture content.

The various states described above have been observed on FDR-foamed asphalt projects when checking the material immediately behind the recycler. It is interesting to note that similar agglomerations as represented by State-D are formed if the compaction water is sprayed onto the recycled material behind the recycler instead of being injected into the mixing chamber as part of the recycling process, or if additional compaction water is sprayed onto the material before initial compaction with the padfoot roller has been completed (i.e., the padfoot roller is too far behind the recycler). These observations support the

need for following recommended construction procedures and for constant evaluation, by trained individuals, of the mix behind the recycler to ensure that adjustments to the mixing moisture content are made promptly as required. The mixing moisture content is likely to change constantly on projects in many areas in California given the changing subgrade and adjacent land use conditions.

7.5.4 Fracture Face Observations

The fracture faces of the tested ITS specimens were studied to obtain an initial indication of the asphalt dispersion. The fracture faces of one replicate of the SR88C soaked ITS-100 mm specimens at each moisture content are shown in Figure 7.20 (one from each replicate). The images have been cropped to facilitate comparison (approximately 80 percent of the fracture face is shown).

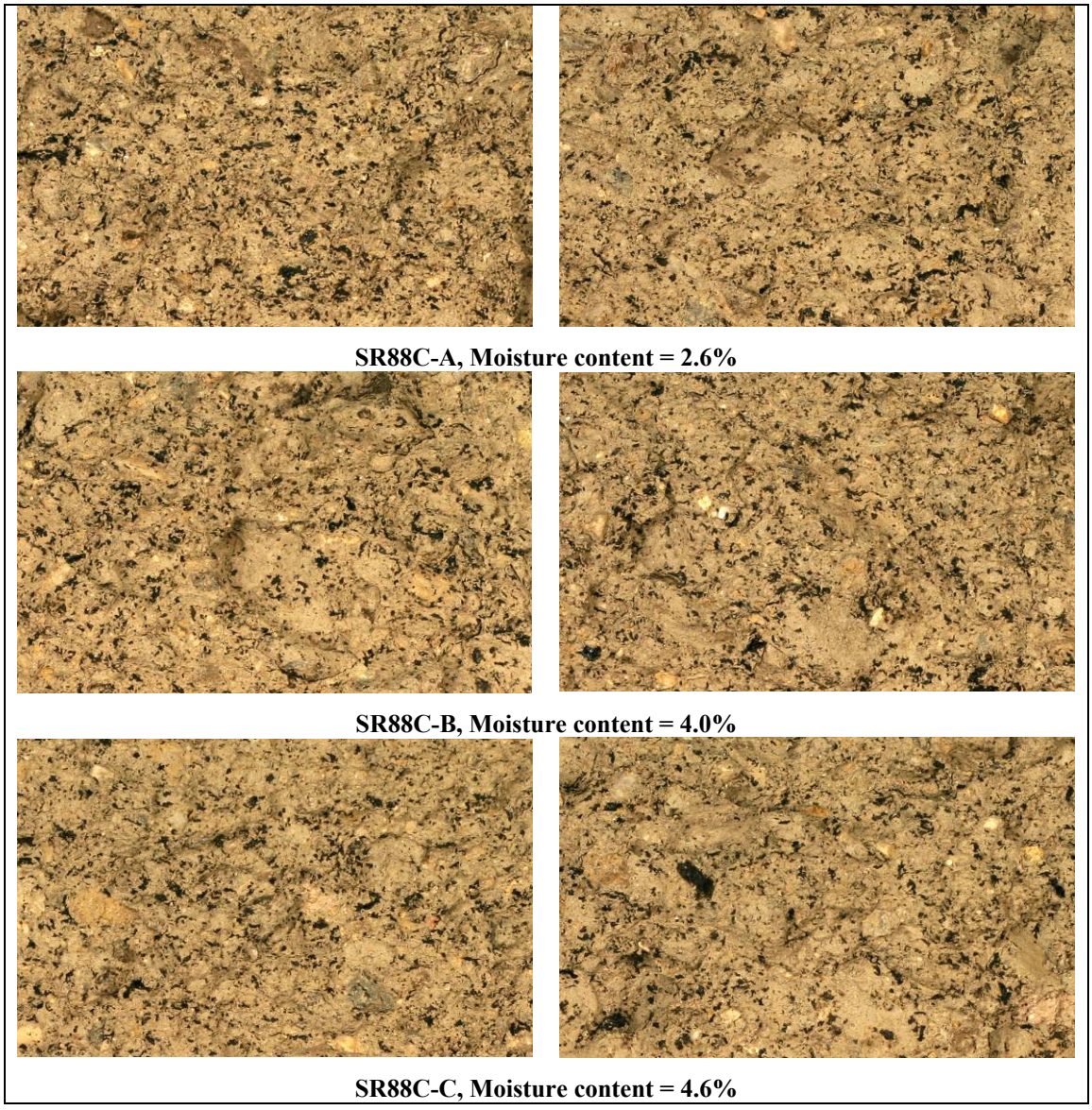

Figure 7.20: Fracture faces of specimens with different mixing moisture contents.

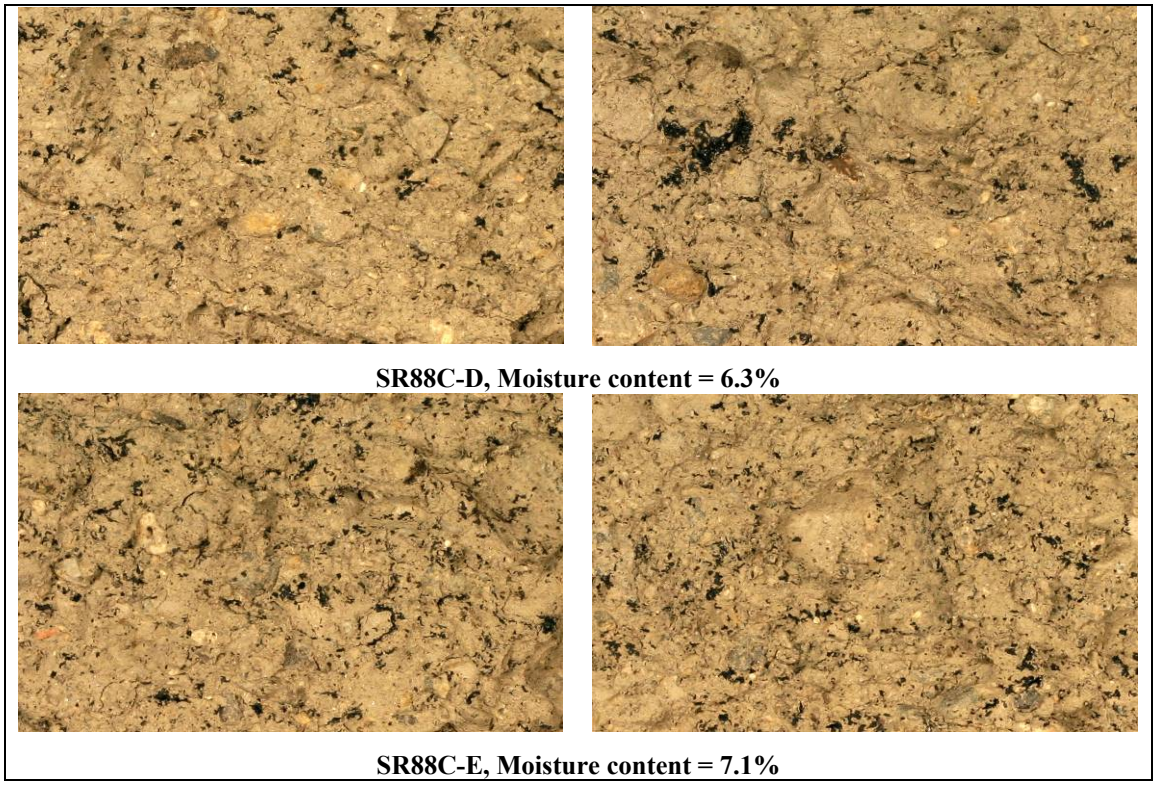

Figure 7.20: Fracture faces of specimens with different mixing moisture contents *(cont.).*

The fracture faces for low mixing moisture content mixes (2.6 to 4.6 percent, corresponding to loose mixes in States-B and -C) show a high number of small asphalt spots, with the visible asphalt mastic distribution features of the two fracture faces from replicate specimens similar for each mix. When the mixing moisture is close to or higher than the optimum moisture content (6.3 percent and higher, corresponding to loose mixes in State-D), the fracture faces show fewer asphalt spots, but the size of these spots is generally larger. The overall asphalt coverage ratios (or FFAC) are lower for these mixes. At the same time, a higher variation between replicate specimens was observed. Generally loose mixes in State-B and State-C, when subject to foamed asphalt treatment, tend to produce a microstructure similar to that shown in Figure 6.13a, which is desirable, while loose mixes in State-D tend to produce a microstructure similar to that shown in Figure 6.13b, which is undesirable. It should be noted that although asphalt distribution appears to be satisfactory for the 2.6 percent mixing moisture content, this would be insufficient moisture to achieve adequate compaction in the field.

7.5.5 Strength and Stiffness Test Results

The strength and resilient modulus (stiffness) test results and the corresponding FFAC results are summarized in Table 7.14.

Table 7.14: Strength Test and FFAC Results for Different Mixing Moisture Contents

Mix[1]		ITS (kPa)	FFAC (%)	ITS (kPa)	FFAC (%)	UCS (kPa)	Triaxial			
							k_1	k_T	k_2	k_3
		Unsoaked		Soaked			Soaked			
33A	A	752	29.8	162	25.3	703	5,827	-0.103	0.28	-0.11
	B	696	34.0	175	33.1	829	6,949	-0.120	0.23	-0.11
	C	780	34.2	146	27.7	790	6,650	-0.116	0.24	-0.10
	D	773	32.9	153	28.3	924	7,216	-0.113	0.24	-0.10
88C	A	564	9.0	104	9.8	643	4,208	-0.106	0.39	-0.15
	B	596	9.0	98	9.2	639	4,042	-0.104	0.41	-0.17
	C	563	7.7	102	8.2	723	4,407	-0.102	0.40	-0.16
	D	449	8.8	65	4.4	516	2,914	-0.088	0.50	-0.20
	E	481	5.8	79	5.6	483	3,604	-0.094	0.44	-0.18

[1] 33A is from Route 33 with gradation A (coarse), 88C is from Route 88 with gradation A (fine). A, B, C, D, E refers to the mixing moisture content.

The unsoaked ITS tests were inconclusive, as expected, while the soaked results showed a general trend of increasing strength with decreasing mixing moisture content. The FFAC results for the soaked ITS specimens followed a similar trend.

Figure 7.21 illustrates the effect of mixing moisture content on the FFAC values. As discussed in Section 6.6, these values can be used as an indicator of the degree of foamed asphalt dispersion in the mix (for materials with the same grading), with higher values representing better dispersion and hence better quality mixes. Mixes with lower moisture contents generally had better asphalt dispersion for the SR88C mixes with the fine gradation, characterized by a high number of small asphalt droplets uniformly distributed in the mixes, which was consistent with the direct observations on the loose mix and on the fracture faces. The effects of mixing moisture contents on the SR33A mixes with the coarse gradation did not show a clear trend.

Figure 7.22 through Figure 7.24 show the correlation between FFAC values and the soaked ITS, unsoaked ITS, and soaked UCS test results respectively. Mixes with better asphalt dispersion generally showed higher strengths, with the trends more distinct for the SR88-C mixes than for the SR33-A mixes. This is attributed to the different fines contents of these two aggregate materials. The evolution of agglomeration states of materials with more fines was more sensitive to moisture change. Figure 7.25a through Figure 7.25d show correlations between the resilient modulus model fitting constants (k_1, k_T, k_2, and k_3) and the FFAC values measured from soaked ITS specimens. The constants k_T, k_2, and k_3 represent the sensitivity of the foamed asphalt mix resilient modulus to loading rates (or load pulse durations), bulk stresses, and deviator stresses, respectively. The constant k_1 is a scalar term: if all the other parameters are the same, the higher the k_1 value, the higher the resilient modulus at low confining stress levels. For each aggregate type (SR88-C or SR33-A), mixes with better asphalt dispersion (higher FFAC values) showed

stiffness less sensitive to stress states (higher value of k_1; lower absolute values of k_2 and k_3) and more sensitive to loading rates (higher absolute values of k_T). The correlations for the SR88-C mixes were more significant than those for the SR33-A materials, similar to observations from the strength test results.

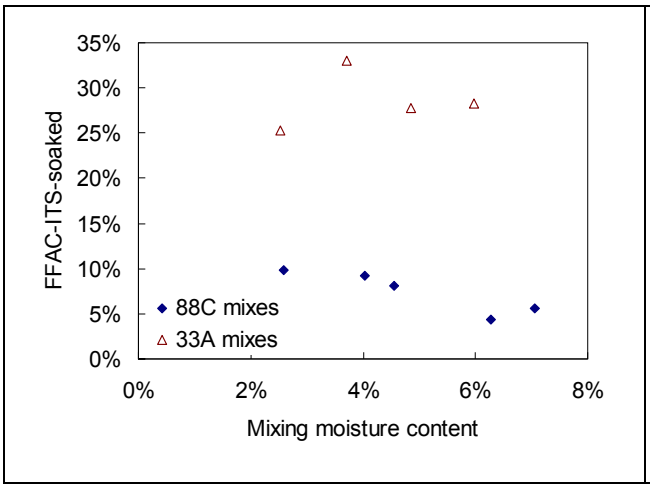

Figure 7.21: Effects of mixing moisture content on FFAC values.

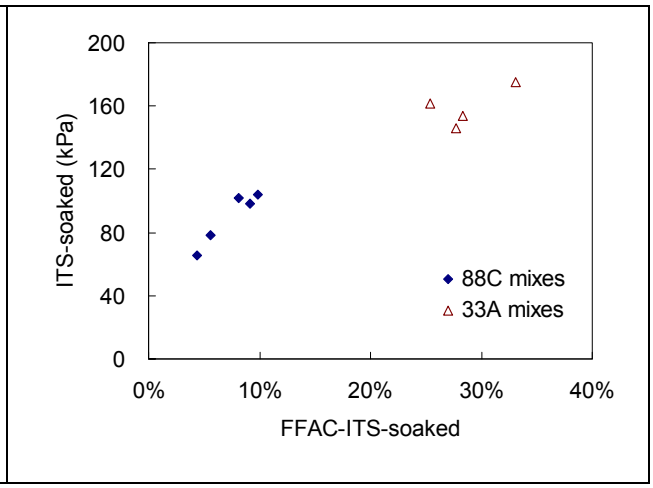

Figure 7.22: Effects of asphalt dispersion on soaked ITS test results.

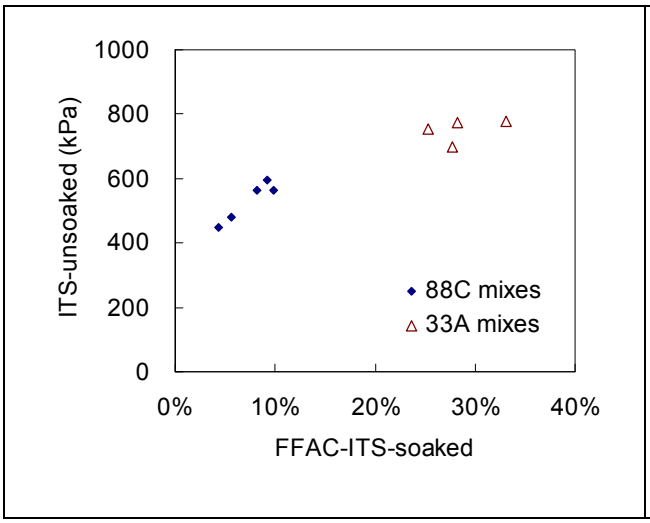

Figure 7.23: Effects of asphalt dispersion on unsoaked ITS test results.

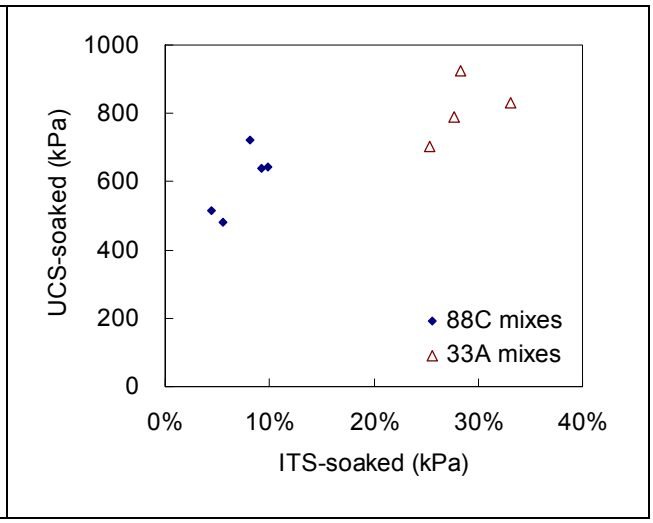

Figure 7.24: Effects of asphalt dispersion on soaked UCS test results.

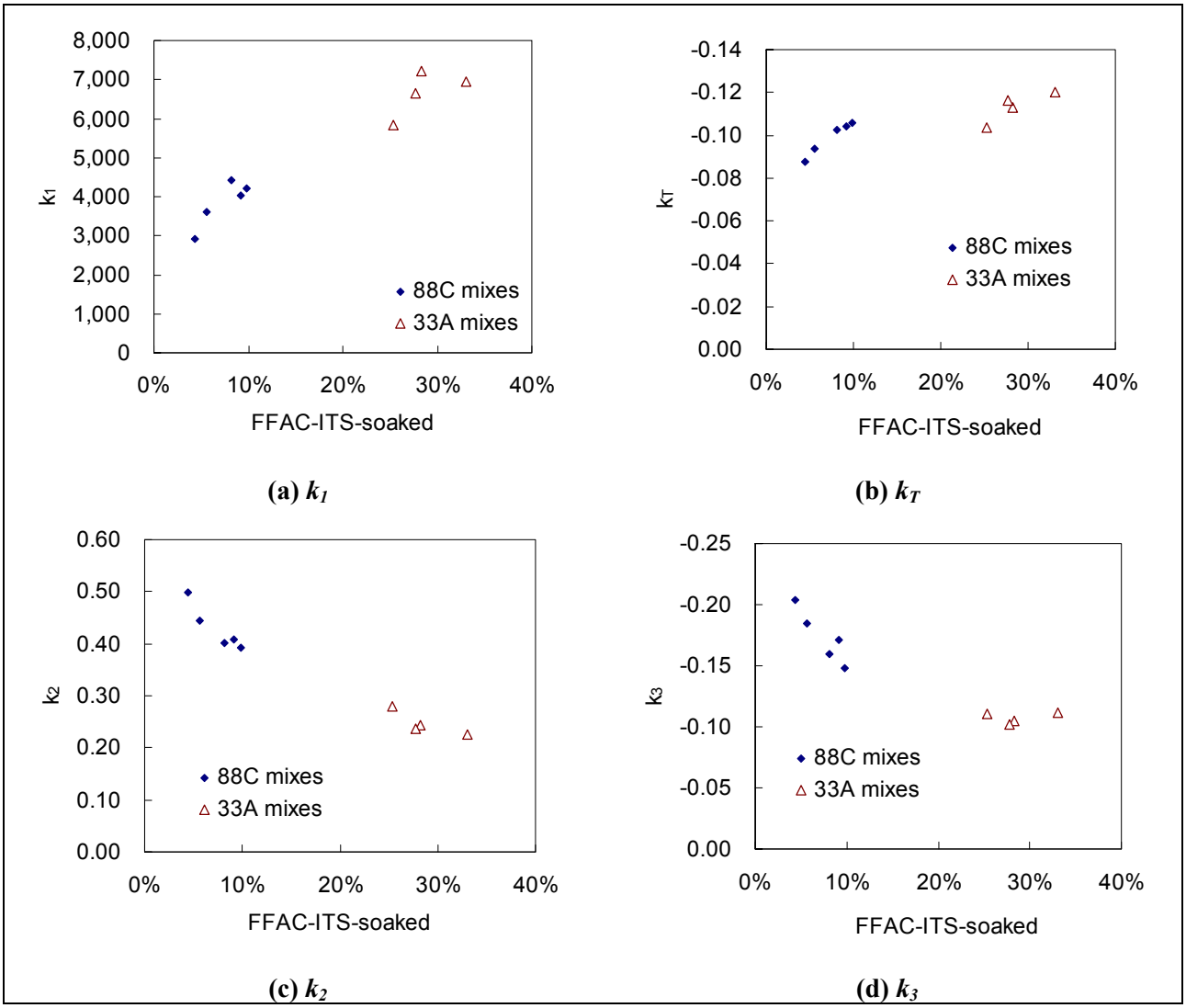

Figure 7.25: Correlations between resilient modulus parameters and FFAC values.

7.5.6 Discussion

Observations of the loose untreated mixes and ITS specimen fracture faces indicate that mixing moisture content affects asphalt distribution in foamed asphalt mixes through its influence on the agglomeration states of aggregate particles, specifically the fine particles. Visual assessments of the ITS specimen fracture faces, supported by the FFAC analysis, indicate that poor dispersion of foamed asphalt is likely if the mix is in agglomeration State–D associated with excessive amounts of mixing moisture, because the exposed surface area of the aggregate particles is small and the asphalt will have a concentrated distribution with a relatively high film thickness. Mixes in State-B typically have good asphalt distribution, but in practice the mixes might be too dry to achieve adequate compaction. Mixes in State-C appear to have a good balance between mix workability (or compactability) and asphalt distribution.

7.5.7 Summary of Recommendations for Mixing Moisture Content

The following recommendations regarding mixing moisture content are made:

- As an interim, a mixing moisture content of between 75 and 90 percent of the optimum compaction moisture content appears to be an appropriate starting point. However, insufficient data was collected during the UCPRC study to determine clear upper and lower limits for the mixing moisture content and therefore these limits should be established during the mix design process.
- Although control of the mixing moisture content is generally applicable to all gradations of material, foamed asphalt dispersion in mixes with coarser gradations appears to be less sensitive to mixing moisture content.

7.6 Assessment of Mixing Temperature

7.6.1 Introduction

The *mixing temperature* (i.e., the aggregate temperature when foamed asphalt is injected) was identified as an important factor affecting foamed asphalt mix properties during both the UCPRC laboratory study and FDR-foamed asphalt projects in California.

The Caltrans Special Provisions that are part of the Project Specifications include the following clause with regard to ambient temperature during FDR with foamed asphalt projects.

> *No cold foam in-place recycling work shall be performed if the ambient air temperature is below 5°C (41°F). Other than the finishing and compaction operations, no work will be allowed if the air temperature drops below 10°C (50°F).*

No mention is made in the specification of measuring the surface temperature of the roadway, the temperature of active fillers after spreading onto the roadway, the temperature in the layer to be recycled, or the temperature of the recycled material immediately behind the recycler. The South African *(3)* and Wirtgen *(6)* guidelines recommend a minimum ambient temperature of 10°C (50°F) and a minimum aggregate temperature (location not specified) of 15°C (59°F). The Wirtgen manual also provides a range of temperatures to obtain acceptable dispersion, based on the expansion ratio of the foam. A similar table, based on the Wirtgen recommendations is provided below (Table 7.15).

Table 7.15: Effect of Aggregate Temperature on Expected Foamed Asphalt Dispersion *(6)*

<8 8–12 >12	Very poor Moderate Good	Poor Good Very good	Moderate Good Very good

Various roadway and ambient temperatures were measured on a number of reclamation projects during the course of the UCPRC study. In all instances, the minimum ambient air temperature requirements in the project specifications were met. However, temperatures on the roadway, in the layer, and of the filler spread onto the road ahead of the recycler were often considerably lower than would typically be tolerated during laboratory testing, where experience has shown that lower temperatures result in poor dispersion of the foamed asphalt. Although heat generated through friction during the pulverization process and from the addition of the binder increases temperatures during recycling, temperature measurements of the recycled material immediately behind the recycler indicated that the processed material was still relatively cold. An example on one specific project is provided in Figure 7.26 through Figure 7.29. In this project, portland cement was spread onto the road ahead of the recycling train. Figure 7.26 and Figure 7.28 show the cement temperatures measured at 07:30 A.M. (8°C [46°F]) and 11:30 A.M. (31°C [88°F]). Figure 7.27 and Figure 7.29 show the temperatures of the foamed material immediately behind the recycling machine at the same times (17°C [62°F] and 32°C [90°F]).

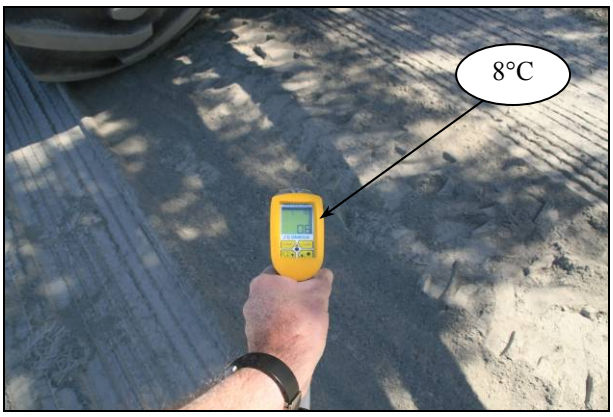

Figure 7.26: Cement temperature (°C) prior to recycling (cold).

Figure 7.27: Recycled material (cold).

Figure 7.28: Cement temperature prior to recycling (warm).

Figure 7.29: Recycled material (warm).

Close inspection of this material revealed poor asphalt distribution and relatively high concentrations of globules and strings of asphalt (Figure 7.30 and Figure 7.31). Higher than normal concentrations of asphalt on the rear tires of the recycler (Figure 7.32 and Figure 7.33) were also observed at these times. Once aggregate temperatures increased to above those recommended in the literature (15°C to 25°C [59°F to 77°F]) *(3,6)*, these problems were no longer observed.

Figure 7.30: Poor asphalt dispersion on cold aggregate.

Figure 7.31: Asphalt strings in recycled material.

Figure 7.32: Asphalt globules on recycler tires.

Figure 7.33: Expected recycler tire appearance.

Although road surface finish after final compaction and blading is dependent on many factors during construction, observations indicated that raveling was often more predominant in areas recycled during colder conditions than those recycled during higher temperatures on the same project (Figure 7.34 and Figure 7.35).

Figure 7.34: Poor surface compaction in areas of recycling in cold temperatures.

Figure 7.35: Good surface compaction in areas of recycling in normal temperatures.

7.6.2 Revised Experiment Factorial

A small-scale laboratory study was included in the work plan to quantitatively investigate the effects described above. Variables considered include mixing temperature and curing durations (Table 7.16). One RAP gradation, one binder, and one test method (100 mm ITS) were used.

Table 7.16: Revised Factorial Design for Mixing Temperature Study

Variable	No. of values	Values
Mixing temperature (aggregate)	5	- Range between 10ºC and 40ºC
Curing durations	2	- 40°C oven curing, unsealed, for 3 days - 40°C oven curing, unsealed, for 7 days
Replicates	5	- 5 specimens per mixing temperature per curing duration
Fixed Values		
RAP	1	- Route 88 RAP, 10% passing the 0.075 mm sieve by mass
Binder source and type	1	- Refinery A, PG64-16, optimized foaming characteristics
Test methods and associated specimen fabrication methods	1	- ITS (100 mm), Marshall compaction, 75 blows/face
Water conditioning method	1	- Soaked, 72 hours soaking
Mixing moisture content	1	- Target value 4.7%; measured average value 4.8% with a standard deviation of 0.3%.

RAP was preconditioned in a forced draft oven at 50°C (122°F) for 24 hours for mixes with target mixing temperatures higher than the ambient air temperature (15°C [60°F]). For mixes with target mixing temperatures lower than the ambient air temperature, the RAP was first subjected to the same 50°C (122°F) preconditioning to standardize any aging effects, and then cooled to the required temperature with ice.

7.6.3 Test Results and Discussion

The mixing temperatures immediately before and after asphalt injection and the ITS test results from the specimens prepared from the respective mixes are summarized in Table 7.17. The average coefficient of variation for strength was eight percent, indicating that repeatable measurements were achieved. The results show that the addition of the hot asphalt foam does not raise the mix temperature by more than about 6°C (11°F) when the aggregate is cold.

Table 7.17: Temperature Sensitivity Test Results

Mixing Temperature (°C)		Soaked ITS (kPa)	
Before Foam Injection	After Foam Injection	3 Day Cure	7 Day cure
11.6	17.8	165	169
11.2	17.2	170	193
15.1	20.3	175	190
31.8	35.4	175	204
41.9	42.6	184	196

The mixes with mixing temperatures ranging between 11.2°C and 15.1°C (52.2°F and 59.2°F) visually appeared to have poor asphalt dispersion in the loose mix, and on the fracture faces of the tested ITS specimens. Relatively large (up to 10 mm [0.4 in.] in diameter) asphalt-and-fine aggregate agglomerations were formed. The mixes with higher mixing temperatures (above 30 C [86°F]) had more uniform asphalt distribution patterns. However, no significant differences were noted in the ITS test results. Possible reasons for this include:

- This effect might be gradation sensitive. Mix properties of the RAP gradation used could have been less sensitive to moderate asphalt dispersion pattern changes.
- Specimen compaction was carried out at similar temperatures for all mixes (± 25°C [77°F]). Compaction at the higher temperature may have facilitated additional asphalt redistribution, which compensated for the poorer dispersion during colder mixing.

7.6.4 Summary of Recommendations for Aggregate Mixing Temperatures

The following recommendations regarding mixing temperature are made:

- Laboratory mixing and compaction temperatures should be monitored and recorded. Aggregate temperatures should exceed 15°C (60°F) at the time of injecting the foamed asphalt. Mix temperatures should exceed 15°C immediately prior to compaction.
- All laboratory testing should be carried out at controlled temperatures (25°C ± 4°C [77°F ± 7°F]).
- The project specifications and special provisions for FDR-foamed asphalt projects should be changed to require measurement of roadway surface temperature and prespread active filler temperature, in addition to ambient temperatures. As an interim measure, ambient temperatures

should exceed 10°C (50°F) and roadway, filler, and aggregate temperatures should exceed 15°C (59°F).

- The effects of low aggregate/active filler temperatures should be studied in more detail and revised project temperatures set if required.

7.7 Relating Laboratory Resilient Modulus Tests to Field Stress States

7.7.1 Introduction

The resilient moduli of foamed asphalt mixes are typically stress dependent, as discussed in Section 7.4. Stiffnesses determined by triaxial resilient modulus tests can be more than ten times higher than those determined by flexural beam tests, especially when the material is soaked prior to testing. The triaxial resilient modulus test characterizes material behavior in stress states of compression/shearing, while the flexural beam test characterizes material behavior in tension. All these stress states exist in foamed asphalt-treated base layers, and the results for triaxial resilient modulus tests and flexural beam tests therefore need to be combined to predict field stiffness behavior more accurately. Predicting resilient modulus values of foamed asphalt mixes under soaked conditions solely based on triaxial tests will not provide sufficiently conservative results. In this section, the test results of the triaxial resilient modulus and flexural beam tests, each of which characterizes one important stress state, were incorporated into a bilinear anisotropic constitutive model to calculate pavement deflection under traffic loading. A virtual FWD backcalculation procedure was used to determine the equivalent resilient modulus of in-service pavement stress states. This numerical analysis procedure involved three main components, namely:

- A bilinear anisotropic elastic constitutive model,
- An axisymmetric finite element model, and
- An FWD backcalculation procedure.

7.7.2 Constitutive Model

A bilinear anisotropic elastic constitutive model is proposed for characterizing the different resilient moduli of foamed asphalt mixes subjected to tension and compression/shearing. Section 7.4 showed that in the unsoaked state, resilient moduli of foamed asphalt mixes in compression/shearing and in tension are similar. Therefore, a conventional isotropic elastic model is sufficient for the unsoaked foamed asphalt mixes discussed in the UCPRC study, and consequently the proposed model focuses on soaked foamed asphalt materials. The constitutive model in a cylindrical axisymmetric coordinate system (Figure 7.36) is shown as Equation 7.2.

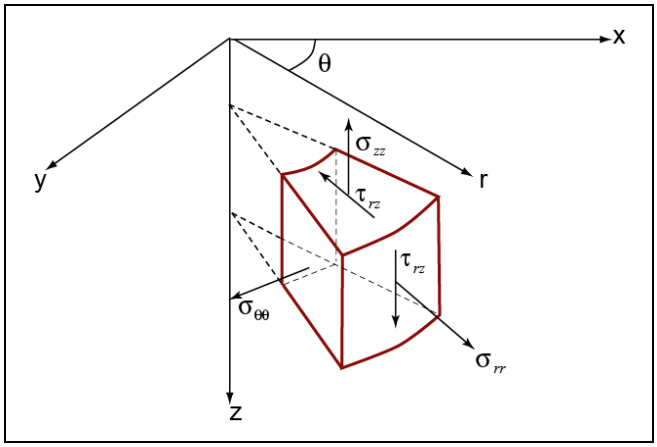

Figure 7.36: Notation of stresses in a cylindrical coordinate system.

$$\sigma = \begin{bmatrix} \sigma_{rr} \\ \sigma_{zz} \\ \sigma_{\theta\theta} \\ \tau_{rz} \end{bmatrix} = \frac{E^*}{(1+v^*)(1-2v^*)} \begin{bmatrix} \alpha_r^2(1-v^*) & \alpha_r v^* & \alpha_r\alpha_\theta v^* & 0 \\ \alpha_r v^* & 1-v^* & \alpha_\theta v^* & 0 \\ \alpha_r\alpha_\theta v^* & \alpha_\theta v^* & \alpha_{\theta\theta}^2(1-v^*) & 0 \\ 0 & 0 & 0 & \frac{\alpha_r(1-2v^*)}{2} \end{bmatrix} \begin{bmatrix} \varepsilon_{rr} \\ \varepsilon_{zz} \\ \varepsilon_{\theta\theta} \\ \gamma_{rz} \end{bmatrix} \quad (7.2)$$

where:
- σ_{rr}, σ_{zz}, $\sigma_{\theta\theta}$, and τ_{xz} are stress components as shown in Figure 7.36.
- ε_{rr}, ε_{zz}, $\varepsilon_{\theta\theta}$, and γ_{xz} are the corresponding strain components.
- E^* and v^* are the Young's modulus and Poisson's ratio, respectively, for compression/shearing of soaked materials. E^* is generally stress level dependent and can be calculated at various mean confining stress and deviator stress levels based on triaxial resilient modulus test results. However, this dependency is ignored in this model to limit the complexity of the analysis and E^* and v^* are assumed to be constants accordingly, regardless of the stress levels.
- α^2 is the ratio of the resilient modulus when the material is in tension (E^+) to the resilient modulus when the material is in compression (E^-) (i.e., $\alpha^2 = E^+/E^-$).
- α_r and α_θ are the anisotropy parameters at the radial and angular directions respectively. If the material is in compression in the radial direction then $\alpha_r = 1$, and if the material is in tension in the radial direction, then $\alpha_r = \alpha < 1$. α_θ follows the same rule. If one point in the material is in tension in both the radial and angular directions, $\alpha_\theta = \alpha_r = \alpha < 1$. α_θ and α_r are two internal state variables depending on the stress state, while α^2 or α is a material-related constant. The procedure to obtain the α^2 value from triaxial and beam test results is elaborated in Appendix C.

Various anisotropic models (mainly cross-isotropic models) have been proposed for granular materials *(61-64)*. These models generally attempt to characterize anisotropy induced by the deposition, compaction, and other vertical loading to the material, with lateral confinement and the model parameters determined by triaxial type laboratory tests *(65,66)*. Although the format of Equation 7.2 is similar to the model proposed by Graham and Houlsby *(62)*, the basic ideas that they convey are somewhat different. The anisotropy expressed in Equation 7.2 is attributed to the different stress states (tension or compression) along different directions at one point in the material, while the initial anisotropy caused by compaction and deposition is ignored, which is the main feature that conventional anisotropic models attempt to capture. Another important difference is that conventional granular materials cannot bear any

tensile strain. The strain states along the two horizontal directions, namely the radial direction and angular direction, are generally different except for along the symmetrical axis, and need to be considered separately. This model is therefore not a cross-isotropic model, but involves an additional parameter compared to Graham and Houlsby's model *(62)*. It should be noted that the anisotropy parameter $\alpha^2 = E^+/E^-$ is different from the horizontal-to-vertical modulus ratio $n = M_r^r/M_r^z$ in conventional cross-isotropy models (e.g., Tutumluer and Thompson *[63]*).

7.7.3 Finite Element Model

An axisymmetric finite element pavement response calculation program was developed as part of the UCPRC study, using an eight-node, isoparametric quadrilateral element for axisymmetric applications. A circular load was applied around the symmetrical axis for the virtual FWD test. The radius of the loading area was 150 mm (6 in.), equivalent to typical FWD equipment. In the finite element mesh, small element sizes (approximately 10 mm x 10 mm [0.4 in.]) were used in the area close to the load, with element sizes gradually increasing in both radial (horizontal) and vertical directions. The dimensions of the entire model were larger than 100 m x 100 m (330 ft) and therefore the boundary effect was negligible. A typical finite element model consisted of 2,000 to 4,000 elements and 6,000 to 12,000 nodes. A layered elastic analysis program *(LEAP2 [19]*) was used to validate the calculation results and satisfactory agreement was achieved. When the anisotropic resilient modulus model was implemented in the FEM model, an iterative procedure, in which the stiffness matrix of each element was updated according to stress calculated from the previous iteration step, was employed until the solution converged. It was also assumed that if at iteration I one element was in tension in a certain direction, the anisotropy parameter would be $\alpha_r = \alpha$ and/or $\alpha_\theta = \alpha$ at the following iterations for this element.

7.7.4 Virtual FWD Backcalculation

In the virtual FWD tests, deflections of the pavement surface at seven locations (0 mm, 200 mm, 300 mm, 450 mm, 600 mm, 900 mm, and 1,525 mm from the center of the load [0, 8, 12, 18, 24, 35, 60 in.) were calculated using the finite element model with the foamed asphalt layer represented by the anisotropic model, and with the subgrade and the asphalt concrete layer represented by the conventional isotropic linear elastic model.

The same FEM model was used as the deflection calculation engine for backcalculation, while the foamed asphalt layer was assumed to be elastic and isotropic with resilient modulus to be determined. An iterative procedure utilizing the constrained Extended Kalman Filter (EKF) method *(24)* was used to estimate equivalent resilient moduli of all pavement layers by minimizing the residual error.

7.7.5 Compaction-Induced Residual Stress and Normalization

Vertical loading (e.g., initial compaction and traffic loading) on granular base materials in pavement structures can induce lateral compressive residual stress (σ_R), which remains (or is contained) after the load is removed, and can partially offset the calculated tensile stress. Typical values of the residual stress are within the range of 10 kPa to 20 kPa (1.5 psi to 3 psi) depending on the soil type and compaction methods *(57,67)*. Details on the in-place measurement of residual stress in foamed asphalt base layers were not found in the literature, and were not attempted in this study. However, in this specific analysis the applied load can be normalized against the value of residual stress. Then, only the proportion between the applied loading stress and the assumed residual stress, and not actual values, affect the backcalculated layer moduli. (For example, two cases [Case-A and Case-B] are considered, both with identical material, structural and loading parameters. Both the applied load and the residual lateral stress of Case-A are twice that of Case-B. The calculated pavement responses [deformation, stress, and strain, etc.] of Case-A would be exactly twice that of Case-B, but the backcalculated equivalent moduli of all layers would be exactly the same for the two cases. For simplicity, all the values reported are based on an assumed residual stress level of 20 kPa (3 psi), unless otherwise stated.)

Lateral compressive deformation was applied to all layers at the radial boundary of the FEM model to produce the desired level of lateral stress in the finite element model. The residual lateral stress was treated as a boundary condition rather than as a stress state. Although lateral stresses were also induced in the asphalt concrete and subgrade layers by this treatment, the materials in these two layers were assumed to be elastic and isotropic, with the effects easily counteracted by subtracting the corresponding uniform deformation, stress, and strain from the calculated pavement responses. The vertical and horizontal stresses induced by gravity of pavement materials were not considered.

7.7.6 General Structural Response Due to Anisotropy

Analysis Scenarios

The factorials listed in Table 7.18 were analyzed to assess the effects of the anisotropy parameters α_r and α_θ, and their interactions with applied loads. Values for each parameter, except for the α value and the applied load p, which were the variables for this sensitivity analysis, were selected according to typical FDR engineering practice in California.

Table 7.18: Factorial for General Structural Response Analysis

Factor	Number of Levels	Values
Layer thickness	1	75 mm for asphalt concrete; 200 mm for foamed asphalt base.
E_{AC}	1	3,000 MPa
E^*_{FA}	1	900 MPa
E_{SG}	1	70 MPa
v_{AC}, v^*_{FA}, and v_{SG}	1	0.35
α^2	5	1.0, 0.5, 0.2, 0.1, 0.05
P	14	100 ~ 1,800 kPa, assuming σ_R = 20 kPa

E_{AC} and E_{SG} are the Young's modulus of the asphalt concrete layer and the subgrade.
v_{AC} and v_{SG} are the Poisson's ratio of the asphalt concrete layer and the subgrade.
P is the applied loading pressure.
σ_R is the assumed residual lateral stress due to compaction.
A or α^2 is a material constant as defined in Section 7.4.5.

Structural Response

Tensile zones in the angular (θ) and radial directions (r) form in the foamed asphalt layer around the loading area under the applied load as the layer deforms. The angular tensile zone is generally much wider than the radial tensile zone. The approximate ranges of the tensile zones for one loading case are illustrated in Figure 7.37. The average radius of the tensile zone in the radial direction ($r_{tensile\_r}$) is always smaller than 260 mm (10 in.) for all the scenarios in Figure 7.37, while the average radius of the tensile zone in the angular direction ($r_{tensile\_\theta}$) increases significantly with the applied load, and can be as high as 1,600 mm (63 in.) as shown in Figure 7.38.

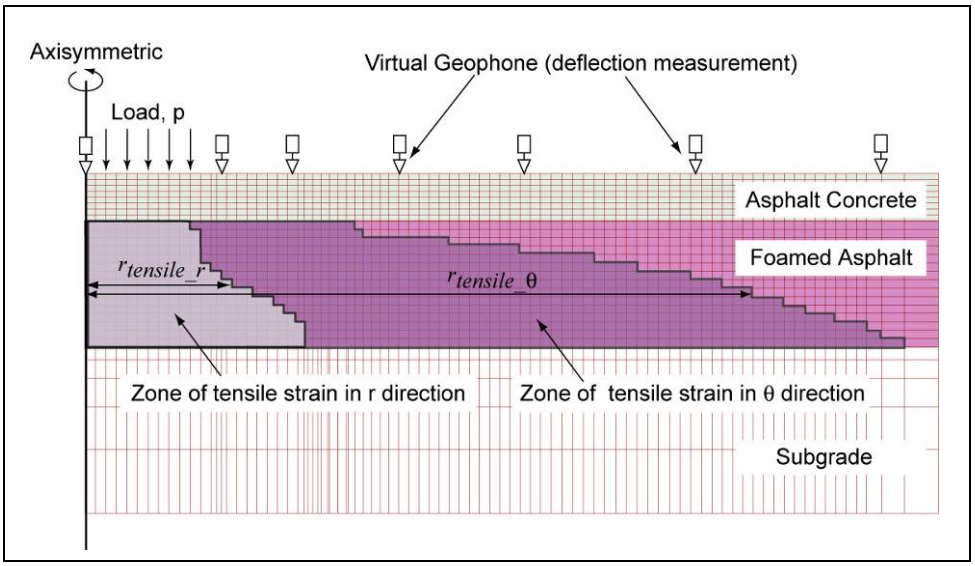

Figure 7.37: A typical FEM mesh (partial) and tensile zones.

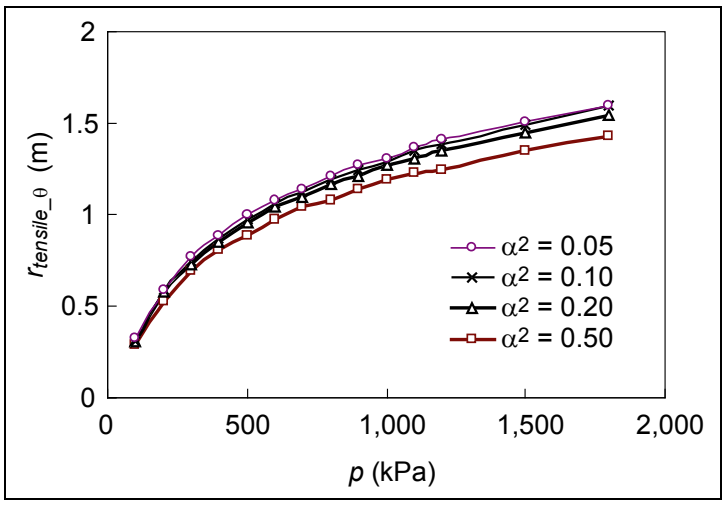

Figure 7.38: Increase in angular tensile zone ($r_{tensile\_\theta}$) with increasing applied loads (p).

Figure 7.39a shows the deflection basins for various α^2 values with a constant applied load of p = 1,000 kPa (145 psi). The deflection basins shown in Figure 7.39b were calculated for various load levels with constant $\alpha^2 = 0.1$, and the deflection values were linearly normalized to p = 1,000 kPa to facilitate comparison. As the applied load (p or α^2) value increases, higher concentrated deflection develops in the area around the applied load, while the deflections at locations further away from the center of the load (e.g., more than four times the radius of the applied load) are only marginally affected. Within the framework of linear elasticity, which is the assumption for the virtual backcalculation procedure, this type of deflection basin corresponds to lower resilient moduli of the upper two layers.

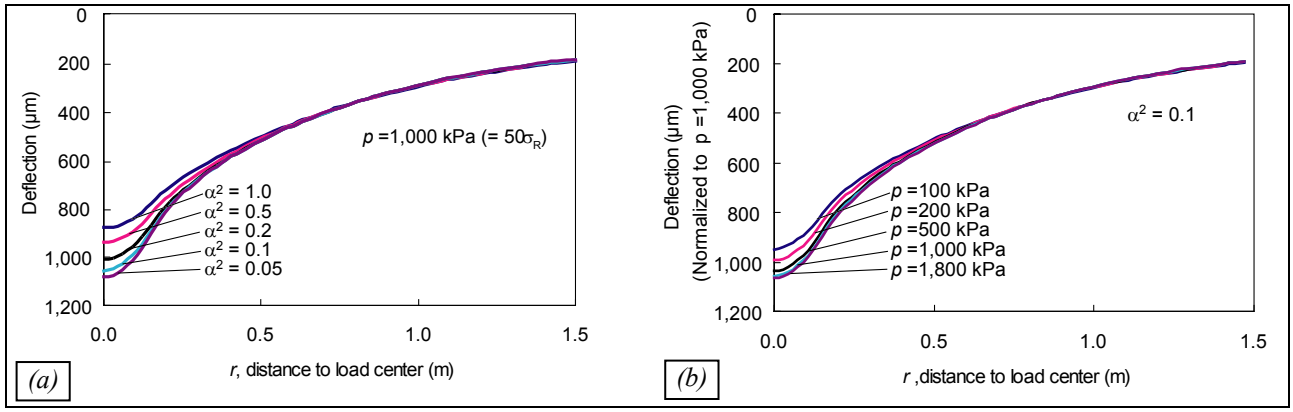

Figure 7.39: Deflection basins for various loads and α^2 values.
(a) Various α^2 values for fixed p = 1,000 kPa; (b) various p values for α^2 = 1.

The average Root Mean Square (RMS) Error (as defined in Equation 7.3) of the backcalculation for all the scenarios was 0.5 percent.

$$RMS\ Error = \sqrt{\frac{\sum_{i=1}^{n}\left(\frac{d_{mi}-d_{ci}}{d_{mi}}\right)^2}{n}} \times 100\% \qquad (7.3)$$

where
- n is the number of geophones.
- d_{mi} and d_{ci} are the measured and calculated deflections of the i^{th} geophone.
- In the virtual FWD test and backcalculation, d_{mi} was calculated with the finite element model, assuming the bilinear anisotropic constitutive model for the foamed asphalt layer, and d_{ci} was calculated with the same finite element model, but assuming linear elasticity.

The calculated deflection basins, assuming an isotropic linear elastic foamed asphalt layer, satisfactorily matched the calculated deflection basins, assuming anisotropy. The backcalculated resilient modulus of the foamed asphalt layer ($E_{FA\_backcal}$) decreased as the applied load increased and/or the α^2 value decreased (Figure 7.40a). The backcalculated resilient modulus of the asphalt concrete layer ($E_{AC\_backcal}$) also decreased with $E_{FA\_backcal}$, as shown in Figure 7.40b.

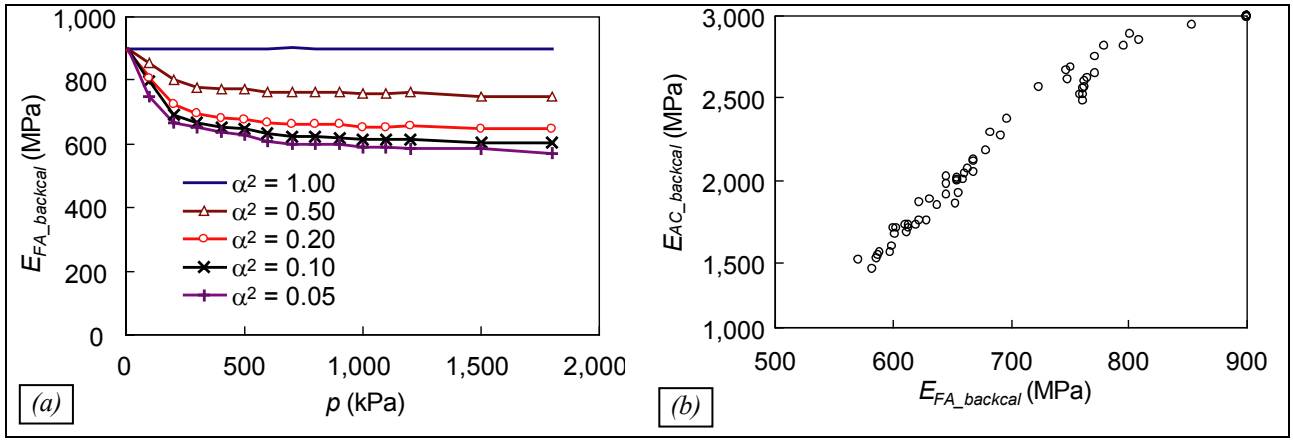

Figure 7.40: Backcalculation results for structural response assessment.
(a) $E_{FA\_backcal}$ decreases with increasing p and/or decreasing α^2;
(b) correlation between $E_{FA\_backcal}$ and $E_{AC\_backcal}$

7.7.7 Effects of Other Structural Parameters

Analysis Scenarios

Based on the above findings, virtual FWD tests and backcalculation were performed on the factorials shown in Table 7.19 to investigate the effects on the resilient moduli of the asphalt concrete layer and the subgrade. Parameters for the foamed asphalt material (E^*_{FA} and α^2) were selected on the basis of the triaxial and flexural beam test results reported earlier. The E^*_{FA} parameter was selected according to typical triaxial resilient modulus test results of soaked foamed asphalt materials at low stress levels (M_{r1} in Table 7.10), and α^2 was calculated based on the ratio ($\lambda^2=E^{bend}/M_{r1}$) of the soaked flexural beam test resilient modulus to the triaxial resilient modulus for the same material (Table 7.11). The equations used to calculate α^2 from λ^2 are provided in Appendix C. Typical California values were used for the other parameters.

Table 7.19: Factorial for Investigating the Effects of Layer Stiffness

Factor	Number of Levels	Values
Layer thickness	1	75 mm for asphalt concrete; 200 mm for foamed asphalt base.
E_{AC}	3	1,500, 3,000, and 9,000 MPa
E^*_{FA}	2	600 and 900 MPa
E_{SG}	3	50, 70, and 100 MPa
v_{AC}, v^*_{FA}, and v_{SG}	1	0.35
α^2	2	0.1, 0.04
p	3	700, 1,000, and 1,500 kPa, assuming σ_R = 20 kPa

The backcalculation results were fitted with the following general log-linear model (Equation 7.4) to investigate the sensitivity of $E_{FA\_backcal}$ to each factor.

$$\ln\left(\frac{E_{FA\_baclcal}}{E^*_{FA}}\right)=\beta_0+\beta_1\ln\left(\frac{E_{AC}}{3000\text{MPa}}\right)+\beta_2\ln\left(\frac{E^*_{FA}}{900\text{MPa}}\right)$$
$$+\beta_3\ln\left(\frac{E_{SG}}{70\text{MPa}}\right)+\beta_4\ln\left(\frac{p}{1000\text{kPa}}\right)+\beta_5\ln\alpha^2 \quad (7.4)$$

where β_1, β_2 , β_3 and β_4 are coefficients of sensitivity for the factors

The constants to nondimensionalize the variables can be selected arbitrarily without affecting the sensitivity analysis results, except for the value of constant β_0. Models of the same format are often used in supply-demand analyses in economics, where the coefficient is termed as "elasticity." An example demonstrating the interpretation of these coefficients is shown in Equations 7.5 and 7.6.

$$\frac{\partial\ln E_{FA\_backcal}}{\partial\ln E_{SG}}=\beta_3 \quad (7.5)$$

$$\frac{\frac{d\ln E_{FA\_backcal}}{dE_{FA\_backcal}}\times dE_{FA\_backcal}}{\frac{d\ln E_{SG}}{dE_{SG}}\times dE_{SG}}=\frac{\frac{dE_{FA\_backcal}}{E_{FA\_backcal}}}{\frac{dE_{SG}}{E_{SG}}}=\frac{\frac{\Delta E_{FA\_backcal}}{E_{FA\_backcal}}}{\frac{\Delta E_{SG}}{E_{SG}}}=\beta_3 \quad (7.6)$$

Therefore, if E_{SG} increases by 10 percent, $E_{FA\_backcal}/E^*_{FA}$ increases by approximately $10\beta_3$ percent. The model fits the backcalculation results reasonably well with a coefficient of determination (R^2) of 80.3 percent. The regression results are shown in Table 7.20.

Table 7.20: Log-Linear Regression Model Fitting Results

Predictor	Coefficient	SE Coefficient	*T*	*P*
β_0	-0.288	0.034	-8.360	<0.001
β_1	-0.006	0.008	-0.800	0.424
β_2	-0.231	0.028	-8.310	<0.001
β_3	0.349	0.020	17.460	<0.001
β_4	-0.041	0.018	-2.270	0.020
β_5	0.029	0.012	2.320	0.022

Statistically, the two most important factors are E_{SG} and E^*_{FA}. The higher the subgrade stiffness, the lower the stiffness reduction due to anisotropy, and the higher the foamed asphalt stiffness, the higher the percentage reduction. The other two factors, namely, the asphalt concrete stiffness and the applied load, have much lower significance than E_{SG} and E^*_{FA}. All backcalculation results are plotted in Figure 7.41 against the resilient modulus of the subgrade. The median value for each "cluster" of data points is also shown.

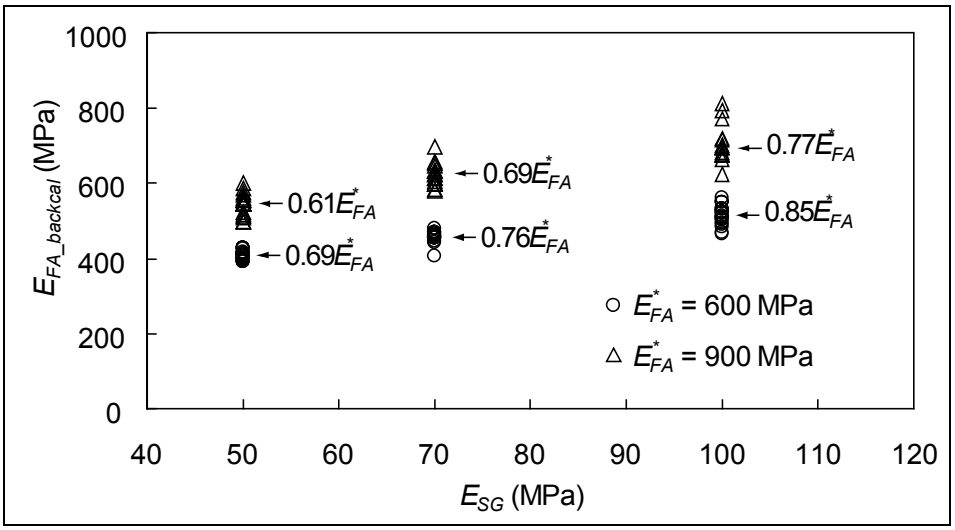

Figure 7.41: Backcalculation results for all scenarios.

This sensitivity analysis shows that the equivalent resilient modulus of the soaked foamed asphalt material with its anisotropy considered in field stress states can be 15 to 40 percent lower than the values that ignore the anisotropy.

The virtual FWD test results also show that as long as the horizontal residual stress is higher than 9.0 kPa (1.3 psi), under load p = 700 kPa (102 psi)(49.5 kN [11,140 lb]), the maximum tensile strain in the foamed asphalt layer does not exceed 1,200 microstrain. According to soaked flexural beam test results, the strain-at-break values for the six mixes tested were within the range of 2,400 microstrain and 4,600 microstrain,

which is much higher than the calculated tensile strain in the numerical analyses. The assumed loads and other boundary conditions will therefore not induce monotonic tensile failure, and the assumptions for the numerical procedure are therefore considered appropriate.

7.7.8 Summary

Tensile stress due to bending and shear/compressive stress with lateral confinement both exist in pavement structures under traffic loading. The triaxial resilient modulus test or the flexural beam test alone can only partially represent the field stress state. The test results from these two test methods were incorporated into a finite element method analysis utilizing a bilinear anisotropic constitutive model. Virtual FWD tests found that an additional 15 to 40 percent reduction of resilient modulus was induced by anisotropy beyond the 5 to 30 percent reduction measured in triaxial tests after water conditioning. Predicting resilient modulus values of foamed asphalt mixes under soaked conditions solely based on triaxial tests will thus not provide sufficiently conservative results. Verification of the findings with FWD deflection measurements on in-service pavements is discussed in Chapter 4.

8. LABORATORY STUDY: PHASE 3

8.1 Introduction

The third phase of the laboratory study extended the objectives of the Phase 2 study discussed in the previous chapter, with more detailed investigations on variables related to recycled asphalt pavement (RAP) sources, RAP gradation, asphalt source, and asphalt grade, but using only one test method (Indirect Tensile Strength [ITS]). A number of tasks were included in this phase that when completed would contribute to addressing the issues identified in the work plan. These tasks included:

- An investigation into the effects of the ITS test loading rate on resultant strength values.
- A study into the effects of RAP source and gradation on the tensile strength of foamed asphalt mixes.
- An investigation into the effects of asphalt binder source, asphalt binder performance grade, foam characteristics, and asphalt content on the tensile strength of foamed asphalt mixes.

8.2 Experiment Design

8.2.1 Testing Matrix

The general factorial design for this phase of the study is summarized in Table 8.1. This entailed a full factorial design consisting of 1,152 ITS tests.

8.2.2 Materials

Aggregate

The Phase 3 study continued with the use of materials sourced from Route 33 (Route 33) and Route 88 (Route 88). Six gradations were constituted for each source. The base gradations were the same as SR33-B and SR88-B described in Phase 2, which had 6.5 percent passing the 0.075 mm (#200) sieve by mass. Additional gradations were constituted by adding various quantities of baghouse dust (Graniterock A.R. Wilson Quarry asphalt plant) to the base gradation to achieve modified gradations of 8.0 percent, 10 percent, 12.5 percent, 16 percent and 20 percent passing the 0.075 mm sieve (#200) by mass. After modification, the Route 33 and Route 88 materials in each gradation group had the same gradation. The grading curves for the Route 33 materials are shown in Figure 8.1.

Asphalt Binder

Three different asphalt binders sourced from three different refineries/terminals in northern California were used in this phase (Table 8.2). The foaming parameters were selected according to the test results in

Phase 1 (Section 6.4) and experience from testing in Phase 2. A tolerance of ±2 Cº (±3.6 F) was allowed for asphalt temperature control. One binder (Asphalt-A) was foamed using two sets of foaming parameters (temperature and foamant water-to-asphalt ratio) to obtain foam with different expansion ratio and half-life characteristics. Foaming parameters for Asphalt-B were selected to maximize the product of the expansion ratio and half-life. Although a foamant water-to-asphalt ratio of 4.0 percent produced a slightly longer half-life, 3.0 percent was selected to suit equipment operational limitations. The foamability of Asphalt-C was poor, with foam characteristics insensitive to the foaming parameters. These were therefore selected arbitrarily, using the same temperature as Foam-A-1 and the same foamant water-to-asphalt ratio as Foam-A-2 and Foam-B.

Table 8.1: Factorial Design for Phase 3 Laboratory Study

Variable	No. of Values	Values
Rap source	2	- Route 33 (Ventura County) and Route 88 (Amador County)
Aggregate gradation based on % passing 0.075 mm[1]	6	- 6.5 (equivalent to SR33/88-B in Phase 2), 8.0, 10.0, 12.5, 16.0, and 20.0 (equivalent to SR33/88-C in Phase 2)
Asphalt source and type	4	- Refinery A PG64-16, foamed at higher temperature - Refinery A PG64-16, foamed at lower temperature - Refinery B PG64-16, optimum foaming characteristics - Refinery C PG64-22, optimum foaming characteristics
Asphalt content (%)[2]	4	- 0 (control), 1.5, 3.0, and 4.5
Loading rates for ITS test[3]	2	- 12.5 mm/minute, 50 mm/minute
Water conditioning method	2	- 24 hours soaking (referred to as soaked) - No conditioning (referred to as unsoaked)
Replicates	2/3/1	- 2 replicates for unsoaked tests - 3 replicates for soaked tests with 50 mm/min loading rate - 1 replicate of soaked tests with 12.5 mm/min loading rate
Fixed Values		
Active filler content (%)	1	- No active filler added
Mixing moisture content (%)	1	- 4.5, 4.6, 4.7, 4.9, 5.2 and 5.5 for the 6 gradations, respectively
Curing method	1	- 40°C oven curing, unsealed, for 7 days
Water conditioning method	1	- 72 hours soaking
Test methods	1	- ITS (100 mm), Marshall compaction, 75 blows on each face
Testing temperature	1	- 20°C

[1] Aggregate gradation based on SR33-B and SR88-B gradation from Phase 2, adjusted with varying quantities of baghouse dust.
[2] Asphalt contents are percent by mass of dry aggregate.
[3] Loading rates are loading head displacement controlled.

Table 8.2: Asphalt Binder Description for Phase 3 Testing

Asphalt Source		PG Grade	Foaming Temp. (ºC)	Foamant Water:Asphalt Ratio (%)	Expansion Ratio	Half-Life (seconds)
Refinery	Foam					
A	A-1	64-16	158	4	24	20
A	A-2	64-16	149	3	20	30
B	B-1	64-22	145	3	11	25
C	C-1	64-16	158	3	6	6

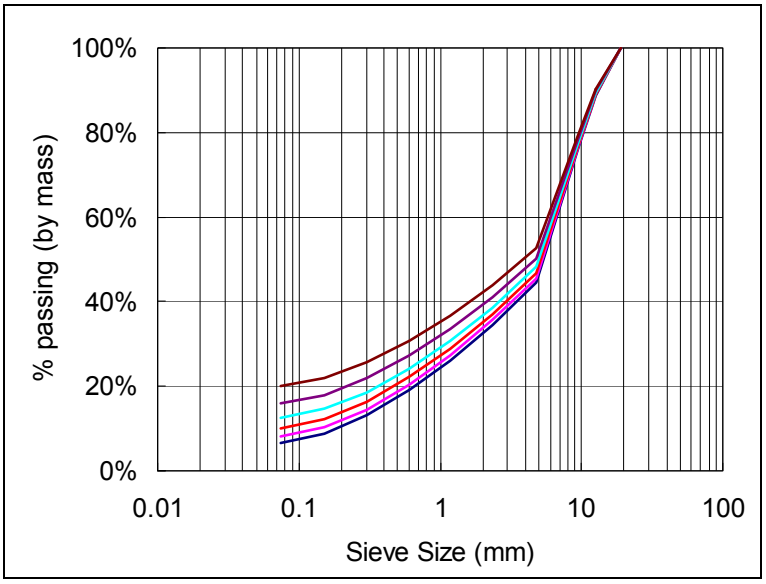

Figure 8.1: Phase 3 RAP gradations (Route 33 material).

The results indicate that there was considerable variation in the foam characteristics of the different binder sources, confirming earlier observations discussed in Chapter 6. This is attributed to different crude oil sources, different refining processes, and the possible effects of the addition of antifoaming additives at various stages of production and transportation.

Maximum Dry Density and Optimum Moisture Content Determination

The maximum dry density and optimum moisture content parameters determined in the previous phases were also used in this phase.

8.2.3 Testing Parameters

Mixing Moisture Content

Target mixing moisture contents for mixes in this phase (and Phase 4) were determined based on the experience gained in Phase 2 (Section 7.5), and direct moist mix agglomeration pattern observations. Target mixing moisture contents were set in a range between 4.5 and 5.5 percent as a linear function of the fines content (Table 8.1). The measured values (mean and standard deviation) are reported in Table 8.3.

Table 8.3: Measured Mixing Moisture Content and Its Variation

Fines Content (%)	Target Moisture Content (%)	Measured Moisture Content (%)	
		Mean	Std. Dev.
6.5	4.50	4.67	0.49
8.0	4.61	4.79	0.45
10.0	4.76	4.87	0.45
12.5	4.94	4.93	0.45
16.0	5.20	5.23	0.37
20.0	5.50	5.56	0.53

ITS Test Loading Rate

The loading rate for the 100 mm ITS test in Phase 2 was displacement controlled at a rate of 12.5 mm (0.5 in.) per minute of movement of the testing machine head, which complied with AASHTO T322 (*Standard Method of Test for Determining the Creep Compliance and Strength of Hot Mix Asphalt (HMA) Using the Indirect Tensile Test Device*). In this phase, the loading rate was changed to 50 mm (2 in.) per minute, which is more commonly used by other researchers. The method complied with AASHTO T283 (*Resistance of Compacted Bituminous Mixture to Moisture Induced Damage*) and LTPP P07 (*Test Method for Determining the Creep Compliance, Resilient Modulus and Strength of Asphalt Materials Using the Indirect Tensile Test Device*). One specimen of each batch of mix was tested at a rate of 12.5 mm (0.5 in.) per minute to obtain a correlation between results tested at the different loading rates.

Fracture Energy Index and Ductility Index

Fracture energy is defined as the area under the load-displacement curve of an ITS test (Figure 8.2) and is measured in Joules (J). During an ITS test, more than one fracture (crack) can develop under loading although not all will propagate completely through the specimen. Fracture energy can therefore be considered as an index for quantifying the energy dissipation capacity of foamed asphalt-treated materials, rather than a strict term as used in fracture mechanics. For example, if two specimens made from two different foamed asphalt mixes have the same ITS values after testing, the specimen with a higher fracture energy value can be assumed to be more ductile than the specimen with the lower fracture energy value.

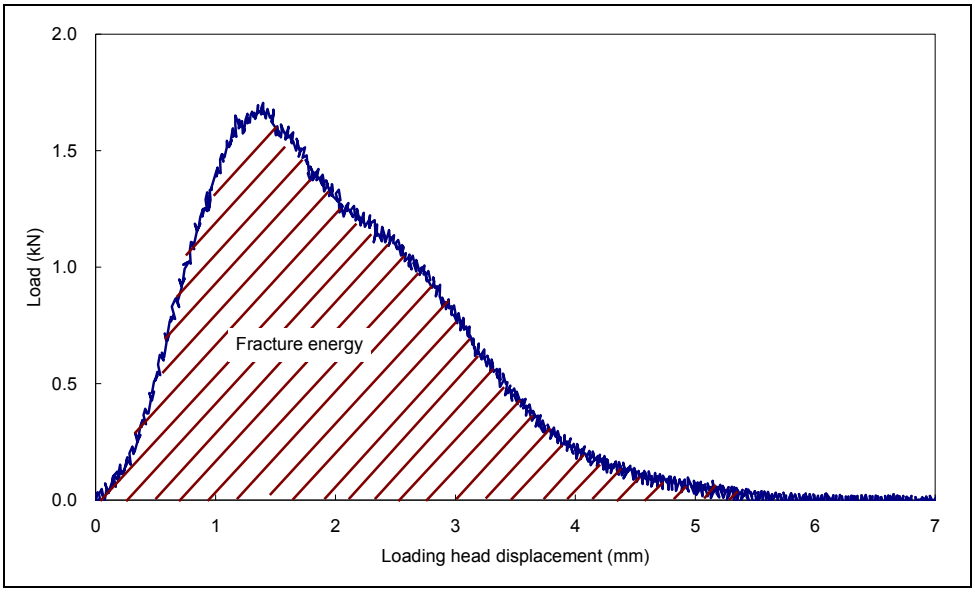

Figure 8.2: Definition of the fracture energy index.

The *ductility index* is defined as the *fracture energy index* (in J) divided by the peak load (in kN) and provides a quantitative indicator of the ductility or tensile deformation resistance of a material. Units are expressed in mm.

8.3 Assessment of Loading Rate

The correlation between ITS values tested at the higher loading rate (50 mm/min) and those tested at the lower loading rate (12.5 mm/min) is summarized in Figure 8.3. The relatively high variance was partially attributed to only one specimen being tested at the lower loading rate for each mix type (i.e., no replicate). Strength was generally higher at the higher loading rate, with the difference more significant for mixes with higher strength. The following bilinear model (Equation 8.1) can be used to convert ITS values between tests at the different loading rates (e.g., when test results from Phase 2 are compared with later phases). The ITS test results discussed in the following sections were all tested at the higher loading rate unless otherwise specified.

$$ITS_{12.5mm/min} = ITS_{50mm/min} \quad \text{if } ITS_{50mm/min} < 70 \text{ kPa}$$
$$ITS_{12.5mm/min} = 0.67ITS_{50mm/min} + 23 \quad \text{if } ITS_{50mm/min} \geq 70 \text{ kPa} \qquad (8.1)$$

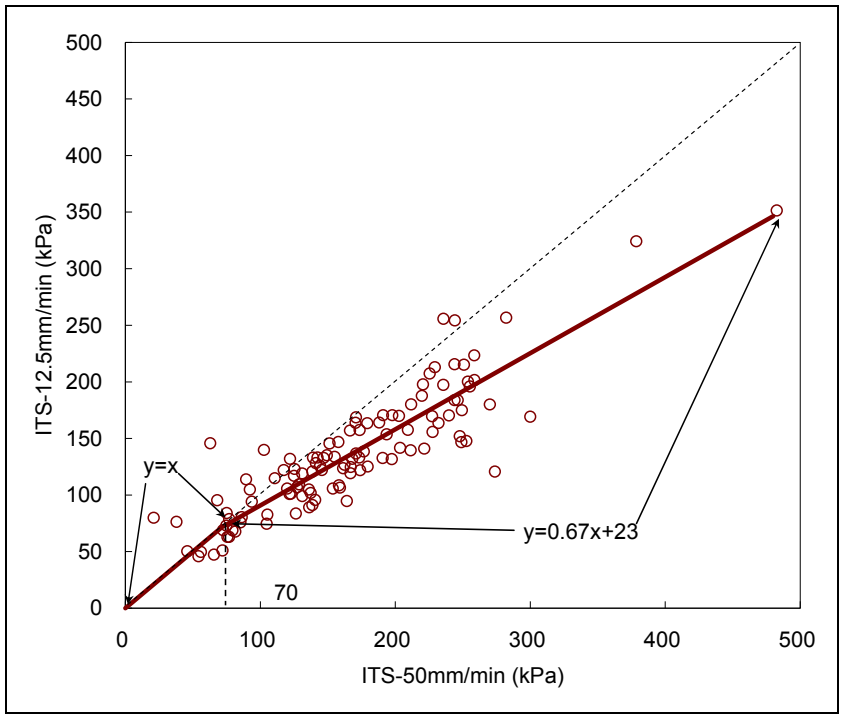

Figure 8.3: Correlation of ITS values at different loading rates.

Table 8.4: Unsoaked ITS Test and Fracture Energy Results for Phase 3 Testing

6.5	632	723	539	723	361	383	283	401	9.8	6.5	5.1	9.0	3.3	3.6	4.0	5.3
8.0	627	710	616	572	361	441	418	462	8.0	6.4	6.6	6.2	4.5	3.8	4.2	4.8
10.0	608	661	574	542	339	393	388	490	6.4	5.6	6.2	5.0	3.0	3.8	4.8	5.2
12.5	459	441	499	562	386	430	291	398	4.2	6.5	5.3	5.3	3.8	4.5	3.2	3.2
16.0	402	443	443	355	304	355	361	341	6.0	4.2	4.0	4.9	3.2	2.7	2.9	3.8
20.0	362	389	323	412	340	328	290	346	3.6	3.9	3.4	3.8	2.5	1.9	2.5	3.4
6.5	922	728	855	893	429	477	512	618	16.1	10.8	13.4	11.5	7.7	8.2	6.9	9.6
8.0	841	741	864	896	599	484	539	NR	19.4	12.3	13.4	14.9	10.9	8.9	9.9	NR
10.0	799	769	825	789	457	493	500	547	14.3	11.1	12.3	12.6	9.8	8.2	7.2	8.4
12.5	741	742	656	749	452	457	455	NR	10.9	9.0	7.8	8.9	7.5	8.7	6.4	NR
16.0	564	562	618	608	480	487	509	NR	7.1	8.8	7.8	8.8	7.1	8.9	4.9	NR
20.0	602	478	550	621	450	486	518	NR	7.1	8.8	6.7	6.0	6.1	6.8	6.3	NR
6.5	901	1,069	833	899	617	633	428	661	22.0	26.2	19.0	20.7	16.9	11.6	7.3	14.0
8.0	972	1,030	735	841	710	699	592	617	22.3	24.5	17.1	20.2	13.1	14.2	12.3	9.5
10.0	990	959	722	795	708	670	532	663	24.1	14.6	16.0	17.0	17.8	13.0	11.8	10.8
12.5	781	832	767	720	655	609	558	574	17.6	20.2	12.4	11.5	13.6	10.6	12.5	8.8
16.0	771	726	656	616	699	602	596	533	13.4	16.9	11.5	11.0	12.2	9.5	11.1	9.1
20.0	699	733	490	501	628	610	477	486	11.1	10.0	11.1	7.2	10.7	9.8	8.9	6.5
	4.5% Asphalt								**4.5% Asphalt**							
6.5	1,063	867	976	1075	715	645	756	706	26.7	22.3	27.4	30.0*	29.2	16.2	17.9	16.2
8.0	872	892	957	995	692	701	778	644	21.3	25.9	22.5	30.2*	19.0	22.8	16.4	16.1
10.0	1,028	882	998	913	746	604	769	665	21.1	25.8	26.2	19.6	19.8	21.5	20.3	18.9
12.5	928	948	890	891	707	670	661	648	25.3	21.9	21.3	21.3	15.0	19.4	15.0	13.2
16.0	821	866	705	805	640	652	716	NR	19.6	26.2	14.3	18.3	14.4	18.2	14.4	NR
20.0	703	694	676	752	624	687	664	581	19.8	14.8	12.7	11.8	13.0	14.5	12.5	11.0

*: Outliers
NR: No Result
Note: For control mixes, the asphalt type has no real meaning because no asphalt was added. Data in different columns from the same source indicate the variability of the RAP material itself and variability introduced in the specimen preparation, conditioning, and testing process.
For soaked ITS test results, the average coefficient of variation was 11 percent.

Table 8.5: Soaked ITS Test and Fracture Energy Results for Phase 3 Testing

6.5	85	112	67	113	76	64	58	102	1.1	1.5	0.8	1.4	0.9	0.7	0.7	1.0
8.0	75	83	59	103	79	90	61	73	1.1	1.1	0.9	1.4	0.9	1.0	0.8	0.9
10.0	75	97	52	68	72	81	68	76	1.1	1.5	1.0	0.9	0.9	1.0	0.7	1.0
12.5	46	52	62	63	73	53	59	60	0.7	0.8	0.9	1.0	1.0	0.7	0.7	0.7
16.0	31	34	39	38	28	43	53	47	0.4	0.5	0.6	0.7	0.4	0.6	0.6	0.7
20.0	10	10	29	21	10	10	10	10	0.1	0.1	0.4	0.2	0.1	0.1	0.1	0.1
6.5	164	118	141	197*	139	177	141	168	2.9	2.8	2.1	3.1	2.3	3.0	2.2	3.2
8.0	159	147	144	174*	158	163	137	183	2.5	2.7	2.8	3.0	3.2	2.9	2.3	3.0
10.0	122	141	149	167	171	155	111	158	2.4	2.5	2.8	2.8	3.3	2.8	1.8	2.9
12.5	117	126	120	136	125	128	126	139	2.6	2.4	2.4	2.3	2.1	2.2	2.2	2.5
16.0	94	97	77	92	89	103	86	126	1.8	1.6	1.4	1.6	1.7	1.9	1.5	2.0
20.0	81	77	56	66	54	73	77	100	1.4	1.9	1.0	1.0	1.0	1.3	1.2	1.6
6.5	212	259	139	244	248	249	142	221	4.7	5.6	2.8	5.4	7.0	6.4	3.5	5.0
8.0	232	244	147	191	244	227	161	203	5.2	5.0	3.6	4.4	6.0	4.8	3.4	4.6
10.0	211	249	161	163	274	191	188	174	5.8	4.9	3.9	3.1	6.0	4.3	3.9	4.0
12.5	185	198	146	154	253	179	171	177	4.7	5.0	2.9	3.8	5.0	4.7	4.0	3.8
16.0	171	151	127	125	180	160	129	132	3.6	3.0	2.6	2.9	5.1	3.9	2.8	2.7
20.0	131	123	105	72	136	122	79	105	3.2	2.3	2.6	1.5	3.2	2.7	1.6	2.2
	4.5% Asphalt								**4.5% Asphalt**							
6.5	236	256	251	483*	300	322	282	307	6.4	7.4	6.6	18.9	10.2	8.6	7.0	9.2
8.0	220	244	255	379*	236	269	246	282	5.8	7.0	7.6	11.6	7.2	7.7	6.3	7.7
10.0	228	229	225	259	270	252	254	255	5.8	6.4	5.3	6.8	9.1	7.8	5.9	7.1
12.5	209	228	194	191	240	226	229	253	5.4	6.0	4.6	5.1	7.2	7.1	5.6	6.8
16.0	220	178	155	162	204	207	173	215	5.8	5.3	3.8	3.7	5.8	6.6	4.8	5.5
20.0	154	160	125	131	167	212	167	185	4.4	4.6	2.7	3.0	4.6	5.9	3.7	4.8

*: Outliers
NR: No Result
Notes: For control mixes, the asphalt type has no real meaning because no asphalt was added. Data in different columns from the same source indicate the variability of the RAP material itself and variability introduced in the specimen preparation, conditioning and testing process.
For soaked ITS test results, the average coefficient of variation was 11 percent.

8.4 Assessment of Fines Content

The ITS results and average coefficient of variation (CoV) for soaked ITS results for Phase 3 testing are summarized in Table 8.4 and Table 8.5. The coefficient of variation for each mix type was determined by first calculating the standard deviation of the ITS values for each mix type (each combination of RAP source-fines content-foam type-asphalt content), and then dividing the standard deviation by the mean strength value. The reported CoV value in the tables is the average over all mix types. The relationship between unsoaked and soaked ITS values and the fines content (gradation) at various asphalt contents are shown in Figure 8.4 and Figure 8.5 respectively for both RAP sources. Each data point represents the average ITS value of mixes treated with the four asphalt binders.

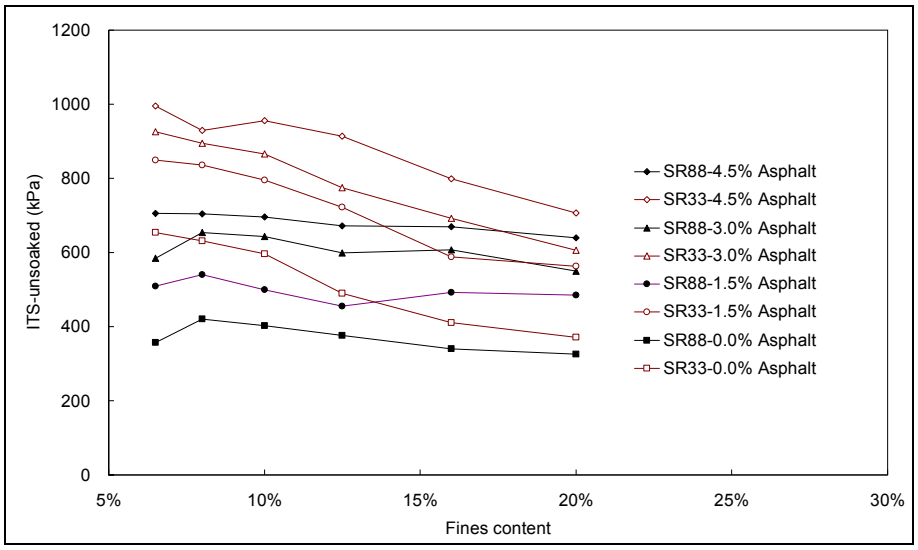

Figure 8.4: Unsoaked ITS values as a function of fines and asphalt content.

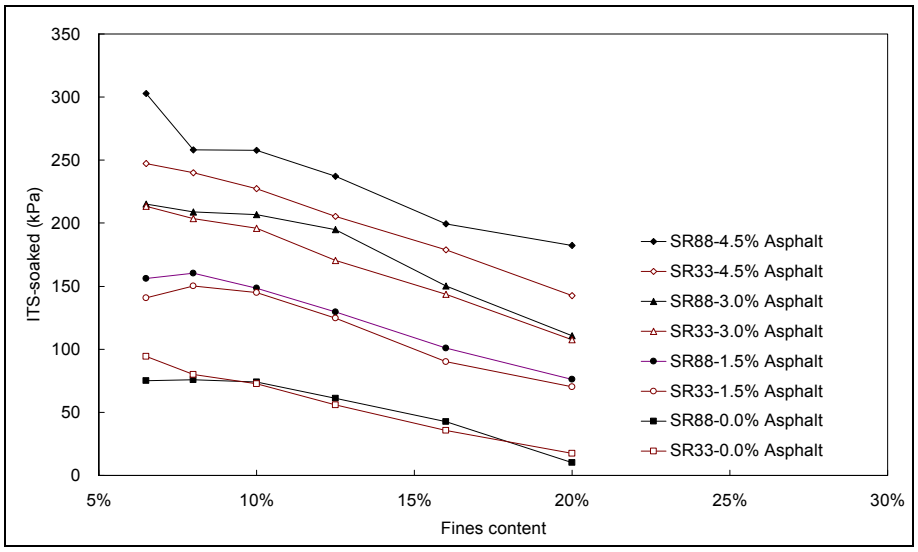

Figure 8.5: Soaked ITS values as a function of fines and asphalt content.

The following observations were made in terms of the effects of fines content, asphalt content, and their interaction under soaked conditions:

- The two RAP sources generally followed a similar trend in behavior for all tests. However, the results for the Route 33 materials were consistently lower than the results for the Route 88 materials throughout the experiment.
- Strength values generally decreased as the fines content increased. This trend was more significant when the fines content was higher than 10 percent. The three coarser gradations (6.5 percent, 8.0 percent, and 10 percent passing the 0.075 mm sieve [#200]) showed similar strengths.
- For each fines content, ITS values increased as the asphalt content increased. The Route 33 materials showed only small strength improvements when the asphalt content increased from 3.0 to 4.5 percent, while the Route 88 materials had a more significant increase.

The following observations were made from the unsoaked test results:

- ITS values increased with increasing asphalt content, with the Route 33 materials showing relatively high tensile strengths even when no asphalt was added, similar to the observations in Phase 2. Consequently, the Route 33 foamed asphalt mixes showed higher unsoaked strengths compared to the Route 88 materials, especially when the fines content was low.
- As the fines content increased, the added baghouse dust diluted the bonding effects of the fines in the original RAP, and the difference in ITS results between the Route 33 RAP and the Route 88 RAP became less significant.

Since the soaked strength was recommended for mix design testing on completion of Phase 2 of the laboratory study, the observations from the unsoaked specimen results do not have any additional practical implications other than confirming the findings from earlier testing, primarily that a more realistic indication of in-service performance will be obtained from soaked testing. Consequently, all further discussion in this section will be limited to soaked testing results unless stated otherwise.

The corresponding fracture energy values are plotted in Figure 8.6. The effects of the fines content on fracture energy were similar to that noted on the ITS test results. The fracture energy increased more significantly with increasing asphalt content compared to the ITS strengths, especially when the asphalt content increased from 3.0 to 4.5 percent. This indicates that increasing the asphalt content not only increases the tensile strength of foamed asphalt mixes, but also improves ductility or flexibility of the materials.

During specimen preparation, it was observed that the RAP materials with higher fines contents produced more “uniform” mixes with “better workability.” After compaction, these specimens appeared to have smoother surfaces when extruded from the compaction molds, and smoother fracture faces after ITS testing. However, when the fines content increases but the asphalt content remains the same, a larger proportion of these fines are not bonded with the available foamed asphalt, and consequently the mineral filler phase occupies more space in the mix. Although such mixes usually have higher densities and lower air-void ratios after compaction, the continuous mineral filler phase, especially when soaked, provides pathways for easy fracture propagation through the specimen during testing. Consequently lower strengths were obtained on specimens with the higher fines contents. During Phase 2 testing, foamed asphalt mixes with high fines contents (20 percent) had lower resilient modulus values and increased sensitivity to stress states. No benefit of high fines content was thus observed.

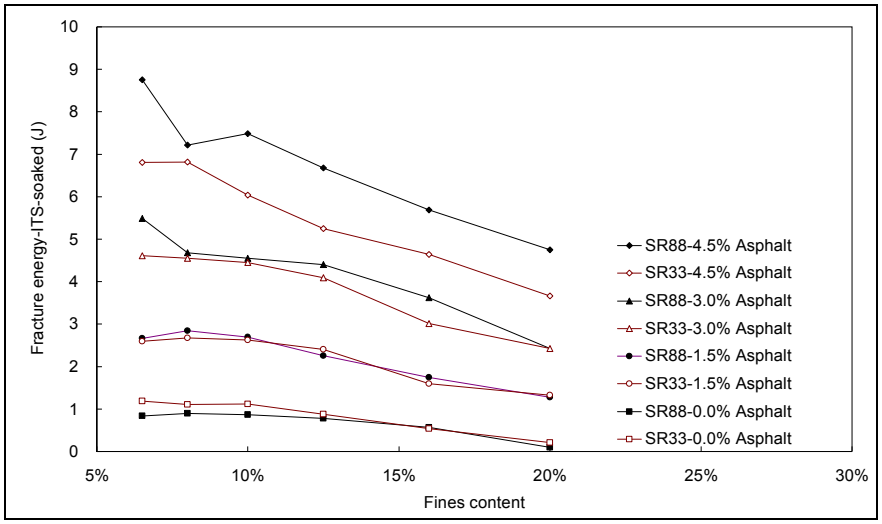

Figure 8.6: Soaked ITS fracture energy as a function of fines and asphalt content.

Although the original Mobil Oil Foam Stabilization Chart *(28)*, followed by the South African guidelines *(3)* and the Wirtgen manual *(6)* all recommend an "ideal zone" of between 5 and 20 percent for the fines content in the material selection criteria, the results of the UCPRC study indicate that better performance is likely if this "ideal" zone is reduced to between 5 and 12 percent. This does not include any active filler that is added, which should react with the aggregate particles, and not effectively increase the fines content of the final mix.

8.4.1 Summary of Recommendations for Fines Content in Mix Designs

The following recommendations regarding fines content are made:

- The mix design fines content (i.e., material finer than 0.075 mm) prior to the application of active filler should not exceed 12 percent as there is no observable improvement in strength or stiffness

above this point, and additional binder may be necessary to counter the effects of seasonal moisture fluctuations.

- The addition of mineral fines to materials with fines contents between 5 and 12 percent is not recommended unless the laboratory mix design testing (without active filler) indicates that the soaked strengths increase by doing so.
- Given that fines content has a significant influence on performance, care should be taken when determining the expected fines content of the pulverized material during mix design. Typically, slabs are removed from test pits during site investigations and these are crushed in the laboratory to obtain an indication of the grading. Observations during the course of the UCPRC study revealed that the actual pulverization process produces higher fines contents than laboratory crushing, which could lead to incorrect mix designs (e.g., low asphalt content). Small cold milling machines (e.g., Wirtgen W35 or W50 series) should be considered for sampling for mix designs as this will provide more representative material.

8.5 Assessment of Asphalt Source

The average soaked ITS values for the six gradations (Table 8.5) were calculated for each asphalt type and asphalt content, and plotted in Figure 8.7. The corresponding fracture energy values are plotted in Figure 8.8.

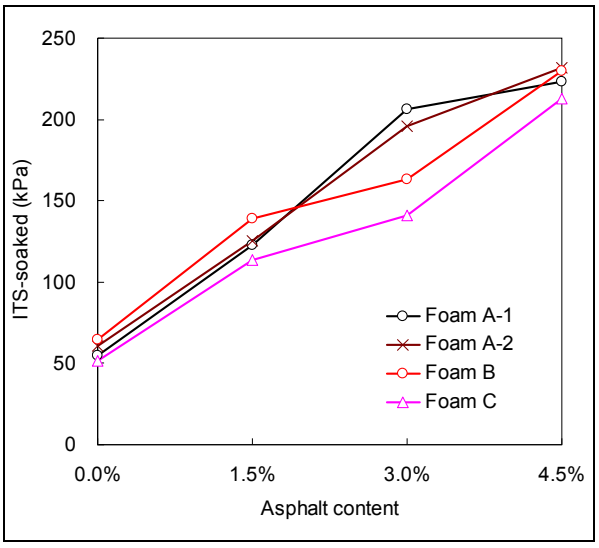

Figure 8.7: Effects of asphalt content on ITS values for different asphalt sources.

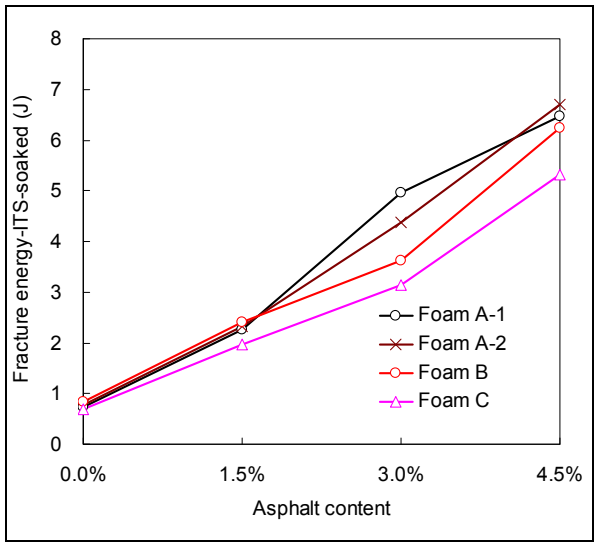

Figure 8.8: Effects of asphalt content on ITS fracture energy for different asphalts.

The following observations were made from the results:

- Tensile strengths and the associated fracture energies for Asphalt-A-1 (higher foaming temperature) and Asphalt-A-2 (lower foaming temperature) were practically the same. This indicates that although the foaming parameters (asphalt temperature and foamant water-to-asphalt ratio) affected the foam characteristics significantly, the effects on mix properties were relatively small. Asphalt-A-1 foam had a higher expansion ratio but a shorter half-life compared to Asphalt-A-2. Finding the "best" combination of foaming parameters is difficult given the variability in foamed asphalt mix properties, and spending additional time and effort in attempting to "optimize" the foam characteristics of a particular mix by adjusting the foaming parameters is not justified based on these findings. Instead, a narrow range of parameter values that have been correlated with known acceptable performance should be set.
- The ranking of ITS and fracture energy values or different asphalt types was generally consistent with their foamability ranking, with Asphalt-A yielding the highest values and Asphalt-C yielding the lowest values. The biggest difference between the binders was recorded for asphalt contents of 3.0 percent, with less significant differences at asphalt contents of 1.5 and 4.5 percent.
- Asphalt-C at 4.5 percent binder content yielded approximately the same ITS and fracture energy values as Asphalt-A mixes with 3.0 percent binder content, indicating that the use of asphalt binders with better foamability can permit lower asphalt contents, which should reduce costs on projects. A more intensive evaluation of this aspect was not carried out, given that obtaining a direct and quantitative link between laboratory strength test results and field performance for each asphalt binder was beyond the scope of the UCPRC study.
- A comparison of the ITS and fracture energy plots confirmed that although asphalt contents higher than 3.0 percent provided only marginal benefits in terms of strength on the materials tested, the material ductility improved significantly at the higher rates.
- According to the performance grading, Asphalt-B should have been the softest. However, the strength of mixes made with this binder was between that of Asphalt-A and Asphalt-C, which is consistent with the foamability rankings. Based on the limited test results, foamability appears to be the primary factor affecting mix properties, and asphalt grade (viscosity) a secondary factor.

8.5.1 Summary of Recommendations for Asphalt Binder Selection

The following recommendations regarding asphalt binders are made:

- A selection of asphalt binders from a number of sources should be assessed during the mix design to ensure that optimum performance in terms of strength and stiffness is obtained.
- As discussed in Section 6.4, the asphalt binders selected during the mix design should be reassessed prior to and during construction to ensure that the foaming characteristics have not changed (e.g., at each tanker change during recycling).

- Fracture energy analyses should be included in the analysis of ITS results when determining mix designs, if the equipment is available, to ensure that optimum strength and ductility is obtained.
- If necessary, a cost-benefit analysis should be undertaken to compare the use of poorer performing asphalt binders at higher asphalt contents to better performing asphalt binders at lower asphalt contents.

9. LABORATORY STUDY: PHASE 4

9.1 Introduction

The fourth and final phase of the laboratory study extended the objectives of the previous phase, with the focus on the role and effects of active fillers. A number of tasks were included in this phase, which further contributed to addressing the issues identified in the work plan. These tasks included assessments of:

- The effects of portland cement and recycled asphalt pavement (RAP) gradation on the behavior of foamed asphalt mixes, considering different cement contents, different gradations, and one foamed asphalt binder content. The Indirect Tensile Strength (ITS) test was used to evaluate the strengths.
- The effects of portland cement and RAP gradation on the behavior of foamed asphalt mixes, considering different foamed asphalt binder contents, different gradations, and one portland cement content. The ITS test was used to assess the strengths.
- The effects of different active and semi-active fillers on early and longer-term strength development of foamed asphalt mixes. Fillers assessed included portland cement, hydrated lime, Class-C fly ash, and cement kiln dust. Factors considered included different filler types, different filler contents, different asphalt contents, and different curing conditions. The ITS test was used for all evaluations.
- The effects of portland cement on the resilient modulus of foamed asphalt mixes, particularly during early curing stages (ITS and Triaxial tests).
- The long-term strength development of foamed asphalt under laboratory curing conditions (ITS tests).
- Potential shrinkage during curing.
- Permanent deformation resistance and potential shrinkage of foamed asphalt mixes (Triaxial tests).
- Curing mechanisms in foamed asphalt mixes and the roles of foamed asphalt and portland cement in the curing process.

9.2 Background

Active (e.g., cement and lime), semi-active (e.g., fly-ash and kiln dust), and inert fillers (e.g., crusher dust and baghouse dust) are often used in FDR-foamed asphalt projects, either to supplement the fines content of the existing milled material and/or to increase the strength and stiffness of the treated material, primarily to provide early strength for accommodating traffic. The use of portland cement (Route 20 in Colusa county, Route 89 in Sierra county), fly ash (Route 132 near Modesto), and cement kiln dust (Route 33 in Ventura county) has been reported in early Caltrans FDR projects. Cement is primarily used as the active filler in South Africa, hydrated lime and cement are used in Australia *(8)*, and the use of inert

crusher dust has been reported in the U.S. state of Maine *(48)*. Strength and stiffness improvements after the addition of the active and semi-active fillers are usually dependent on the material characteristics, and the choice of filler and application rate need to be determined during the mix design process.

A number of studies have been carried out internationally to compare the properties of foamed asphalt mixes with and without portland cement *(16,17,68,69)*. In all of these studies, the addition of the portland cement had a significant and dominating influence on the measured soaked and unsoaked properties of the mixes, even at low cement contents (between one and two percent). Although the addition of foamed asphalt and portland cement both serve the same purpose of bonding aggregate particles together, their roles are complementary rather than interchangeable. Portland cement strength development occurs during a hydration process in the presence of moisture, and under typical field conditions it progresses faster than the strength development of the foamed asphalt, which relies on evaporation of moisture from the treated layer *(28)*. The bonds formed by hydrated cement are strong but brittle compared to those of foamed asphalt which are weaker but more ductile.

Many foamed asphalt reclamation projects, including those in California, typically require that the recycled section of road be opened to traffic before darkness each day. Early strength is therefore a key issue in the design, thereby supporting the use of an active filler in conjunction with the foamed asphalt.

9.3 Experiment Design

9.3.1 Testing Matrix

The general factorial design for this phase of the study is summarized in Table 9.1. This matrix was modified to suit the requirements of each task and revised matrices are provided in the relevant sections. Tests to assess the effects of fines content and asphalt content on the behavior of mixes with active filler were carried out first with portland cement to establish appropriate rates for testing with other fillers. Once these had been established, the tests were repeated using a number of different fillers, but only one gradation and asphalt content. Although a full-factorial of testing would have been preferable, time and testing constraints dictated that a partial factorial approach be followed.

9.3.2 Materials

Aggregate

The Phase 4 study was carried out on materials sourced from Route 88 (Route 88) only, since results from earlier testing showed consistent trends between the Route 88 and Route 33 materials. The aggregate chemistry, which is important to consider when assessing active fillers, was also similar for the two materials. Various gradations were used and these are discussed in more detail under each task. Gradation

modifications where required were achieved by the addition of mineral fines (baghouse dust) sourced from the Graniterock Company A.R. Wilson asphalt plant.

No testing was carried out on aggregates with different chemical compositions. The results discussed in this chapter are therefore not necessarily applicable to all aggregates used in roads in California.

Table 9.1: Factorial Design for Phase 4 Laboratory Study

Variable	No. of Values	Values
Aggregate gradation	Various	- See Task matrices
Asphalt binder content (%)		
Active filler type		
Active filler content		
Curing method		
Water conditioning method		
Replicates		
Fixed Values		
Rap source	1	- Route 88 (Amador County)
Asphalt source and type	1	- Refinery-A, PG64-16, foamed at 150°C with 3% foamant water
Mixing moisture content	1	- Gradation dependent (see Task matrices)
Test method	1	- ITS (100 mm), Marshall compaction, 75 blows on each face. Loading rate of 50 mm/minute - Triaxial resilient modulus (see Section 7.2.3) - Triaxial permanent deformation
Ambient testing temperature	1	- 20°C

Asphalt Binder

Only one asphalt binder (PG64-16 from Refinery-A) was used in this phase of the laboratory study.

Fillers

The fillers used in this phase of the study were sourced as follows:

- Portland cement: Type II portland cement, sourced from a local hardware store. The same brand and type was used throughout the study.
- Hydrated lime: sourced from a local hardware store.
- Fly-ash: sourced from Cemex® fly-ash terminal at Pittsburg, California.
- Kiln dust: sourced from Cemex® cement plant at Davenport, California.

Filler Contents

Filler contents were based on the findings of initial consumption of stabilizer tests *(70)*. In this test, the lowest percentage stabilizer at which the soil paste remains constant is the saturation stabilizer content for this particular material. (The saturation pH of lime at 25°C [77°F] is usually 12.4. Portland cement and lime contents are typically set at the saturation pH level plus at least 1.0 percent on stabilization projects,

depending on the required strength.) The saturation pH levels for the four fillers assessed in the UCPRC study are plotted in Figure 9.1. It was not clear from the limited testing whether saturation pH level is an appropriate indicator for determining fly ash content, as changes continued above 5.0 percent. Active filler contents above 3.0 percent are unlikely to be considered in FDR projects in California because of the likelihood of shrinkage cracking, and were therefore not assessed in the UCPRC study.

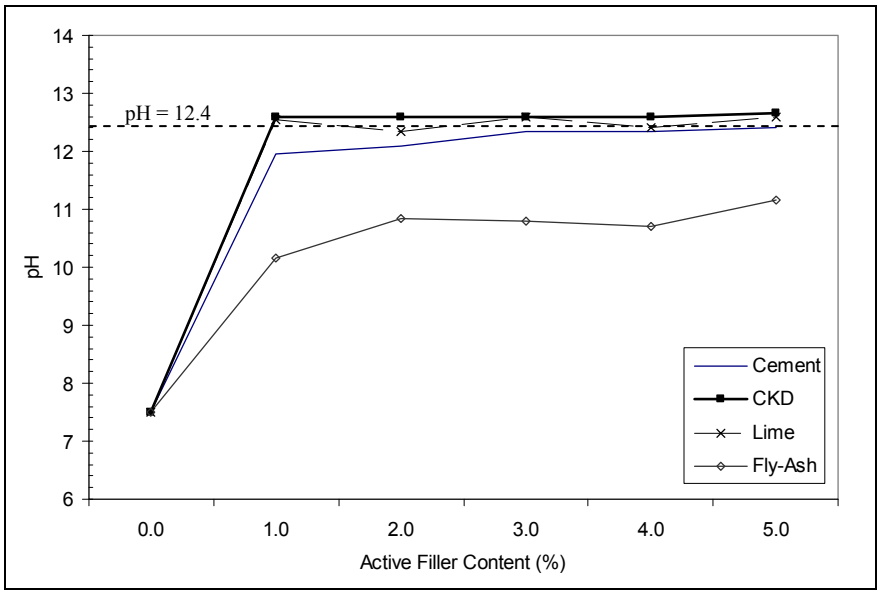

Figure 9.1: Saturation pH levels for various active fillers.

Maximum Dry Density, Optimum Moisture Content, and Mixing Moisture Content Determination

The experimental design for this phase required a large number (>25) of mix types. Performing a precise mix design procedure for each to determine the optimum mixing/compaction moisture content was considered impractical. A semi-empirical process using data collected throughout the study was therefore adopted. The measured moisture contents and variation for all subtasks are reported in the respective sections.

9.3.3 Testing Parameters

Specimen Curing and Soaking

In conjunction with the standard curing procedure adopted in earlier phases, a new curing procedure was adopted in this phase to simulate the conditions during the early life (a few hours to a few days) of a recently recycled pavement. This entailed sealing the specimen in a plastic bag immediately after compaction, curing at 20°C (68°F) for 24 hours, removal of the specimen from the bag, followed by immediate testing without further soaking or drying. The moisture content at the time of testing was usually slightly lower than the compaction moisture content as some moisture was lost through

evaporation and condensation on the inside of the bag. Moisture contents at the actual time of testing were not controlled or measured.

In some subtasks, the curing duration for the long cure (40°C [104°F], unsealed) of ITS specimens was reduced to 72 hours, and soaking duration to 24 hours for productivity considerations, as well as for comparisons with other research reported in the literature where this curing procedure was followed (longer curing and soaking durations were used in some of the previous phases to compensate for the effects of different specimen sizes on water infiltration rates).

9.4 Assessment of Cement Content and Fines Content

9.4.1 Introduction and Revised Experimental Design

This task investigated the effects of different cement contents and different RAP gradations (characterized by the fines content) on the behavior of foamed asphalt mixes. One asphalt binder content (3.0 percent) was used for all tests. The task was included to better understand the role of active fillers at fixed asphalt contents. Variables in this task included aggregate gradation and portland cement content. The revised test matrix for this task is summarized in Table 9.2. Aggregate gradation was based on the SR88-B gradation used in previous phases, with fines content adjusted with baghouse dust. It should be noted that the active filler content was not included in the aggregate gradation determination (i.e., a mix with an aggregate gradation of 20 percent passing the 0.075 mm [#200] sieve and 4 percent cement would actually have a combined fines content of 24 percent prior to the injection of the foamed asphalt.)

Table 9.2: Revised Factorial Design for Cement and Fines Content Assessment

Variable	No. of Values	Values
Aggregate gradation (% passing 0.075 mm sieve)	4	- 6.5, 10, 16, and 20 (see Figure 8.1)
Active filler content (%)[1]	5	- 0, 1, 2, 3, and 4
Mixing moisture content	Various	- See Table 9.3
Water conditioning method	2	- 24 hours soaking (referred to as "soaked") - No conditioning (referred to as "unsoaked")
Replicates	3/5	- 3 replicates for unsoaked test, 5 replicates for soaked tests
Fixed Values		
Asphalt binder content (%)[1]	1	- 3
Active filler type	1	- Portland cement
Curing method	1	- 40°C oven curing, unsealed, for 7 days
[1] % of mass of dry aggregate		

The mixing moisture content measurements for this task are summarized in Table 9.3.

Table 9.3: Mixing Moisture Content Measurements for Phase 4, Task 1

Fines Content (%)	Measured Moisture Content (%)	
	Mean	Std. Deviation
6.5	4.55	0.39
10.0	4.82	0.48
16.0	5.25	0.49
20.0	5.63	0.85

9.4.2 Results

The test results for this task are summarized in Table 9.4 and Figure 9.2 through Figure 9.4. The results of unsoaked testing are provided in the table, however, only soaked test results are provided in the figures and in the discussion below, given that these results are more relevant to in-service performance. The following observations were made based on the results:

- The addition of cement significantly increased the strengths measured when compared to the untreated control specimens.
- Strengths increased with increasing cement contents up to three percent cement. Cement contents above 3.0 percent did not appear to further increase the strength of the materials tested. Optimum cement contents are likely to be influenced by the physical and chemical properties of the soil and will need to be determined during the mix design.
- The effects of increasing fines content on mixes containing cement differed from the results of tests assessing the effects of increasing fines content on the behavior of foamed asphalt with no active fillers, carried out in Phase 3 (Section 8.4). When cement was added, the influence of increasing fines content had less effect compared to the tests with no active filler, with strengths generally insensitive to or positively affected by the fines content. The addition of cement therefore appears to be more effective in strengthening the mineral filler phase than foamed asphalt alone.
- The addition of cement to the mix also increased the fracture energy index of the ITS tests, but to a smaller extent than the increase in strength improvement.
- The effect of the fines content on the fracture energy index were somewhat inconsistent, but followed a general trend of higher fracture energy indexes at lower fines contents.
- The addition of cement reduced the ductility index of the mixes, as expected. Mixes with higher fines contents had lower ductility.

Table 9.4: Results Summary for Assessment of Cement and Fines Contents

Cement Content (%)	Indirect Tensile Strength (kPa)				Fracture Energy Index (J)				Ductility Index (J)			
	Fines Content (%)											
	6	10	16	20	6	10	16	20	6	10	16	20
Unsoaked Test Results[1]												
0	512	576	598	576	14.2	11.9	11.2	11.0	2.73	2.06	1.85	1.92
1	642	682	746	686	12.5	13.5	11.6	8.6	1.97	1.96	1.52	1.24
2	744	785	907	1,070	16.9	12.6	12.4	11.9	2.26	1.75	1.37	1.09
3	890	1,079	1,263	1,207	13.4	15.3	17.1	13.6	1.49	1.41	1.33	1.11
4	962	933	1,315	1,157	14.6	13.3	15.1	11.5	1.50	1.38	1.17	1.01
Soaked Test Results[1]												
0	251	177	160	111	6.4	4.6	3.5	2.5	2.54	2.58	2.19	2.25
1	434	445	505	501	8.9	8.6	8.0	6.5	2.07	1.92	1.56	1.27
2	588	719	679	696	10.7	12.0	10.2	9.3	1.80	1.67	1.49	1.32
3	825	909	1,111	927	12.7	14.4	13.5	10.8	1.57	1.52	1.19	1.15
4	676	814	918	1,060	12.8	11.8	9.8	10.7	1.89	1.43	1.06	1.11

[1] Average of replicate specimens

Note: The average coefficient of variation for soaked ITS test results was 9 percent.

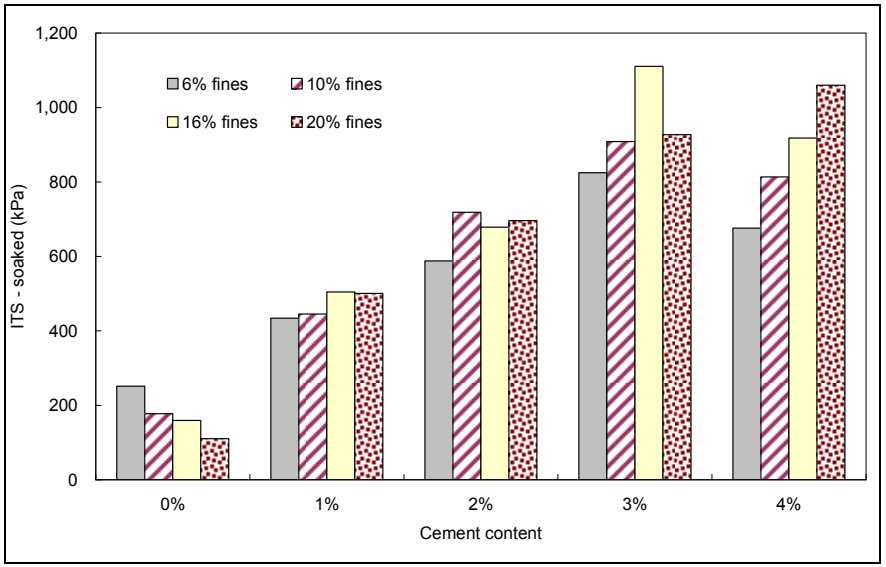

Figure 9.2: Effect of cement and fines contents on ITS values.

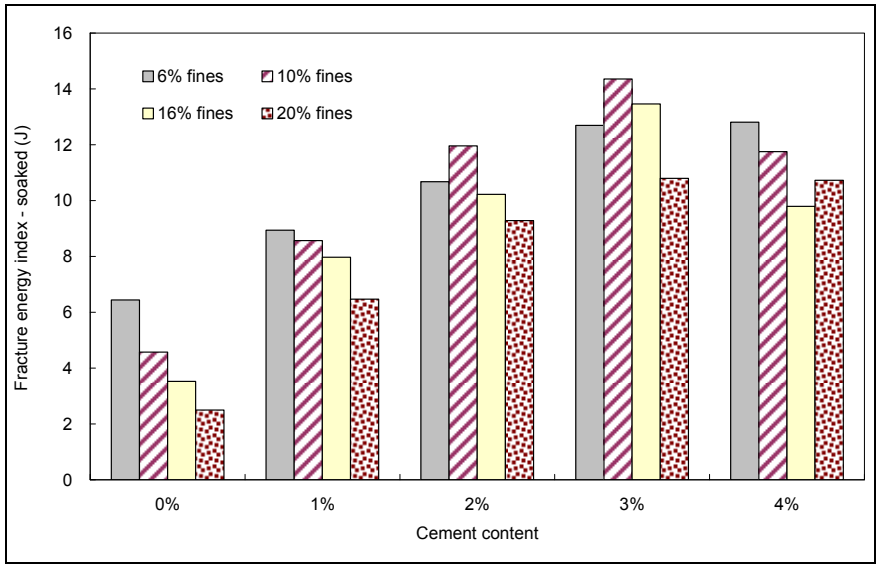

Figure 9.3: Effect of cement and fines contents on fracture energy index.

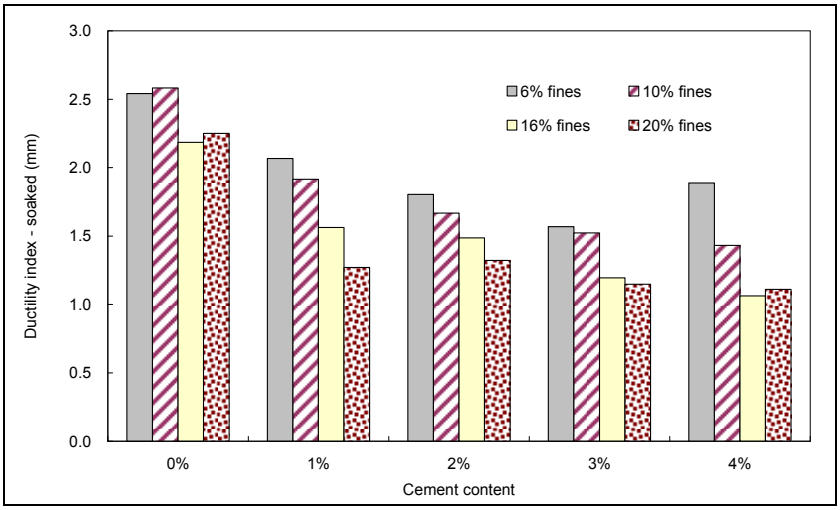

Figure 9.4: Effect of cement and fines contents on ductility index.

- The waterproofing effects of increasing cement contents were clearly apparent on the fracture faces of the specimens after ITS testing. Figure 9. shows the specimen fracture faces from three tests with cement contents of 1.0, 2.0, and 3.0 percent respectively (foamed asphalt content fixed at 3.0 percent and percent passing 0.075 mm [#200] fixed at 10 percent). No dry areas were observed on the specimens with one percent cement, however, a dry "core" can be seen in the middle of the fracture faces of the specimens with two and three percent cement, with the size of the dry core increasing with increasing cement content. Soaking time and conditions for all specimens were the same.

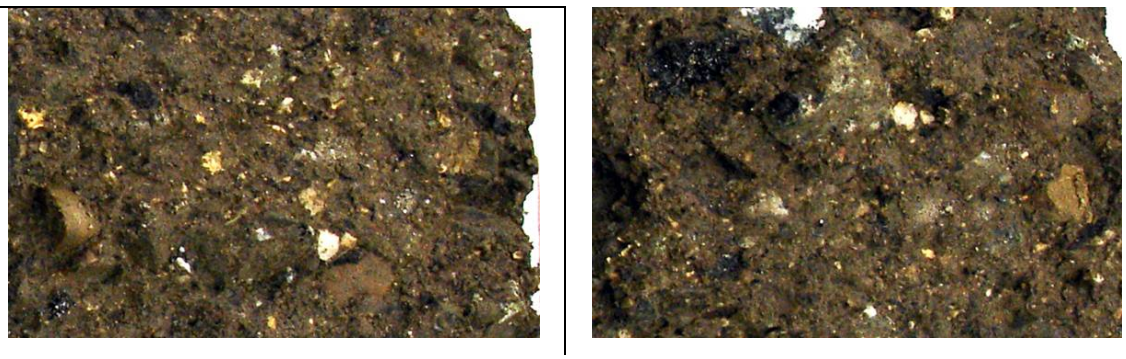

(a) Mix with 3% foamed asphalt and 1% cement

Figure 9.5: Fracture faces of soaked ITS specimens at various cement contents.

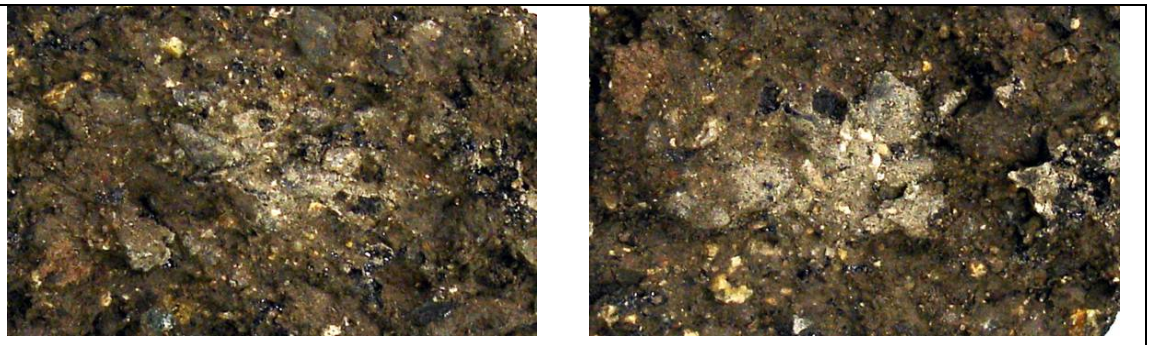

(b) Mix with 3% foamed asphalt and 2% cement

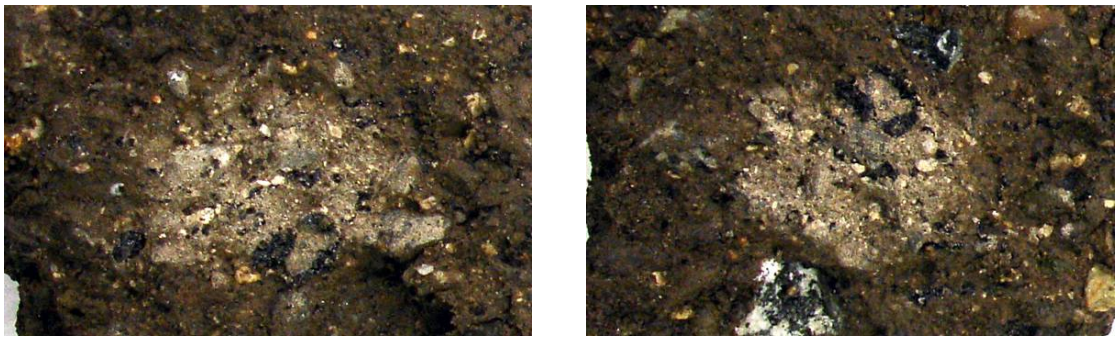

(c) Mix with 3% foamed asphalt and 3% cement

Figure 9.5: Fracture faces of soaked ITS specimens at various cement contents (*continued*).

9.4.3 Summary of Recommendations for Cement and Fines Contents

No recommendations are made based on the findings of this task.

9.5 Assessment of Asphalt Content and Fines Content

9.5.1 Introduction and Revised Experimental Design

This task investigated the effects of different asphalt binder contents and different RAP gradations (characterized by the fines content) on the behavior of foamed asphalt mixes. One portland cement content (two percent) was used for all tests. The task was included to better understand the role of active fillers with varying asphalt contents. Variables in this task included aggregate gradation and asphalt binder content. The revised test matrix for this task is summarized in Table 9.5. The aggregate gradation was based on the SR88-B gradation used in previous phases, with fines content adjusted with baghouse dust.

Table 9.5: Revised Factorial Design for Asphalt and Fines Content Assessment

Variable	No. of Values	Values
Aggregate gradation (% passing 0.075 mm sieve)	4	- 6.5, 10, 16, and 20
Asphalt binder content (%)	4	- 0, 2, 3, and 4 (0% binder for 10% fines content only)
Mixing moisture content	Various	- See Table 9.6
Water conditioning method	2	- 24 hours soaking (referred to as "soaked") - No conditioning (referred to as "unsoaked")
Replicates	3/5	- 3 replicates for unsoaked tests, 5 for soaked tests
Fixed Values		
Active filler type	1	- Portland cement
Active filler content (%)	1	- 2
Curing method	1	- 40°C oven curing, unsealed, for 7 days

The mixing moisture content measurements for this task are summarized in Table 9.6.

Table 9.6: Mixing Moisture Content Measurements for Phase 4, Task 2

Fines Content (%)	Measured Moisture Content (%)	
	Mean	Std. Deviation
6.5	4.55	0.37
10.0	4.42	0.09
16.0	4.93	0.04
20.0	5.38	0.21

9.5.2 Results

The test results for this task are summarized in Table 9.7 and Figure 9.6 through Figure 9.8. Although the results of unsoaked testing are provided in the table, only soaked test results are provided in the figures and referred to in the discussion below. The following observations were made based on the results:

- There was no significant difference in the indirect tensile strengths measured between the different asphalt binder contents, and strengths appeared to be insensitive to the fines content, similar to the findings in the previous task. This indicates that the influence of the foamed asphalt on the indirect tensile strength, observed in tests during Phase 3 when no active fillers were added (Section 8.4), is masked by the presence of portland cement.
- Although no differences were observed in the strength test results, the effects of the foamed asphalt were apparent in the fracture energy and ductility indices. Mixes with higher foamed asphalt contents appeared to be more ductile than the mixes with lower asphalt contents. The indices dropped with increasing fines contents, but not to the same extent as that observed in Phase 3.

Table 9.7: Results Summary for Assessment of Asphalt and Fines Contents

Asphalt Content (%)	Indirect Tensile Strength (kPa)				Fracture Energy Index (J)				Ductility Index (J)			
	Fines Content (%)											
	6	10	16	20	6	10	16	20	6	10	16	20
Unsoaked Test Results[1]												
0	–	776	–	–	–	8.5	–	–	–	1.08	–	–
2	672	806	893	987	11.0	9.0	8.4	10.4	1.69	1.14	0.94	1.05
3	744	785	907	1,070	16.9	12.6	12.4	11.9	2.26	1.75	1.37	1.09
4	825	833	846	1,019	17.2	15.2	14.0	14.2	2.07	1.82	1.64	1.44
Soaked Test Results[1]												
0	–	645	–	–	–	6.6	–	–	–	1.01	–	–
2	523	708	635	656	8.8	11.3	7.2	6.7	1.67	1.57	1.12	1.00
3	588	719	679	696	10.7	12.0	10.2	9.3	1.80	1.67	1.49	1.32
4	649	645	690	723	18.2	14.2	10.7	9.8	2.80	2.18	1.57	1.34

[1] Average of replicate specimens
Note: The average coefficient of variation for soaked ITS test results was 9 percent.

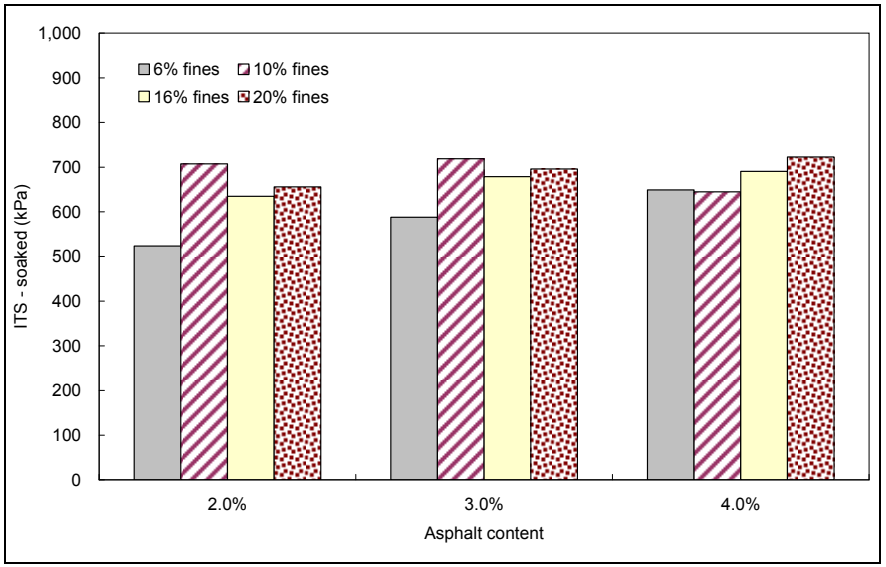

Figure 9.6: Effect of asphalt and fines contents on ITS values.

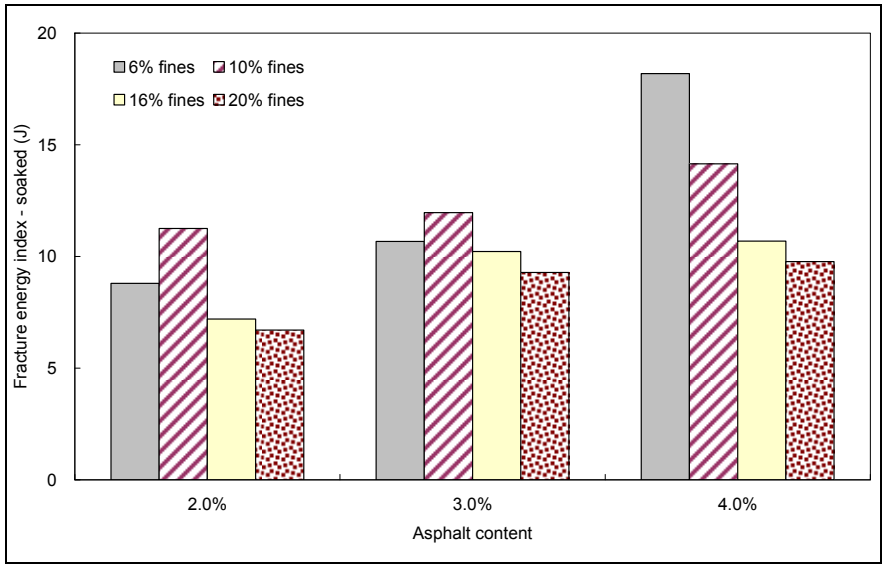

Figure 9.7: Effect of asphalt and fines contents on fracture energy index.

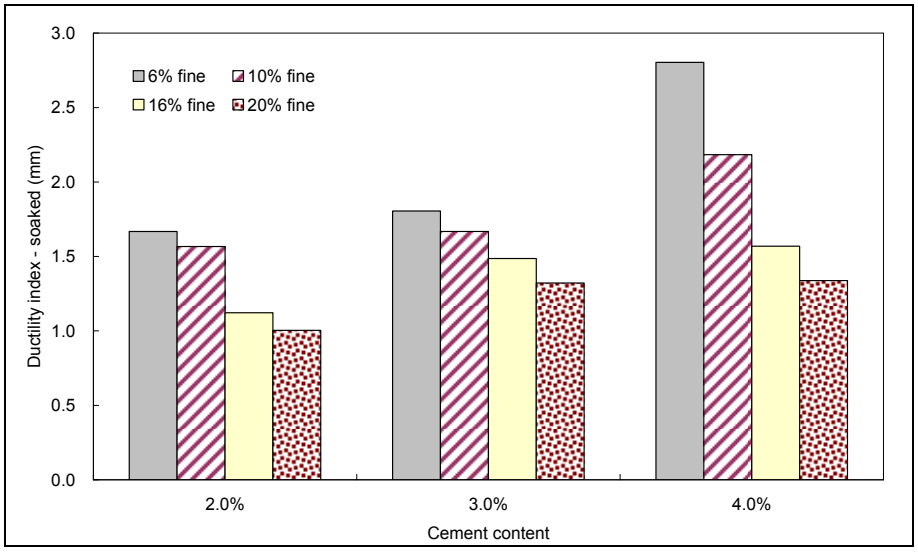

Figure 9.8: Effect of asphalt and fines contents on ductility index.

- The moisture resistance of the mixes improved with the addition of cement, as expected. This was attributed to improved binding of the fines by the cement in the mineral filler of the mix, thereby reducing the effects of weaker fracture paths through this material. This supports the use of cement for strengthening the mineral filler phase in foamed asphalt reclamation projects.

9.5.3 Summary of Recommendations for Asphalt Binder and Fines Contents

No recommendations are made based on the findings of this task.

9.6 Assessment of Filler Type and Content

9.6.1 Introduction and Revised Experimental Design

This task investigated the effects of different active and semi-active fillers at different application rates on the behavior of foamed asphalt mixes under different curing conditions and at different curing stages. To date, a variety of fillers have been used on foamed asphalt projects in California, including portland cement, fly-ash, and kiln dust, while the use of lime has been reported in other countries. One gradation (characterized by the fines content) and two foamed asphalt contents (zero and 3.0 percent) were tested. Two curing methods were included in the experimental design; one a shortened version of the method used throughout the study (72-hour unsealed cure at a moderately elevated temperature) and the other to assess early strength gain and the potential impacts of early opening to traffic (24-hour sealed cure at ambient temperature). The revised test matrix for this task is summarized in Table 9.8. The aggregate gradation was based on the SR88-B gradation used in previous phases, with fines content adjusted with baghouse dust.

Table 9.8: Revised Factorial Design for Filler Type Assessment

Asphalt binder content (%)	2	- 0 (control) and 3
Active filler type	4	- Portland cement, hydrated lime, fly-ash, kiln dust
Active filler content (%)	4	- 0, 1, 2, and 3
Mixing moisture content	Various	- See Table 9.9
Curing method	2	- 20°C room temperature, sealed, for 24 hours - 40°C oven curing, unsealed, for 3 days
Water conditioning method	3	- 24 hours soaking (soaked) for 40°C cured specimens - No conditioning (unsoaked) for 40°C cured specimens - Tested as is without further soaking or drying for 20°C cured specimens (as is)
Replicates	2/4/3	- 2 replicates for unsoaked test - 4 replicates for soaked tests - 3 replicates for 20°C cure
Aggregate gradation (% passing 0.075 mm sieve)	1	- 10

The mixing moisture content measurements for this task are summarized in Table 9.9.

Table 9.9: Mixing Moisture Content Measurements for Phase 4, Task 3

1	5.70	5.70
2	5.64	5.64
3	5.87	5.87

9.6.2 Results

The test results for this task are summarized in Table 9.10 and Figure 9.9 through Figure 9.12. Although the results of unsoaked testing are provided in the table, only soaked test results are provided in the figures and referred to in the discussion below. It should be noted that the strengths obtained from the various fillers are usually related to the chemistry of the aggregates and the fines, and the reaction between these and the filler. The results obtained are thus not necessarily indicative of all RAP mixes.

The following observations were made based on the results of specimens cured for 72 hours, unsealed:

- Portland cement had the most significant effect on the soaked indirect tensile strength of the four active fillers tested, followed by cement kiln dust, lime, and fly-ash. Strengths increased with increasing portland cement content, but were not influenced by the presence of foamed asphalt.
- The addition of cement kiln dust increased the soaked strengths of the specimens considerably, with strengths increasing with increasing application rate, specifically above 2.0 percent. Specimens treated with both cement kiln dust and foamed asphalt had higher strengths than specimens treated with cement kiln dust alone.

Table 9.10: Results Summary for Assessment of Filler Type and Content

Cement	24-hour, S	As is	57	279	438	506	62	256	398	433
	72-hour, US	Soaked	34	379	594	725	211	418	721	748
	72-hour, US	Unsoaked	319	384	705	853	535	602	838	819
Lime	24-hour, S	As is	57	71	76	84	62	92	111	128
	72-hour, US	Soaked	34	106	186	182	211	272	413	393
	72-hour, US	Unsoaked	319	175	199	301	535	413	519	596
Cement Kiln Dust	24-hour, S	As is	57	76	103	133	62	101	113	111
	72-hour, US	Soaked	34	138	400	412	211	286	526	611
	72-hour, US	Unsoaked	319	226	556	860	535	401	766	947
Fly ash	24-hour, S	As is	57	90	62	68	62	97	96	112
	72-hour, US	Soaked	34	89	94	91	211	190	221	275
	72-hour, US	Unsoaked	319	357	249	226	535	506	480	497
Cement	24-hour, S	As is	0.6	3.4	5.1	5.7	1.4	3.7	6.8	7.3
	72-hour, US	Soaked	0.3	4.3	5.4	6.0	4.3	6.9	9.4	13.1
	72-hour, US	Unsoaked	3.2	5.6	8.6	7.4	12.0	12.0	10.0	11.4
Lime	24-hour, S	As is	0.6	1.0	1.2	1.4	1.4	1.6	1.9	2.3
	72-hour, US	Soaked	0.3	1.3	2.3	2.1	4.3	5.8	8.7	7.2
	72-hour, US	Unsoaked	3.2	2.0	2.6	3.2	12.0	8.1	10.1	9.4
Cement Kiln Dust	24-hour, S	As is	0.6	1.1	1.3	1.6	1.4	1.5	2.1	2.0
	72-hour, US	Soaked	0.3	1.7	4.5	3.5	4.3	5.7	8.4	11.5
	72-hour, US	Unsoaked	3.2	2.8	5.6	7.5	12.0	8.3	13.2	14.8
Fly ash	24-hour, S	As is	0.6	1.2	0.9	1.0	1.4	1.7	1.4	1.8
	72-hour, US	Soaked	0.3	1.0	1.1	1.1	4.3	3.1	4.8	5.0
	72-hour, US	Unsoaked	3.2	3.9	2.5	2.2	12.0	10.7	9.7	10.6
			Ductility Index (J)							
Cement	24-hour, S	As is	1.37	1.21	1.15	1.11	2.20	1.44	1.67	1.67
	72-hour, US	Soaked	1.21	1.10	0.90	0.82	2.00	1.63	1.29	1.74
	72-hour, US	Unsoaked	1.07	1.43	1.23	0.86	2.20	1.97	1.18	1.37
Lime	24-hour, S	As is	1.37	1.45	1.58	1.59	2.20	1.67	1.70	1.73
	72-hour, US	Soaked	1.21	1.16	1.22	1.17	2.00	2.09	2.07	1.81
	72-hour, US	Unsoaked	1.07	1.10	1.28	1.06	2.20	1.95	1.91	1.54
Cement Kiln Dust	24-hour, S	As is	1.37	1.44	1.28	1.20	2.20	1.49	1.82	1.75
	72-hour, US	Soaked	1.21	1.25	1.11	0.85	2.00	1.95	1.57	1.90
	72-hour, US	Unsoaked	1.07	1.23	1.00	0.87	2.20	2.07	1.67	1.53
Fly ash	24-hour, S	As is	1.37	1.29	1.39	1.48	2.20	1.68	1.50	1.62
	72-hour, US	Soaked	1.21	1.13	1.18	1.20	2.00	1.63	2.16	1.78
	72-hour, US	Unsoaked	1.07	1.06	1.00	0.98	2.20	2.10	1.98	2.09

[1] S: sealed during curing; US: unsealed during curing.
[2] As is—tested immediately after removal from bag with no further conditioning.

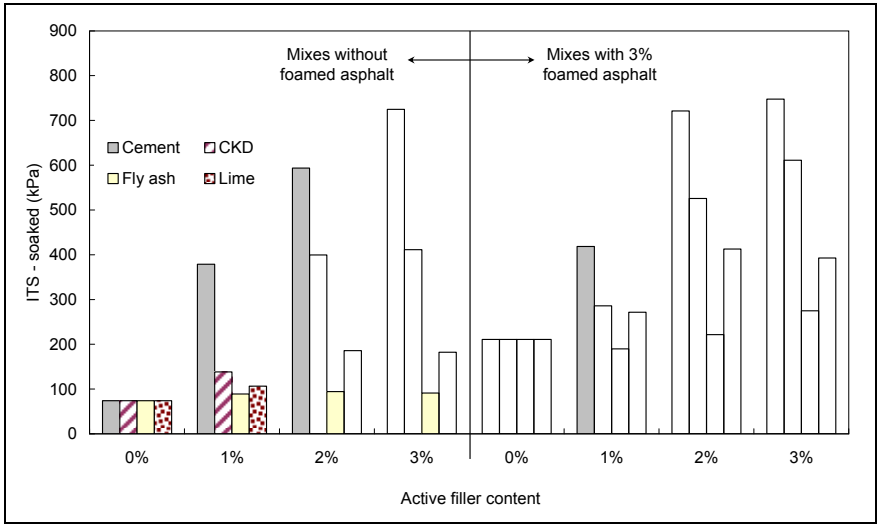

Figure 9.9: Effect of filler type and content on soaked ITS results.
(40°C, 72-hr, unsealed)

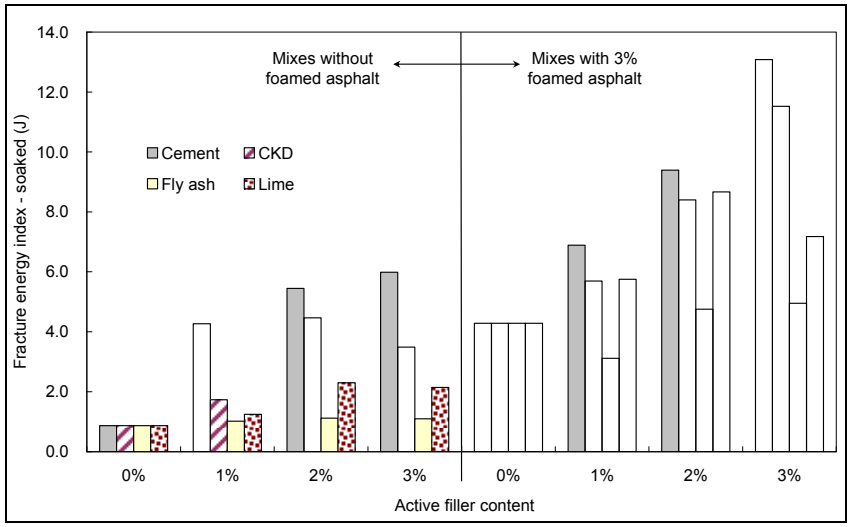

Figure 9.10: Effect of filler type and content on fracture energy index.
(40°C, 72-hr, unsealed)

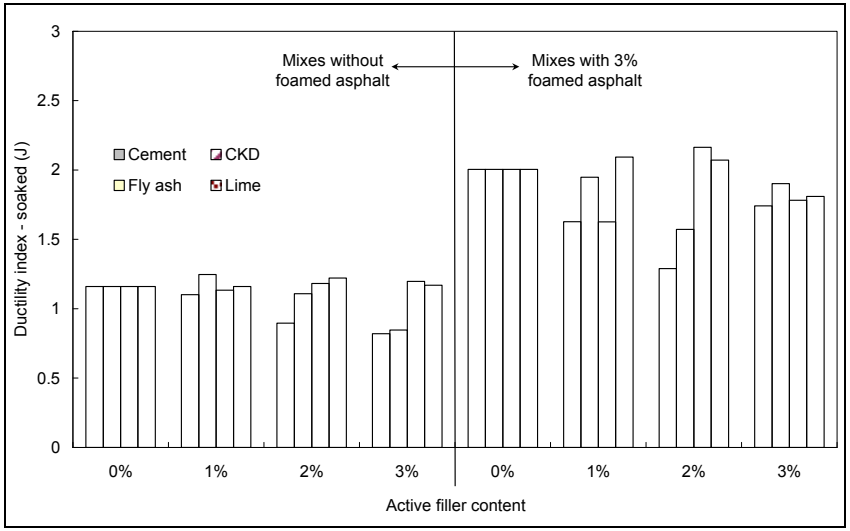

Figure 9.11: Effect of filler type and content on ductility index.
(40°C, 72-hr, unsealed)

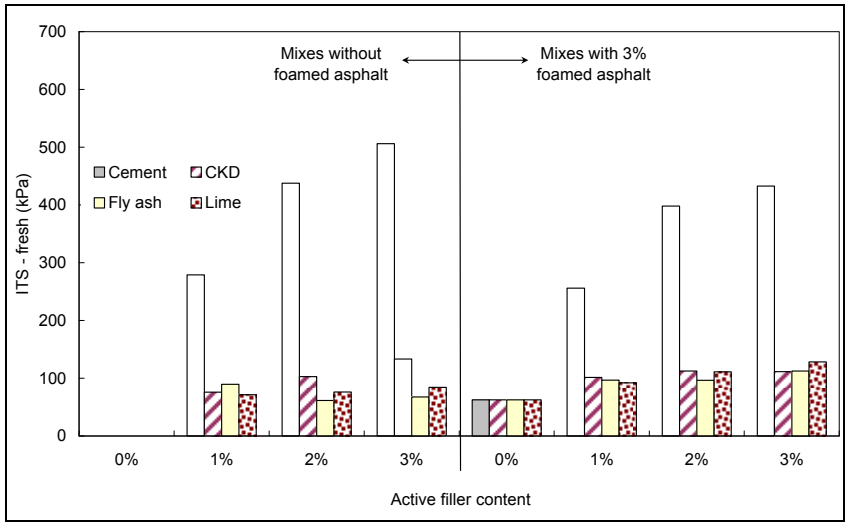

Figure 9.12: Effect of filler type and content on soaked ITS results.
(20°C, 24-hr, sealed)

- The addition of hydrated lime provided only a marginal increase in strength to the specimens with no foamed asphalt, with strengths increasing slightly with increasing application rate. When combined with foamed asphalt, higher strengths were recorded.
- The fly-ash had little influence on the strength, with only slight increases recorded at an application rate of 3.0 percent. Slightly higher strengths were recorded when the fly-ash (3.0 percent) and foamed asphalt were combined. Although these results could be attributed to fly-ash source, content, and/or curing times, further studies were not considered to be justified, given that early strength gain is a primary requirement.
- Fracture energy indices for each of the fillers showed similar trends to those observed from the ITS test results. The only significant exception was the mixes treated with portland cement, where the addition of foamed asphalt showed no significant benefits in strength gain but showed significant improvement in fracture energy, indicating that portland cement and foamed asphalt in combination provide a less brittle but equally strong layer than if portland cement is used alone.
- The ductility indices of the cement and cement kiln dust specimens without foamed asphalt were lower than the untreated control specimens at application rates of 2.0 percent and higher, but were not affected by the addition of lime and fly-ash. When combined with foamed asphalt, the ductility indices of the specimens with filler treatments were generally lower than the control specimens, with cement and cement kiln dust showing the greatest change.

The following observations were made based on the results of specimens cured in sealed plastic bags for 24 hours at 20°C±1°C (68°F ±1.8°F) and then tested at the cured moisture content (i.e., without soaking or further drying):

- The addition of portland cement significantly increased the strength of the specimens after the limited period of curing, with strengths increasing with increasing cement content. When combined with foamed asphalt, the strength increases, although still significant, were lower compared to the specimens treated only with cement.
- The other three fillers tested showed very little strength gain in the short curing period compared to the untreated controls.

9.6.3 Interaction Between Active Fillers and Foamed Asphalt

Based on the results and observations during specimen preparation and testing, the potential interactions between foamed asphalt and active fillers were evaluated quantitatively to provide additional insights into the selection of appropriate active fillers for reclamation projects with foamed asphalt.

If a certain type of active filler (F) does not interact with foamed asphalt, then the strength of a mix containing X percent of such filler and Y percent of foamed asphalt can be approximately predicted by Equation 9.1.

$$ITS_{XFYA\text{-}pred} = ITS_{XF0A} + ITS_{0FYA} - ITS_{0F0A} \quad (9.1)$$

where: $ITS_{XFYA\text{-}pred}$ = predicted (indirect tensile) strength of mix containing X% of active filler and Y% of foamed asphalt (in this section, Y=3);

ITS_{XF0A} = measured strength of the mix containing X% of active filler and no foamed asphalt;

ITS_{0FYA} = measured strength of the mix containing no active filler and Y% foamed asphalt;

ITS_{0F0A} = measured strength of the control mix without active filler or foamed asphalt.

If the measured strength ITS_{XFYA} is higher than the corresponding predicted value $ITS_{XFYA\text{-}pred}$, then a positive interaction between this active filler and the foamed asphalt will be apparent, which implies that improved strengths will result from a combination of the filler and the foamed asphalt compared to the strengths obtained if only one of the two additives is used. A comparison of measured ITS test results and values based on Equation 9.1 is shown in Figure 9.13. The following interactions can be observed from the figure:

- A positive interaction between lime and asphalt
- A negative interaction between portland cement and asphalt
- No notable interaction between cement kiln dust or fly ash and asphalt.

A similar analysis was carried out with the fracture energy index results, as shown in Figure 9.14. All of the active filler types showed more or less positive interaction with foamed asphalt, with the exception of fly-ash. The interactions were stronger with increasing applications rates of the active filler.

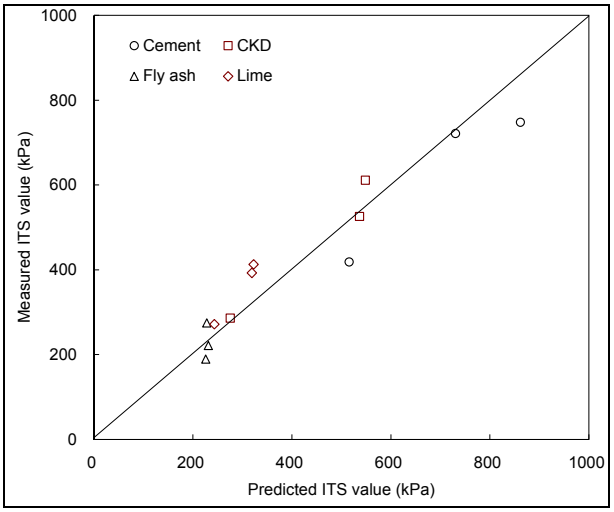

Figure 9.13: Comparison of predicted and measured ITS results.

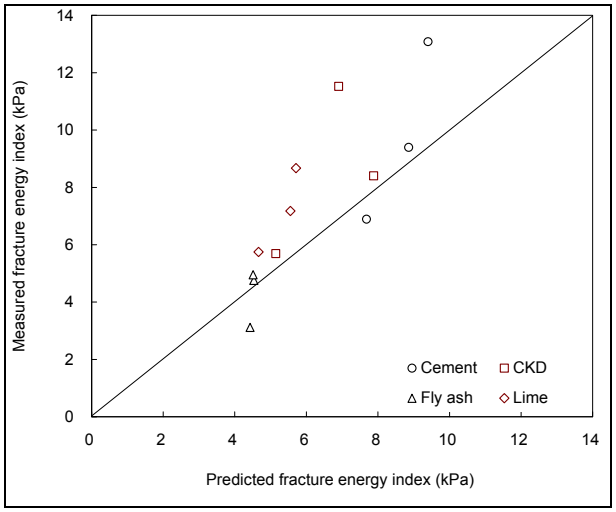

Figure 9.14: Comparison of predicted and measured fracture energy index results.

9.6.4 Summary of Recommendations for Filler Type and Content

The following interim recommendations regarding filler type and content are made:

- Active fillers should be considered in all foamed asphalt FDR projects, as they complement the foamed asphalt by improving early strengths and reducing the moisture sensitivity of the mineral filler phase. The foamed asphalt improves the ductility of materials treated with cementitious fillers.
- Portland cement appears to offer the most advantages compared to the other active fillers tested. However, insufficient testing was carried out on a range of materials to exclude other fillers, and these should be considered in the mix design until sufficient information has been collected on local materials. Hydrated lime may perform better on materials of basic crystalline origin (e.g. basalt).
- Specimens cured for 24-hours (sealed at ambient temperature [20°C (68°F)]) should be included in the mix design testing along with the 3-day or 7-day unsealed cured (at 40°C [104°F]) specimens to select the most appropriate active filler, to determine the optimum active filler content, and to assess the effectiveness of the active filler in developing early strength in the material.

9.7 Assessment of Resilient Modulus with Portland Cement

9.7.1 Introduction and Revised Experimental Design

This task investigated the effects of portland cement and curing condition (1 day and 7 days, 20ºC and 40ºC, sealed and unsealed) on the resilient modulus of prepared specimens. Three cement contents (zero [control], 1.0, and 2.0 percent) were used for all tests. The revised test matrix for this task is summarized in Table 9.11. ITS tests were performed as a reference to compare results under these test conditions to those in earlier phases.

Table 9.11: Revised Factorial Design for Resilient Modulus Testing

Variable	No. of Values	Values
Asphalt binder content (%)	2	- 0 and 3
Active filler content (%)	3	- 0, 1, and 2 (1% used for mixes with 3% foamed asphalt)
Mixing moisture content	Various	- See Table 9.12
Curing method	2	- 20°C room temperature, sealed, for 24 hours (short cure) - 40°C oven curing, unsealed, for 7 days (long cure)
Test method	2	- ITS (100 mm), Marshall compaction, 75 blows on each face. Loading rate of 50 mm/minute - Triaxial resilient modulus, adjusted Modified Proctor compaction
Replicates	5	- 4 ITS specimens per mix per test condition - 1 Triaxial specimen per mix per test condition
Fixed values		
Aggregate gradation (% passing 0.075 mm sieve)	1	- 10
Active filler type	1	- Portland cement
Soaking condition	1	- ITS: 24 hours - Triaxial: various for each specimen, 1 day to 38 days - Short cure tested immediately after curing

9.7.2 Test Methods

The specimen fabrication and testing for both the ITS and triaxial resilient modulus tests complied with the procedures discussed in Phase 2 (Chapter 7). Multiple tests were carried out on cured specimens after the various soaking durations listed in Table 9.12. The testing procedures followed in this task were similar to those followed in Section 9.6, except that the curing duration was extended from three days to seven days to allow for more uniform moisture distribution in the relatively large triaxial specimens.

Table 9.12: Phase 4 Triaxial Specimen Mix Design and Test Condition

Specimen Label	Mix Design		Mixing Moisture (%)	Test Conditions (Multiple tests for selected specimens)
	Asphalt (%)	Cement (%)		
TriA	3	0	5.3	- 24-hour cure, sealed, unsoaked - 7-day cure, unsealed, and 6-day soak
TriB	3	0	6.0	- 7-day cure, unsealed, and 7 day soak
TriC	3	2	5.8	- 24-hour cure, sealed, unsoaked - 7-day cure, unsealed, and 1 day soak - 7-day cure, unsealed, and 7 day soak - 7-day cure, unsealed, and 38 day soak
TriD	3	2	5.8	- 7-day cure, unsealed, and 1 day soak - 7-day cure, unsealed, and 7 day soak - 7-day cure, unsealed, and 38 day soak
TriE TriF TriG TriH	0 0 3 0	2 2 1 0	5.1 5.5 4.3 7.1	- 24-hour cure, sealed, unsoaked - 7-day cure, unsealed, and 5 day soak - 24-hour cure, sealed, unsoaked - 24-hour cure, sealed, unsoaked
TriI	3	0	5.6	- Triaxial permanent deformation test

9.7.3 Results

The ITS test results for this task are summarized in Table 9.13.

Table 9.13: ITS Test Results for Preliminary Curing Experiment

Test Condition	Asphalt Content (% of dry aggregate mass)				
	0		3		
	Cement Content (%)				
	0	2	0	1	2
24-hour cure, sealed, unsoaked	58	426	66	213	335
7-day cure, unsealed, unsoaked	36	–	353	435	900

The behavior trends observed were similar to those discussed in Section 9.6 and include:

- Mixes containing 2.0 percent cement developed considerable strength in the first 24 hours during which time the specimens were sealed and little or no evaporation occurred.
- The strengths of the mixes containing only foamed asphalt (no cement) and cured for 24 hours were similar to the strengths of the untreated control mixes cured under the same sealed condition and for the same period of time. The tensile strength measured under these conditions was mostly attributed to matrix suction in the mineral filler phase.

- When comparing results in Table 9.10 to those in Table 9.13, the soaked ITS values (355 kPa [50 psi]) for the cured-soaked mixes containing 3.0 percent foamed asphalt and no cement was significantly higher than the corresponding value (211 kPa [31 psi]) in later testing. This was attributed in part to the three-day cure of the specimens in the earlier task (Section 9.6) compared with the seven-day cure of the specimens tested in this task, indicating better strength associated primarily with longer curing times. This aspect is discussed in more detail in Section 9.11. Other factors, such as uncontrolled environmental factors (ambient air temperature during mixing, compaction mix temperature, etc.) and inherent variation in the materials would also influence these results.

Selected Triaxial Resilient Modulus results for mixes tested under various conditions are plotted against the confining stress applied in Figure 9.15. Only the results for one pulse loading duration of 0.1 seconds with 0.4 seconds of relaxation are shown. Data point scattering at each confining stress for each mix is attributed to the different deviator stress levels applied. All test data were fitted to the model (Equation 7.1) discussed in Section 7.4, and model fitting results are summarized in Table 9.14. The mean R^2 value for model fitting was 0.98.

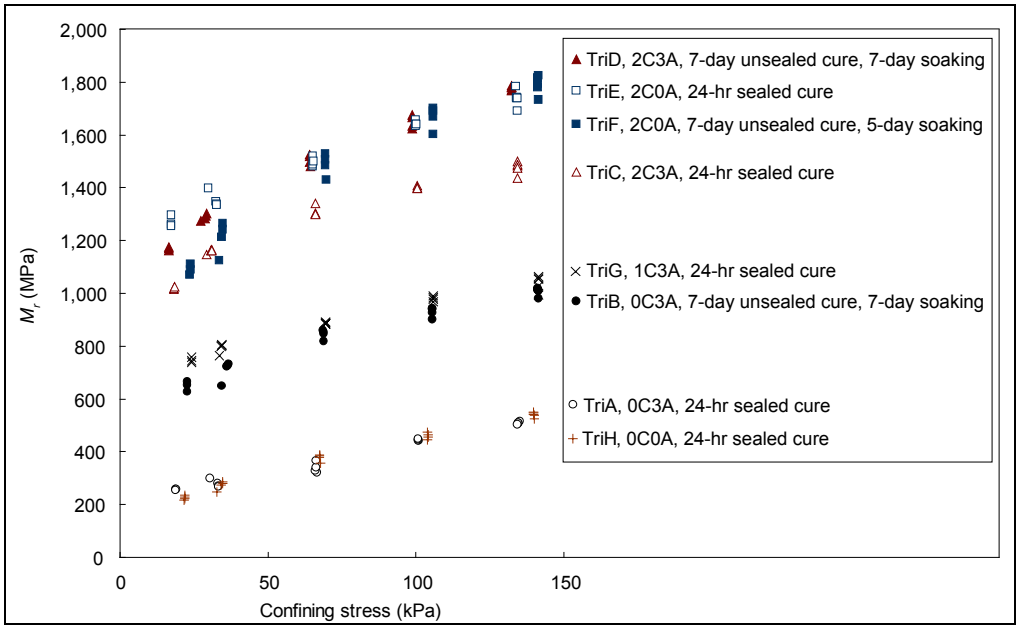

Figure 9.15: Triaxial Resilient Modulus test results under various conditions.
("XCYA" represents the mix design. For example, "2C3A" indicates that the mix contained 2% cement and 3% foamed asphalt.)

The results indicate that:

- Similar trends to those observed during ITS tests were recorded for the triaxial resilient modulus tests.

Table 9.14: Model Fitting Results for Triaxial Resilient Modulus Testing

Specimen	Mix Design	Pre-Test Conditioning[1]	MMC[2] (%)	Model Fitting Results[3]					
				k_1	k_T	k_2	k_3	M_{r1} (MPa)	M_{r2} (MPa)
TriA	0C3A	24-hour, no soak	5.3	1,599	-0.05	0.59	-0.23	244	499
		7-day/6-day soak	5.7	6,087	-0.08	0.28	-0.10	737	1,042
TriB	0C3A	7-day/7-day soak	5.3	5,503	-0.06	0.31	-0.10	667	996
TriC	2C3A	24-hour, no soak	5.8	8,630	-0.05	0.28	-0.10	1,052	1,496
		7-day/1-day soak	3.8	11,112	-0.05	0.24	-0.07	1,281	1,747
		7-day/7-day soak	4.4	11,634	-0.05	0.21	-0.08	1,349	1,747
		7-day/38-day soak	4.9	11,882	-0.05	0.22	-0.06	1,355	1,797
TriD	2C3A	7-day/1-day soak	3.8	8,832	-0.05	0.35	-0.11	1,095	1,720
		7-day/7-day soak	4.4	10,104	-0.05	0.30	-0.08	1,201	1,762
		7-day/38-day soak	4.9	9,651	-0.05	0.32	-0.08	1,151	1,737
TriE	2C0A	24-hour cure	5.1	10,257	-0.05	0.27	-0.12	1,267	1,742
TriF	2C0A	7-day/5-day soak	4.5	9,083	-0.04	0.36	-0.10	1,114	1,781
TriG	1C3A	24-hour, no soak	4.3	5,846	-0.06	0.29	-0.14	744	1,048
TriH	0C0A	24-hour, no soak	7.1	1,623	-0.01	0.63	-0.17	232	523

[1] 24-hour cure was sealed; 7-day cure was unsealed.
[2] Mixing moisture content
[3] M_{r1} and M_{r2} are resilient modulus values at two reference stress states as discussed in Section 7.4.5.

- The measured resilient modulus values of mix containing foamed asphalt and no cement (Specimen TriA) with a 24-hour (unsealed) cure were similar to those of the control mix (Specimen TriH).
- The resilient modulus increased substantially after a longer unsealed cure and 7-day soak (Specimen TriB), even though the moisture content as tested (5.3%) was similar to that measured after the short cure (Specimen TriA). These two specimens showed higher sensitivity to loading rates and lower sensitivity to stress states after curing and soaking.
- The ITS and triaxial resilient modulus test results indicated that the strength gains of the specimens with foamed asphalt and no cement only developed during the curing/drying process associated with water evaporation.
- Strength gain development in cement-treated materials showed significant development in the first 24 hours, and consequently mixes containing cement (Specimens TriC, TriE, and TriG) had much higher stiffnesses after any of the curing periods. Stiffnesses increased with increasing cement content as expected.
- Specimens TriA and TriC had similar resilient modulus values to those of Specimens TriB and TriD respectively after curing and soaking. This indicates that the loading history after the 24-hour sealed cure did not alter the post-cured material properties.
- Specimens TriC and TriD were also subjected to triaxial resilient modulus testing after various durations (1 day to 38 days) of soaking. No significant changes in material properties were observed during soaking, while moisture contents increased moderately. The effects of moisture damage and longer-term strength gain under these curing conditions were not apparent.

9.7.4 Summary of Recommendations for Resilient Modulus Testing

No additional recommendations are made based on the findings of this task.

9.8 Assessment of Long-Term Strength Development

9.8.1 Introduction and Revised Experimental Design

This task entailed a small-scale experiment to assess the development of strength of foamed asphalt mixes with portland cement during curing. It was included to investigate the potential longer-term strength development of foamed asphalt mixes, and to provide a reference for comparing ITS test results of specimens with different curing durations. Variables included cement content and curing duration. The revised test matrix for this task is summarized in Table 9.15 and the mixing moisture content measurements are summarized in Table 9.16.

Table 9.15: Revised Factorial Design for Strength Development Testing

Variable	No. of Values	Values
Active filler content (%)	5	- 0, 1, 2, 3, and 4
Mixing moisture content (%)	Various	- See Table 9.16
Curing method Curing period	1 5	- 40°C oven curing, unsealed - 1, 3, 15, 29, and 107 days
Replicates	2	- 2 ITS specimens per mix per curing duration
Fixed Values		
Aggregate gradation (% passing 0.075 mm sieve)	1	- 10
Asphalt binder content (%)	1	- 3
Active filler type	1	- Portland cement
Soaking condition	1	- 24 hours soaking
Test method	1	- ITS (100 mm), Marshall compaction, 75 blows on each face. Loading rate of 50 mm/minute.

Table 9.16: Mixing Moisture Content Measurements for Phase 4, Task 5

Cement Content (%)	Measured Moisture Content (%)	
	Mean	Std. Deviation
0	4.89	
1	4.78	
2	3.80	One sample per mix type.
3	4.11	
4	4.07	

9.8.2 Results

The ITS test results for the task are shown in Table 9.17 and Figure 9.16. The *strength ratio* is defined as the ratio between the strength of a mix after one day or three days of curing to the average strength measured after 15, 29, and 107 days of curing, and is an indicator of the maturity of strength development at early curing stages. Since only two replicate specimens per mix type per curing duration were available,

a high variation was expected. Strengths measured after 15 days of curing showed fairly significant variation instead of a steady trend. The average ITS values for three curing durations were used to represent the long-term or "ultimate" strengths when defining the strength ratio to obtain a more representative value. It should be noted that the conditions in a forced draft oven at 40°C (104°F) are more severe than typical field conditions in terms of the speed of moisture evaporation in foamed asphalt mixes. The South African guidelines *(3)* suggest that three days of curing under these conditions is equivalent to six months of curing in the field for average climate conditions in South Africa.

Table 9.17: ITS Results for Strength Development Testing

Cement Content (%)	Curing Duration (days)					Strength Ratio (%)	
	1	3	15	29	107	1 day	3 days
0	110	180	201	233	270	47	77
1	372	442	524	474	428	78	93
2	570	699	649	599	869	81	99
3	647	689	734	770	751	86	92
4	840	898	1,014	781	877	94	101

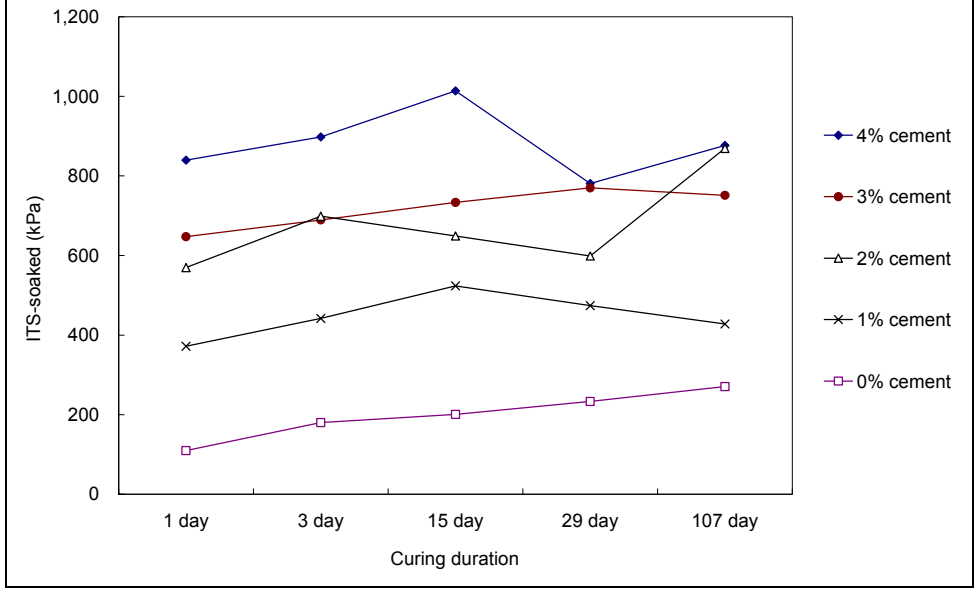

Note

Inconsistent results for the 1% (29 & 107 day), 2% (3 day)and 4% (29 & 107 day) are attributed to the poor repeatability of the ITS test under this type of testing program (i.e. multiple specimens produced and then tested at intervals.

Figure 9.16: ITS results for strength development testing in 40°C forced draft oven.

The results indicate that:

- The foamed asphalt mix without portland cement developed approximately half of its ultimate strength in the first 24 hours.
- The rate of strength gain in the first 24 hours for mixes containing cement was faster, and the higher the cement content, the faster the strength gain.
- After three days, all mixes except for that with no cement had developed more than 90 percent of the ultimate strength measured during the experiment. Although a definitive relation between field

and laboratory curing conditions cannot be established at this stage, these results provide useful additional information for interpreting test results from previous phases, such as comparing ITS test results for 3-day and 7-day cured specimens.

9.8.3 Summary of Recommendations for Strength Development

No additional recommendations are made based on the finding of this task. However, the findings further reinforce that cementitious active fillers should be considered in all FDR-foamed asphalt projects to provide early strength for early trafficking of the rehabilitated road. They also support earlier findings that the foamed asphalt does not contribute to stiffness and strength until the compaction moisture has evaporated from the mix, implying that poor strength and stiffness can be expected if the recycled layer does not dry back before surfacing.

9.9 Assessment of Potential Shrinkage During Curing

Shrinkage is a potential concern when certain active fillers (e.g., cementitious materials) are added to foamed asphalt mixes. Long and Ventura *(17)* concluded that up to 2.0 percent cement would not cause significant shrinkage and that any shrinkage measured would mainly be due to moisture loss.

Potential free shrinkage during the curing process was measured on ten selected cylindrical triaxial specimens (150 mm [6 in.] in diameter and 305 mm [12 in.] in height) in this task of the UCPRC study. The height of each specimen was measured immediately after compaction and again after curing (unsealed at 40°C [104°F] for seven days), and the ratio of the height change after curing to the height of the specimen immediately after compaction was calculated as the *shrinkage value.* The apparatus, shown in Figure 9.17, is able to measure the height change of a triaxial specimen to a precision of 0.001 mm (0.039 mils). However, the surfaces of the selected triaxial specimens were not absolutely flat and smooth, and some variability in measurements was expected. Ten replicate measurements were therefore taken and a mean value calculated to limit this variability. Measurement results are summarized in Table 9.18.

The results indicate that variation of the shrinkage values was large compared to the absolute values, and therefore no clear trend was identified in terms of the effects of RAP gradation (fines content), asphalt content, and cement content on shrinkage. Two specimens showed negative shrinkage values, which was attributed to measurement variation. The highest shrinkage value measured was 413 microstrain, which is considerably lower than the strain-at-break values measured for foamed asphalt mixes containing no active filler (Table 7.11). These observations confirm that shrinkage cracking is not a major concern in foamed asphalt mixes using the materials tested in this study and containing up to 2.0 percent cement.

Shrinkage tests should be carried out in project mix designs if high portland cement contents (e.g. between 1.5 and 2.0 percent) are considered until more experience is gained.

Figure 9.17: Apparatus for measuring shrinkage of cured specimens.

Table 9.18: Shrinkage Measurements for Selected Triaxial Specimens

Specimen	Fines Content (%)	Asphalt Content (%)	Cement Content (%)	Shrinkage[1] (μ)
1	10.0	0	1	+216
2	10.0	0	2	-47
3	10.0	3	0	-51
4	10.0	3	1	+20
5	10.0	3	1	+276
6	10.0	3	1	+22
7	6.5	3	1	+47
8	16.0	3	1	+413
9	10.0	3	2	+356
10	16.0	3	2	+159

[1] Positive values indicate shrinkage and negative values indicate elongation.

9.9.1 Summary of Recommendations for Shrinkage

No additional recommendations are made based on the findings of this task.

9.10 Assessment of Permanent Deformation Resistance

A limited series of triaxial permanent deformation tests were performed on selected triaxial specimens listed in Table 9.19 to compare the permanent deformation resistance of different mixes under different

curing and soaking conditions. Most of these specimens had already been subjected to triaxial resilient modulus tests before the permanent deformation tests were carried out (Table 9.12). It was considered reasonable to assume that the resilient modulus tests were essentially nondestructive, considering that the stress levels applied in the permanent deformation tests are much higher than those applied during the resilient modulus tests.

Table 9.19: Permanent Deformation Resistance Test Details

Specimen	Mix Design	Test Condition	Moisture Content (%)
TriB	3% asphalt, 0% cement	7-day cure, unsealed, and 7-day soak	5.3
TriC	3% asphalt, 2% cement	7-day cure, unsealed, and 40-day soak	4.9
TriG	3% asphalt, 1% cement	24-hour cure, sealed, unsoaked	4.3
TriH	0% asphalt, 0% cement	24-hour cure, sealed, unsoaked	7.1
TriI	3% asphalt, 0% cement	24-hour cure, sealed, unsoaked	5.6

One confining stress level (70 kPa [10 psi]) was adopted, which is the median confining stress level for the triaxial resilient modulus test procedure. During permanent deformation testing, 20,000 load repetitions were first applied at a deviator stress level (σ_d) of 300 kPa (44 psi), followed by another 20,000 load repetitions at 500 kPa (75 psi), and then up to 210,000 load repetitions applied at 700 kPa (100 psi). The duration of each haversine loading pulse was 0.1 seconds and the relaxation time was 0.2 seconds. All testing was carried out at an ambient temperature of 20°C ± 2°C (68°F ± 3.5°F).

The axial strain development of the five specimens is shown in Figure 9.18. Compression was considered as positive strain. The mix design, and curing and soaking condition for each specimen prior to testing are also shown. The following observations were made from these results:

- The mix containing 3.0 percent foamed asphalt and no cement (Specimen TriI) and cured for 24 hours had the poorest permanent deformation resistance, with performance worse than that of the untreated control (Specimen TriH). This was attributed to the asphalt mastic phase behaving as a lubricant and reducing the permanent deformation resistance.
- After longer (unsealed) curing, the permanent deformation resistance of the mix containing 3.0 percent foamed asphalt and no cement (Specimen TriB) improved significantly.
- The permanent deformation resistance improved significantly (Specimens TriG and TriC) when cement was added (1.0 and 2.0 percent). The permanent deformation resistance improved with increasing cement content, as expected.
- The results of this limited testing show the role of cement in preventing early permanent deformation in foamed asphalt-treated materials.

9.10.1 Summary of Recommendations for Deformation Resistance

No additional recommendations are made based on the findings of this task.

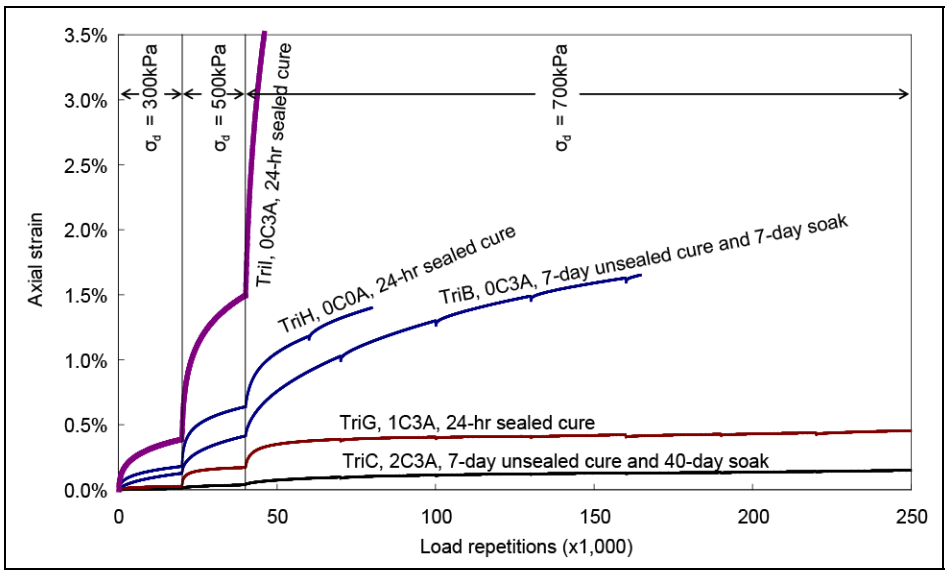

Figure 9.18: Triaxial permanent deformation test results.

9.11 Assessment of Curing Mechanisms

A number of insights into the curing mechanisms of foamed asphalt-treated materials were made based on the test results and observations of fractured specimens in this and previous phases.

The curing processes of foamed asphalt and active fillers appear to take place relatively independently. In most of the tests undertaken, there was no evidence that the foamed asphalt chemically reacted with any of the active fillers and therefore existing theory, knowledge, and experience pertaining to specific active fillers (e.g., portland cement) also generally applies to foamed asphalt mixes when the curing of these active fillers is concerned.

The curing and strength development mechanisms associated with foamed asphalt are illustrated in Figure 9.19. When foamed asphalt is injected onto agitated moist aggregate (RAP), it partially bonds the mineral filler to form an asphalt mastic, visible in the loose mix as small droplets (Figure 9.19a). Aggregate particles in the loose mix are mostly coated with a water membrane. After compaction, the asphalt mastic droplets are in tight contact with the aggregate particles (Figure 9.19b), but due to the presence of the water membrane, they do not physically bond to the aggregates until most of the molding moisture has evaporated (Figure 9.19c) during the curing process (Figure 9.19d). Once the physical bonds between the aggregate particles and asphalt mastic droplets have formed, only partial damage to these

bonds will occur if water is re-introduced into the mix. This explains why specimens TriA (24-hour sealed cure) and TriB (7-day unsealed cure and soak [Figure 9.18]) had the same moisture contents, but the stiffness of the latter specimen was higher and less sensitive to stress states (with smaller absolute values of k_2 and k_3).

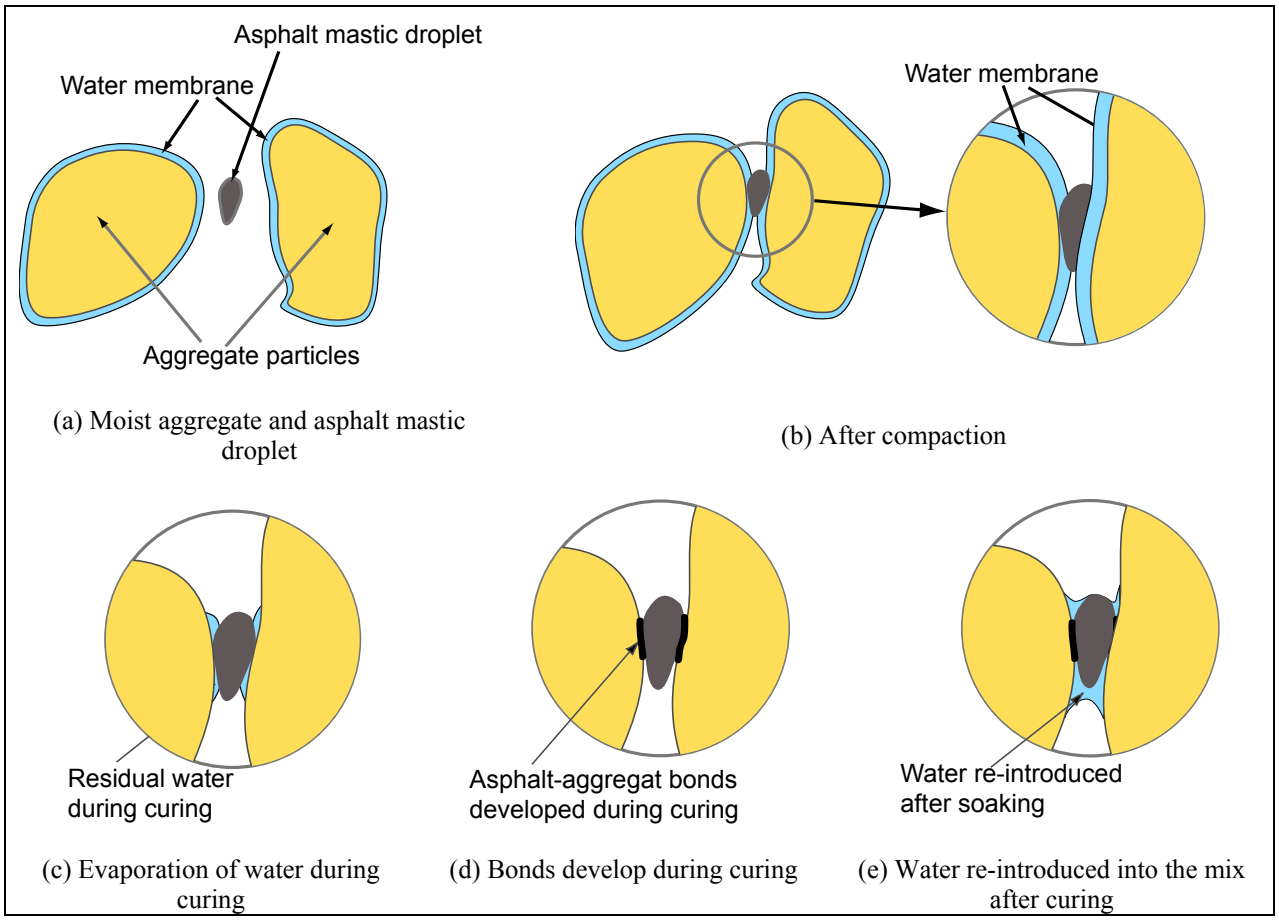

Figure 9.19: Curing process for foamed asphalt.
(Conceptual illustration of the relationship between asphalt mastic, aggregate skeleton, and the bonds between them. The mineral filler phase and air voids are not explicitly shown.)

The influence of the mineral filler phase (excluding asphalt and active filler) was not explicitly considered in the above discussion. This phase is distributed through the mix along with the foamed asphalt mastic, partially filling the voids in the mix. The mineral filler phase also develops strength during the curing process as discussed previously, but when water is re-introduced, its strength is significantly reduced.

This discussion was supported by evidence from specimen fracture face observations. When a fracture propagates in a "fresh" foamed asphalt specimen (i.e., uncured or partially cured specimen with a considerable amount of molding water retained), it travels primarily through the interface of the foamed asphalt mastic and aggregate particles, where the bonds have not fully developed (Figure 9.20a). However, in a 7-day cured and soaked specimen, the fracture is more likely to propagate through the

asphalt mastic droplets as shown in Figure 9.20b. It could also break the asphalt mastic-aggregate interface, but the likelihood of the fracture precisely splitting the asphalt and aggregate is small.

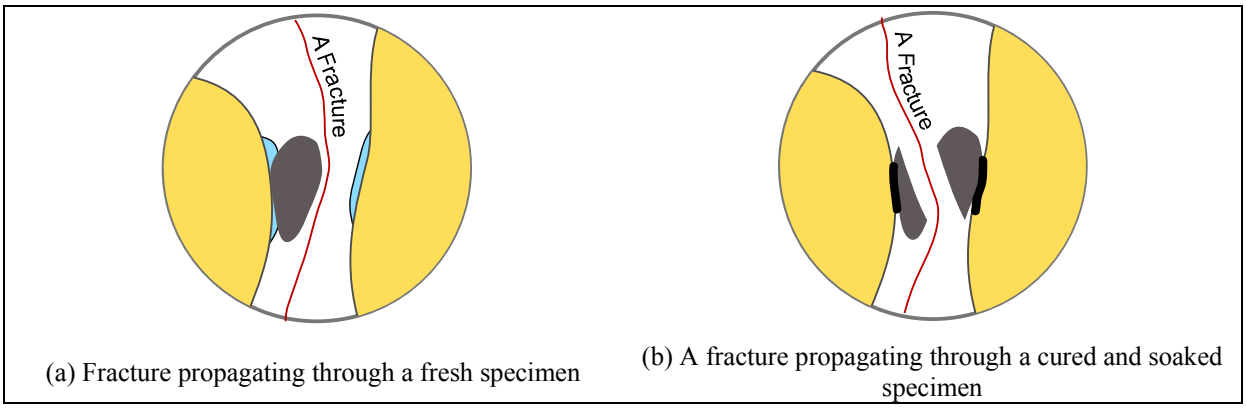

(a) Fracture propagating through a fresh specimen

(b) A fracture propagating through a cured and soaked specimen

Figure 9.20: Theoretical fracture paths for uncured and cured specimens.

The fracture faces of fresh, and cured-and-soaked ITS specimens are shown in Figure 9.21a and Figure 9.21b respectively. These two specimens were selected from the ITS tests carried out in parallel with triaxial tests TriA and TriB respectively discussed in Section 9.10, which had identical mix designs. The images represent approximately 80 percent of the fracture face of a specimen (80 mm x 50 mm [3.2 in. x 2 in.]). Magnified images (various magnification factors) of these two fracture faces are shown in Figure 9.21c through Figure 9.21f. The asphalt mastic droplets were partially covered by mineral filler in the 24-hour cured specimen, and are thus not visible in Figure 9.21c, but are visible in Figure 9.21e. The fracture face of the fully cured and soaked specimen had a notably different appearance, with asphalt mastic droplets split along the fracture face.

These observations have important implications for full-depth reclamation of pavement structures in that the bonding provided by the foamed asphalt develops as the mixing/compaction water evaporates, and only fully develops once this water is no longer present. If, under certain conditions, this water is retained after compaction (e.g., by early placement of the asphalt wearing course or because of inadequate drainage) the bonds will not develop, even after a prolonged period of time (months or years). However, once the bonds have formed, occasional reintroduction of water into the treated layer will only partially damage the bonding, provided that extended soaking periods do not occur. It is therefore crucial to allow the initial mixing/compaction water to evaporate from the recycled layer before the asphalt concrete surface layer is placed, to ensure that the road is adequately drained and to ensure that roadside practices (e.g., irrigation) do not adversely affect the moisture condition of the pavement.

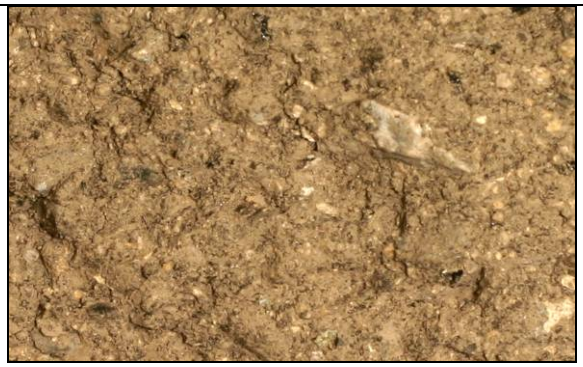

(a) Fracture face of an uncured (fresh) specimen, split through mineral filler phase (actual size)

(b) Fracture face of a cured and soaked specimen, split through asphalt mastic phase (actual size)

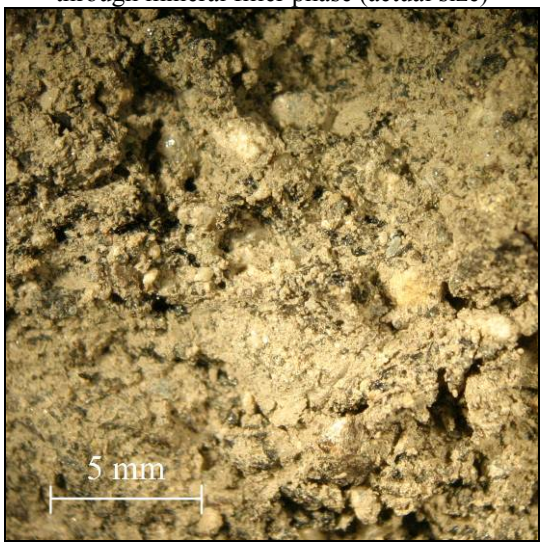

(c) Microscope image of the fracture face of an uncured specimen

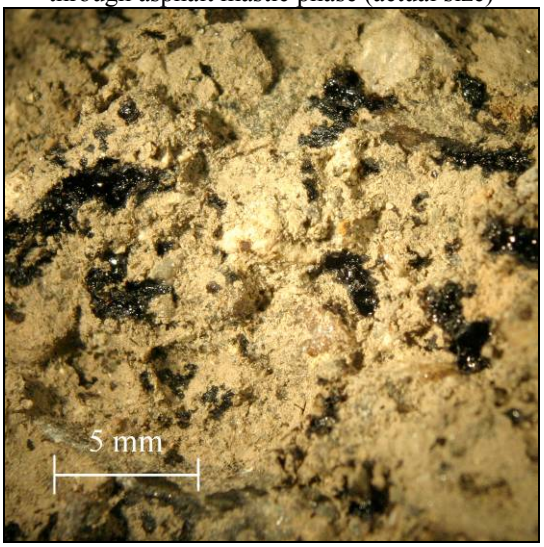

(d) Microscope image of the fracture face of a cured and soaked specimen

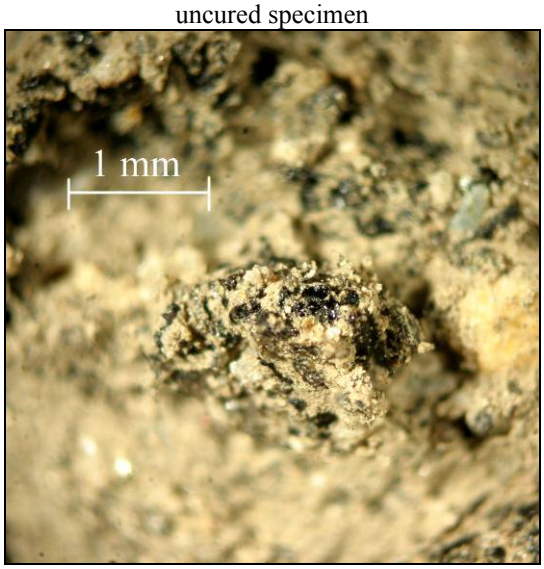

(e) Microscope image of the fracture face of an uncured specimen

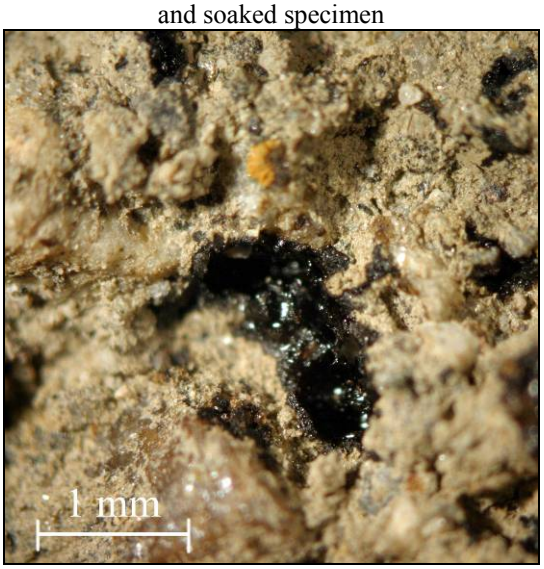

(f) Microscope image of the fracture face of a cured and soaked specimen

Figure 9.21: Fracture face and magnified images of uncured and cured specimens.

9.11.1 Summary of Recommendations for Curing

The following recommendations regarding curing are made:

- Recycled layers should be allowed to dry back to at least 50 percent (preferably 30 percent) of the compaction moisture content before new aggregate layers or the wearing course is placed.
- Adequate drainage measures should be incorporated into the design and construction of recycled roadways.
- Roadside activities, such as irrigation and agricultural land preparations, should be appropriately managed to ensure that the pavement structure is not subjected to unnatural and/or extreme moisture fluctuations.

10. DERIVED GRAVEL FACTORS FOR FOAMED ASPHALT

10.1 Introduction

This chapter derives the Gravel Factors (G_f) of foamed asphalt-treated base materials, which are required for the current Caltrans empirical flexible pavement design method. Since the Gravel Factor is a generic characteristic of a pavement material, and is not directly and explicitly related to any strength or stiffness tests, a mechanisitic-empirical design exercise involving typical material and structural parameters was undertaken to relate the findings of this study to a Gravel Factor. The procedure followed is summarized below:

- Several pavement structures using pulverized asphalt concrete as the base course (PAB) are designed with the Caltrans empirical design method for different traffic volumes. The critical pavement responses pertaining to asphalt concrete fatigue failure and to rutting failure are then calculated as reference values.
- In these structures, the pulverized asphalt concrete layer is replaced with a foamed asphalt-treated base (FA), which is generally stiffer than PAB, yielding smaller pavement responses.
- The asphalt concrete (AC) layer thickness is reduced iteratively until the same pavement responses as the reference values are achieved. The reduction of the Gravel Equivalent (GE) in the asphalt concrete layer is assumed to be the Gravel Equivalent improvement achieved by foamed asphalt stabilization. The Gravel Factor values of the foamed asphalt-treated material are calculated accordingly.

10.2 Experimental Design

The parameters for the design exercise are summarized in Table 10.1.

Table 10.1: Parameters for the Gravel Factor Design Exercise

Variable or Parameter	Values
Subgrade resilient modulus ($M_{r\text{-}SG}$)	- 50 MPa (R-Value = 28) - 70 MPa (R-Value = 36) - 100 MPa (R-Value = 43)
PAB or FA layer thickness (H_{PAB} or H_{FA})	- 200 mm
Gravel Factor of PAB ($G_{f\text{-}PAB}$)	- 1.2[1]
Gravel Factor of AC ($G_{f\text{-}AC}$)	- Dependent on traffic index (TI) (see Table 10.2)
AC resilient modulus ($M_{r\text{-}AC}$)	- 1,500, 3,000, and 9,000 MPa
Resilient modulus of PAB ($M_{r\text{-}PAB}$)	- 360 MPa
Resilient modulus of FA ($M_{r\text{-}FA}$)	- 450 and 650 MPa
Design Traffic Index	- 8, 10 and 13

[1] $G_{f\text{-}PAB}$ based on study undertaken by UCPRC and was based on conservative inputs at all levels of the calculation.

The values for resilient modulus of the asphalt concrete and subgrade ($M_{r\text{-}AC}$ and $M_{r\text{-}SG}$,), thickness of the foamed asphalt base (H_{FA}), and Gravel Factor of the asphalt concrete ($G_{f\text{-}AC}$) were selected according to typical full-depth reclamation practice in California. The California empirical design method uses the Gravel Factor as the main parameter for material characterization while typically a mechanistic-empirical (M-E) design method requires material resilient modulus. An example correlation between subgrade R-value and subgrade resilient modulus ($M_{r\text{-}SG}$) can be found in several publications *(71,72)*. Those from the *Shell Pavement Design Manual* were used for these calculations. Similar correlations for asphalt concrete materials were not found in the literature, therefore the resilient modulus of the asphalt concrete ($M_{r\text{-}AC}$) was treated as a variable and the sensitivity of the derived Gravel Factor ($G_{f\text{-}FA}$) values to this variable was investigated. The following properties were assumed based on the previous study *(73)*. Gravel Factor, R-value, and resilient modulus for the pulverized asphalt concrete base materials were assumed to be 1.2, 80, and 360 MPa (52.2 ksi) respectively on the basis of another University of California Pavement Research Center (UCPRC) study on this material *(73)*.

The resilient modulus of foamed asphalt-treated materials is sensitive to temperature and moisture conditions, as discussed in Chapters 4 and 7, and therefore need to be considered in a mechanistic evaluation. Two values, namely 450 MPa and 650 MPa (65 ksi and 94 ksi), were therefore selected in this study to represent foamed asphalt-treated materials in typical California FDR projects in the wet and dry seasons, respectively. The Gravel Factors for these two seasons were investigated separately and the average of the two used for further calculations.

Structures with a pulverized asphalt concrete base course are typically designed for different subgrade moduli and Traffic Indices complying with the Caltrans empirical design method as shown in Table 10.2.

Table 10.2: Empirical Design Results of Pulverized Asphalt Concrete Bases

Traffic Index	Subgrade Characteristics		H_{FA} (mm)	H_{AC} (mm)
	$M_{r\text{-}SG}$ (MPa)	R-Value		
8	50	28	200	165
8	70	36	200	135
8	100	43	200	105
10	50	28	200	225
10	70	36	200	195
10	100	43	200	165
13	50	28	200	330
13	70	36	200	300
13	100	43	200	255

10.3 Derivation of Gravel Factors

Two general pavement responses, namely the maximum tensile strain in the asphalt concrete layer ($\varepsilon_{t\text{-}AC}$) and the maximum compressive strain in the subgrade ($\varepsilon_{v\text{-}SG}$) for each designed structure were calculated with *LEAP2 (19)* and are shown in Table 10.3. The asphalt concrete strain ($\varepsilon_{t\text{-}AC}$) is believed to be the critical pavement response for asphalt concrete fatigue failure and subgrade strain ($\varepsilon_{v\text{-}SG}$) the critical pavement response for rutting failure.

When the pulverized asphalt concrete base material is replaced with stiffer foamed asphalt-treated materials, the thickness of the asphalt concrete layer needs to be reduced to yield the same pavement responses. The required thickness was calculated iteratively for fatigue and rutting respectively, and for the wet season and the dry season respectively as shown in Table 10.3.

Table 10.3: Structure Design Exercise Results

Empirical Design Results for Structures Containing PAB				Pavement Response		H_{AC} to Yield Same Responses			
						Wet Season		Dry Season	
TI	$M_{r\text{-}SG}$ (MPa)	$M_{r\text{-}AC}$ (MPa)	H_{AC} (mm)	$\varepsilon_{t\text{-}AC}$	$\varepsilon_{v\text{-}SG}$	Fatigue	Rutting	Fatigue	Rutting
8	50	1,500	165	253	761	126	154	–	132
	50	3,000	165	193	605	146	157	–	140
	50	9,000	165	104	384	158	161	140	152
	70	1,500	135	285	798	–	124	–	104
	70	3,000	135	224	653	112	128	–	111
	70	9,000	135	126	436	124	131	107	123
	100	1,500	105	312	829	–	96	–	77
	100	3,000	105	258	704	–	98	–	83
	100	9,000	105	155	501	95	102	–	93
10	50	1,500	225	186	541	199	214	-	192
	50	3,000	225	136	411	210	218	175	201
	50	9,000	225	68	241	219	222	205	214
	70	1,500	195	211	551	168	185	–	165
	70	3,000	195	156	428	180	188	141	174
	70	9,000	195	80	261	188	192	174	185
	100	1,500	165	241	555	133	157	–	139
	100	3,000	165	180	442	148	159	–	146
	100	9,000	165	95	281	158	163	143	157
13	50	1,500	330	113	331	306	319	255	297
	50	3,000	330	79	238	316	323	285	308
	50	9,000	330	37	126	324	328	312	322
	70	1,500	300	124	328	277	291	227	271
	70	3,000	300	87	240	286	295	256	281
	70	9,000	300	42	132	294	299	282	293
	100	1,500	255	148	342	232	248	181	230
	100	3,000	255	105	257	241	251	211	239
	100	9,000	255	52	149	249	254	236	250

Strains in the foamed asphalt treated layer were compared with those in an untreated pulverized asphalt base layer to calculate the asphalt concrete layer thickness. The results were not dependent on transfer functions relating pavement mechanical responses (such as strains) to service life.

In the twenty-seven scenarios investigated, maintaining the vertical strain at the top of the subgrade ($\varepsilon_{v\text{-}SG}$) between the existing and new structures always required a thicker asphalt concrete layer than did keeping the tensile strain at the bottom of the asphalt concrete ($\varepsilon_{t\text{-}AC}$) unchanged. Although rutting is seldom more critical than fatigue in terms of pavement performance, limiting both $\varepsilon_{v\text{-}SG}$ and $\varepsilon_{t\text{-}AC}$ for the new structures to less than that for the existing structures ensured that the performance of the new structures was at least as good as that of the existingstructures.

For certain structures, the required asphalt concrete thickness for fatigue is not provided in Table 10.3 because a search for such a value was unsuccessful. In these cases, the foamed asphalt-treated layer stiffness was relatively high; the asphalt concrete stiffness relatively low, and the neutral axis of the combined layer was located in the base layer. Decreasing the asphalt concrete thickness did not reduce the maximum tensile strain in this layer and under this condition (relatively flexible asphalt concrete layer supported by a stiff base layer), pavement structures typically fail by permanent deformation in the base or subgrade, and not by fatigue in the asphalt concrete (i.e. fatigue is not the critical distress mode). Therefore, determining the asphalt concrete thickness on the basis of rutting performance was considered appropriate for the purposes of this study.

Table 10.4 compares the designed structures in which pulverized asphalt concrete was used as the base course and the structures in which foamed asphalt-treated materials were used as the base course. In the foamed asphalt structures, the asphalt concrete thicknesses were generally reduced. From an empirical pavement design perspective, this implies that the Gravel Equivalent provided by foamed asphalt materials is greater that that provided by untreated pulverized materials and hence the required thickness (or *GE*) for the asphalt concrete layer is reduced. The reduction of Gravel Equivalent in the asphalt concrete layer (GE_{AC}) is assumed to equal the Gravel Equivalent improvement of foamed asphalt materials over untreated pulverized materials. Since the base course thickness remained constant, the improvement of the Gravel Factor was calculated accordingly as shown in Equation 10.1.

$$H_{FA}\,(G_{f\text{-}FA} - G_{f\text{-}PAB}) = GE_{AC\text{-}PAB} - GE_{AC\text{-}FA} \qquad (10.1)$$

10.4 Recommended Gravel Factors

Based on the findings of the above analysis, the average Gravel Factor of foamed asphalt-treated materials in the wet and dry seasons is 1.32 and 1.47, respectively. Slight dependencies on traffic index (positive), subgrade stiffness (negative), and asphalt concrete stiffness (negative) were observed. These values assume a mix design of 3.0 percent foamed asphalt and 2.0 percent portland cement for the foamed asphalt base, as well as a period of curing.

Given that the Caltrans empirical design method does not explicitly consider seasonal variation of material properties, a Gravel Factor of 1.4 is recommended as an interim for designing foamed asphalt-treated pavements in California, until additional information from long-term field studies is obtained.

Table 10.4: Comparison of Design Structures

Empirical Design Results for Structures Containing PAB					Equivalent Structure in Wet Season			Equivalent Structure in Dry Season		
TI	$M_{r\text{-}SG}$ (MPa)	$M_{r\text{-}AC}$ (MPa)	H_{AC} (mm)	$GE_{AC\text{-}PAB}$ (mm)	H_{AC} (mm)	$GE_{AC\text{-}FA}$ (mm)	$G_{f\text{-}FA}$	H_{AC} (mm)	$GE_{AC\text{-}FA}$ (mm)	$G_{f\text{-}FA}$
8	50	1,500	165	1.12	154	1.00	1.38	132	0.87	1.58
	50	3,000	165	1.12	157	1.02	1.34	140	0.92	1.50
	50	9,000	165	1.12	161	1.06	1.29	152	1.00	1.38
	70	1,500	135	0.90	124	0.82	1.33	104	0.68	1.53
	70	3,000	135	0.90	128	0.84	1.29	111	0.73	1.46
	70	9,000	135	0.90	131	0.86	1.26	123	0.81	1.34
	100	1,500	105	0.70	96	0.63	1.31	77	0.51	1.50
	100	3,000	105	0.70	98	0.64	1.29	83	0.55	1.44
	100	9,000	105	0.70	102	0.67	1.25	93	0.61	1.34
10	50	1,500	225	1.51	214	1.38	1.39	192	1.20	1.68
	50	3,000	225	1.51	218	1.42	1.34	201	1.27	1.56
	50	9,000	225	1.51	222	1.45	1.29	214	1.38	1.39
	70	1,500	195	1.25	185	1.14	1.37	165	0.98	1.61
	70	3,000	195	1.25	188	1.16	1.33	174	1.05	1.50
	70	9,000	195	1.25	192	1.20	1.28	185	1.14	1.37
	100	1,500	165	1.00	157	0.92	1.33	139	0.82	1.48
	100	3,000	165	1.00	159	0.93	1.30	146	0.86	1.41
	100	9,000	165	1.00	163	0.96	1.26	157	0.92	1.33
13	50	1,500	330	2.20	319	2.06	1.42	297	1.88	1.70
	50	3,000	330	2.20	323	2.10	1.36	308	1.97	1.56
	50	9,000	330	2.20	328	2.14	1.30	322	2.09	1.38
	70	1,500	300	1.94	291	1.83	1.38	271	1.66	1.63
	70	3,000	300	1.94	295	1.86	1.33	281	1.74	1.50
	70	9,000	300	1.94	299	1.89	1.27	293	1.84	1.35
	100	1,500	255	1.56	248	1.48	1.33	230	1.34	1.55
	100	3,000	255	1.56	251	1.50	1.30	239	1.40	1.44
	100	9,000	255	1.56	254	1.52	1.26	250	1.49	1.31

11. RECOMMENDATIONS FOR GUIDELINES

11.1 Introduction

A separate guideline document has been prepared as part of this University of California Pavement Research Center (UCPRC) study *(74)*. It provides recommendations for project selection, mix design, structural design, and construction, based on observations during projects in California and elsewhere, and on the results of the laboratory testing and studies described in this report. A summary of key recommendations considered for the guideline, based on the findings from the UCPRC study, are provided below.

11.2 Project Selection

Key recommendations for project selection include:

- All FDR-foamed asphalt projects should be individually designed, based on the findings of a comprehensive field investigation. This investigation includes Falling Weight Deflectometer (FWD) measurements, visual assessment, coring, Dynamic Cone Penetrometer (DCP) measurements, test pit investigations, and material sampling, carried out by the designer, together with the maintenance staff from the responsible maintenance station. Maintenance staff or the Pavement Management System (PMS) should be able to provide the designer with historical information about the performance and maintenance of the road, and identify problem areas. The assessment should be carried out toward the end of the rain year (i.e., late winter, early spring in California).
- FWD measurements should be taken at 65-ft (20-m) intervals. The results (deflection of 600 mm sensor) should be used to identify uniform sections and problem areas. Locations for test pits and additional cores and DCP measurements should be based on this analysis. FDR-foamed asphalt should not be considered on roads where the backcalculated deflection modulus ($E_{def\text{-}600}$) is less than 25 MPa (600 mm sensor deflection greater than 1.25 mm [49 mils]). On roads or sections of the road where the calculated deflection modulus is between 25 MPa and 45 MPa (3.6 and 6.5 ksi), subgrade problems are likely and these should be corrected prior to recycling.
- Cores should be taken every 1,500 ft to 2,250 ft (2 to 3/mile [500 m to 750 m, 2 to 3/1.5km]) to determine the thickness of the asphalt and to provide an indication of underlying materials. Core spacing will depend on the perceived variability of asphalt thickness and the number of patches. DCP measurements should be taken in the core holes to evaluate the strength of the underlying

material. Care should be taken when interpreting the DCP results as water from the coring operation will weaken the materials under the asphalt.

- The visual assessment should include drainage and adjacent land use, with specific attention given to irrigation practices in agricultural areas. FDR-foamed asphalt should not be considered on roads with poor drainage.
- Test pits should be excavated with a cold milling machine to ensure that representative samples are collected for mix design. The moisture content of the underlying granular material should be determined.

11.3 Mix Design

Key recommendations for mix design include:

- General recommendations:
  - A mix design must be carried for each project.
- Recommendations on asphalt binder selection:
  - A selection of asphalt binders should be assessed to ensure that optimal foamability is achieved. The use of softer asphalt binder grades is encouraged, as these have better dispersion than harder binders for the same or similar foaming characteristics. A cost-benefit analysis should be undertaken to justify transporting binders with better foaming characteristics.
  - The minimum requirements for the Expansion Ratio and Half-Life are 10 times and 12 seconds (from time foam nozzle is switched off), respectively. Instead of defining one "optimum" combination of foaming parameters, an acceptance range of the asphalt temperature and the foamant water-to-asphalt ratio should be determined in the mix design stage to serve as a guideline for construction. The foamability check should at least cover a temperature range of 150°C to 180°C (300°F to 360°F) with even increments of 10°C (15°F), and a foaming water ratio range of 1.0 to 5.0 percent.
- Recommendations on aggregate:
  - The aggregate and ambient temperatures should be controlled and recorded during mixing and prior to compaction. Ambient temperatures should be maintained at approximately 77°F (25°C). Aggregate temperatures should be maintained in a range of 70°F to 77°F (20°C to 25°C). A control test should also be carried out at the minimum expected field mixing temperature to assess the influence of this parameter on performance of the mix. This temperature should not be lower than 60°F (15°C).

- Recommendations on active filler:
  - Active fillers should be used in all foamed asphalt projects. Semi-active and inactive fillers (e.g., mineral fines, kiln dust, and fly-ash) can be considered in conjunction with the active filler in the unlikely event that the true fines content after milling is less than 5.0 percent.
  - Portland cement should be used as the active filler if the aggregates in the recycled material are predominantly of granitic, quartzitic, or sandstone origin. Both portland cement and lime should be considered in the mix design for other materials until sufficient knowledge on the performance of these fillers on specific material types has been gathered.
- Recommendations on testing:
  - Assuming that a representative sample grading has been obtained from the test pits using a cold milling machine, the target grading should have a fines content (material passing the #200 sieve [0.075 mm]) of between 5 and 12 percent. In the unlikely event of the fines content being below 5.0 percent, extra fines in addition to the active filler may be required. If the fines content is between 12 and 15 percent, a slightly higher asphalt binder content may be required. If the fines content is above 15 percent the soaked strengths should be monitored carefully. Fines contents higher than 20 percent should not be considered.
  - The Atterberg limits of the pulverized fines collected from sampling to the proposed milling depth, as well as those for the underling base, subbase, or subgrade material should be determined. The plasticity index of the pulverized layer material should not exceed six. The limits for the underlying layers should not exceed those specified for the respective material (e.g., Caltrans Specification *[75]*).
  - A mixing moisture content of between 75 and 90 percent of the optimum compaction moisture content should be used as a basis for preparing laboratory materials. Within this range, higher moisture contents might benefit compaction but attention should be paid to the physical states of the loose mix to assure that no visible agglomerations larger than 2 mm (0.01 in.) in diameter are formed.
  - All mix designs should be based on testing after soaking. Unsoaked tests (preferably dried back to the equilibrium moisture content determined during the project assessment) can be included to determine a tensile strength ratio to assess moisture sensitivity.
  - The Indirect Tensile Strength test (soaked) can be used for mix design testing provided that sufficient replicates are tested (at least four) and that tests are repeated if there is high variability between replicates (e.g., standard deviation of the strength is more than 15 percent of the average strength [i.e. coefficient of variation is more than 15 percent]).
  - If triaxial resilient modulus and flexural beam tests are used in a mix design, the results need to be combined to better understand foamed asphalt mix behavior.

- The fracture faces of tested specimens should be carefully scrutinized to assess mix behavior.

11.4 Structural Design

Key recommendations for structural design include:

- Standard pavement design procedures should be followed, based on traffic predictions, site investigations (visual assessment, Falling Weight Deflectometer and Dynamic Cone Penetrometer), and laboratory testing.
- For designs performed using the Caltrans R-value method, a Gravel Factor of 1.4 (based on results from the testing of soaked specimens) should be used in the interim for designing pavement structures with a foamed asphalt layer, until additional information is collected from long-term studies. This Gravel Factor is considered conservative.

11.5 Construction

Key recommendations for construction include:

- The contractor's crew should include an experienced technician who is required to walk behind the recycling train at all times while the recycler is moving. This individual should check the material characteristics, material consistency, and mixing moisture content, and for asphalt "stringers" or globules, the presence of which indicate that the asphalt is not being sufficiently foamed. The technician should monitor the initial compaction and ensure that the distance between the recycling train and the padfoot roller is acceptable. In addition, the technician should be in constant contact with the recycler operator and should be sufficiently experienced to call for adjustments to the asphalt and moisture contents.
- Recycling should not begin until the air temperature is above 50°F (10°C), and the temperatures of the road surface and prespread active filler are all equal to or above 60°F (15°C).
- Mixing moisture content should be strictly controlled and should be achieved in the mixing chamber of the recycler. This requires a water tanker to be coupled to the recycling machine. Water should not be added behind the recycler and moisture contents should not be adjusted on the recycled material until initial compaction with the padfoot roller has been completed.
- The binder temperature, expansion ratio and half-life should be checked after each tanker change.
- The required weights of the compaction equipment should be specified in the Project Special Provisions, and should be strictly enforced. Guidelines for roller requirements are provided in the Wirtgen manual *(6)*. Padfoot roller specifications should include a requirement of a blade.
- Optimal rolling patterns should be determined during construction of the test strip. The padfoot roller should continue until no further indentations are observed on the road. The blade on the roller

should be used to smooth the material after each pass. Refusal density should be considered instead of a target density as it has been clearly shown that higher strengths and reduced moisture sensitivity result from higher densities. However, care should be taken to ensure that the material is not crushed by the rollers, or that recycled material is "punched" into the subgrade.

- If more than one recycling train is used on a project, each train should have a padfoot roller for initial compaction.
- Quality control measurements, including but not limited to milling depth, the presence of unfoamed asphalt, the presence of oversize material, the presence of loose material prior to surfacing, compaction moisture content, and density should be clearly defined in the Project Special Provisions, and strictly enforced. Nuclear gauges should be calibrated on foamed asphalt material. Densities should meet the requirement throughout the layer.
- The surface should be sealed with a light fog spray of diluted asphalt emulsion (diluted 50:50 with water and applied at 0.7 L/m^2 [0.15 gal/yd^2]) on the second day after compaction to prevent raveling.
- Raveled areas and any areas exhibiting signs of distress (e.g. associated with inadequate compaction, over compaction, over watering, etc) should be repaired prior to surfacing (distressed material removed and replaced with excess foamed material from the side of the road, or emulsion treated base course material. The replaced material should be compacted to specification). Asphalt concrete should not be applied to loose material under any circumstances.

12. CONCLUSIONS AND RECOMMENDATIONS

12.1 Conclusions

A comprehensive study on full-depth reclamation with foamed asphalt has been completed for the California Department of Transportation by the University of California Pavement Research Center. The study culminated in the preparation of interim guidelines for project selection, mix design, structural design, and construction, which can be used in conjunction with the South African *Guidelines for the Design and Use of Foamed Bitumen Treated Materials* and the *Wirtgen Cold Recycling Manual.* The California guideline provides additional information for recycling thick asphalt pavements, and is based on extensive laboratory testing and the assessment of reclamation projects in the state.

A literature review of current practice revealed that very little research had been carried out on the reclamation of thick asphalt pavements (multiple overlays over a relatively weak base or subgrade). Most research worldwide has been carried out on pavements consisting of relatively thick granular layers and thin surface treatments. A mechanistic sensitivity analysis was carried out to identify key variables in the design of recycled pavements consisting primarily of recycled asphalt pavement. The findings of the literature review and the sensitivity analysis were used to formulate a work plan for laboratory and field studies that would address the issues specific to reclamation these thick asphalt pavements.

A number of recently completed construction projects were visited, and construction on projects on state and county routes was observed. Material for laboratory testing was collected from these projects. Visual assessments and Falling Weight Deflectometer testing were carried out in the spring and fall each year during the course of the study. Heavy Vehicle Simulator testing was carried out on one of the projects, however, the test site was not representative of the mainline (or typical foamed asphalt pavements) and little useful information was gained. A comprehensive laboratory investigation identified a number of key issues that have been incorporated into the mix design guideline. These include appropriate test methods for California, preparation of specimens (mixing moisture content and aggregate temperature), asphalt binder selection, target asphalt and active filler contents, aggregate gradations (fines content), specimen curing, and the interpretation of results.

The study concluded that full-depth reclamation with foamed asphalt combined with a cementitious filler is an appropriate pavement rehabilitation option for California. Projects should be carefully selected with special care given to roadside drainage. Appropriate mix and structural design procedures should be followed, and construction should be strictly controlled to ensure that optimal performance and life are

obtained from the pavement. Premature failures will in most instances be attributed to poor project selection (e.g., weak subgrades and/or poor drainage) or to poor construction (e.g., poor asphalt dispersion, incorrect mixing moisture content, poor compaction, and poor surface finish).

12.2 Recommendations

The following recommendations are made:

- Full-depth reclamation with foamed asphalt combined with a cementitious filler should be considered as a rehabilitation option on thick, cracked asphalt pavements on highways with a Traffic Index (TI) less than 12 (or annual average daily traffic volume not exceeding 20,000 vehicles per day), provided that an appropriate design can be achieved. The technology is particularly suited to pavements where multiple overlays have been placed over a relatively weak base course layers, and where cracks reflect through the overlay in a relatively short time. Higher traffic volumes can be considered provided that strength and durability requirements meet or exceed the requirements for the pavement design. Alternatively, the recycled layer can be used as a subbase underneath a new base layer if a pavement structure with higher strength is required.
- Project selection, mix design, and construction should be strictly controlled to ensure that optimal performance is obtained from the rehabilitated roadway.
- Full-depth reclamation with asphalt emulsions and partial-depth reclamation with asphalt emulsions and foamed asphalt should also be evaluated, and guidelines prepared for choosing the most appropriate technology for a given set of circumstances.

13. REFERENCES

1. **Full-Depth Recycling with Foamed Asphalt Study: Work plan.** 2005. Davis and Berkeley, CA: University of California Pavement Research Center. (WP-2005-05).
2. MUTHEN, K.M. 1999. **Foamed Asphalt Mixes, Mix Design Procedure.** Pretoria, South Africa: CSIR Transportek. (Contract Report CR-98/077, 31 pp).
3. **The Design and Use of Foamed Bitumen Treated Materials.** 2002. Pretoria, South Africa: Asphalt Academy. (Interim Technical Guideline, TG2).
4. JENKINS, K.J. 2000. **Mix Design Considerations for Cold and Half-cold Bituminous Mixes with Emphasis on Foamed Bitumen.** PhD Thesis. University of Stellenbosch, South Africa.
5. SALEH, M.F. and Herrington, P. 2003. **Foamed bitumen stabilisation, for New Zealand roads.** Christchurch, New Zealand: Transfund. (Research Report No. 250).
6. **Wirtgen Cold Recycling Manual.** 2004. Windhagen, Germany: Wirtgen GmbH.
7. JENKINS, K.J., Robroch, S., Henderson, M.G., Wilkinson, J., and Molenaar, A.A.A. 2004. *Advanced Testing for Cold Recycling Treatment Selection on N7 Near Cape Town.* **Proceedings 8th Conference on Asphalt Pavements for Southern Africa (CAPSA'04).** Sun City, South Africa. (pp 537-552).
8. RAMANUJAM, J.M. and Jones, J.D. 2007. *Characterization of Foamed-Bitumen Stabilization.* **International Journal of Pavement Engineering, Vol 8, No 2.** (pp 111-122.
9. THEYSE, H.L., Long, F. Harvey, J.T., and Monismith, C.L. 2004. **Discussion of Deep In-Situ Recycling (DISR).** Davis and Berkeley, CA: University of California Pavement Research Center. (UCPRC-TM-2004-6).
10. LONG, F. M. 2001. **The Development of Structural Design Models for Foamed Bitumen Treated Pavement Layers.** Pretoria, South Africa: Transportek, CSIR. (Report CR 2001/76).
11. LONG, F.M. and Theyse, H.L. 2004. *Mechanistic Empirical Structural Design Models for Foamed and Emulsified Bitumen Treated Materials.* 2004. **Proceedings 8th Conference on Asphalt Pavements for Southern Africa (CAPSA).** Sun City, South Africa. (pp 553-568).
12. THEYSE, H.L., De Beer, M., and Rust, F.C. 1996. *Overview of the South African Mechanistic Pavement Design Method.* **Transportation Research Record: Journal of the Transportation Research Board, No 1539.** Washington, DC: Transportation Research Board, National Research Council. (pp 6-17).
13. THEYSE, H.L. 2003. **1st Level Analysis Report of the Foamed Bitumen Treated Crushed Stone Base on the Slow Lane of the Southbound Carriageway of the N7 near Cape Town.** Pretoria, South Africa: Transportek, CSIR. (Report CR-2003/23).

14. COLLINGS, D., Lindsay, R., and Shunmugam, R. 2004. *LTPP Exercise on a Foamed Bitumen Treated Base - Evaluation of almost 10 Years of Heavy Trafficking on MR 504 in KwaZulu-Natal.* **Proceedings 8th Conference on Asphalt pavements for Southern Africa (CAPSA'99).** Sun City, South Africa: (pp 468-499).
15. **AASHTO Guide for the Design of Pavement Structures.** 1993. Washington, DC: American Association of State Highway and Transportation Officials.
16. LONG, F.M., and Theyse, H.L. 2002. **Laboratory Testing for the HVS Sections on Road P243/1**. Pretoria, South Africa: Transportek, CSIR. (Report CR 2001/32).
17. LONG, F.M. and Ventura, D.F.C. 2003. **Laboratory Testing for the HVS Sections on the N7 (TR11/1)**. Pretoria, South Africa: Transportek, CSIR. (Report CR-2003/56).
18. SHOOK, J.F., Finn, F.N., Witczak, M.W., and Monismith, C.L. 1982. *Thickness Design of Asphalt Pavements—The Asphalt Institute Method.* **Proceedings 5th International Conference on the Structural Design of Asphalt Pavements.** University of Michigan and Delft Technical University. (pp 17-44).
19. **LEAP 2.0 Layered Elastic Analysis Program.** 2004. Berkeley, CA: Symplectic Engineering Corporation. (Release 2.0).
20. **Annual Average Daily Truck Traffic on the California State Highway System.** 2006. Sacramento, CA: California Department of Transportation Traffic and Vehicle Data Systems Unit.
21. **Final Completion Report for Cold Foam in Place Reclamation Col-20 PM 10.2-28.2.** 2006. Marysville, CA: California Department of Transportation North Region Materials Office.
22. THEYSE, H.L., Long, F.M., Jones, D., and Harvey, J.T. 2004. **Full-Depth Reclamation with Foamed Asphalt: First-Level Analysis Report on HVS Testing on Route 89.** Davis and Berkeley, CA: University of California Pavement Research Center. (UCPRC-RR-2004-07).
23. PETERSON, J.F. 2006. **Preliminary Failure Analysis and Remediation on SLO/SB-33.** Marysville, CA: California Department of Transportation. (Unpublished Internal Report).
24. CHOI, J.W., Wu, R. and Pestana, J. 2007. *Application of Constrained Extended Kalman Filter in Layer Moduli Backcalculation.* **Proceedings of the 86th Annual Meeting of Transportation Research Board (CD-ROM)**. Washington, D.C.: Transportation Research Board, National Research Council.
25. HARVEY, J.T, Fu, P., Jeon, E.J., and Ullidtz, P. 2006. *Granular Base Layer Stiffness Characterization for Analytical Design of Flexible Pavements.* **Proceedings of the 10th International Conference on Asphalt Pavements (CD-Rom).** Quebec City, Canada.
26. HOUSTON, M. and Long, F.M. 2004. *Correlations Between Different ITS and UCS Test Protocols for Foamed Bitumen Treated Materials.* **Proceedings 8th Conference on Asphalt Pavements for Southern Africa (CAPSA'04).** Sun City, South Africa. (pp 522-536).

27. TWAGIRA, M.E., Jenkins K.J., and Ebels, L.J. 2006. *Characterisation of Fatigue Performance of Selected Cold Bituminous Mixes.* **Proceedings of the 10th International Conference on Asphalt Pavements (CD-Rom).** Quebec City, Canada.

28. BOWERING, R.H. 1970. *Upgrading Marginal Road-Building Materials with Foamed Bitumen.* **Highway Engineering in Australia**. Melbourne, Australia: Mobil Oil Australia.

29. RUCKEL, P.J., Acott, S.M., and Bowering, R.H. 1983. *Foamed-Asphalt Paving Mixtures: Preparation of Design Mixes And Treatment of Test Specimens.* **In Transportation Research Record: Journal of the Transportation Research Board, No. 911.** Washington, D.C.: Transportation Research Board, National Research Council. (pp 88-95).

30. SALEH, M. F. 2006. *Characterisation of Foam Bitumen Quality and the Mechanical Properties of Foamed Bitumen Stabilised Mixes.* **Proceedings of the 10th International Conference on Asphalt Pavements (CD-Rom).** Quebec City, Canada.

31. **Foamed Bitumen Mix Design Procedure Using the Wirtgen WLB 10.** 2001. Windhagen, Germany: Wirtgen GmbH.

32. ABEL, F. 1978. *Foamed Asphalt Base Stabilization.* **Proceedings 6th Annual Asphalt Paving Seminar.** Denver, CO: Colorado State University.

33. JENKINS, K.J., Van de Ven, M.F.C., and de Groot, J.L.A. 1999. *Characterisation of Foamed Bitumen.* **Proceedings 7th Conference on Asphalt Pavements for Southern Africa (CAPSA'99)**, Victoria Falls, Zimbabwe.

34. HARVEY, J.T., Chong, A., and Roesler, J. 2000. **Climate Regions for Mechanistic-Empirical Pavement Design in California and Expected Effects on Performance**. Davis and Berkeley, CA: University of California Pavement Research. (Draft report prepared for California Department of Transportation, UCPRC-RR-2000-07).

35. ONGEL, A. and Harvey, J.T. 2004. **Analysis of 30 Years of Pavement Temperatures Using the Enhanced Integrated Climate Model (EICM).** Davis and Berkeley, CA: University of California Pavement Research. (Draft report prepared for the California Department of Transportation, UCPRC-RR-2004-05).

36. NATAATMADJA, A. 2001. *Some Characteristics of Foamed Bitumen Mixes.* **Transportation Research Record: Journal of the Transportation Research Board, No. 1767.** Washington, D.C.: Transportation Research Board, National Research Council. (pp 120-125).

37. UZAN, J. 1985. *Characterization of Granular Material.* **Transportation Research Record, No.1022.** Washington, D.C.: Transportation Research Board, National Research Council. (pp. 52–59).

38. YUE, Z., Bekking, W., and Morin, I. 1995. *Application of Digital Image Processing to Quantitative Study of Asphalt Concrete Microstructure.* **In Transportation Research Record: Journal of the**

Transportation Research Board. No. 1492. Washington, D.C.: Transportation Research Board, National Research Council, (pp 53-60)

39. BHASIN, A. Button, J.W., Chowdhury, A., and Masad. E. 2006. *Selection of Optimum Gravel Aggregate Size To Resist Permanent Deformation In Hot-Mix Asphalt.* **In Transportation Research Record: Journal of the Transportation Research Board, No. 1952.** Washington, D.C.: Transportation Research Board, National Research Council, (pp 39-47).
40. SAADEH, S, Tashman, L, Masad E, and Mogawer W. 2002. *Spatial and Directional Distribution of Aggregates in Asphalt Mixes.* **Journal of Testing and Evaluation**. Vol. 30. (pp 483-491).
41. MASAD, E. 2004. *X-ray Computed Tomography of Aggregates and Asphalt Mixes.* **Materials Evaluation Journal, American Society for Nondestructive Testing.** Vol. 62. (pp 775-783).
42. MASAD, E. and Button, J.W. 2004. *Implications of Experimental Measurements and Analyses of the Internal Structure of Hot-Mix Asphalt.* **In Transportation Research Record: Journal of the Transportation Research Board. No. 1891.** Washington, D.C.: Transportation Research Board, National Research Council. (pp 212-220).
43. PAN, T., Tutumluer, E. and Anochie, J. 2006. *Aggregate Morphology Affecting Resilient Behavior of Unbound Granular Materials.* **In Transportation Research Record: Journal of the Transportation Research Board. No. 1952.** Washington, D.C.: Transportation Research Board, National Research Council. (pp 12-20).
44. **Mix Design Methods for Asphalt Concrete and Other Hot-Mix Types (MS-2).** 1974. Lexington, KY: Asphalt Institute.
45. NAZARIAN, S., Yuan, D., and Williams, R.R. 2003. *A Simple Method for Determining Modulus of Base and Subgrade Materials.* **ASTM Special Technical Publication, No.1437.** West Conshohocken, PA: ASTM. (pp. 152-164).
46. HILBRICH, S. and Scullion, T.A. 2007. *Rapid Alternative for Laboratory Determination of Resilient Modulus Input Values on Stabilized Materials for the AASHTO M-E Design Guide.* **Proceedings of the 86th Annual Meeting of Transportation Research Board (CD-Rom)**. Washington, D.C.: Transportation Research Board, National Research Council.
47. ROMANOSCHI, S.A., Hossain, M., Gisi, A., and Heitzman, M. 2004. *Accelerated Pavement Testing Evaluation of the Structural Contribution of Full-Depth Reclamation Material Stabilized with Foamed Asphalt.* **Transportation Research Record: Journal of the Transportation Research Board, No. 1896.** Washington, D.C.: Transportation Research Board, National Research Council. (pp 199-207).
48. MARQUIS, B., Bradbury, R.L., Colson, S., Malick, R.B., Nanagiri, Y.V., Gould, J.S., O'Brien, S., and Marshall, M. 2003. *Design, Construction and Early Performance of Foamed Asphalt Full Depth Reclaimed (FDR) Pavement in Maine.* **Proceedings of the 82nd Annual Meeting of**

Transportation Research Board (CD-ROM). Washington, D.C.: Transportation Research Board, National Research Council.

49. KIM, Y. and Lee, H.D. 2006. *Development of a Mix Design Procedure for Cold In-Place Recycling with Foamed Asphalt.* **Journal of Materials in Civil Engineering, Vol 18, No 1.** (pp 116-124).
50. MITCHELL, J.K. 1993. **Fundamentals of Soil Behavior.** New York, NY: Wiley.
51. LU, N., Wu, B., and Tan, C.P. 2007. *Tensile Strength Characteristics of Unsaturated Sands.* **Journal of Geotechnical and Geoenvironmental Engineering, Vol 133, No 2.** (pp 144-154).
52. EBELS, L.J. and Jenkins, K.J. 2006. *Determination of Material Properties of Bitumen Stabilised Materials Using Tri-axial Testing.* **Proceedings of the 10th International Conference on Asphalt Pavements (CD-Rom).** Quebec City, Canada.
53. FU, P. and Harvey, J.T. 2007. *Temperature Sensitivity of Foamed Asphalt Mix Stiffness: Field and Laboratory Study.* **International Journal of Pavement Engineering, Vol 8, No 2.** (pp 137-145).
54. JENKINS, K.J., Long, F.M., and Ebels, L.J. 2007. *Foamed Bitumen Mixes = Shear Performance?* **International Journal of Pavement Engineering, Vol 8, No 2.** (pp 85-98).
55. CHIU, C. T. and Lewis A. J. N. 2006. *A Study on Properties of Foamed-Asphalt-Treated Mixes.* **Journal of Testing and Evaluation, Vol 34, No 1.** (pp 5-10).
56. KHWEIR, K. 2007. *Performance of Foamed Bitumen-Stabilised Mixtures.* **Proceedings of the Institution of Civil Engineers: Transport, Vol 160, No 2.** (pp 67-72).
57. FILZ, G.M. and Duncan, J.M. 1996. *Earth Pressures Due to Compaction: Comparison of Theory with Laboratory and Field Behavior.* **Transportation Research Record: Journal of the Transportation Research Board, No 1526.** Washington, D.C.: Transportation Research Board, National Research Council. (pp 28-37).
58. JENKINS, K.J., Van de Ven, M.F.C., Molenaar, A.A.A., and de Groot, J.L.A. 2002. *Performance Prediction of Cold Foamed Bitumen Mixes.* **Proceedings of the 9th International Conference on Asphalt Pavements (CD-ROM).** Copenhagen, Denmark.
59. LANE, B. and Kazmierowski, T. 2005. *Implementation of Cold In-Place Recycling with Expanded Asphalt Technology in Canada.* **Transportation Research Record: Journal of the Transportation Research Board, No 1905.** Washington, D.C.: Transportation Research Board, National Research Council. (pp 17-24).
60. ULLIDTZ, P. 2001. *Distinct Element Method for Study of Failure in Cohesive Particulate Media.* **Transportation Research Record: Journal of the Transportation Research Board, No 1757.** Washington, D.C.: Transportation Research Board, National Research Council. (pp 127-133).
61. PICKERING, D.J. 1970. *Anisotropic Elastic Parameters for Soil.* **Geotechnique, Vol 20, No 3.** (pp 271–276).

62. GRAHAM, J. and Houlsby, G.T. 1983. *Elastic Anisotropy of a Natural Clay.* **Geotechnique, Vol 33, No 2.** (pp 165-180).

63. TUTUMLUER, E. and Thompson, M.R. 1997. *Anisotropic Modeling of Granular Bases in Flexible Pavements.* **Transportation Research Record: Journal of the Transportation Research Board, No 1577.** Washington, D.C.: Transportation Research Board, National Research Council. (pp 18-26).

64. ADU-OSEI, A., Little, D.N. and Lytton, R.L. 2001. *Cross-Anisotropic Characterization of Unbound Granular Materials.* **Transportation Research Record: Journal of the Transportation Research Board, No 1757.** Washington, D.C.: Transportation Research Board, National Research Council. (pp 82-91).

65. DESAI, C.S., Siriwardane, H.J., and Janardhanan, R. 1983. **Interaction and Load Transfer in Track Support Structures, Part 2: Testing and Constitutive Modeling of Materials and Interfaces.** Washington, D.C.: Office of University Research, U.S. Department of Transportation. (Final Report, Contract DOT-US-05-80013).

66. TUTUMLUER, E. and Seyhan, U. 1999. *Laboratory Determination of Anisotropic Aggregate Resilient Moduli Using an Innovative Test Device.* **Transportation Research Record: Journal of the Transportation Research Board, No 1687.** Washington, D.C.: Transportation Research Board, National Research Council. (pp 13-21).

67. DUNCAN, J.M. and Seed, R.B. 1986. *Compaction-Induced Earth Pressures Under K_0-Conditions.* **Journal of the Geotechnical Engineering Division, ASCE, Vol 112, No 1.** (pp 1–22).

68. LEWIS, A.J.N. and Collings, D.C. 1999. *Cold In-Place Recycling: a Relevant Process for Road Rehabilitation and Upgrading.* **Proceedings 7th Conference on Asphalt Pavements for Southern Africa (CAPSA'99).** Victoria Falls, Zimbabwe.

69. HODGKINSON, A. and Visser, A.T. 2004. *The Role of Fillers and Cementitious Binders when Recycling with Foamed Bitumen or Bitumen Emulsion.* **Proceedings 8th Conference on Asphalt Pavements for Southern Africa (CAPSA'04).** Sun City, South Africa. (pp 512-521).

70. **Stabilization Manual.** 2004. Pretoria, South Africa: Gauteng Department of Public Transport, Roads and Works. (Manual L2/04).

71. VAN TIL, C.J., McCullough, B.F., Vallerga, B.A., and Hicks, R.G. 1972. **Evaluation of AASHO Interim Guides for Design of Pavement Structures, NCHRP 128**. Washington, DC: Highway Research Board.

72. **Shell Pavement Design Manual.** 1978. London, UK: Shell International Petroleum Company, Limited.

73. STEVEN, B.D., Jeon, E.J. and Harvey, J.T. 2006. **Initial Recommendation of a Gravel factor for Pulverized Asphalt Concrete Used as an Unbound Base.** Davis and Berkeley, CA: University of California Pavement Research Center. (Technical Memorandum: UCPRC-TM-2006-13).

74. JONES, D., Fu, P. and Harvey, J.T. 2008. **Full-Depth Pavement Reclamation with Foamed Asphalt: Guideline for Project Selection, Design, and Construction.** Davis and Berkeley, CA: University of California Pavement Research Center. (UCPRC-GL-2008-01).

75. **Standard Specifications. State of California Business, Transportation and Housing Agency. Department of Transportation.** 2006. Sacramento, CA: California Department of Transportation.

APPENDIX A

BACKCALCULATED FALLING WEIGHT DEFLECTOMETER RESULTS

APPENDIX A: BACKCALCULATED FWD RESULTS

The backcalculated resilient moduli of the asphalt concrete layer (E_{AC}), the foamed asphalt layer (E_{FA}), and the subgrade (E_{SG}) for Sections on Route 20 (Colusa County) and Route 33 (San Luis Obispo/Santa Barbara and Ventura Counties) as measured during the course of the study are plotted in Figure A.1 through Figure A.14.

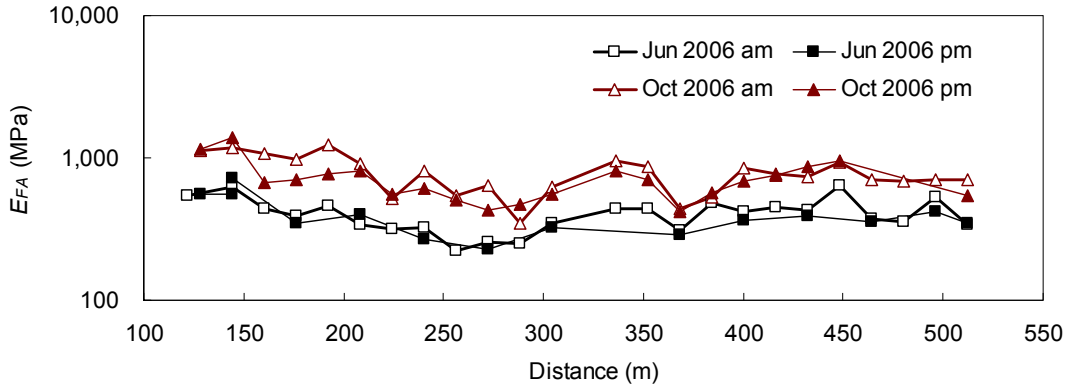

(a)

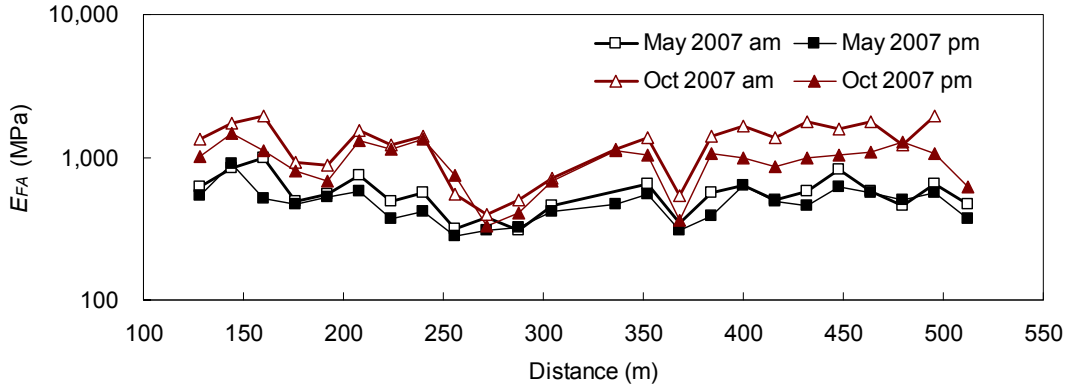

(b)

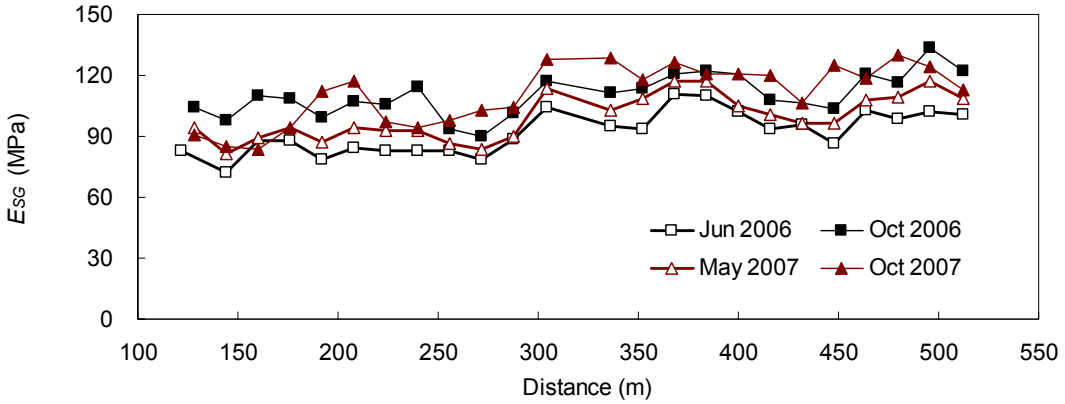

(c)

Figure A.1: Backcalculated Resilient Modulus for Section SR20-A.
([a] Foamed asphalt-treated layer in 2006; [b] foamed asphalt-treated layer in 2007; and [c] subgrade)

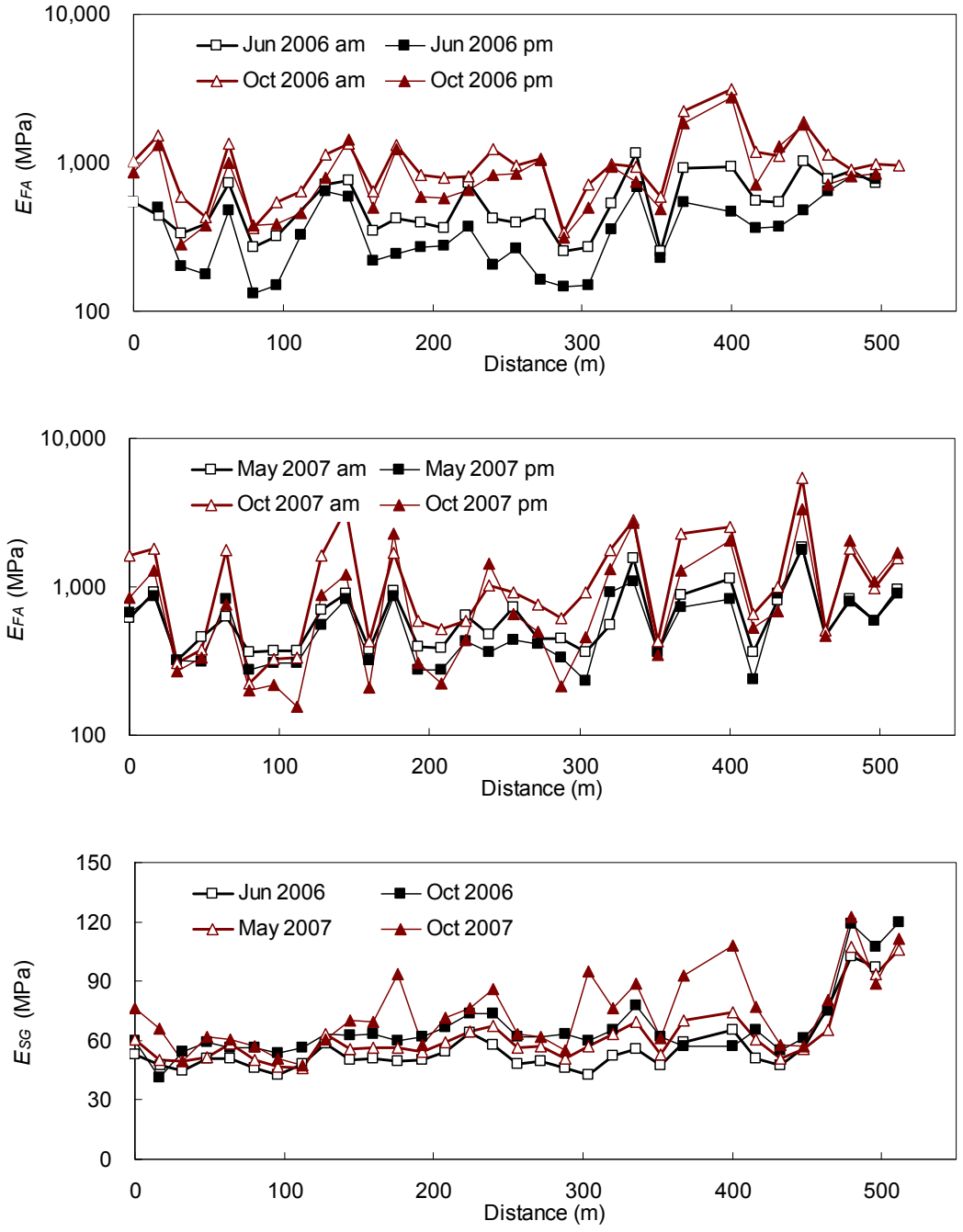

Figure A.2: Backcalculated Resilient Modulus for Section SR20-B.
([a] Foamed asphalt-treated layer in 2006; [b] foamed asphalt-treated layer in 2007; and [c] subgrade)

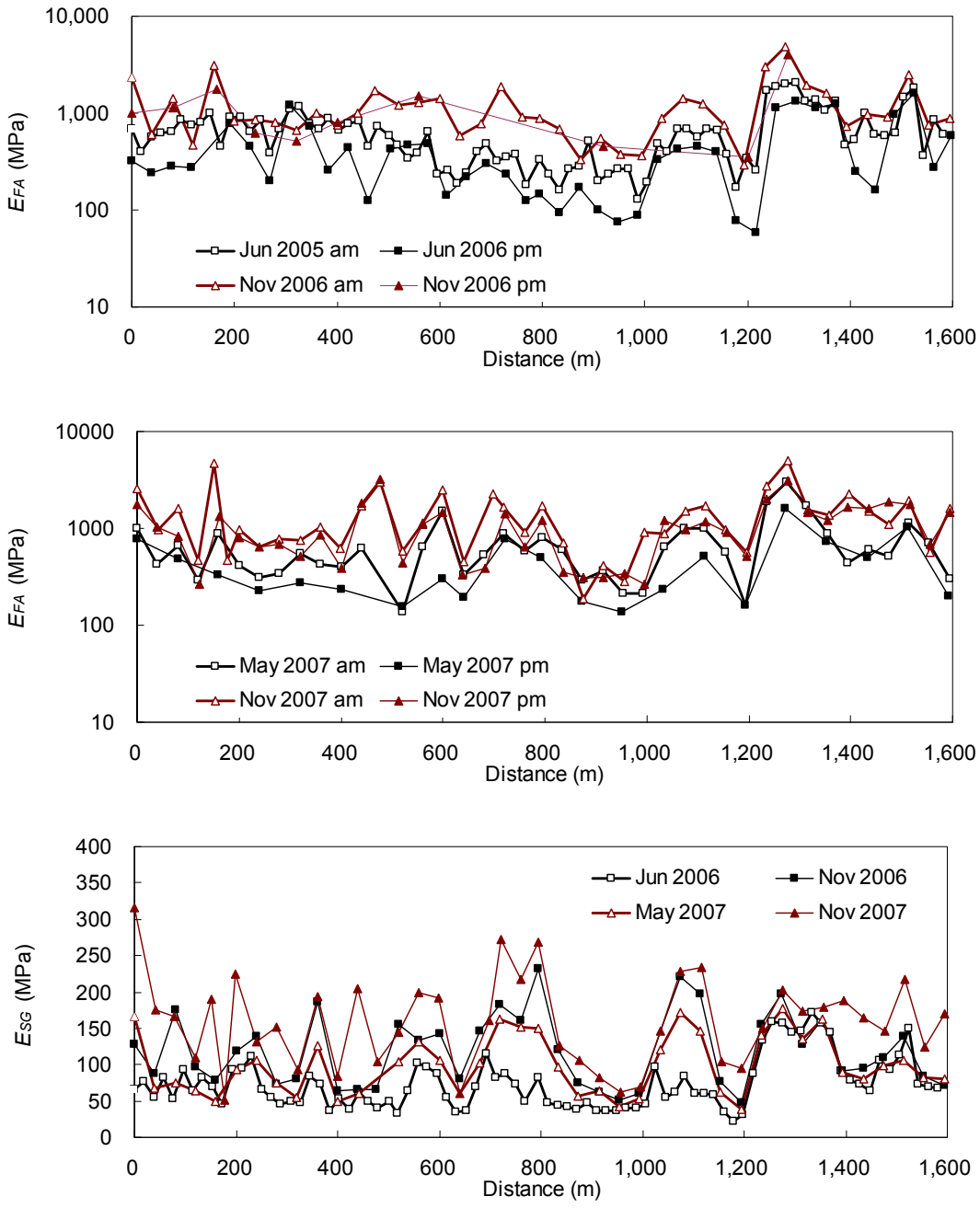

Figure A.3: Backcalculated Resilient Modulus for Section SR33-Ven-A.
([a] Foamed asphalt-treated layer in 2006; [b] foamed asphalt-treated layer in 2007; and [c] subgrade)

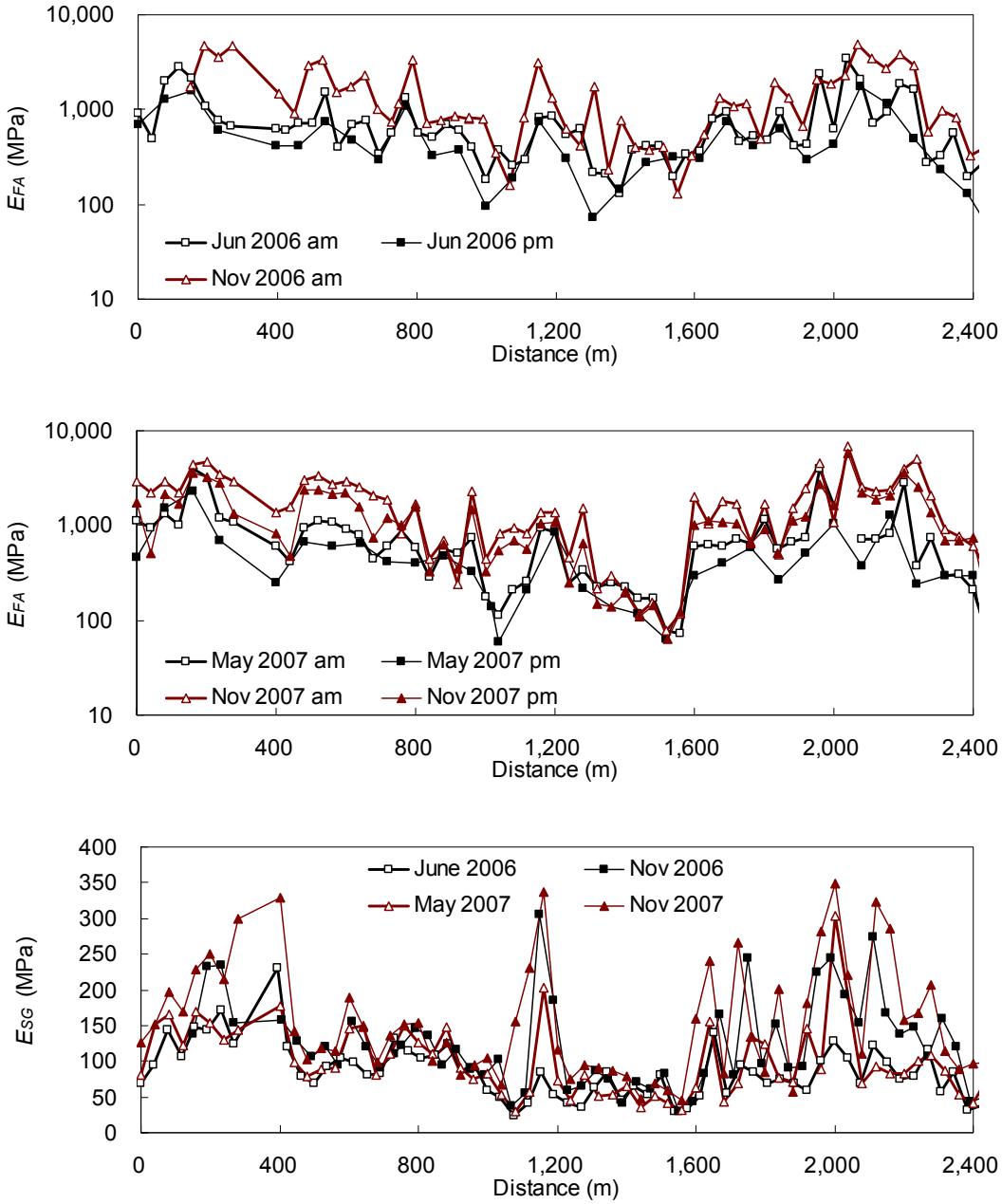

Figure A.4: Backcalculated Resilient Modulus for Section SR33-Ven-B.
([a] Foamed asphalt-treated layer in 2006; [b] foamed asphalt-treated layer in 2007; and [c] subgrade)

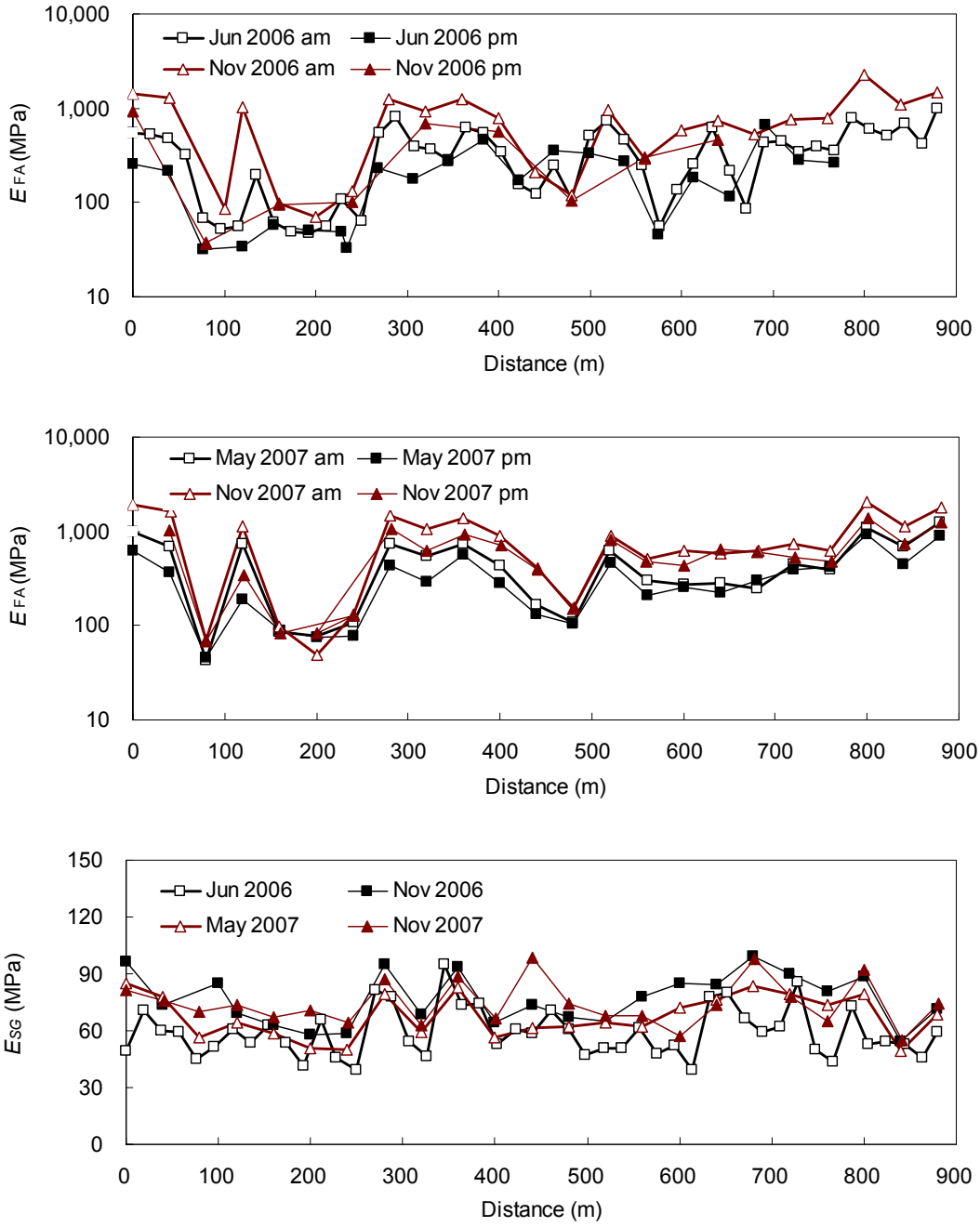

Figure A.5: Backcalculated Resilient Modulus for Section SR33-SB/SLO-A.
([a] Foamed asphalt-treated layer in 2006; [b] foamed asphalt-treated layer in 2007; and [c] subgrade)

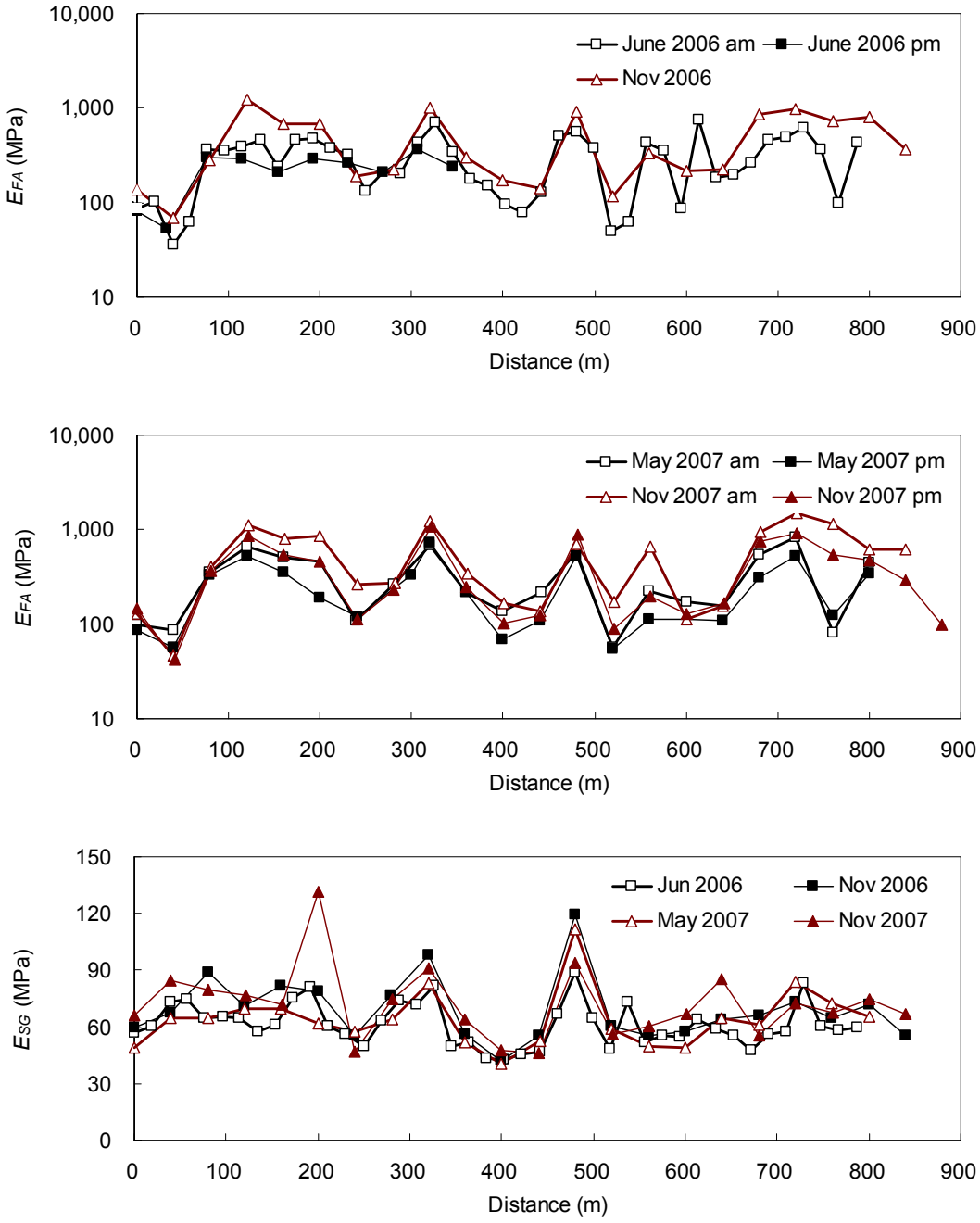

Figure A.6: Backcalculated Resilient Modulus for Section SR33-SB/SLO-B.
([a] Foamed asphalt-treated layer in 2006; [b] foamed asphalt-treated layer in 2007; and [c] subgrade)

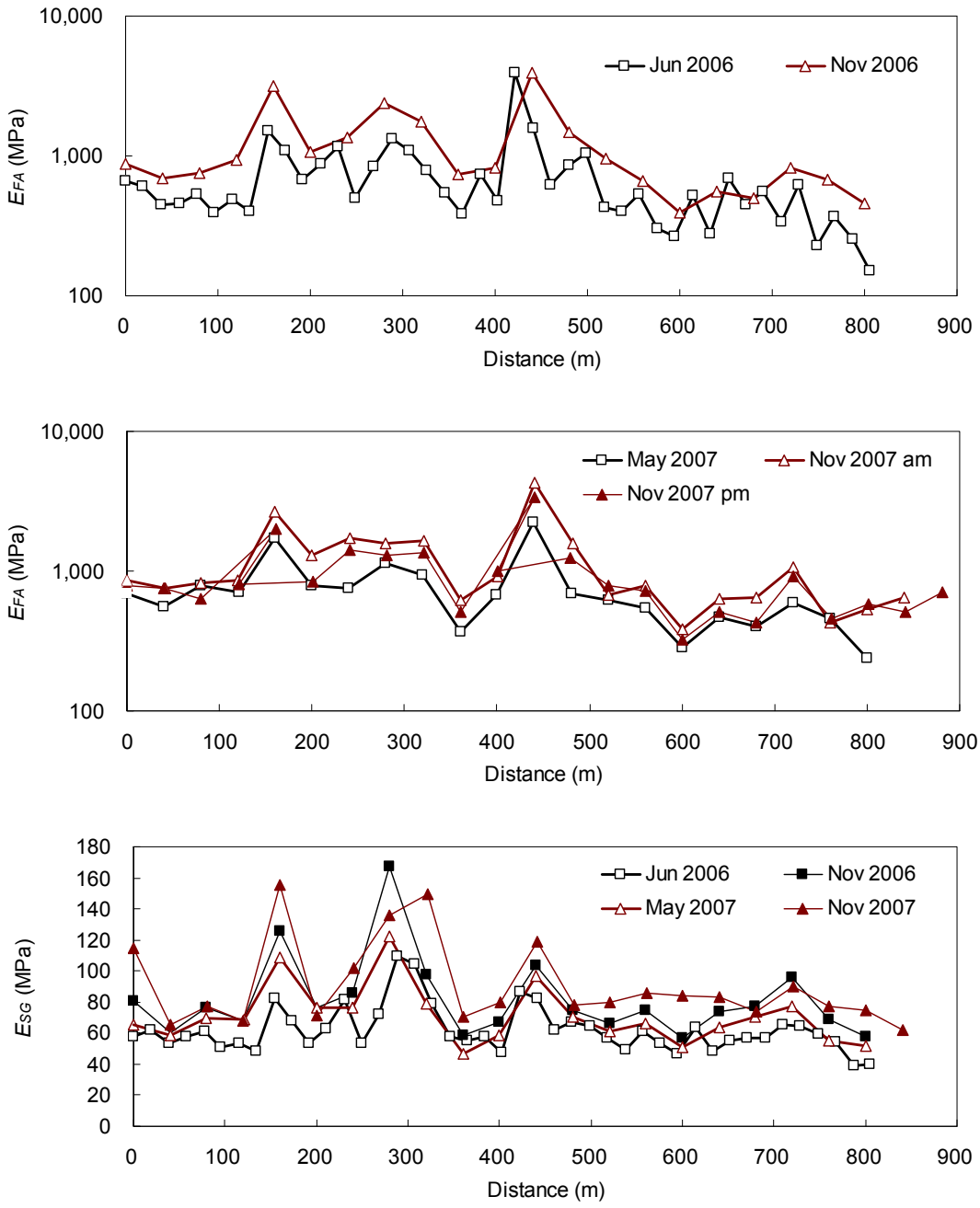

Figure A.7: Backcalculated Resilient Modulus for Section SR33-SB/SLO-C.
([a] Foamed asphalt-treated layer in 2006; [b] foamed asphalt-treated layer in 2007; and [c] subgrade)

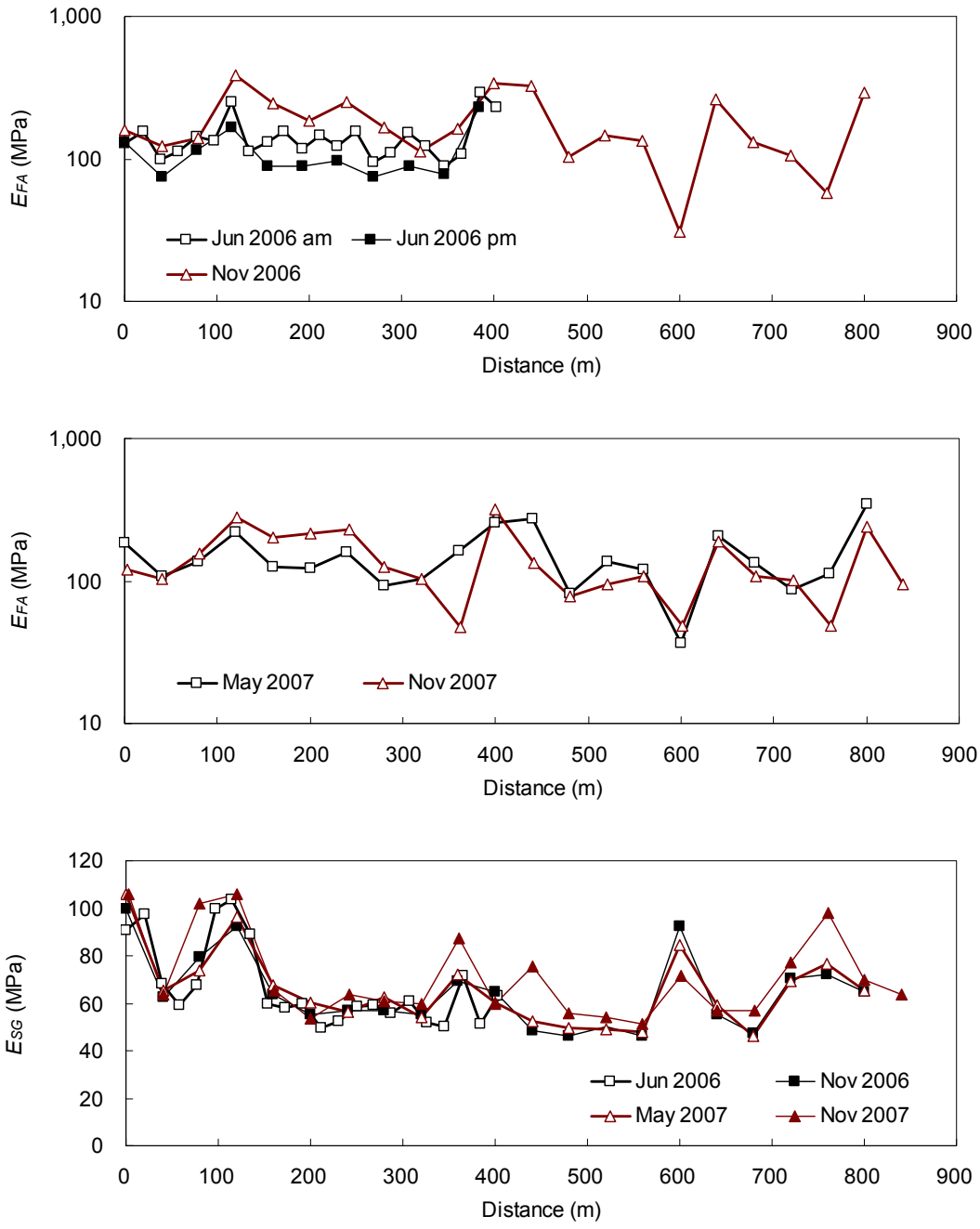

Figure A.8: Backcalculated Resilient Modulus for Section SR33-SB/SLO-D.
([a] Foamed asphalt-treated layer in 2006; [b] foamed asphalt-treated layer in 2007; and [c] Subgrade)

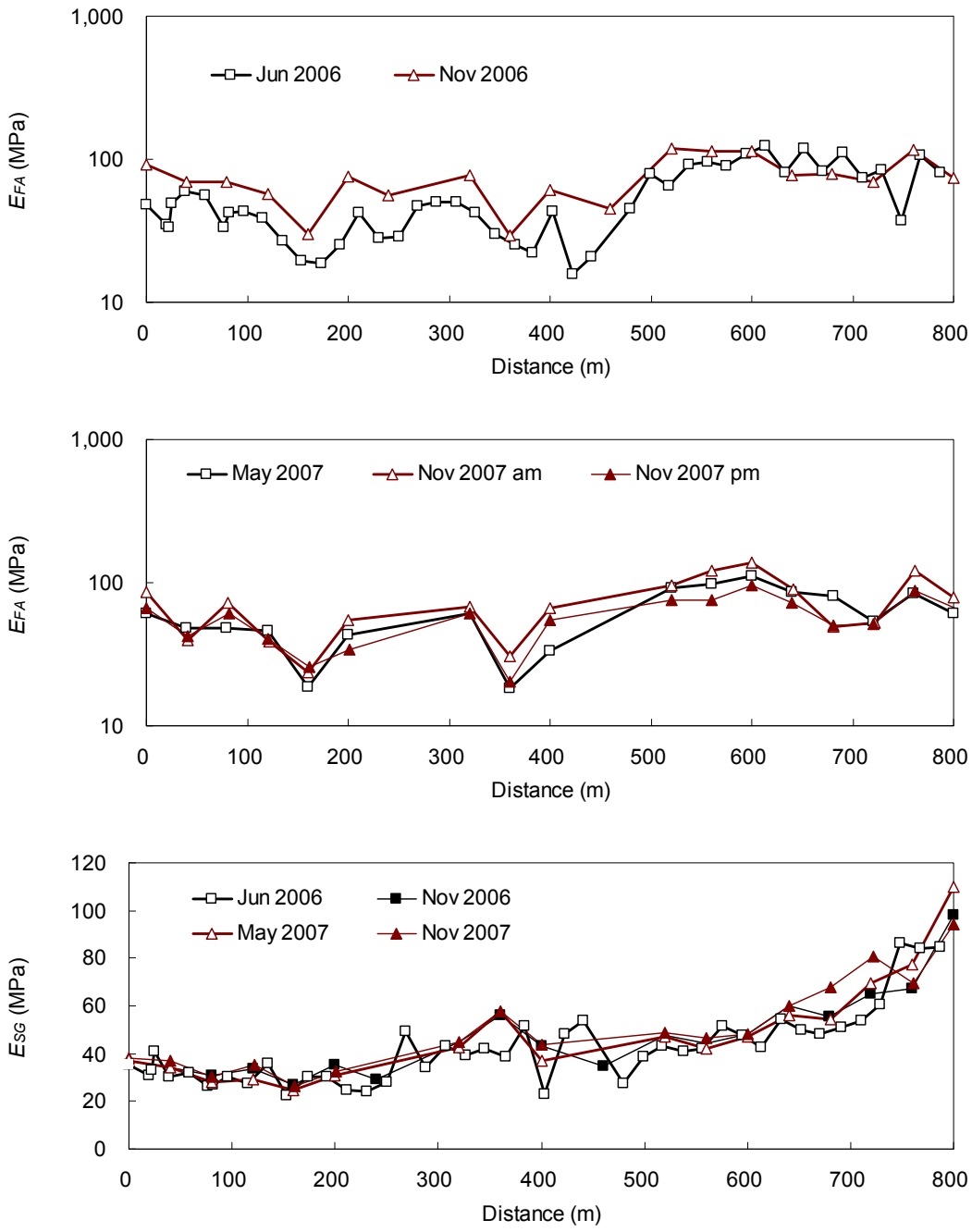

Figure A.9: Backcalculated Resilient Modulus for Section SR33-SB/SLO-E.
([a] Foamed asphalt-treated layer in 2006; [b] foamed asphalt-treated layer in 2007; and [c] subgrade)

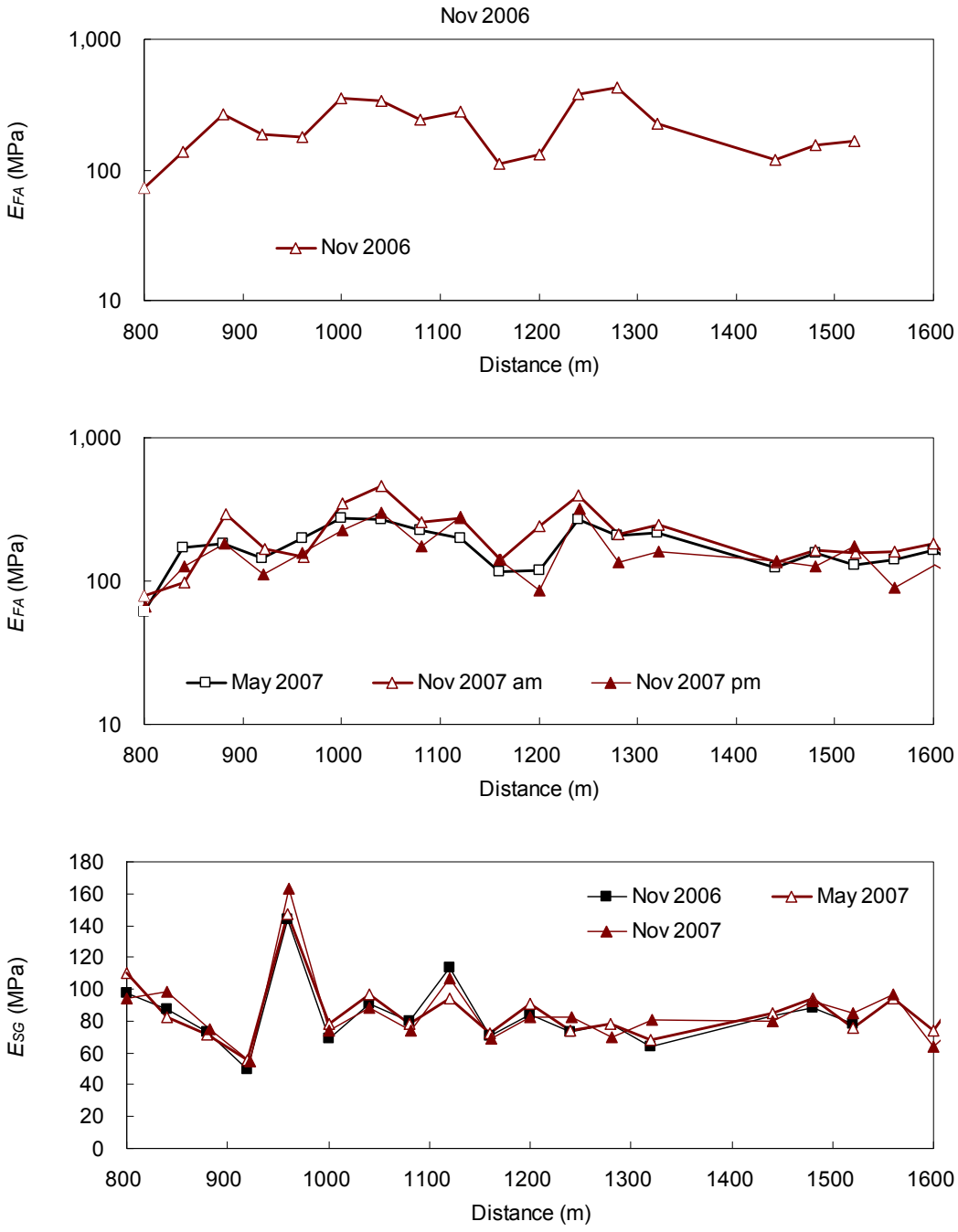

Figure A.10: Backcalculated Resilient Modulus for Section SR33-SB/SLO-F.
([a] Foamed asphalt-treated layer in 2006; [b] foamed asphalt-treated layer in 2007; and [c] subgrade)

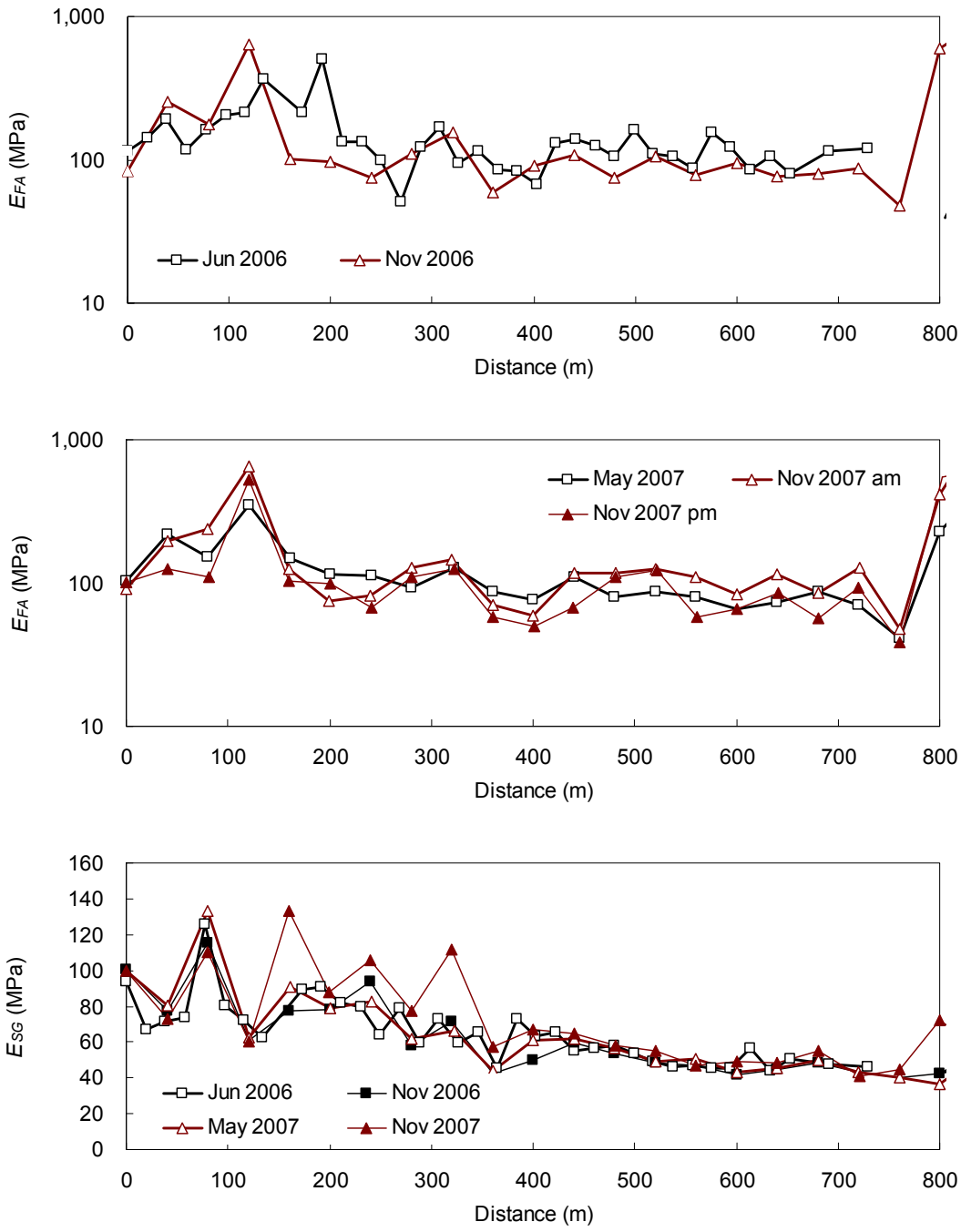

Figure A.11: Backcalculated Resilient Modulus for Section SR33-SB/SLO-G.
([a] Foamed asphalt-treated layer in 2006; [b] foamed asphalt-treated layer in 2007; and [c] subgrade)

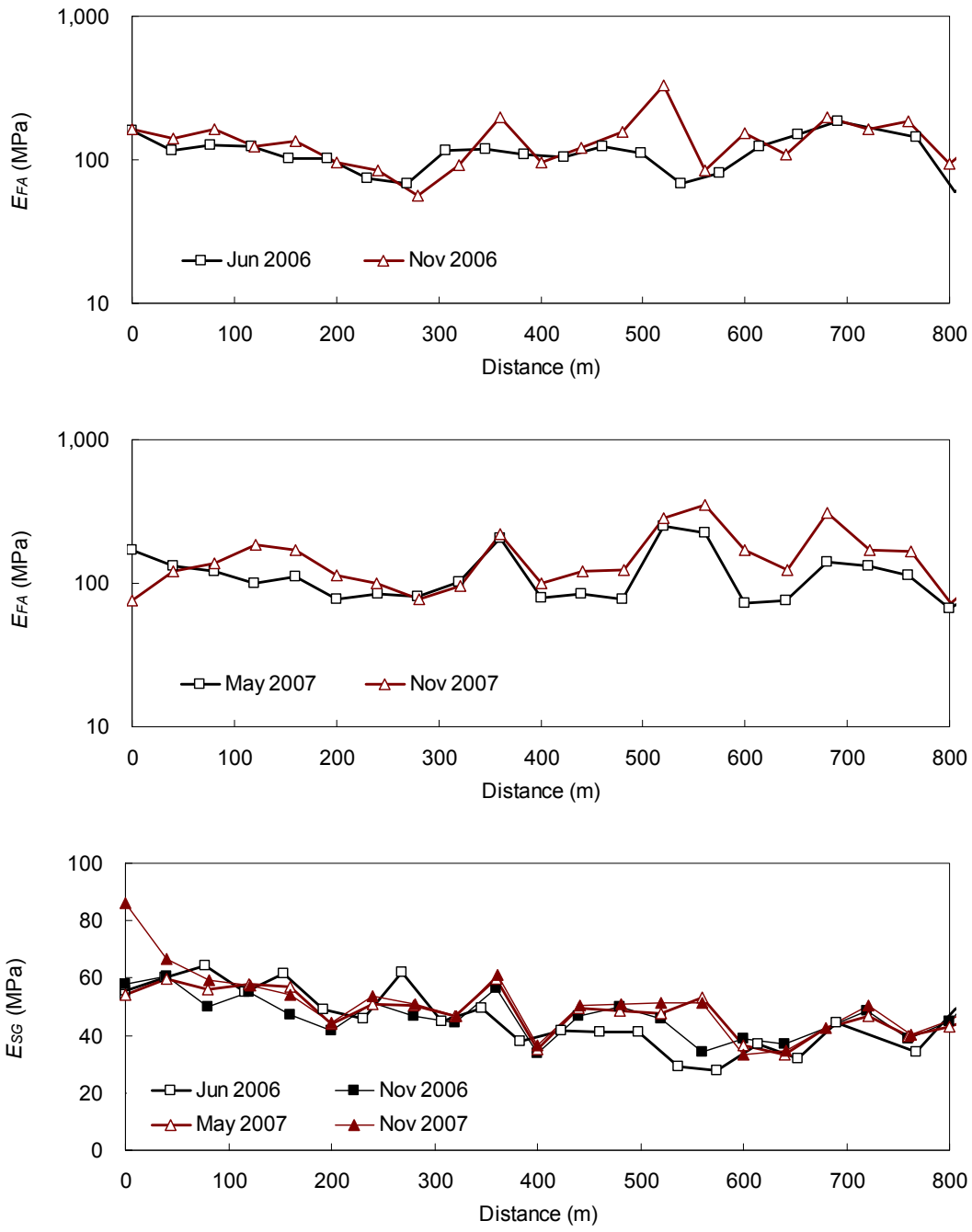

Figure A.12: Backcalculated Resilient Modulus for Section SR33-SB/SLO-H.
([a] Foamed asphalt-treated layer in 2006; [b] foamed asphalt-treated layer in 2007; and [c] subgrade)

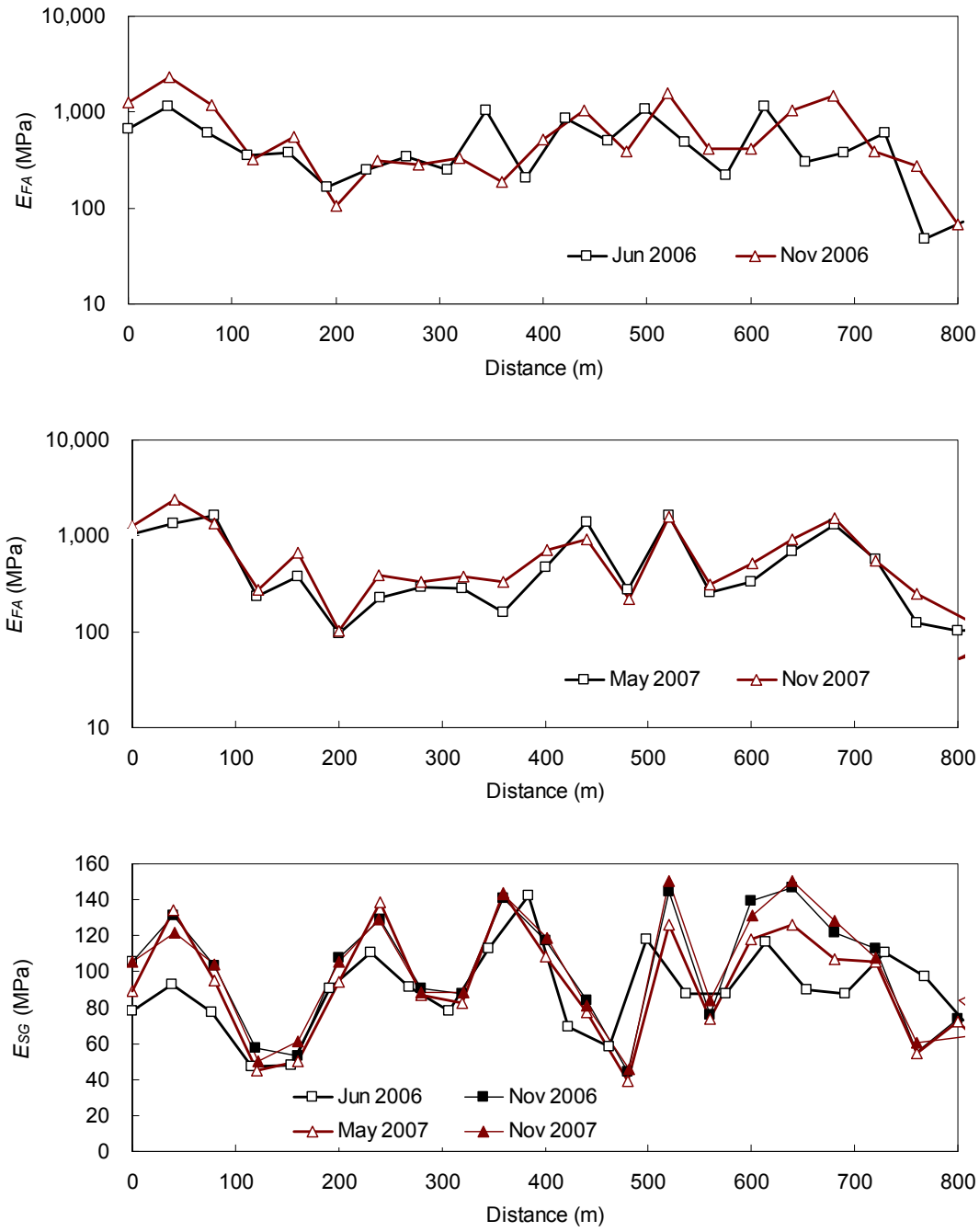

Figure A.13: Backcalculated Resilient Modulus for Section SR33-SB/SLO-I
([a] Foamed asphalt-treated layer in 2006; [b] foamed asphalt-treated layer in 2007; and [c] subgrade)

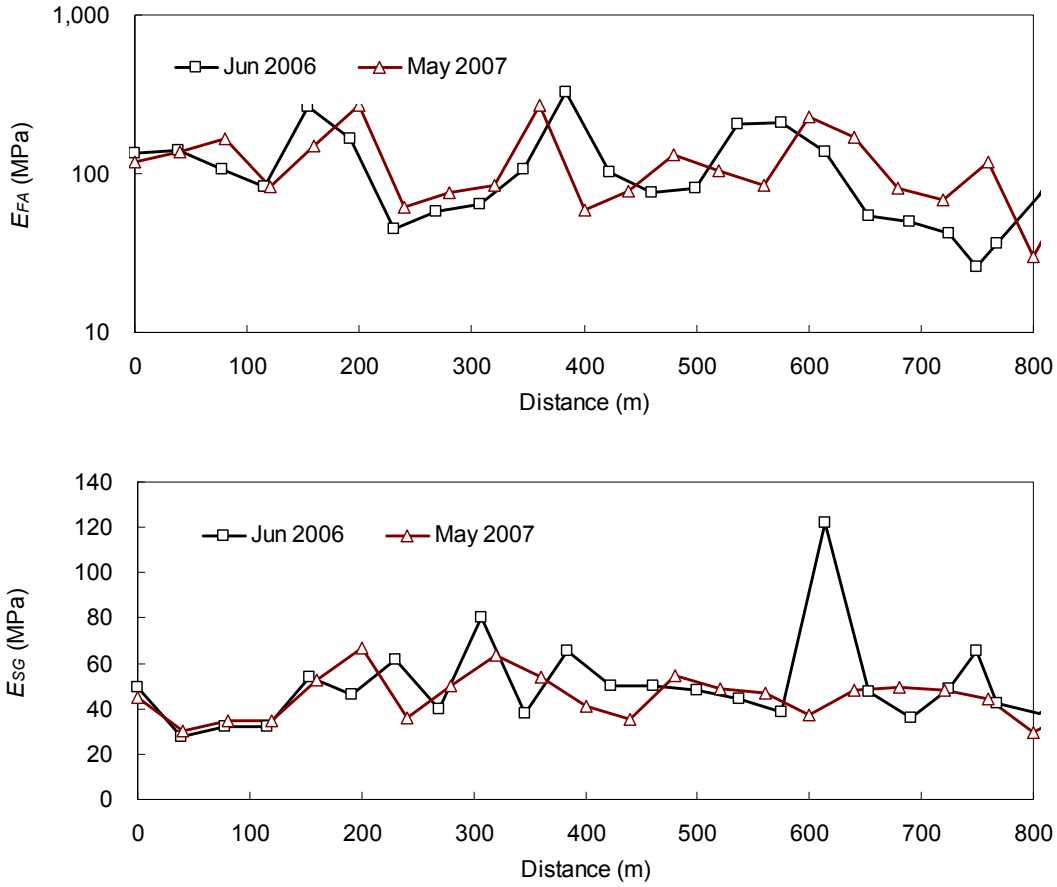

Figure A.14: Backcalculated Resilient Modulus for Section SR33-SB/SLO-J
([a] Foamed asphalt-treated layer in 2006; and [b] subgrade)

APPENDIX B

ASPHALT BINDER PERFORMANCE GRADE CERTIFICATION TESTS

APPENDIX B: PERFORMANCE GRADE CERTIFICATION TESTS

The results of performance grade certification tests for the various asphalt binders used in the UCPRC laboratory study are shown on the following pages. Tests were undertaken by the binder suppliers.

Shell Oil Products US

Martinez Refinery
PO BOX 711 Martinez, CA 94553

CERTIFICATE OF ANALYSIS

22-AUG-2006

Consignee: Asphalt Customer

Shipping Date: 22-AUG-2006

Asphalt

SMR Code	APH-PGGRADING
SMR Blend ID	PG-GRADING-06-0099
Certification Date	8-19-2006
Tender Type	PG 64-10
Tender Name/Number	Tank 00561

Sample Point TK-00561

Properties	Specifications	Units	Results
PAV Aging Temp		deg	100
0 C Average Stiffness, M	<=300	MPa	116
0 C Average m-Value	>=0.300	m	0.420
Viscosity, Brookfield	<=3	PaS	0.425
64C G*/SinAngle, calc	>=1000	Pa	2202
28C G* x SinAngle, calc	<=5000000	Pa	7459399
64C G*/SinAngle, calc	>=2200	Pa	4966
Flash, COC, deg C	>=230	deg_C	308
Ductility on RTFO		cm	>150
Mass Loss, RTFO, %		%	-0.198

- Samples for CAL Berkeley
-

Kevin A. Cray
SMR REPRESENTATIVE

Approved Cray, Kevin A SOPUS-CMU/334 Page 1 of 1

Shell Oil Products US

Martinez Refinery
PO BOX 711 Martinez, CA 94553

CERTIFICATE OF ANALYSIS

22-AUG-2006

Consignee: Asphalt Customer

Shipping Date: 22-AUG-2006

Asphalt

SMR Code	APH-PGGRADING
SMR Blend ID	PG-GRADING-06-0098
Certification Date	8-19-2006
Tender Type	PG 64-16
Tender Name/Number	Tank 00560

Sample Point TK-00560

Properties	Specifications	Units	Results
PAV Aging Temp		deg	100
-6 C Average Stiffness,	<=300	MPa	182
-6 C Average m-Value	>=0.300	m	0.354
Viscosity, Brookfield	<=3	PaS	0.344
64C G*/SinAngle, calc	>=1000	Pa	1341
28C G* x SinAngle, calc	<=5000000	Pa	4229060
64C G*/SinAngle, calc	>=2200	Pa	2925
Flash, COC, deg C	>=230	deg_C	282
Ductility on RTFO		cm	>150
Mass Loss, RTFO, %		%	-0.202

- Samples for CAL Berkeley
-

Kevin A. Cray
SMR REPRESENTATIVE

Approved Cray, Kevin A SOPUS-OMU/334

Page 1 of 1

Martinez, Paul H SOPUS-DMW/311

From: sampman-houhdcs908-S
Sent: Monday, January 08, 2007 4:30 PM
To: Martinez, Paul H SOPUS-DMW/311
Subject: Martinez G-LIMS Report

Laboratory Quality Control Summary
Requestor: BACKGROUND
Date/Time: 08-JAN-2007 16:28:03

Blend ID: LC-WKSPLT-07-0002 Product Name:50264
Blend Type: LC-Asphalt Weekly Split Version: 1
Blend Status: Authorised Product Code:50264
Created on: 05-JAN-2007 12:37:15 Description: PG64-16
Test Lab: NOGROUP
Requesting Unit: OMULO-APH
Source: TK-00560
Source Description: TK-00560

Certified ON-SPEC for Level MZ-SPEC

Levels	Tests	Component	Spec Limits	Results
Units	S	SmpRef		
50264				
MZ-SPEC (Martinez Specifications)				
Sample Tests				
	R29	PG Grade		PG64-16
Y	1			
	T240	Mass Loss, RTFO, %	-1.000 <=> 1.000	-0.245
%	Y	1		
	T313--6C	PAV Aging Temp		100
deg_C	Y	1		
	T313--6C	-6 C Average Stiffness, MPa	0 <=> 300	200
MPa	Y	1		
	T313--6C	-6 C Average m-Value	0.300 <=> 1000.000	0.372
m	Y	1		
	T316	Viscosity, Brookfield	0.000 <=> 3.000	0.300
PaS	Y	1		
	T315-ORG	58C G*/SinAngle, calc		0
Pa	Y	1		
	T315-ORG	Average Viscostiy at 60C		0.00
Pa	Y	1		
	T315-ORG	64C G*/SinAngle, calc	>=1000	1100
Pa	Y	1		
	T315-ORG	70C G*/SinAngle, calc		0
Pa	Y	1		
	T315-PAV	PAV Aging Temp		100.00
deg	Y	1		
	T315-PAV	22C G* x SinAngle, calc		0
Pa	Y	1		
	T315-PAV	25C G* x SinAngle, calc		7161132
Pa	Y	1		
	T315-PAV	28C G* x SinAngle, calc	<=5000000	4631522
Pa	Y	1		
	T315-PAV	31C G* x SinAngle, calc		0
Pa	Y	1		
	T315-PAV	34C G* x SinAngle, calc		0
Pa	Y	1		
	T315-PAV	37C G* x SinAngle,calc		0
a	Y	1		
	T315-RTFO	58C G*/SinAngle, calc		0
Pa	Y	1		
	T315-RTFO	Average Viscostiy at 60C		0

1

Pa	Y	1			
	T315-RTFO	64C G*/SinAngle, calc		>=2000	2494
Pa	Y	1			
	T315-RTFO	70C G*/SinAngle, calc			0
Pa	Y	1			
	T48	Flash, COC, deg C		>=232	304
deg_C	Y	1			
	T51	Ductility on RTFO		>=75	>150
cm	Y	1			
	T44	Soluable Material			99.99
%	Y	1			
	D-00070	Specific Gravity at 77F			1.0153
Y	1				

SmpRef	Sample	Status
1	196858	Authorised

Page 1

2

Martinez, Paul H SOPUS-DMW/311

From: sampman-houhdcs908-S
Sent: Sunday, January 07, 2007 5:24 PM
To: Martinez, Paul H SOPUS-DMW/311
Subject: Martinez G-LIMS Report

Laboratory Quality Control Summary
Requestor: BACKGROUND
Date/Time: 07-JAN-2007 17:22:31

Blend ID: LC-WKSPLT-07-0003 Product Name:50266
Blend Type: LC-Asphalt Weekly Split Version: 2
Blend Status: Authorised Product Code:50266
Created on: 05-JAN-2007 12:38:07 Description: PG64-10
Test Lab: NOGROUP
Requesting Unit: OMULO-APH
Source: TK-00561
Source Description: TK-00561

Certified ON-SPEC for Level MZ-SPEC

Levels Units	Tests S	Component SmpRef	Spec Limits	Results
50266				
MZ-SPEC (Martinez Specifications)				
Sample Tests				
	R29	PG Grade		PG64-10
Y	1			
	T240	Mass Loss, RTFO, %	-1.000 <=> 1.000	-0.238
%	Y	1		
	T313-0C	PAV Aging Temp	100 <=> 100	100
deg_C	Y	1		
	T313-0C	0 C Average Stiffness, MPa	0 <=> 300	100
MPa	Y	1		
	T313-0C	0 C Average m-Value	0.300 <=> 0.900	0.452
m	Y	1		
	T316	Viscosity, Brookfield	0.000 <=> 3.000	0.384
PaS	Y	1		
	T315-ORG	58C G*/SinAngle, calc		0
Pa	Y	1		
	T315-ORG	Average Viscostiy at 60C		0.00
Pa	Y	1		
	T315-ORG	64C G*/SinAngle, calc	>=1000	1711
Pa	Y	1		
	T315-ORG	70C G*/SinAngle, calc		0
Pa	Y	1		
	T315-PAV	PAV Aging Temp		100.00
deg	Y	1		
	T315-PAV	22C G* x SinAngle, calc		0
Pa	Y	1		
	T315-PAV	25C G* x SinAngle, calc		0
Pa	Y	1		
	T315-PAV	28C G* x SinAngle, calc		7191080
Pa	Y	1		
	T315-PAV	31C G* x SinAngle, calc	0 <=> 5000000	4567428
Pa	Y	1		
	T315-PAV	34C G* x SinAngle, calc		0
Pa	Y	1		
	T315-PAV	37C G* x SinAngle,calc		0
a	Y	1		
	T315-RTFO	58C G*/SinAngle, calc		0
Pa	Y	1		
	T315-RTFO	Average Viscostiy at 60C		0

1

Pa	Y	1			
	T315-RTFO	64C G*/SinAngle, calc		>=2200	4031
Pa	Y	1			
	T315-RTFO	70C G*/SinAngle, calc			0
Pa	Y	1			
	T48	Flash, COC, deg C		232 <=> 343	290
deg_C	Y	1			
	T51	Ductility on RTFO		>=75	>150
cm	Y	1			
	D-00070	Specific Gravity at 77F			1.0183
Y	1				
	Perodic Tests				
	T44	Soluable Material			99.99
%	Y	1	2006/07/13		

SmpRef	Sample	Status
1	196859	Authorised

Laboratory Quality Control Condensed Summary

Requestor: MARTIPH
Date/Time: 16-JAN-2007 15:00:30

Sample Desc: Weekly Split on TK-00558
Sample ID: 188741
Sample Type: LC-WKSPLT
Sample Status: Authorised
Sampled on: 21-DEC-2006 13:50:38
Test Lab: NOGROUP
Blend ID: LC-WKSPLT-06-0097
Requesting Unit: OMULO-APH
Source: TK-00558
Source Description: TK-00558

Product Name: 50399
Version: 1
Product Code: 50399
Description: PG70-10

Certified ON-SPEC for Level MZ-SPEC

Tests	Component	Results
50399		
Sample Tests		
R29	PG Grade	PG70-10
T240	Mass Loss, RTFO, %	-0.236
T313-0C	PAV Aging Temp	110
T313-0C	0 C Average Stiffness, MPa	182
T313-0C	0 C Average m-Value	0.365
T316	Viscosity, Brookfield	0.458
T315-ORG	58C G*/SinAngle, calc	0
T315-ORG	Average Viscostiy at 60C	0.00
T315-ORG	64C G*/SinAngle, calc	0
T315-ORG	70C G*/SinAngle, calc	1100
T315-PAV	PAV Aging Temp	110.00
T315-PAV	22C G* x SinAngle, calc	0
T315-PAV	25C G* x SinAngle, calc	0
T315-PAV	28C G* x SinAngle, calc	0
T315-PAV	31C G* x SinAngle, calc	5494286
T315-PAV	34C G* x SinAngle, calc	3956118
T315-PAV	37C G* x SinAngle,calc	0
T315-RTFO	58C G*/SinAngle, calc	0
T315-RTFO	Average Viscostiy at 60C	0
T315-RTFO	64C G*/SinAngle, calc	-1.$
T315-RTFO	70C G*/SinAngle, calc	2594
T48	Flash, COC, deg C	313
T51	Ductility on RTFO	>150
D-00070	Specific Gravity at 77F	1.0205

Page 1

Laboratory Quality Control Summary

Requestor:	MARTIPH		
Date/Time:	16-JAN-2007 12:13:42		
Sample Desc:	Weekly Split on TK-00558		
Sample ID:	188741	Product Name:	50399
Sample Type:	LC-WKSPLT	Version:	1
Sample Status:	Authorised	Product Code:	50399
Sampled on:	21-DEC-2006 13:50:38	Description:	PG70-10
Test Lab:	NOGROUP		
Blend ID:	LC-WKSPLT-06-0097		
Requesting Unit:	OMULO-APH		
Source:	TK-00558		
Source Description:	TK-00558		

Certified ON-SPEC for Level MZ-SPEC

Levels	Tests	Component	Spec Limits
50399			
MZ-SPEC (Martinez Specifications)			
Sample Tests			
	R29	PG Grade	
	T240	Mass Loss, RTFO, %	-1.000 <=> 1.000
	T313-0C	PAV Aging Temp	
	T313-0C	0 C Average Stiffness, MPa	0 <=> 300
	T313-0C	0 C Average m-Value	0.300 <=> 0.900
	T316	Viscosity, Brookfield	0.000 <=> 3.000
	T315-ORG	58C G*/SinAngle, calc	
	T315-ORG	Average Viscostiy at 60C	
	T315-ORG	64C G*/SinAngle, calc	
	T315-ORG	70C G*/SinAngle, calc	1000 <=> 10000
	T315-PAV	PAV Aging Temp	
	T315-PAV	22C G* x SinAngle, calc	
	T315-PAV	25C G* x SinAngle, calc	
	T315-PAV	28C G* x SinAngle, calc	
	T315-PAV	31C G* x SinAngle, calc	
	T315-PAV	34C G* x SinAngle, calc	0 <=> 5000000
	T315-PAV	37C G* x SinAngle,calc	
	T315-RTFO	58C G*/SinAngle, calc	
	T315-RTFO	Average Viscostiy at 60C	
	T315-RTFO	64C G*/SinAngle, calc	
	T315-RTFO	70C G*/SinAngle, calc	2200 <=> 10000
	T48	Flash, COC, deg C	232 <=> 343
	T51	Ductility on RTFO	75 <=> 150
	D-00070	Specific Gravity at 77F	

VALERO
MARKETING AND SUPPLY COMPANY
1100 Willow Pass Road • Pittsburg, California 94565 • Telephone (925) 427-6880

CERTIFICATE OF COMPLIANCE

PG64-16

TANK: 5004 **Batch #073106031** **DATE: 08/01/06**

CONTRACTOR: _____ **PROJECT#:** _____

DESTINATION: _____

WT. TICKET #: _____ **SHIPMENT DATE:** _____

QUANTITY TONS: _____ **METRIC TONS:** _____

TEST DESCRIPTION	METHOD	RESULTS	SPEC.
Test on PAV Residue:	AASHTO		
Dynamic Shear @ 31°C, 10 rads^{-1}, G*/sinδ	T315	3760	5000 kPa max.
Creep Stiffness @ -6°C, 60s	T313	130	300 Mps max.
m-value	T313	0.354	0.300 min.
Test on RTFOT Residue:			
Mass Loss	T240	0.0440	0.5% max
Dynamic Shear @ 64°C, 10 rads^{-1}, G*/sinδ	T5	4.30	2.2 kPa min.
Ductility @ 25 C, 5 cm/min, cm	T51	80+	75 min.
Test on Original Asphalt:			
Flash Point Temp, °C	T48	230+	230°C min.
Rotational Viscosity @ 135 C, Pa.S	T316	0.096	3 Pa.S max
Dynamic Shear @ 64°C, 10 rads^{-1}, G*/sinδ	T315	2.00	1.0 kPa min

Valero Marketing & Supply-Pittsburg California hereby certifies that the asphalt product accompanying this certification was produced in accordance with the California Department of Transportation's Certification Program for Suppliers of Asphalt, and that this product complies in all respects with the requirements of the applicable specifications for the asphalt product identified on this document.

I hereby certify by my signature that I have the authority to represent the supplier providing the accompanying asphalt product.

Reviewed and approved
Patrick Sendegeya
Laboratory Supervisor

VALERO
MARKETING AND SUPPLY COMPANY
1100 Willow Pass Road • Pittsburg, California 94565 • Telephone (925) 427-6880

CERTIFICATE OF COMPLIANCE

PG64-10

TANK: 5004 **Batch #073106045** **DATE: 08/01/06**

CONTRACTOR: _____ **PROJECT#:** _____

DESTINATION: _____

WT. TICKET #: _____ **SHIPMENT DATE:** _____

QUANTITY TONS: _____ **METRIC TONS:** _____

TEST DESCRIPTION	METHOD	RESULTS	SPEC.
Test on PAV Residue:	AASHTO		
Dynamic Shear @ 31°C, 10 rads^{-1}, G*/sinδ	T315	2460	5000 kPa max.
Creep Stiffness @ 0°C, 60s	T313	48	300 Mps max.
m-value	T313	0.430	0.300 min.
Test on RTFOT Residue:			
Mass Change.	T240	0.0440	0.5%max
Dynamic Shear @ 64°C, 10 rads^{-1}, G*/sinδ	T5	4.30	2.2 kPa min.
Ductility @ 25 C, 5 cm/min, cm	T51	80+	75 min.
Test on Original Asphalt:			
Flash Point Temp, °C	T48	230+	230°C min.
Rotational Viscosity @ 135 C, Pa.S	T316	0.096	3 Pa.S max
Dynamic Shear @ 64°C, 10 rads^{-1}, G*/sinδ	T315	2.00	1.0 kPa min

Valero Marketing & Supply-Pittsburg California hereby certifies that the asphalt product accompanying this certification was produced in accordance with the California Department of Transportation's Certification Program for Suppliers of Asphalt, and that this product complies in all respects with the requirements of the applicable specifications for the asphalt product identified on this document.

I hereby certify by my signature that I have the authority to represent the supplier providing the accompanying asphalt product.

Reviewed and approved
Patrick Sendegeya
Laboratory Supervisor

PARAMOUNT-NEVADA
ASPHALT COMPANY, LLC

425 Logan lane
P.O. Box 2247
Fernley, NV 89408
(775) 690-8513

Product : ***PG64-22 Asphalt Cement***
Code #: Nox147
Date:3/1/2007
Tank#2

Purchaser:
Destination: UC Berkley
Transporter:
Truck No:
Bill of Lading No:
Contract No: Research Purposes
Purchase Order No:

MEETS SPECIFICATIONS: *Federal Highway Administration ASTM D6373, AASHTO M320, Nevada DOT, RTC*

CERTIFICATE OF COMPLIANCE

TESTS	***ASTM #***	***AASHTO #***	***SPEC***	***RESULT***
Test on Original Asphalt:				
Dynamic Shear, 64°C, G/Sin δ, kPa*		*T315*	*1.00 min*	*1.07*
Viscosity, 135°C, 21 Spindle, 20 RPM, Pa-s	*D4402*	*T316*	*3 max*	*0.37*
Flash Point, C.O.C., °C	*D92*	*T48*	*230 min*	*306*
Density,60°F,Lb/Gallon	*D70*	*T228*	*--*	*8.55*
Specific Gravity, 77/77°F	*D70*	*T228*	*--*	*1.0208*
Specific Gravity, 60/60°F	*D70*	*T228*	*--*	*1.0268*
API Gravity, 60°F	*D70*	*T228*	*--*	*6.3*
Test on Residue from Rolling Thin Flim Oven:	*D2872*	*T240*		
Dynamic Shear, 64°C, G/Sin δ, kPa*		*T315*	*2.20 min*	*2.67*
Mass Loss, %	*D2872*	*T240*	*1.00 max*	*0.22*
Tests on Residue from PAV Test @ 100°C:	*D6521*	*R28*		
Dynamic Shear, 25°C, G·Sin δ, kPa*		*T315*	*5000 max*	*3276*
BBR Creep Stiffness,-12C°, MPa	*D6648*	*T313*	*300 max*	*168*
BBR m-value, -12°C	*D6648*	*T313*	*0.300 min*	*0.337*

We hereby certify that the above material was sampled and tested according to the applicable ASTM and AASHTO standards and that it complies with all specifications.

This certification is valid for 30 days from the day of issued

Certified By: _____
Paramount - Nevada Asphalt Company L.L.C.

PARAMOUNT PETROLEUM

10090 Waterman Road
Elk Grove, CA 95624
(916) 685-9253
(916) 685-8701 Fax

PRODUCT: PG 64-16 ASPHALT CEMENT
CODE No: 13223
DATE:
TANK No.: 100M1

Purchaser: _____
Destination: _____
Transporter: _____
Truck No.: _____
Bill of Lading No.: _____

Meets Specifications: ASTM D 6373; AASHTO M 320.

CERTIFICATE OF COMPLIANCE

TESTS	ASTM No.	AASHTO No.	SPECIFICATION	RESULT
Tests on Original Asphalt:				
Dynamic Shear, 64°C, G/Sinδ, kPa*	D 7175	T 315	1.00 min	1.11
Viscosity, 135°C, 21 Spindle, 20 RPM, Pa-s	D 4402	T 316	3 max	0.265
Flash Point, C.O.C., °C	D 92	T 48	230 min	302
Density, 15°C, Kg/m³	D 70	T 228	--	1.0241
Solubility in Trichloroethylene, wt.%	D 2042	T 44	99 min	99.99
Tests on R.T.F.O. Residue:	D 2872	T 240		
Dynamic Shear, 64°C, G/Sinδ, kPa*	D 7175	T 315	2.20 min	2.86
Mass Loss, %	D 2872	T 240	1.00 max	0.235
Ductility, 25°C, 5 cm/min, cm	D 113	T 51	75 min	100+
Tests on P.A.V. Residue @ 100°C:	D 6521	R 28		
Dynamic Shear, 25°C, G·Sinδ, kPa*	D 7175	T 315	5000 max	4230
Creep Stiffness, -6°C, S, MPa	D 6648	T 313	300 max	177
m-Value, -6°C	D 6648	T 313	0.300 min	0.360

Paramount Petroleum Corporation hereby certifies that the asphalt product accompanying this certificate was produced in accordance with an accepted certification program for suppliers of asphalt, and the above test data is representative of the shipment.

Data Compiled By: Jack Dougherty
Lab Chemist

Released By: John Dumas
Refinery Shift Supervisor

PARAMOUNT PETROLEUM

10090 Waterman Road
Elk Grove, CA 95624
(916) 685-9253
(916) 685-8701 Fax

PRODUCT: PG 64-10 ASPHALT CEMENT
CODE No: 13221
DATE:
TANK No.: 10M2

Purchaser: _____
Destination: _____
Transporter: _____
Truck No.: _____
Bill of Lading No.: _____

Meets Specifications: ASTM D 6373; AASHTO M 320.

CERTIFICATE OF COMPLIANCE

TESTS	ASTM No.	AASHTO No.	SPECIFICATION	RESULT
Tests on Original Asphalt:				
Dynamic Shear, 64°C, G/Sinδ, kPa*	D 7175	T 315	1.00 min	1.11
Viscosity, 135°C, 21 Spindle, 20 RPM, Pa·s	D 4402	T 316	3 max	0.265
Flash Point, C.O.C., °C	D 92	T 48	230 min	302
Density, 15°C, Kg/m³	D 70	T 228	- -	1.0241
Solubility in Trichloroethylene, wt.%	D 2042	T 44	99 min	99.99
Tests on R.T.F.O. Residue:	D 2872	T 240		
Dynamic Shear, 64°C, G/Sinδ, kPa*	D 7175	T 315	2.20 min	2.86
Mass Loss, %	D 2872	T 240	1.00 max	0.235
Ductility, 25°C, 5 cm/min, cm	D 113	T 51	75 min	100+
Tests on P.A.V. Residue @ 100°C:	D 6521	R 28		
Dynamic Shear, 31°C, G·Sinδ, kPa*	D 7175	T 315	5000 max	3440
Creep Stiffness, 0°C, S, MPa	D 6648	T 313	300 max	68
m-Value, 0°C	D 6648	T 313	0.300 min	0.443

Paramount Petroleum Corporation hereby certifies that the asphalt product accompanying this certificate was Produced in accordance with an accepted certification program for suppliers of asphalt, and the above test data is representative of the shipment.

Data Compiled By: Jack Dougherty
Lab Chemist

Released By: John Dumas
Refinery Shift Supervisor

PARAMOUNT-NEVADA
ASPHALT COMPANY, LLC

PG64-22

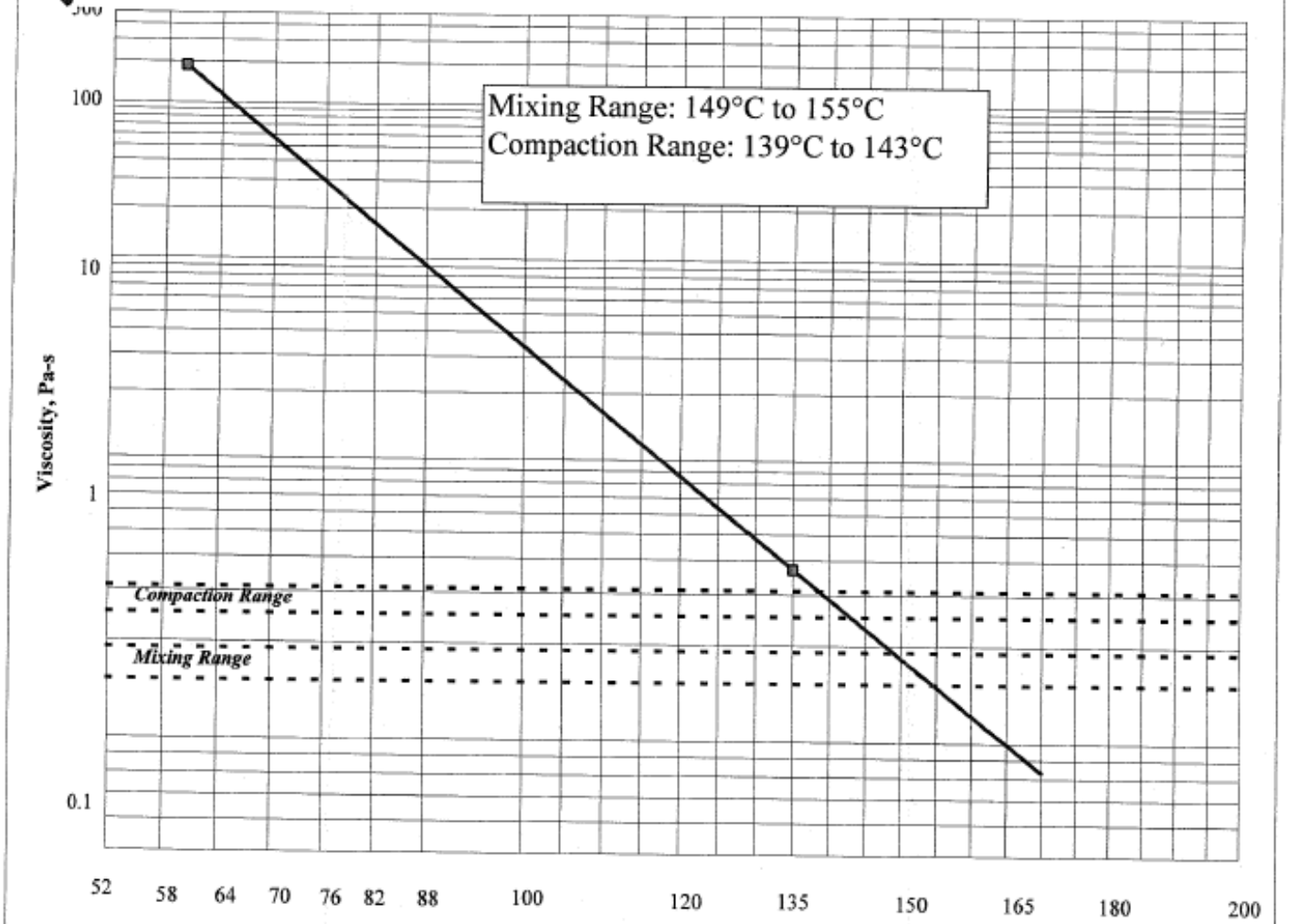

Note: Mixing temperatures are relative to the binder properties for mix design purposes, these may not reflect the actual mixing and compaction experienced in the field and may need to be adjusted to within 25°F for field mixing and 50°F for compaction.

3/1/2007

APPENDIX C

CALCULATION OF THE ANISOTROPY PARAMETER

APPENDIX C: CALCULATION OF THE ANISOTROPY PARAMETER

The derivation of the equations to calculate the anisotropy parameter α^2 used in Section 7.4 is explained below.

The cross section of a beam is shown in Figure C.1. Figure parameters are explained in Equations C.1 through C.3. It is assumed that the Young's modulus for tension is E^+ and E^- for compression. When this cross section is subjected to a bending moment (M), the neutral axis is generally not located at the mid-height.

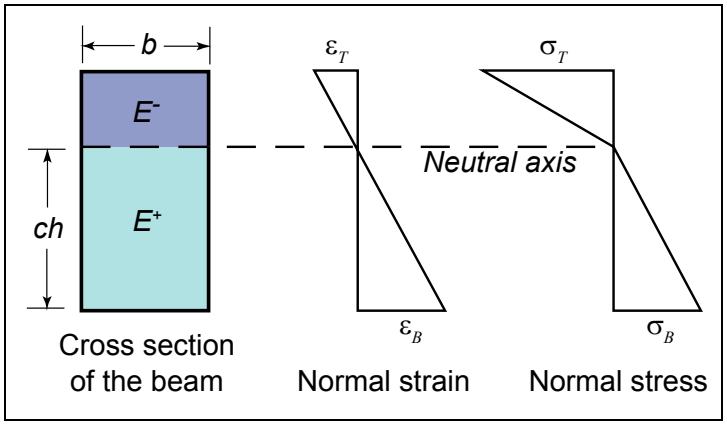

Figure C.1: Cross section of a beam and the strain and stress distributions.

$$E^+ = \alpha^2 E^- \tag{C.1}$$

$$\frac{\varepsilon^T}{\varepsilon^B} = \frac{h-ch}{ch} = \frac{1-c}{c} \tag{C.2}$$

$$\sigma^T = E^- \varepsilon^T \; ; \quad \sigma^B = E^+ \varepsilon^B \tag{C.3}$$

where ε^T and ε^B are the normal strains at the top and the bottom of the beam respectively, and σ^T and σ^T are the corresponding normal stresses.

The tensile (F^+) and compressive (F^-) forces on the cross section should balance each other as shown in Equation C.4. By inserting Equations C.1 through C.3 into Equation C.5, the relation as shown in Equation C.6 can be obtained, which shows the vertical location of the neutral axis as a function of α.

$$F^+ = 0.5chb\sigma^B = F^- = 0.5(1-c)h\sigma^T \tag{C.4}$$

$$\frac{E^+}{E^-}\frac{\varepsilon_B}{\varepsilon_B}=\alpha^2\frac{c}{1-c}=\frac{1-c}{c} \tag{C.5}$$

$$c=\frac{1}{1+\alpha} \tag{C.6}$$

The bending stiffness provided by the beam cross section is (Equation C.7):

$$\sum EI=\frac{1}{3}E^-b\left(\frac{\alpha h}{1+\alpha}\right)^3+\frac{1}{3}E^+b\left(\frac{h}{1+\alpha}\right)^3=\frac{1}{3}\left(\frac{\alpha}{1+\alpha}\right)^2E^-bh^3 \tag{C.7}$$

The equivalent tangential Young's modulus for bending (E^{bend}) was calculated by assuming a homogeneous beam with the same stiffness for compression and tension as shown in Figure C.2 and Equation C.8. The resilient modulus values from triaxial tests at low confining stress levels can be used to approximate E^- (i.e., M_{r1} in Table 7.10).

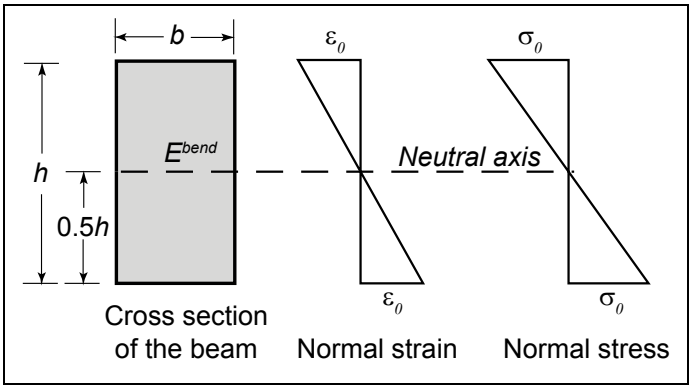

Figure C.2: Equivalent homogeneous beam and stress and strain distributions.

$$\frac{E^{bend}}{E^-}\approx\frac{E^{bend}}{M_{r^1}}\lambda^2 \tag{C.8}$$

The bending stiffness provided by the equivalent beam should be the same as that of the beam in Figure C.1 (Equation C.9).

$$E^{bend}I^{equi}=\frac{1}{12}E^{bend}bh^3 \tag{C.9}$$

The relation between α^2 and λ^2 as shown in Equation C.10 can be obtained by inserting Equation C.9 into Equation C.7.

$$\alpha^2=\left(\frac{\lambda}{2-\lambda}\right)^2 \tag{C.10}$$

The values of $\lambda^2 = E^{bend}/M_{r1}$ in Table 7.11 under the soaked condition range between 9 and 27 percent. In the sensitivity analysis discussed in Chapter 3, two values (0.1 and 0.04) of α^2 were considered. Using Equation C.10, the corresponding λ^2 values are 11 percent and 23 percent.